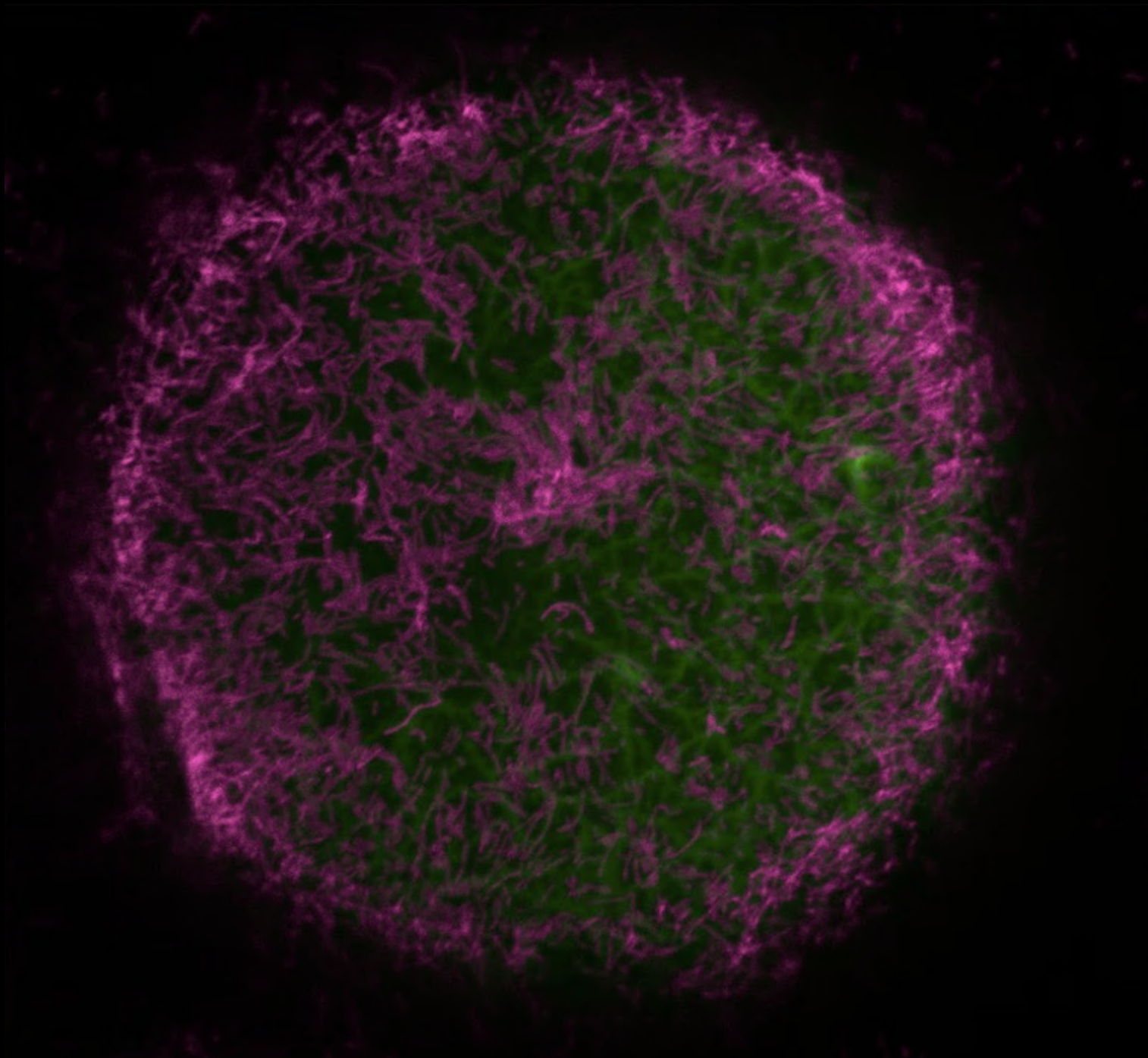
UNDERSTANDING THE CONTRIBUTION OF RESISTANCE-NODULATION-DIVISION FAMILY EFFLUX PUMPS TO THE LIFESTYLE OF *PSEUDOMONAS AERUGINOSA*

DANIELLE SCALES





University of Nottingham
UK | CHINA | MALAYSIA

Supported by wellcome trust

Understanding the contribution of Resistance-Nodulation-Division family efflux pumps to the lifestyle of *Pseudomonas aeruginosa*

Danielle Scales, MSc., MRes.

Thesis submitted to the University of Nottingham for the degree of

Doctor of Philosophy

Biomolecular Discovery Institute

School of Life Sciences

The University of Nottingham

April 2023

Declaration

I hereby declare that, unless otherwise acknowledged, the work presented in this thesis is my own. None of this work has been submitted in whole or in part for another degree at the University of Nottingham or any other institute of learning.



Danielle Scales, 2023

Abstract

Resistance-Nodulation-Division (RND) family efflux pumps are important antibiotic resistance determinants that extrude a range of structurally diverse antibiotics from the cell before they reach their target. Of the 12 RND efflux pumps in *Pseudomonas aeruginosa*, the best characterised are MexAB-OprM, MexCD-OprJ, MexEF-OprN and MexXY. The physiological requirement for so many efflux pumps is unclear given their varied and overlapping substrate profiles. To understand the reasons underlying so much redundancy, the impact of the loss of 10 of the individual efflux pumps and 9 combinatorial mutants lacking different combinations of efflux pumps was studied. In addition to changes in drug susceptibility, this study demonstrates that efflux also plays an important role in motility, quorum sensing, biofilm formation and virulence.

Transcriptomic analysis revealed differences between a mutant lacking MexAB-OprM, MexCD-OprJ, MexEF-OprN and MexXY and the parental PAO1-L strain. Results validation using a combination of transcriptional promoter fusions and phenotypic assays revealed genes involved in quorum sensing, pyocyanin biosynthesis and efflux were upregulated at exponential growth phase. During stationary phase, genes related to anthranilate and glycerol metabolism were upregulated, while 13 tRNAs were downregulated. Interestingly, though the genes encoding several secreted exoenzymes were upregulated, the mutant produced significantly less alkaline protease, elastase B and protease IV than the parent strain.

The results of this work provide new insights into the physiological roles of RND efflux pumps and demonstrate their role as much more than antibiotic resistance determinants.

Acknowledgements

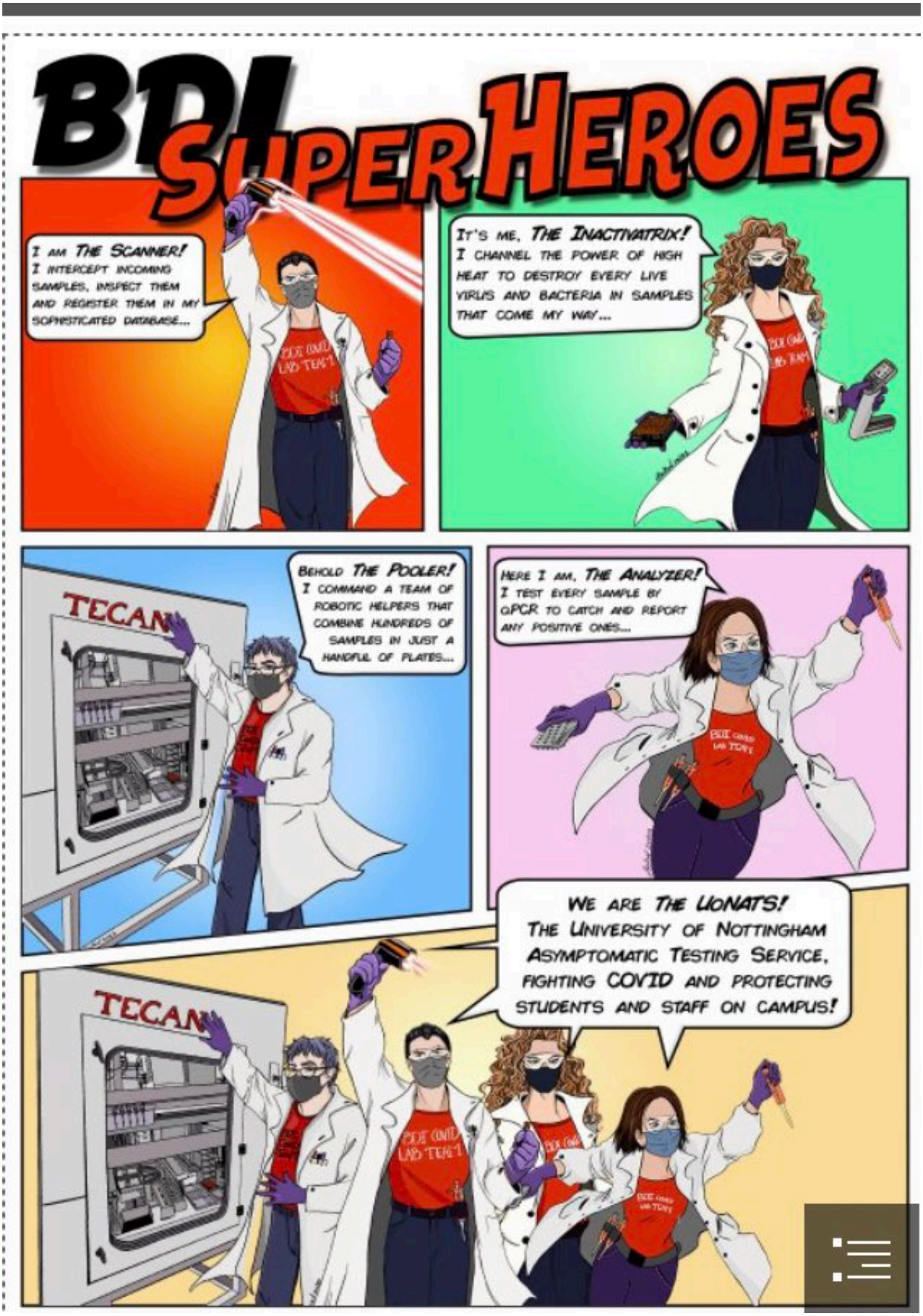
This body of work would not have been possible without the support and guidance of a huge number of people over the past 6 years. First and foremost, I would like to thank my PhD supervisors Professor Paul Williams, Dr Jeni Luckett and Dr Phil Hill. Thank you for your unwavering support and guidance throughout, for allowing me the space to try new things, make mistakes and learn from them, and for talking me down from one particular supervision meeting 12 months into my PhD when I was ready to drop out because I couldn't make a mutant. You had the foresight and experience to know that I could, and 19 mutants later I'm very glad I persevered!

Thank you to all the collaborators who shared their knowledge and expertise with me during this project: Dr Jeni Luckett for the mice experiments and microscopy expertise, Nigel Halliday for the LC-MS analysis, Dr Shaun Robertson for assistance setting up the *Galleria mellonella* infection model and Dr Adriano Gigante for running the Biolog plates. I would also like to give thanks to everyone who helped with work that did not make it into this thesis due to time constraints: Dr Jean Dubern for all your help setting up the fermenters, Dr Ana Da Silva for your help with the Congo-Red plates, Dr Vanina Garcia for your help with the catheter biofilm model, and Professor Jessica Blair and Dr Ilyas Alev at the University of Birmingham for allowing me to visit their lab and learn the ethidium bromide efflux assay.

I would like to thank Professor Ian Henderson and Dr Steve Atkinson for their supervision during my rotation projects. I would also like to thank everyone else I met during my rotation at the University of Birmingham; Dr Jack Bryant, Dr Jess Gray, Samantha McKeand, Dr Chris Icke, Dr Georgia Isom, and Dr Emily Goodall. Thanks for making my time in Birmingham such fun.

Thanks to Dr Katie Hardy and everyone else I met at the Heartlands Hospital (Birmingham, UK) during my placement with Public Health England. I learned a huge amount about clinical microbiology and was inspired to pursue a career in public health.

Between September 2020 and July 2021 I interrupted my PhD to help set up the University of Nottingham Asymptomatic Testing Service (UoNATS) in response to the COVID-19 pandemic. Collectively, the UoNATS processed more than 110,000 PCR tests, broke more than 500 transmission chains on campus and was the first laboratory to gain UKAS



Artwork by Dr Sara Pijuan-Galito and comic by Dr Francesco Tarantini.

accreditation for a saliva-based PCR test. I am incredibly proud of all we achieved and would like to thank Professor Chris Denning and Moira Petrie for the opportunity and for funding my PRINCE2 qualifications in Project Management. I would also like to thank the rest of the COVID-19 dream team: Dr Claire Seedhouse, Dr Andrew Benest, Dr Sara Pijuan-Galito, Dr Francesco Tarantini, Dr Hannah Tomlin, Dr Harry Jenkins, Dr Ana Tellechea Lopez, Dr Kazuyo Kaneko, Dr Siyu Wu, Lara Doolan, Dr Asta Tranholm, Dr I-ning Lee, Dr Jamie Thompson, Caroline Reffin, Penny Gwynne and Joanne Porte for all the good times along the way.

Many thanks to all the past and present members of the lab for their helpful discussions, especially Dr Carolina Paiva, Dr Frances Smith, Dr Will Richardson, Dr Claire Laxton, Dr Sam Fenn, Dr Maria Papaggeli, Dr Dean Walsh, Isobel Blower, Marina Serder, Dr Erik Hanko, Dr Bashir Rumah, Dr Chris Stead, Dr Josh Petch, Dimitra Panagiotopoulou and Bethan Roberts. I have particularly fond memories of all our coffee breaks and our trips to the peak district, Lisbon and the Azores.

I would like to thank the Wellcome Trust and the University of Nottingham for their financial support, and the rest of the Antimicrobials and Antimicrobial resistance (AAMR) 2016 cohort: Dr Jess Gray, Dr Farhana Burnett, Dr Alistair Middlemiss, Dr Tom Armstrong, Dr Nikki Osborne, Dr Alice Lanne and Dr Emily Whittle. It’s been a pleasure to know you and watch you succeed in and out of the lab.

Last but not least, I would like to thank my family especially my mum, dad and Ed for all the sacrifices they made to enable me to finish my PhD. I would not be here without your support.

Collaborative work

This work was supported by funding from the University of Nottingham in collaboration with the Wellcome Trust (grant number A136WB)

Genome sequencing was provided by MicrobesNG (http://www.microbesng.com)

RNA extraction and transcriptome sequencing was performed by Novogene (Cambridge, UK)

Liquid Chromatography-Mass spectrometry analysis of quorum sensing signalling molecules and anthranilate was performed by Nigel Halliday.

Biolog phenotypic plates were prepared by Dr Adriano Gigante

Confocal microscopy was performed with assistance from Dr Jeni Luckett

G. mellonella infection model was performed with assistance from Dr Shaun Robertson

The murine infection model was performed by Dr Jeni Luckett

Publications during this project

Jenkins, H.H., Lopez, A.A.T., Tarantini, F.S., Tomlin, H., **Scales, D.**, Lee, I., Wu, S., Hyde, R., Lis-Slimak, K., Byaruhanga, T. and Thompson, J.L., 2022. Performance evaluation of a non-invasive one-step multiplex RT-qPCR assay for detection of SARS-CoV-2 direct from saliva. Scientific Reports, 12(1).

Tarantini, F.S., Wu, S., Jenkins, H., Tellechea Lopez, A., Tomlin, H., Hyde, R., Lis-Slimak, K., Thompson, J.L., Pijuan-Galitó, S., **Scales, D**. and Kaneko, K., 2022. Direct RT-qPCR Assay for the Detection of SARS-CoV-2 in Saliva Samples. Methods and Protocols, 5(2), p.25.

Pijuan-Galito, S., Tarantini, F.S., Tomlin, H., Jenkins, H., Thompson, J.L., **Scales, D**., Stroud, A., Tellechea Lopez, A., Hassall, J., McTernan, P.G. and Coultas, A., 2021. Saliva for COVID-19 testing: Simple but useless or an undervalued resource?. Frontiers in Virology, p.29.

Table of Contents

LIST OF FIGURES **XVI**

LIST OF TABLES **XIX**

LIST OF ABBREVIATIONS **XXI**

1 INTRODUCTION **2**

1.1 *Pseudomonas* **2**

1.1.1 *Pseudomonas aeruginosa* 2

1.1.1.1 Infection 3

1.1.1.2 Treatment 4

1.1.1.3 Antimicrobial resistance 4

1.2 Transmembrane export **8**

1.2.1 Secretion systems 8

1.2.2 Efflux pumps 11

1.2.2.1 RND efflux pumps 12

1.2.2.1.1 Structure 15

1.2.2.1.2 Substrates 19

1.2.2.1.3 Expression 21

1.2.2.1.4 Regulation 23

1.2.2.1.5 Lifestyle 28

1.2.2.1.6 Efflux pump inhibitors as a target to reduce antimicrobial resistance 29

1.3 Gene regulation **30**

1.3.1 Two-component systems 30

1.3.2 Quorum sensing 34

1.3.2.1 *las* system 34

1.3.2.2 *rhl* system 36
1.3.2.3 *pqs* system 37
1.3.2.4 Quorum sensing and efflux 38

1.4 Virulence 38
1.4.1 Pyocyanin 39
1.4.2 Rhamnolipids 42
1.4.3 Siderophores 42
1.4.4 Exoproteases 43
1.4.4.1 Elastase A 43
1.4.4.2 Elastase B 44
1.4.4.3 Protease IV 44
1.4.4.4 Alkaline protease 45
1.4.5 Flagella 45
1.4.6 Pili 46
1.4.7 Virulence and efflux 48

1.5 Biofilm formation 49
1.5.1 Biofilm composition 50
1.5.2 Life cycle 51
1.5.3 Biofilms and efflux 53

1.6 Hypothesis 54

1.7 Aims 54

2. CONSTRUCTION OF RND EFFLUX PUMP MUTANTS IN *P. AERUGINOSA* PAO1-L-DS 56

2.1 Introduction 56

2.2 Aims 58

2.3 Construction of a series of isogenic *P. aeruginosa* PAO1-L-DS efflux pump deletion mutants 59

2.3.1 Construction of pEX18 suicide plasmids and insertion into *E. coli* S17-1λpir 59
2.3.2 Construction of single *P. aeruginosa* PAO1-L-DS chromosomal efflux pump deletion mutants 60
2.3.3 Construction of combinatorial *P. aeruginosa* PAO1-L-DS chromosomal efflux pump deletion mutants 64

2.4 Confirmation of efflux pump deletion by whole genome sequencing (WGS) 64
2.4.1 Assessment of raw read and alignment quality 64
2.4.2 Analysis of variants 68
2.4.2.1 Identification of variants responsible for QS defects in K2732 68
2.4.2.2 Comparison of variants found in PAO1-L 70
2.4.2.3 Comparison of variants in the RND efflux pump mutants 70

2.5 Discussion 80

2.6 Summary of key findings 82

2.7 Future work 82

3. TRANSCRIPTOMIC CHANGES CAUSED BY LOSS OF MEXAB-OPRM, MEXCD-OPRJ, MEXEF-OPRN AND MEXXY IN *P. AERUGINOSA* PAO1-L-DS 84

3.1 Background 84

3.2 Aims 86

3.3 Hypothesis 86

3.4 Transcriptomic changes arising from loss of MexAB-OprM, MexCD-OprJ, MexEF-OprN and MexXY in *P. aeruginosa* PAO1-L-DS 87
3.4.1 Quality control of RNA-Seq results 89
3.4.2 Analysis of differentially expressed genes identified by RNA-Seq 91
3.4.3 Enrichment analysis of RNA-Seq results 98

3.5 Validation of transcriptomic changes associated with loss of MexAB-OprM, MexCD-OprJ, MexEF-OprN and MexXY in *P. aeruginosa* PAO1-L-DS 98

3.5.1 Differential transcription of the alkaline protease gene *aprA* 100
3.5.3 Differential transcription of the rhamnolipid synthesis gene *rhlA* 100
3.5.4 Differential transcription of the pyocyanin synthesis gene *phzA1* 105
3.5.4 Differential transcription of the *pqs* quorum sensing system 108
3.5.5 Differential transcription of the anthranilate degradation genes *antA* and *antR* 111
3.5.6 Elastase production decreases with the loss of MexAB-OprM, MexCD-OprJ, MexEF-OprN and MexXY in *P. aeruginosa* PAO1-L-DS 114

3.6 Discussion 118

3.7 Summary of key findings 123

3.8 Future work 123

4. PHENOTYPIC CHANGES CAUSED BY LOSS OF EFFLUX 125

4.1 Background 125

4.2 Aims 126

4.3 Hypotheses 126

4.4 Phenotypic characterisation of the *P. aeruginosa* PAO1-L-DS efflux pump deletion mutants 126
4.4.1 Growth profiles 126
4.4.2 Antimicrobial susceptibility of the RND efflux pump mutants 130
4.4.3 Changes in motility 131
4.4.4 Changes in pyocyanin production 136
4.4.5 Changes in rhamnolipid production 136
4.4.6 Changes in protease production 138

4.5 Metabolic profiling 143

4.6 Biofilm formation 146

4.7 Virulence **148**

4.7.1 *Galleria mellonella* infection 148

4.7.2 Murine infection 150

4.8 Discussion **152**

4.9 Summary of key findings **157**

4.10 Future work **157**

5. OVERALL DISCUSSION **159**

6. MATERIALS AND METHODS **163**

6.1 Strains and culture conditions **163**

6.1.1 Bacterial strains and growth conditions 163

6.1.2 Plasmids 163

6.1.3 Media 163

6.1.4 Antibiotic selection 164

6.1.5 Storage 164

6.1.6 Growth curves 164

6.1.7 Transcriptional promoter fusion assays 173

6.1.8 Antimicrobial susceptibility testing 173

6.2 General molecular techniques **174**

6.2.1 Primers 174

6.2.2 Polymerase chain reaction 174

6.2.3 Gel electrophoresis and extraction 181

6.2.4 Restriction digests 181

6.2.5 Ligation 181

6.2.6 Bacterial transformation 181

6.2.6.1 *E.coli* electro-competent cells 181

6.2.6.2 *P. aeruginosa* electro-competent cells 182

6.2.6.3 Electroporation 182

6.2.6.3 Conjugation 182
6.2.7 DNA extraction 183
6.2.8 Construction of a series of RND efflux pump mutants 183
6.2.8.1 Construction of a series of suicide vectors 185
6.2.8.2 Allelic replacement of the wild-type loci with the deletion variant in *P. aeruginosa* PAO1-L-DS 185
6.2.8.3 Allelic replacement of the wild-type loci with the deletion variant in previously constructed RND efflux pump mutants 186

6.3 Phenotypic assays 186
6.3.1 Rhamnolipids 186
6.3.2 Pyocyanin 187
6.3.3 Exoenzyme activity assays 187
6.3.3.1 Universal protease 187
6.3.3.2 Alkaline protease 187
6.3.3.3 Elastase A 188
6.3.3.4 Elastase B 188
6.3.3.5 Protease IV 189
6.3 Motility assays 189
6.3.4.1 Swimming 189
6.3.4.2 Swarming 189
6.3.4.3 Twitching 190
6.3.5 LC-MS/MS analysis 190
6.3.5.1 AHL and AQ quantification 190
6.3.5.2 Anthranilate quantification 190
6.3.6 Biolog phenotype assays 190

6.4 Biofilm formation 191
6.4.1 Biofilm formation on glass beads 191
6.4.2 Biofilm imaging 191

6.5 Sequencing 191
6.5.1 Sanger sequencing 191

6.5.2 Whole genome sequencing and data analysis 192
6.5.3 Transcriptome sequencing and data analysis 194

6.6 *In vivo* infection models 196
6.6.1 Excision of gentamicin resistance cassette 196
6.6.2 *Galleria mellonella* infection model 196
6.6.3 Murine infection model 197

6.7 Statistical analysis 197

REFERENCES 198

APPENDIX 241

List of figures

Figure 1.1: Secretion systems and associated substrates in *P. aeruginosa* 9
Figure 1.2: RND efflux pumps in *P. aeruginosa* 13
Figure 1.3: Multiple sequence alignment of major Gram-negative RND transporter protein sequences 14
Figure 1.4 Genomic arrangement of *P. aeruginosa* PAO1-UW RND efflux pumps. 16
Figure 1.5: Two Component Systems in *P. aeruginosa* 31
Figure 1.6: The Las, Rhl and PQS quorum sensing systems of *P. aeruginosa* 35
Figure 1.7 Pyocyanin biosynthesis and regulation 41
Figure 1.8: Organisation and assembly of Type IV pili in *P. aeruginosa* 47
Figure 1.9 Lifecycle of a biofilm 52
Figure 2.1: Lineage of the efflux pump deletion mutants 63
Figure 2.2: Comparative genome assembly of the K2732 (PAO1 WT) and K2733 (Δ*mexAB-oprM* Δ*mexCD-oprJ* Δ*mexEF-oprN* Δ*mexXY* against the PAO1-UW reference genome 65
Figure 2.3: Comparative genome assembly of the PAO1-L-DS single efflux pump deletion mutants against PAO1-UW reference genome 66
Figure 2.4 Comparative genome assembly of the PAO1-L-DS combinatorial efflux pump deletion mutants against PAO1-UW reference genome. 67
Figure 3.1 Summary of known links between RND efflux pumps and bacterial physiology in *P. aeruginosa* 85
Figure 3.2. Selection of samples for RNA-Seq 88
Figure 3.3: Unsupervised clustering analysis of RNA-Seq results indicates a strong correlation between replicates of each strain and time-point 90
Figure 3.4: Volcano plots displaying differentially expressed genes (DEGs) in the ΔABCDEFXY mutant compared to PAO1-L-DS 92
Figure 3.5: Visualization of gene expression between samples 97
Figure 3.6: Gene Ontology classification of differentially expressed gene products in the ΔABCDEFXY mutant compared to PAO1-L-DS. 99

Figure 3.7: Loss of MexAB-OprM, MexCD-OprJ, MexEF-OprN and MexXY decreases alkaline protease production. 101
Figure 3.8: Rhamnolipid production decreases with loss of MexAB-OprM, MexCD-OprJ, MexEF-OprN and MexXY 103
Figure 3.9: Pyocyanin production increases with loss of MexAB-OprM, MexCD-OprJ, MexEF-OprN and MexXY. 106
Figure 3.10: PQS production increases with loss of MexAB-OprM, MexCD-OprJ, MexEF-OprN and MexXY 109
Figure 3.11: Anthranilate metabolism changes with loss of MexAB-OprM, MexCD-OprJ, MexEF-OprN and MexXY. 112
Figure 3.12: Elastase production decreases with loss of MexAB-OprM, MexCD-OprJ, MexEF-OprN and MexXY. 115
Figure 3.13: Summary of changes in gene expression and virulence caused by loss of MexAB-OprM, MexCD-OprJ, MexEF-OprN and MexXY at exponential phase 119
Figure 3.14: Summary of changes in gene expression and virulence caused by loss of MexAB-OprM, MexCD-OprJ, MexEF-OprN and MexXY at stationary phase 120
Figure 4.1: Growth profiles of PAO1-L-DS and the RND efflux system mutants in LB. ... 127
Figure 4.2: Growth profiles of PAO1-L-DS and the RND efflux system mutants in M9 .. 128
Figure 4.3: Swimming motility of PAO1-L-DS and the RND efflux system mutants..... 133
Figure 4.4: Swarming motility of PAO1-L-DS and the RND efflux system mutants. 134
Figure 4.5: Twitching motility of PAO1-L-DS and the RND efflux system mutants..... 135
Figure 4.6: Pyocyanin and rhamnolipid production of PAO1-L-DS and the RND efflux system mutants 137
Figure 4.7: Universal protease, Elastase B and Protease IV production of PAO1-L-DS and the RND efflux system mutants. 140
Figure 4.8: Elastase A production of PAO1-L-DS and the RND efflux system mutants... 141
Figure 4.9: Alkaline protease production of PAO1-L-DS and the RND efflux system mutants 142
Figure 4.10: Carbon, nitrogen, phosphorus and sulphur utilisation of PAO1-L-DS, ΔABCDEFXY and ΔABCDEFPQXY. 144
Figure 4.11: Confocal microscopy of PAO1-L-DS, ΔABCDEFXY and ΔABCDEFPQXY biofilm production on cytodex beads. 147

Figure 4.12: *G. mellonella* infection with PAO1-L-DS and ΔABCDEFXY..... 149
Figure 4.13: Murine infection with PAO1-L-DS, ΔABCDEFXY and ΔABCDEFPQXY 151
Figure 6.1: Overview of the construction of a series of RND efflux pump mutants..... 184
Figure 6.2: WGS data analysis pipeline..... 193
Figure 6.3: RNA-Seq data analysis pipeline 195

List of tables

Table 1.1 Antibiotics used for the treatment of *P. aeruginosa* infections and associated mechanisms of resistance 5

Table 1.2: *P. aeruginosa* PAO1-UW RND efflux pump coding regions 17

Table 1.3 Substrate profiles of the *P. aeruginosa* RND efflux pumps..... 20

Table 1.4 Expression of *P. aeruginosa* RND family efflux pumps 22

Table 1.5 Transcriptional regulators of *P. aeruginosa* RND family efflux pumps 24

Table 1.6: Two-Component Systems (TCS) regulating virulence and/or biofilm development in *P. aeruginosa*..... 32

Table 1.7 Virulence factors produced by *P. aeruginosa* 40

Table 2.1: Expected fragment sizes following the construction of the pEX18Gm suicide vectors 61

Table 2.2: Expected fragment sizes for second recombination event where upstream integration results in gene deletion and downstream integration reverts to wild-type (WT)62

Table 2.3: Single nucleotide polymorphisms, insertions and deletions in K2732 compared to the PAO1-UW reference genome that were not observed in PAO1-L-DS. 69

Table 2.4: Single nucleotide polymorphisms, insertions and deletions identified in PAO1-L-DS and PAO1-L-HN compared to the PAO1-UW reference genome 71

Table 2.5: Predicted impact of single nucleotide polymorphisms, insertions and deletions found in PAO1-L-DS compared to PAO1-UW on the biological function of the protein 74

Table 2.6 Single nucleotide polymorphisms, insertions and deletions present in PAO1-L-HN but not PAO1-L-DS, when compared to the PAO1-UW reference genome. 76

Table 2.7 Single nucleotide polymorphisms, insertions and deletions in the efflux pump deletion mutants compared to the PAO1-L-DS parent strain 78

Table 2.8: Predicted impact of single nucleotide polymorphisms, insertions and deletions in the efflux pump deletion mutants compared to PAO1-L-DS on the biological function of the protein..... 79

Table 3.1: Differentially expressed genes in the ΔABCDEFXY mutant compared to PAO1-L-DS at exponential growth phase growth 93

Table 3.2: Differentially expressed genes in the ΔABCDEFXY mutant compared to PAO1-L-DS at early stationary growth phase growth. 95
Table 4.1: Minimum inhibitory concentrations of antibiotics for PAO1-L-DS and the efflux pump mutants. 129
Table 6.1: Bacterial strains used in this study 165
Table 6.2: Plasmids 168
Table 6.3: Media composition 171
Table 6.4: Antibiotics used in this study 172
Table 6.5: Primers used in this study 175
Table 6.6: Generic PCR thermocycling condition using Q5® High-Fidelity Master Mix . 179
Table 6.7: Generic PCR thermocycling condition using GoTaq® Master Mix 180

List of abbreviations

Abbreviation	Definition
μg	Micrograms
μL	Microlitres
μM	Micromolar
3-oxo-C_{12}-HSL	*N*-(3-oxododecanyl)-L-homoserine lactone
5-Me-PCA	5-methylphenazine-1-carboxylate
ABC	ATP-binding cassette family
AHL	Acyl-homoserine lactone
AIDS	Acquired immune deficiency syndrome
AME	Aminoglycoside-modifying enzymes
AMR	Antimicrobial resistant
AQ	Alkyl quinolone
ATP	Adenosine triphosphate
BLI	β-lactamase inhibitor
C_4-HSL	*N*-butanoyl-L-homoserine lactone
c-di-GMP	Bis-(3'-5')-cyclic dimeric guanosine monophosphate
CCCP	Carbonyl cyanide 3-chlorophenylhydrazone
CF	Cystic Fibrosis
CRE	Carbapenem-resistant Enterobacteriaceae
CRISPR	Clustered regularly interspaced short palindromic repeats
cUTI	Complicated urinary tract infection
DNA	Deoxyribonucleic acid
DBP	Distal binding pocket

eDNA	Extracellular DNA
EPI	Efflux pump inhibitor
EPS	Extracellular polymeric substance
ESBL	Extended-spectrum β-lactamase
FD	Funnel domain
FDA	United Stated Food and Drug Administration
HOAc	Acetic acid
HHQ	4-hydroxy-2-heptylquinoline
Indel	Insertion/deletion
LC-MS/MS	Liquid chromatography-tandem mass spectrometry
LPS	Lipopolysaccharide
MATE	Multidrug and toxic-compound extrusion family
MCS	Multiple cloning site
MDR	Multi-drug resistant
MFS	Major facilitator superfamily
MPD	Membrane-proximal domain
ND	Not determined
nM	Nanomolar
NS	Not significant
OMP	Outer-membrane protein
PAβN	Phenylalanine-arginine-β-naphthylamide
PAP	Periplasmic adapter protein
PBP	Proximal binding pocket
PBS	Phosphate buffered saline
PCR	Polymerase chain reaction
PD	Pore domain

PIV	Protease IV
pmol	Picomole
PQS	*Pseudomonas* quinolone signal; 2-heptyl-3-hydroxy-4-quinolone
QS	Quorum sensing
QSSM	Quorum sensing signalling molecule
RNA	Ribonucleic acid
RNA-seq	RNA-sequencing
RND	Resistance-nodulation-cell division family
SMR	Small multidrug resistance family
SNP	Single nucleotide polymorphism
T1SS	Type I secretion system
T2SS	Type II secretion system
T3SS	Type III secretion system
T4SS	Type IV secretion system
T5SS	Type V secretion system
T6SS	Type VI secretion system
TCA	Tricarboxylic acid
TCS	Two-component system
TFP	Type IV pili
TMD	Transmembrane domain
UHT	Ultra-heat treated
UTI	Urinary tract infection
WGS	Whole genome sequencing
WT	Wild-type

CHAPTER 1:

Introduction

1 Introduction

1.1 *Pseudomonas*

Belonging to the Pseudomonadota phylum, the *Pseudomonas* genus comprises over 100 species of Gram-negative, flagellated, aerobic, non-spore-forming, rod-shaped bacilli. Pseudomonads can colonise a wide range of ecological niches and are found in aquatic, soil and plant environments. Many are commensals although some are fish, insect or plant pathogens such as *P. syringae* which produces the ice nucleation active protein InaZ to freeze water and cause frost damage (Roeters *et al*., 2021). Some species are opportunistic human pathogens including *P. fluorescens*, *P. stutzeri* and *P. aeruginosa*.

1.1.1 *Pseudomonas aeruginosa*

P. aeruginosa is a ubiquitous environmental organism characterised by the fruity, grape-like odour of 2-aminoacetophenone, and a blue-green pigmentation produced by a combination of pyocyanin (non-fluorescent blue pigment) and pyoverdine (fluorescent green pigment). Strains are divided into three main lineages, where PAO1, PA14 and PA7 are the reference strains for group 1, group 2 and group 3 respectively (Freschi *et al*., 2015). The best characterised of these is PAO1, which is a chloramphenicol-resistant mutant of the PAO strain originally isolated from a burn wound in 1954 (Holloway, 1955), however distinct PAO1 lineages have evolved as the original strain has undergone multiple passages in laboratories around the world (Klockgether *et al*., 2010). The first PAO1 subline to be sequenced was PAO1-UW (Stover *et al*., 2000), which has since become the reference for the scientific community. PAO1 grows on a range of non-selective media where colonies appear large and flat with rough edges, though other strains produce smooth or mucoid colonies. Identification is confirmed by Gram-stain, with positive oxidase and catalase tests (Public Health England, 2015). This laboratory strain can grow at temperatures ranging from 5 – 42°C, respire both aerobically and anaerobically, and utilise various carbon sources.

P. aeruginosa is a major source of water contamination in both industrial and hospital settings, where it readily forms biofilms on taps and associated pipework. Biofilms can also

form on medical implants and catheters, which are almost impossible to treat without surgical removal of the device. The organism is a leading cause of hospital-acquired infections and the World Health Organisation has declared the pathogen a major cause for concern (WHO, 2017). Although *P. aeruginosa* rarely infects healthy individuals, high-risk groups including neonates and those with neutropenia, burn wounds or the autosomal recessive disorder Cystic Fibrosis (CF) are susceptible to life-threatening infections.

1.1.1.1 Infection

P. aeruginosa infections can be categorised as either acute or chronic. Acute infections are characterised by the rapid onset of symptoms and range from milder skin infections to surgical site infections and urinary tract infections (UTIs) while pneumonia, burn wound infections and bacteremia are more severe, spread rapidly and carry a high mortality rate. Occasionally, *Pseudomonas* bacteremia presents as ecthyma gangrenosum where gangrenous ulcers rapidly transform into necrotic ulcers and the prognosis is poor. During acute infections, *P. aeruginosa* is motile and displays a more virulent phenotype secreting T3SS effector proteins, hydrogen cyanide and exotoxin A (Furukawa *et al*., 2006).

Chronic infections are a significant cause of morbidity and mortality for those with pre-existing conditions including AIDS, lung cancer, bronchiectasis and CF; a disease caused by a mutation in the cystic fibrosis transmembrane conductance regulator (CFTR) gene, of which Phe508del accounts for approximately two-thirds of cases in European populations (Castellani *et al*., 2008). The CFTR gene encodes an ion channel which normally allows the passage of chloride ions across epithelial cell membranes. Disease severity is dependent on the genotype and whether the mutation results in defective regulation of the CFTR protein, insufficient CFTR production, or a complete lack of CFTR altogether (Elborn, 2016). The symptoms of CF are caused by the build-up of mucus in the lungs, pancreas and other organs resulting in breathing problems and increased susceptibility to lung infections.

By age 26, more than 80% of people with CF are infected with *P. aeruginosa* (FitzSimmons, 1993). Chronic infections are associated with decreased lung function and increased morbidity and mortality (Emerson *et al*., 2002). Over time, chronic isolates accumulate mutations in genes resulting in less virulent phenotypes. Commonly mutated

genes include *mucA* which gives rise to the mucoid phenotype resulting from overproduction of the exopolysaccharide alginate and *lasR* which downregulates quorum sensing (Ciofu *et al*., 2010). Other important changes include reduced motility and reduced production of virulence factors (Moradeli *et al*., 2017).

1.1.1.2 Treatment

Eight classes of antibiotics are routinely used for the treatment of *P. aeruginosa* infections: aminoglycosides, carbapenems, cephalosporins, fluoroquinolones, monobactams, penicillin in combination with a β-lactamase inhibitor (BLI), phosphonic acids and polymyxins (Bassetti *et al*., 2018). Current clinical guidelines recommend an initial combination therapy of two broad-spectrum antibiotics from different classes, followed by a single antibiotic dependent upon antibiotic sensitivity testing results (Bassetti *et al*., 2018). For people with CF, long-term inhaled antibiotics such as tobramycin inhalation solution (TIS) are prescribed for chronic maintenance therapy, while pulmonary exacerbations are alleviated with intravenous antibiotics selected according to the results of antibiotic susceptibility testing (Castellani *et al*., 2018).

Antibiotics from each class recommended for the treatment of *P. aeruginosa* infection and associated resistance mechanisms are summarised in **Table 1.1.** Due to many intrinsic and acquired resistance mechanisms treatments for *P. aeruginosa* infections are limited.

1.1.1.3 Antimicrobial resistance

Antimicrobial-resistant (AMR) bacteria survive exposure to a drug concentration that would normally kill the organism. AMR *P. aeruginosa* can be further subdivided into multidrug-resistant (MDR) strains that are resistant to antibiotics from at least three of the eight different classes detailed in **Table 1.1**, extensively drug-resistant (XDR) strains that are resistant to antibiotics from at least six of the eight different classes and pandrug-resistant (PDR) strains that are resistant to antibiotics from each of the eight different classes (Magiorakos *et al*., 2012).

Table 1.1 Antibiotics used for the treatment of *P. aeruginosa* infections and associated mechanisms of resistance

Antibiotic Class	Examples	Molecular Target	Resistance Mechanism
Aminoglycosides	Amikacin, gentamicin, tobramycin	Protein synthesis: 30S ribosomal subunit inhibition	Over-expression of MexXY, aminoglycoside modifying enzymes (AME)
Carbapenems	Imipenem, meropenem	Cell wall biosynthesis: transpeptidase inhibition	Carbapenemases
Cephalosporins	3rd generation: ceftazidime, 4th generation: cefepime	Cell wall biosynthesis: transpeptidase inhibition	Extended-spectrum β-lactamases (ESBLs)
Fluoroquinolones	2nd generation: ciprofloxacin, 3rd generation: levofloxacin	DNA replication: DNA gyrase and topoisomerase IV inhibition	Quinolone Resistance Determining Region (QRDR), plasmid-mediated quinolone resistance (PMQR) genes
Monobactams	Aztreonam	Cell wall biosynthesis: transpeptidase inhibition	β-lactamases
Penicillin with BLI	Piperacillin/tazobactam, ticarcillin/clavulanic acid	Cell wall biosynthesis: transpeptidase inhibition	Hyperproduction of β-lactamases
Phosphonic acids	Fosfomycin	Cell wall biosynthesis: MurA (UDP-N-acetylglucosamine-3-enolpyruvyltransferase) inhibition	Fosfomycin-resistance enzymes
Polymyxins	Polymyxin B and polymyxin E (colistin)	Outer membrane disruption; competitively displaces divalent cations (Ca^{2+} and Mg^{2+})	LPS additions, activation of the two-component systems PhoPQ and PmrAB

Resistance mechanisms can either be intrinsic or acquired. *P. aeruginosa* is intrinsically resistant to many classes of antibiotics due to an impermeable cell envelope, the presence of multidrug efflux pumps and chromosomally encoded antibiotic-inactivating enzymes. Acquired drug resistance occurs through the transfer of antibiotic resistance genes on mobile genetic elements such as integrons, plasmids, prophages and transposons. These genes may be transferred between and within species by mechanisms of horizontal gene transfer, including conjugation, transduction and transformation (Thomas & Nielson, 2005). Antibiotic resistance genes can be broadly divided into four functions which are discussed below with examples: a reduction in cell membrane permeability to prevent antibiotic entry, antibiotic modification, target modification or increased expression of multidrug efflux pumps. The resistance genes found in PAO1-L are detailed in **Appendix T**.

Many antibiotics need to cross the outer membrane to reach their intracellular targets: an asymmetric lipid bilayer comprised of phospholipids and lipopolysaccharides (LPS). While hydrophilic molecules such as β-lactams, fluoroquinolones and chloramphenicol enter the cell through porins, macrolides and other hydrophobic antibiotics diffuse through the lipid bilayer. *P. aeruginosa* is intrinsically resistant to vancomycin and other large molecules that are unable to pass through porins, and many clinical isolates downregulate porin expression to reduce cell membrane permeability and increase expression of efflux pumps (Quale *et al*., 2006; Xavier *et al.,* 2010).

Several groups of enzymes directly modify the antibiotic structure. β-lactams are characterised by the eponymous β-lactam ring in their molecular structure and inhibit cell wall biosynthesis by inhibiting transpeptidases. These enzymes remove the terminal D-alanine of the N-acetylmuramic acid (NAM) pentapeptide side chain, to enable peptidoglycan cross-links to form. As β-lactams are structural analogues of D-alanine-D-alanine, they block the active site of the transpeptidase inhibiting cross-linking and peptidoglycan biosynthesis so cell lysis occurs. However, bacteria produce β-lactamases that hydrolyse the β -lactam ring, preventing its reaction with the transpeptidase. Penicillinase was the first β-lactamase to be identified (Abraham & Chain, 1940), and shows specificity for penicillins. For this reason, β-lactamase inhibitors (BLI) are co-prescribed with ß-lactams to overcome resistance. Penicillins routinely prescribed for the treatment of *P. aeruginosa*

infection include piperacillin/tazobactam and ticarcillin/clavulanic acid (Bassetti *et al*., 2018).

Cephalosporins are a subclass of β-lactams originally isolated from the fungus Acremonium. First-generation cephalosporins had low activity against Gram-negative bacteria, however subsequent generations have an increased spectrum of activity. Cephalosporins commonly used in the treatment of *P. aeruginosa* infection include the third-generation ceftazidime and the fourth-generation cefepime (Bassetti *et al*., 2018). Plasmid-encoded extended-spectrum β-lactamases (ESBLs) such as TEM-1 and SHV-1 hydrolyze cephalosporins with an oxyimino side chain, reducing treatment options as these plasmids often carry multiple resistance genes. For this reason, carbapenems remain the treatment choice for ESBL-producing strains.

Carbapenems are another subclass of β-lactams which have a broader spectrum of activity than penicillins and cephalosporins. For this reason, they are usually reserved for treating MDR infections. Carbapenems commonly used to treat *P. aeruginosa* infection include imipenem and meropenem (Bassetti *et al*., 2018). Carbapenems are unaffected by β-lactamases and ESBLs but are susceptible to carbapenemases. In strains carrying carbapenemases, resistance to non-β-lactams is also common and severely limits treatment options.

Other enzymes alter the antibiotic structure including the aminoglycoside modifying enzyme (AME) AAC(6')-Ib which acetylates the NH_2 group of kanamycin B to prevent ribosomal binding. However, mutations D179Y & W102R in this enzyme also enable the acetylation of the NH_2 group in fluoroquinolones, giving rise to multi-drug resistant strains (Robicsek *et al.*, 2006). Two fosfomycin-resistance enzymes have been identified in *P. aeruginosa*. FosA (Bernat *et al*., 1997) and FosX (Fillgrove *et al*., 2007) open up the epoxide ring with glutathione or water respectively to render the structure ineffective.

Target modification is a major cause of fluoroquinolone resistance, where mutations in genes located on the Quinolone Resistance Determining Region (QRDR) such as S87L in the *parC* gene of topoisomerase IV, and T83I in the *gyrA* gene of DNA gyrase so ciprofloxacin is no longer able to bind (Wang *et al.*, 2015). Plasmid-mediated quinolone resistance (PMQR) genes such as *qnr* can also confer mild fluoroquinolone resistance through the formation of a structure which mimics B-DNA (Hegde *et al.*, 2011). This protein then binds to the enzyme

to prevent drug inhibition. Resistance to polymyxins can also occur through the acquisition of the mobilized colistin resistance *(mcr-1)* (Liu *et al*., 2016) which encodes a phosphatidylethanolamine transferase and transfers a phosphoethanolamine residue to the lipid A moiety of LPS, lowering its affinity for colistin and other polymyxins.

Resistance-nodulation-cell division (RND) family efflux pumps are frequently upregulated in clinical isolates, due to mutations in pump regulators. Cabot *et al.* (2011) found that clinical isolates from bloodstream samples were most likely to overexpress MexAB-OprM or MexXY, while Shigimura *et al*. (2015) found that isolates from UTIs were more likely to overexpress MexAB-OprM or MexCD-OprJ. Pump overexpression is likely to correlate with the antibiotic treatment of the patient.

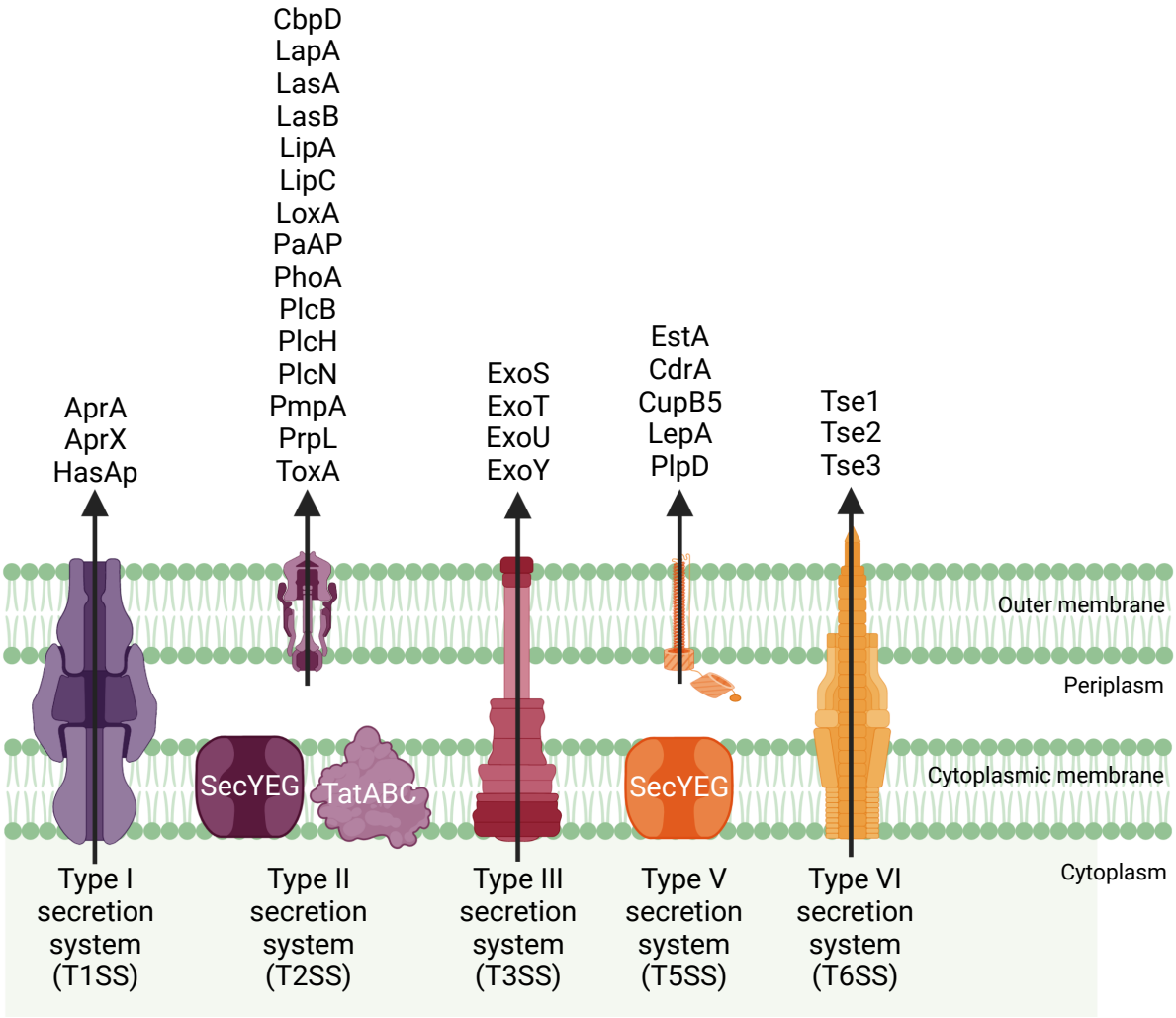
1.2 Transmembrane export

The Gram-negative cell envelope has three distinct layers: a cytoplasmic membrane, a peptidoglycan cell wall and an outer membrane which together form an effective barrier against environmental attack. The double membrane also prevents the passage of molecules including enzymes, proteins and toxins into the extracellular environment. To overcome this biological challenge, bacteria have evolved secretion systems and efflux pumps.

1.2.1 Secretion systems

Six families of secretion systems are conserved across Gram-negative bacteria, of which 5 have been identified in *P. aeruginosa.* The Type IV secretion system (T4SS) is the only secretion system which has not yet been described. These systems are diverse and differ in their ability to transport folded or unfolded proteins, across one or both membranes into the extracellular environment or directly into the cytosol of cells or competing bacteria. An overview of each secretion system is presented in **Figure 1.1**.

Figure 1.1: Secretion systems and associated substrates in *P. aeruginosa*. The Type I (T1SS), Type III (T3SS) and Type VI (T6SS) secretion systems transport substrates directly from the cytoplasm to the extracellular environment, while the Type II (T2SS) and Type V (T5SS) secretion systems only span the outer membrane. Proteins are translocated across the cytoplasmic membrane and into the periplasm through either the Sec or Tat pathways, where they can then be transported into the extracellular environment by the T2SS or T5SS as applicable. Image created using BioRender.



Two systems employ a two-step secretion mechanism, whereby the first step involves protein translocation across the cytoplasmic membrane and into the periplasm through either the Sec or Tat pathways. Substrates can then be transported across the outer membrane by the Type II (T2SS) or Type V (T5SS) secretion systems. The T2SS is mechanistically related to the Type IV pilus and three systems have been described in *P. aeruginosa* encoded by the *xcp*, *hxc* and *txc* (Cadoret *et al*., 2014) operons respectively. The Xcp system secretes virulence factors including LasA (Braun *et al*., 1998), LasB (Braun *et al*., 1998) and ToxA (Lu *et al*., 1993). The Type Va (T5aSS) secretion system encodes all the secretory information within a single polypeptide and is also known as an autotransporter. These systems transport unfolded proteins across the outer membrane to be folded in the extracellular space. The best characterised are EstA (Wilhelm *et al*., 1999) and PlpD (Salacha *et al*., 2010). *P. aeruginosa* is also predicted to encode five Type Vb (T5bSS) systems which differ from T5aSS as the β-barrel domain and the passenger domain are encoded by two separate polypeptides. LepA/LepB is the best characterised (Kida *et al*.,2008).

Other systems can transport substrates directly from the cytoplasm to the extracellular environment including Type I (T1SS), Type III (T3SS) and Type VI (T6SS) secretion systems. T1SSs are also known as ABC-transporters and are comprised of an ATP-binding cassette, an outer membrane protein and an inner membrane protein. Two T1SS have been described in *P. aeruginosa* to date: AprDEF exports AprA (Guzzo *et al*., 1991) and AprX (Duong *et al*., 2001), while HasDEF secretes the heme-acquisition protein HasAp (Létoffé *et al*., 1998). The Type III secretion system (T3SS) shares homology with the flagella and uses a needle-like projection to inject unfolded cytotoxins ExoS, ExoT, ExoU and ExoY directly into the host cell periplasm (Engel & Balachandran, 2009). The Type VI secretion system (T6SS) is another contact-dependent secretion system which resembles an inverted phage. The Hcp secretion island 1 (Hcp1) T6SS exports toxins Tse1, Tse2 and Tse3 which can degrade bacterial peptidoglycan and provide a competitive advantage during chronic infections (Hood *et al*., 2010).

1.2.2 Efflux pumps

Six major superfamilies of efflux pumps have been described in *P. aeruginosa*: the adenosine triphosphate (ATP)-binding cassette (ABC) family, the multidrug and toxic-compound extrusion (MATE) family, the major facilitator superfamily (MFS), the small multidrug resistance (SMR) family, the resistance-nodulation-cell division (RND) family and the recently described proteobacterial antimicrobial compound efflux (PACE) family.

All efflux pump families are found throughout Gram-positive and Gram-negative bacteria, except PACE and RND pumps which are unique to Gram-negative bacteria as they span the inner membrane and outer membranes to transport substrates directly from the cytoplasm to the periplasm. To enable ABC, MATE, MFS and SMR family pumps to export substrates across the double membrane, they form a complex with outer membrane components in Gram-negative bacteria, similar to the RND family. For example, the *P. aeruginosa* ABC family pump PvdRT-OpmQ includes the outer membrane component OmpQ to export the siderophore pyoverdine (Imperi *et al*., 2009).

Substrates are actively transported against a concentration gradient. The MFS, PACE, RND and SMR families are driven by proton motive force where the separation of protons (H^+) and hydroxide ions (OH^-) on either side of a membrane causes differences in pH and charge to generate a huge amount of potential energy. The MATE family employs a Na^+/H^+ antiport system where Na^+ ions are exchanged for H^+ ions, although an H^+-coupled MATE family pump designated PmpM has also been identified (He *et al.*, 2004). ABC pumps use ATP hydrolysis to transport substrates across the membrane where energy is generated through the conformational changes required for ATP binding and hydrolysis.

Efflux pumps have expansive substrate profiles including antibiotics, biocides, metabolites, dyes, and metal ions. For example, the RND pump CzcCBA exports heavy metal ions Zn^{2+}, and Cd^{2+} (Hassan *et al.,* 1999) while the PACE family pump PA2880 exports the disinfectant chlorhexidine diacetate (Zhao *et al.,* 2022). Several pumps have also been linked to antibiotic resistance including RND family pumps MexAB-OprM, MexCD-OprJ, MexEF-OprN and MexXY, and the SMR family pump EmrE which confers resistance to aminoglycosides (Li *et al.,* 2003).

1.2.2.1 RND efflux pumps

Chromosomally-encoded RND pumps are highly conserved between *P. aeruginosa* strains and 12 systems have been described: MexAB-OprM (Poole *et al*., 1993), MexCD-OprJ (Poole *et al*., 1996b), MexEF-OprN (Köhler *et al*., 1997), MexGHI-OpmD (Aendekerk *et al*., 2002), MexJK (Chuanchuen *et al*., 2002), MexMN (Mima *et al*., 2005), MexPQ-OpmE (Mima *et al*., 2005), MexVW (Li *et al*., 2003), MexXY (Mine *et al*., 1999), MuxABC-OpmB (Mima *et al*., 2009), TriABC (Mima *et al*., 2007), and CzcCBA (Hassan *et al*., 1999) (**Figure 1.2**). All of these efflux systems are broadly conserved throughout the *Pseudomonas* genus, with the exception of MexXY which is unique to *P. aeruginosa* (Henderson *et al*., 2021).

Multiple sequence alignment of the RND transport proteins of Gram-negative bacteria shows that *P. aeruginosa* RND proteins are split into two distinct clades highlighted in purple (**Figure 1.3**). with MexB, MexD, MexF, MexI, MexK, MexN and MexQ most similar to RND proteins found in *Vibrio parahaemolyticus* while MexW, MexY, CzcA, MuxB, MuxC and TriC are more similar to the AdeB and AdeJ transporters of *Acinetobacter baumannii*. MexB shares 69% sequence similarity with the prototypical RND transporter AcrB from *E. coli*.

Figure 1.2: RND efflux pumps in *P. aeruginosa*. RND pumps are characterised by a tripartite structure which spans the inner and outer membranes to transport substrates directly from the cytoplasm to the extracellular environment. MexGHI-OpmD and TriABC each encode a second periplasmic adapter proteins (PAP), while MuxABC-OpmB encodes a second RND family transport proteins (RND). RNDs are shown in purple, PAPs are shown in pink and outer membrane proteins (OMP) are shown in yellow. Image created using BioRender.

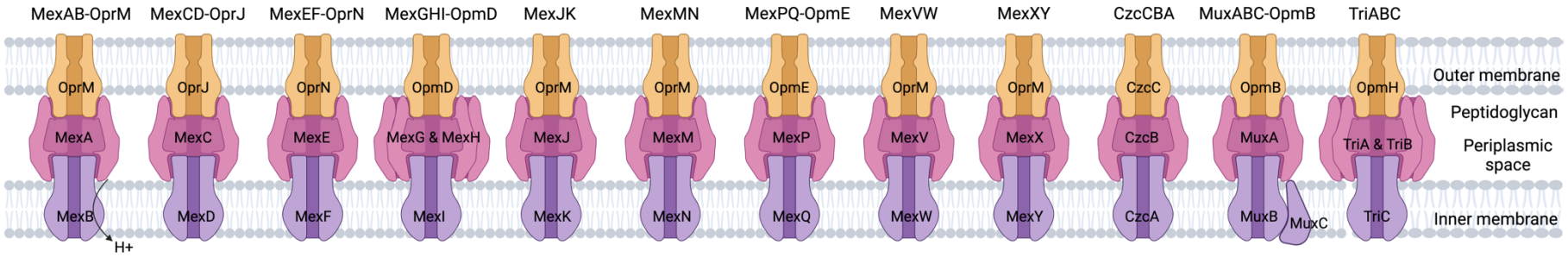
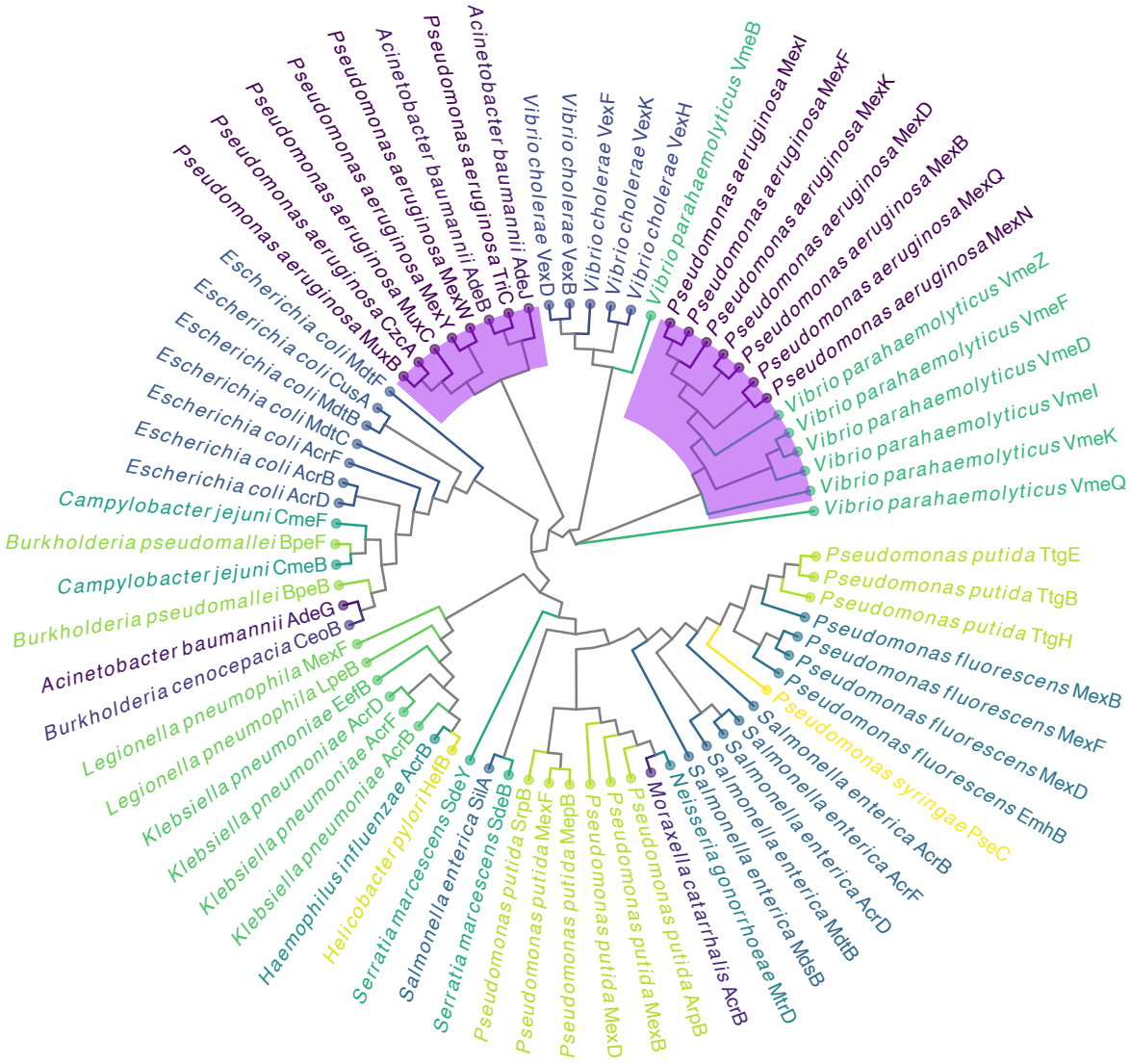


Figure 1.3: Multiple sequence alignment of major Gram-negative RND transporter protein sequences. Amino acid sequences were downloaded from GenBank using the R package [Rentrez] (Winter, 2017) and multiple sequence alignment was performed using [ape] (Paradis & Schliep, 2019). Pairwise distances from the aligned sequences were calculated using [seqinr] (Sharif & Lobry, 2007) and displayed as a phylogenetic tree using [ggTree] (Yu *et al*., 2017). The two distinct clades of *P. aeruginosa* RND transporters are highlighted in purple. The GenBank accession numbers of the protein sequences used are detailed in **Appendix A**.



1.2.2.1.1 Structure

RND pumps are characterised by a tripartite structure comprising an inner membrane-bound RND family transport protein (RND) to bind substrates and transport them across the cytoplasmic membrane, an outer membrane protein (OMP) to form a duct to allow the substrate to cross the outer membrane and prevent a return to the cytosol, and a periplasmic adapter protein (PAP) to bind the aforementioned proteins together. The chromosomal arrangements of the 12 RND systems in *P. aeruginosa* PAO1-UW are visualised in **Figure 1.4** and the coding regions are provided in **Table 1.2**.

Much of our structural and functional knowledge of RND efflux pumps comes from the extensive characterization of the AcrAB-TolC system of *E. coli* and *Salmonella enterica* serovar Typhimurium, though bound (Sennhauser *et al*., 2009) and whole (Tsutsumi *et al*., 2019) crystal structures of MexAB-OprM have also been resolved. The functional pump assembles as a trimeric RND, a trimeric OMP and a hexameric PAP (Yum *et al*., 2009; Xu *et al*., 2012).

AcrB is an RND protein which exports substrates by rotating through three distinct conformations known as Access (A), bound (B) and extrusion (E) (Murakami *et al*., 2006). The transition between the three states is powered by the entry of a hydrogen ion each time (ie. proton motive force). During the A stage, the monomer is open to acquiring a substrate. When a substrate enters the monomer rotates to the B conformation where the substrate cannot flow back into the cell. The system then rotates to the E conformation where the substrate is transported in a one-directional way through the OMP and released into the extracellular environment (Murakami *et al*., 2006).

Each protomer within the asymmetric trimer of an RND transporter has three domains: the transmembrane (TMD) domain located in the inner membrane converts chemical energy to mechanical energy, the pore domain (PD) located in the periplasm recruits and transports substrates, and the funnel domain (FD) connects the RND protein to the OMP (Tsutsumi *et al*., 2019). Unusually for an RND pump, MuxABC-OpmB encodes a second RND transporter, the function of which is unknown.

Figure 1.4 Genomic arrangement of *P. aeruginosa* PAO1-UW RND efflux pumps. Arrows indicate known promoter binding regions. Figure created using the R package [gggenes].

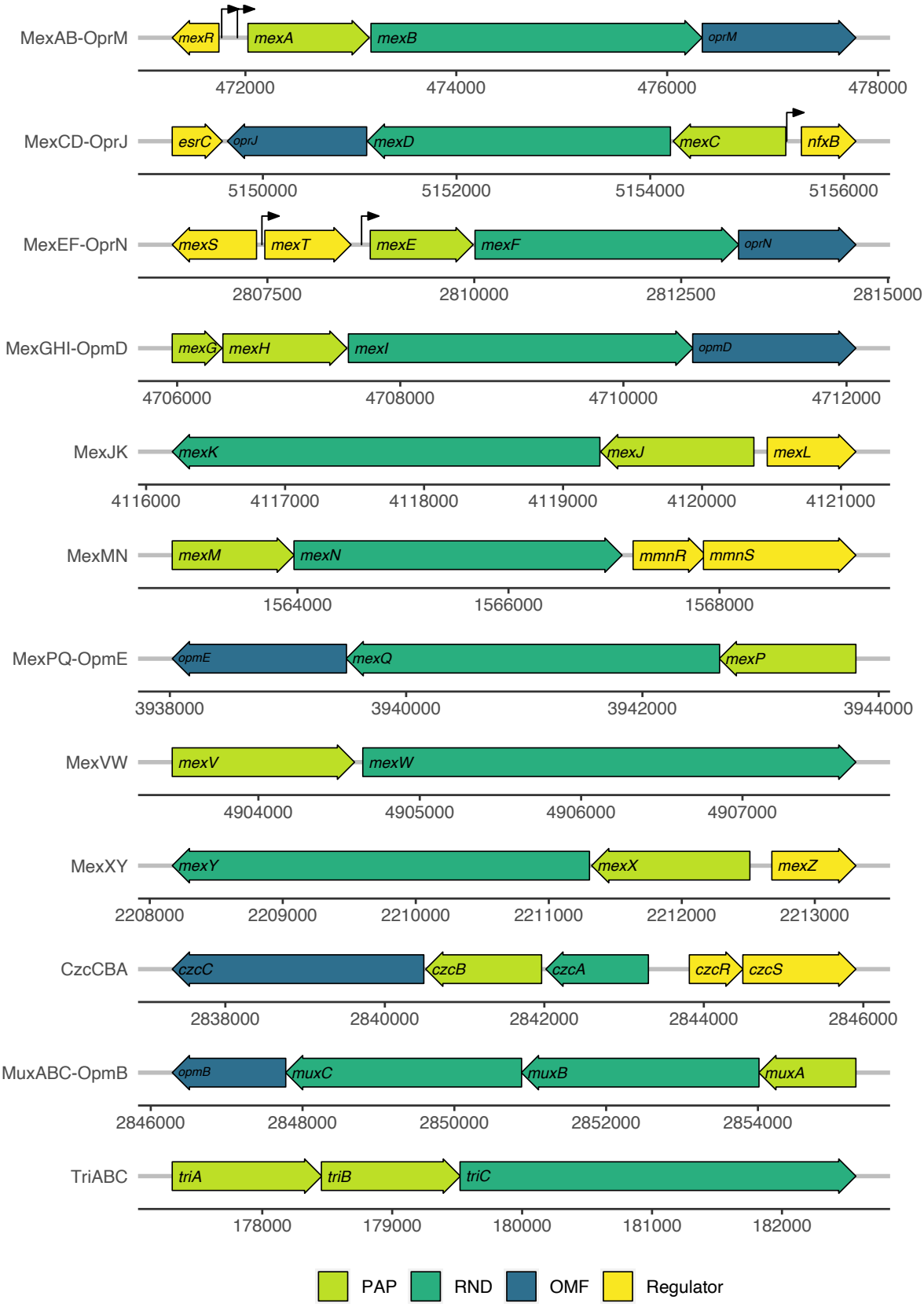


Table 1.2: *P. aeruginosa* PAO1-UW RND efflux pump coding regions

Efflux pump	Gene	Locus Tag	Start*	End*	Strand direction	Function**
MexAB-OprM	*mexA*	PA0425	472024	473175	forward	PAP
	mexB	PA0426	473191	476331	forward	RND
	oprM	PA0427	476333	477790	forward	OMP
	mexR	PA0424	471306	471749	reverse	Local regulator
MexCD-OprJ	*mexC*	PA4599	5154237	5155400	reverse	PAP
	mexD	PA4598	5151078	5154209	reverse	RND
	oprJ	PA4597	5149633	5151072	reverse	OMP
	nfxB	PA4600	5155561	5156124	forward	Local regulator
	esrC	PA4596	5149064	5149582	forward	Local regulator
MexEF-OprN	*mexE*	PA2493	2808743	2809987	forward	PAP
	mexF	PA2494	2810009	2813197	forward	RND
	oprN	PA2495	2813194	2814612	forward	OMP
	mexS	PA2491	2806350	2807369	reverse	Local regulator
	mexT	PA2492	2807469	2808512	forward	Local regulator
MexXY	*mexX*	PA2019	2211322	2212512	reverse	PAP
	mexY	PA2018	2208169	2211306	reverse	RND
	mexZ	PA2020	2212677	2213309	forward	Local regulator
MexGHI-OpmD	*mexG*	PA4205	4705956	4706402	forward	PAP
	mexH	PA4206	4706410	4707522	forward	PAP
	mexI	PA4207	4707535	4710624	forward	RND
	opmD	PA4208	4710621	4712084	forward	OMP
MexJK	*mexJ*	PA3677	4119270	4120373	reverse	PAP
	mexK	PA3676	4116188	4119265	reverse	RND
	mexL	PA3678	4120469	4121107	forward	Local regulator

MexMN	*mexM*	PA1435	1562813	1563970	forward	PAP
	mexN	PA1436	1563967	1567077	forward	RND
	mmnR	PA1437	1567181	1567870	forward	Local regulator
	mmnS	PA1438	1567848	1569293	forward	Local regulator
MexPQ-OpmE	*mexP*	PA3523	3942650	3943807	reverse	PAP
	mexQ	PA3522	3939492	3942653	reverse	RND
	opmE	PA3521	3938020	3939495	reverse	OMP
MexVW	*mexV*	PA4374	4903466	4904596	forward	PAP
	mexW	PA4375	4904647	4907703	forward	RND
CzcCBA	*czcB*	PA2521	2840512	2841966	reverse	PAP
	czcC	PA2522	2837334	2840489	reverse	OMF
	czcA	PA2520	2842019	2843305	reverse	RND
	czcR	PA2523	2843818	2844492	forward	Local regulator
	czcS	PA2524	2844489	2845907	forward	Local regulator
MuxABC-OpmB	*muxA*	PA2528	2854011	2855291	reverse	PAP
	muxB	PA2527	2850883	2854014	reverse	RND
	muxC	PA2526	2847776	2850886	reverse	RND
	opmB	PA2525	2846283	2847779	reverse	OMP
TriABC	*triA*	PA0156	177307	178458	forward	PAP
	triB	PA0157	178455	179525	forward	PAP
	triC	PA0158	179522	182569	forward	RND

* The start and end coordinates for each gene were obtained from www.pseudomonas.com and correspond to the sequence of PAO1-UW (Stover *et al*., 2000)

** PAP denotes periplasmic adapter protein; RND denotes RND protein; OMP signifies outer membrane protein

The OMP has a coiled-coil domain, an equatorial domain and an α-barrel domain located in the periplasm, and a β-barrel domain which spans the inner and outer membranes. In contrast to TolC, the OprM monomers do not exhibit three-fold symmetry (Phan *et al.,* 2010). Of the 12 RND pumps, seven operons encode an OMP: MexAB-OprM, MexCD-OprJ, MexEF-OprN, MexGHI-OpmD, MexPQ-OpmE, CzcCBA and MuxABC-OpmB. Complete assembly of the other pumps requires a divergent OMP that is normally OprM.

Each PAP monomer exhibits a "hairpin-like" topology which is comprised of a membrane-proximal domain (MPD), β-barrel domain, lipoyl domain, and α-hairpin domain joined by flexible linkers (Xu *et al*., 2012). MexGHI-OpmD and TriABC each encode two PAP genes: *mexG* and *mexH*, and *triA* and *triB* respectively. Weeks *et al*., (2015) found TriAB functioned as an asymmetric dimer, with TriA stabilising interactions with the OMP and TriB stimulating the RND transporter.

1.2.2.1.2 Substrates

RND systems export a range of structurally diverse compounds including those which are lipophilic (e.g. macrolides), anionic (e.g. β-lactams), cationic (e.g. aminoglycosides) and neutral (e.g. chloramphenicol). The substrate profile of each pump is summarised in **Table 1.3**. They export a diverse range of substrates due to the presence of two distinct binding pockets: the proximal binding pocket (PBP) binds high molecular weight substrates and the distal binding pocket (DBP) binds low molecular weight substrates (Nakashima *et al*., 2013). In *S.* Typhimurium, the MPD of the PAP AcrA impacts substrate preference and selection (McNeil *et al*., 2019; Alev *et al*., 2022) and is likely to have a similar gatekeeping role in *P. aeruginosa*.

Many efflux pumps have overlapping substrate profiles. For example, almost all pumps can export fluoroquinolones and five efflux pumps can efflux the biocide triclosan: MexAB-OprM, MexCD-OprJ, MexEF-OprN, MexJK and TriABC. Other substrates are only exported by a specific pump such as CzcCBA which is the only pump able to export trace metals (Hassan *et al*., 1999). Aminoglycosides are mainly exported by MexXY, however, MexAB-OprM expression has also been shown to increase in the presence of paromomycin (Fruci & Poole, 2018).

Table 1.3 Substrate profiles of the *P. aeruginosa* RND efflux pumps

Efflux pump	Substrates	References
MexAB-OprM	Aminoglycosides, β-lactams, chloramphenicol, colistin, ethidium bromide, fluroquinolones, macrolides, SDS, sulfonamides, tetracycline, trimethoprim, triclosan	Li *et al*., 1995; Masuda *et al*., 2000
MexCD-OprJ	β-lactams, chloramphenicol, chlorhexidine, colistin, fluroquinolones, HHQ, kynurenine, macrolides, quaternary ammonium compounds, tetracyclines, trimethoprim, triclosan	Masuda *et al*., 2000; Alcalde-Rico *et al*., 2018
MexEF-OprN	Chloramphenicol, fluoroquinolones, HHQ, kynurenine, tetracycline, trimethoprim, triclosan	Köhler *et al*., 1997; Lamarche and Déziel, 2011; Olivares *et al*., 2012
MexGHI-OpmD	5-Me-PCA, acriflavine, ethidium bromide, fluroquinolones, tetracycline	Sekiya *et al.,* 2003; Aendekerk *et al*., 2005; Sakhtah *et al*., 2016
MexJK	Erythromycin, tetracycline, triclosan	Chuanchuen *et al*., 2002
MexMN	Chloramphenicol	Mima *et al*., 2005
MexPQ-OpmE	Fluroquinolones, macrolides, phenoxyethanol	Mima *et al*., 2005; Green *et al*., 2018
MexVW	Acriflavine, chloramphenicol, ethidium bromide, erythromycin, fluroquinolones, tetracycline	Li *et al*., 2003
MexXY	Aminoglycosides, β-lactams, chloramphenicol, fluroquinolones, macrolides, tetracycline, tigecycline	Masuda *et al*., 2000
CzcCBA	β-lactams, trace metal ions (Cd^{2+}, Zn^{2+})	Hassan *et al*., 1999; Perron *et al*., 2004
MuxABC-OpmB	Aztreonam, erythromycin, fluroquinolones, novobiocin, tetracycline	Mima *et al*., 2009
TriABC	Nile Red, SDS, triclosan	Mima *et al*., 2007; Weeks *et al*., 2015

In addition to antimicrobial compounds, several pumps have been linked to metabolite export. MexCD-OprJ and MexEF-OprN export kynurenine, which is produced from tryptophan catabolism and used for the production of anthranilate (Olivares *et al*., 2012; Alcalde-Rico *et al*., 2018), although MexEF-OprN has a higher affinity for this substrate than MexCD-OprJ (Olivares *et al*., 2012). MexCD-OprJ and MexEF-OprN have been shown to export HHQ from the cell (Lamarche and Déziel, 2011; Alcalde-Rico *et al*., 2018), though MexCD-OprJ overexpressing strains produce higher amounts of HHQ than MexEF-OprN overexpressing strains leading to reduced production of PQS Alcalde-Rico *et al*., 2018). MexGHI-OpmD has also been shown to export the pyocyanin precursor molecule 5-methylphenazine-1-carboxylate (5-Me-PCA) (Sakhtah *et al*., 2016).

1.2.2.1.3 Expression

As the *P. aeruginosa* genome encodes multiple efflux pumps, expression is tightly regulated to avoid issues with membrane structure and solidity. Most pumps are silent or weakly expressed under laboratory conditions and upregulated in response to stress given that efflux pumps are energy intensive; not only in terms of the energy required to create the proteins but also for the proton motive force used as an energy source. The expression state of each efflux pump is provided in **Table 1.4**.

MexAB-OprM, and to a lesser extent MexJK, MexVW, MexXY and MuxABC-OpmB are constitutively expressed in BHI, LB and M9 media (Yang *et al*., 2011) contributing to the intrinsic resistance of several antibiotic classes including β-lactams and β-lactamase inhibitors, fluoroquinolones, chloramphenicol and macrolides. MexGHI-OpmD, MexMN and MexPQ-OpmE are weakly expressed in LB, though the expression of MexGHI-OpmD increases in a rich medium (ie. BHI), while the expression of MexMN and MexPQ-OpmE increases in a nutrient limited medium (ie. M9) (Yang *et al*., 2011). Each of these pumps displays a similar expression profile in LB and M9, with low expression during lag phase and much higher expression during exponential and stationary phases of growth. In BHI, expression tends to decrease in exponential phase (Yang *et al*., 2011).

Table 1.4 Expression of *P. aeruginosa* RND family efflux pumps

Efflux pump	Expression state	Inducible expression	Hyper expression	Reference
MexAB-OprM	High	Oxidative stress, autoinducers (HSL's)	Mutations in MexR (*nalB* phenotype)	Yang *et al*., 2011; Chen *et al*., 2008
MexCD-OprJ	None	Envelope stress	Mutations in NfxB (*nfxB* phenotype)	Yang *et al*., 2011; Morita *et al.*, 2003; Fraud *et al.*, 2008
MexEF-OprN	None	Nitrosative stress, chloramphenicol	Mutations in MexT (*nfxC* phenotype)	Yang *et al*., 2011; Fetar *et al*., 2011
MexGHI-OpmD	Low	ND	ND	Chuanchuen *et al*., 2002; Yang *et al*., 2011
MexJK	Medium	ND	Mutations in MexL	Yang *et al*., 2011; Amieva *et al*., 2022
MexMN	Low	Cu^{+}	ND	Mima *et al*., 2005; Teitzel *et al*.,2006; Yang *et al*., 2011
MexPQ-OpmE	Low	Cu^{+}, Phenoxyethanol	ND	Mima *et al*., 2005; Teitzel *et al*.,2006; Yang *et al*., 2011; Green *et al*., 2018
MexVW	Medium	ND	ND	Yang *et al*., 2011
MexXY	Medium	Oxidative stress, ribosome-targeting antibiotics	Mutations in MexZ	Yang *et al*., 2011; Fraud & Poole, 2011; Morita *et al*., 2006; Morita *et al*., 2009;
CzcCBA	None	Cd^{2+}, Cu^{+}, Zn^{2+}	ND	Perron *et al*., 2004; Teitzel *et al*.,2006; Yang *et al*., 2011
MuxABC-OpmB	Medium	ND	ND	Yang *et al*., 2011
TriABC	None	Triclosan	ND	Mima *et al*., 2007; Yang *et al*., 2011

The expression of MexCD-OprJ, MexEF-OprN, CzcCBA and TriABC is strictly repressed in wild-type strains (Poole *et al*., 1996b; Köhler *et al*., 1997; Yang *et al*., 2011), and these pumps are only associated with antibiotic resistance following mutations in pump regulators which result in the hyper-expression of these pumps.

Some RND efflux pumps can be induced in response to environmental signals or an increased intracellular concentration of toxic substances. These inducer molecules bind to either positive transcriptional regulators or their negative regulators. The expression of MexCD-OprJ can be induced in the presence of membrane stress from compounds including benzalkonium chloride and ethidium bromide (Morita *et al*., 2003), whilst expression of MexXY can also be induced in response to envelope stress and aminoglycosides (Lau *et al*., 2015). The CzcCBA efflux pump is expressed in the presence of heavy metal substrates zinc, cadmium and cobalt (Perron *et al*., 2004; Ducret *et al*., 2020), while pyocyanin has been shown to activate the transcription factor SoxR to induce the expression of MexGHI-OpmD (Dietrich *et al*., 2006).

In clinical isolates, MexA-OprM and MexXY are commonly overexpressed though MexCD-OprJ and MexEF-OprN overexpression has also been reported (Yoneda *et al.,* 2005; Quale *et al.*, 2006; Xavier *et al.,* 2010; Rahbar *et al.,* 2021). It is also common to see increased expression of two or more efflux pumps, particularly MexAB-OprM and MexXY (Rahbar *et al.,* 2021).

1.2.2.1.4 Regulation

RND efflux pumps are regulated by a range of local and global transcriptional regulators (**Table 1.5**). Local transcriptional regulators are normally located adjacent to the efflux pump operon and fine-tune gene expression in response to external signals giving rise to acquired resistance. While global regulators play an important role in intrinsic resistance and regulate many cell processes including efflux pump expression (Hernando-Amado *et al*., 2016). Mutations in transcriptional regulators give rise to varying degrees of antimicrobial resistance. Many MDR clinical strains contain mutations in pump regulators *mexR*, *nfxB* or *mexZ* leading to the overexpression of the MexAB-OprM, MexCD-OprJ or MexXY efflux pumps respectively.

Table 1.5 Transcriptional regulators of *P. aeruginosa* RND family efflux pumps

Efflux pump	Locus Tag	Gene	Family	Description	Reference
MexAB-OprM	PA0424	*mexR*	MarR-type transcriptional regulator	Negative regulation of MexAB-OprM	Poole *et al*., 1996a
	PA2492	*mexT*	LysR-type transcriptional regulator	Negative regulation of MexAB-OprM	Maseda *et al*., 2004
	PA3045	*rocA2*	Two-component response regulator	Negative regulation of MexAB-OprM	Sivaneson *et al*., 2011
	PA3204	*cpxR*	CpxRA two-component response regulator	Positive regulation of MexAB-OprM	Tian *et al*., 2016
	PA3225	-	LysR-type transcriptional regulator	Negative regulation of MexAB-OprM	Hall *et al*., 2017
	PA3574	*nalD*	TetR-type transcriptional regulator	Negative regulation of MexAB-OprM	Sobel *et al*., 2005a; Chen *et al*., 2016
	PA3719	*armR*	ND	Antirepressor of MexR	Daigle *et al*., 2007
	PA3721	*nalC*	TetR-type transcriptional regulator	Negative regulation of ArmR	Cao *et al*., 2004
	PA3898	*mdrR1*	ND	Negative regulation of MexAB-OprM	Heacock-Kang *et al*., 2018
	PA4109	*ampR*	LysR-type transcriptional regulator	Negative regulation of MexR	Balasubramanian *et al*., 2012
	PA4878	*brlR*	MerR-type transcriptional regulator	Positive regulation of MexAB-OprM	Liao *et al*., 2013
MexCD-OprJ	PA4596	*esrC*	AraC-type transcriptional regulator	Negative regulation of MexCD-OprJ	Purssell et al., 2015
	PA4600	*nfxB*	LacI/GalR-type transcriptional regulator	Negative regulation of MexCD-OprJ	Shiba *et al*., 1995
MexEF-OprN	PA1431	*rsaL*	ND	Positive regulation of MexEF-OprN	Rampioni *et al*., 2009

	PA1799	*parR*	ParRS-two-component response regulator	Positive regulation of MexS	Wang *et al*., 2013
	PA2449	-	TyrR-type transcriptional regulator	Negative regulation of MexEF-OprN	Lundgren *et al*., 2013
	PA2491	*mexS*	Probable oxidoreductase	Negative regulation of MexEF-OprN	Sobel *et al*., 2005b
	PA2492	*mexT*	LysR-type transcriptional regulator	Positive regulation of MexS and MexEF-OprN	Köhler *et al*., 1999; Tian *et al*., 2009a
	PA3271	*mxtR*	Two-component response regulator	Negative regulation of MexEF-OprN	Zaoui *et al*., 2012
	PA4109	*ampR*	LysR-type transcriptional regulator	Negative regulation of MexEF-OprN	Balasubramanian *et al*., 2012
	PA4203	*nmoR*	LysR-type transcriptional regulator	Positive regulation of MexEF-OprN	Vercammen *et al*., 2015
	PA4315	*mvaT*	ND	Negative regulation of MexEF-OprN	Westfall *et al*., 2006
	PA4878	*brlR*	MerR-type transcriptional regulator	Positive regulation of MexEF-OprN	Liao *et al*., 2013
MexGHI-OpmD	PA1431	*rsaL*	ND	Negative regulation of MexGHI-OpmD	Rampioni *et al*., 2009
	PA2273	*soxR*	MerR-type transcriptional regulator	Positive regulation of MexGHI-OpmD	Palma *et al*., 2005
	PA4209	*phzM*	*N*-methyltransferase	Positive regulation of MexGHI-OpmD	Sakhtah *et al*., 2016
MexJK	PA3678	*mexL*	TetR-type transcriptional regulator	Negative regulation of MexJK	Chuanchuen *et al*., 2005
MexMN	PA1438	*mmnS*	MmnRS two-component sensor kinase	Negative regulation of MexMN	Ranjitkar *et al*., 2019
MexPQ-OpmE	PA4778	*cueR*	MerR-type transcriptional regulator	Positive regulation of MexPQ-OpmE	Thaden *et al*., 2010

MexVW	ND	ND	ND	ND	ND
MexXY	PA1799	*parR*	ParRS two-component response regulator	Positive regulation of MexXY	Muller *et al*., 2013
	PA2020	*mexZ*	TetR-type transcriptional regulator	Negative regulation of MexXY	Matsuo *et al.,* 2006
	PA5200	*amgR*	ND	Aminoglycoside-dependent regulation of MexXY	Lau *et al*., 2015
	PA5471	*armZ*	RtcB family of RNA-splicing ligases	Anti-repressor of *mexZ*	Morita *et al*., 2006
CzcCBA	PA2523	*czcR*	Two-component response regulator	Positive regulation of CzcCBA	Perron *et al*., 2004
	PA2809	*copR*	Two-component response regulator	Positive regulation of CzcCBA	Caille *et al*., 2007
MuxABC-OpmB	PA3204	*cpxR*	CpxRA two-component response regulator	Positive regulation of MuxABC-OpmB	Tian *et al*., 2016
TriABC	NA	*pcaR-triA* intergenic region	ND	Positive regulation of TriABC	Mima *et al*., 2007

Transcriptional regulators can be broadly divided into one-component and two-component systems which contain their sensory and output functions on either a single or multiple polypeptides. If the binding of the transcriptional regulator is required for transcription to begin then the regulatory protein is known as an activator and the operon is said to be positively regulated, whereas if binding inhibits transcription then the regulatory protein is known as a repressor and the operon is said to be negatively regulated.

There are at least 20 different families of one-component regulatory systems named after the first characterised member of each family. Many of these regulate efflux pumps in *P. aeruginosa*. The largest family are the LysR-type transcriptional regulators (LTTR) which function as both activators and repressors. Examples include MexT, which positively regulates the expression of both MexS and the MexEF-OprN efflux pump (Köhler *et al*., 1999) and AmpR which negatively regulates the expression of MexR and MexEF-OprN (Balasubramanian *et al*., 2012). The TetR-family of transcriptional regulators (TFTR) is characterised by an N-terminal DNA-binding domain and functions as a dimer (Cuthbertson & Nodwell, 2013). Type I TFTR's regulate divergent genes, such as *mexL* which regulates the expression of the *mexJK* operon (Chuanchuen *et al*., 2005) while type III TFTRs regulate distant genes such as *nalD*, which binds to the proximal promoter of the *mexAB-oprM* operon (Sobel *et al*., 2005a). The *mexAB-oprM* operon also has a distal promoter which is modulated by the local repressor *mexR* (Poole *et al*., 1996a), a MarR family transcriptional regulator. The MerR family have an N-terminal DNA-binding domain and typically function as transcriptional repressors, though *brlR* has been shown to activate the expression of both MexAB-OprM and MexEF-OprN (Liao *et al*., 2013).

Other RND pumps fall under the regulation of two-component regulatory systems (TCS) including CzcRS which regulates the expression of the CzcCBA efflux pump (Perron *et al*., 2004) and ParRS which regulates the expression of MexEF-OprN (Wang *et al*., 2013). TCS are discussed in more detail in **Section 1.3.1**.

1.2.2.1.5 Lifestyle

In addition to their role in antimicrobial resistance, RND efflux pumps also contribute to the survival of Gram-negative bacteria in host environments in several key ways. Firstly, they enable adaptation to changes in the host environment by pumping out toxic compounds so bacteria can survive in environments that would otherwise be inhospitable. Many efflux systems export heavy metals: CusCFBA exports Cu^{2+} and Ag^{+} in *E. coli* (Franke *et al*., 2003), GesCBA exports Au^{+} in *S. enterica* (Pontel *et al*., 2007), and CzcCBA exports $Cd^{2+}$and Zn^{2+} in *P. aeruginosa* (Hassan *et al*., 1999). Others, such as SprABC in *P. putida* (Yao *et al*., 2017) and MexAB-OprM, MexCD-OprJ and MexEF-OprN in *P. aeruginosa* (Li *et al*., 1998) export aromatic hydrocarbons which would otherwise alter membrane fluidity and disrupt essential downstream processes.

The RND family also play a role in homeostasis by regulating the intracellular concentration of certain compounds such as pH, salts and primary metabolites. Acid stress has been shown to induce the TolC outer membrane channel TolC in *E. coli* (Yohannes *et al.,* 2004) suggesting that EmrAB-TolC and MdtAB-TolC are important for acid adaptation (Deininger *et al*., 2011). Primary metabolites are used as energy sources and building blocks for macromolecules, and TolC has also been implicated in the efflux of the amino acid L-cysteine (Wiriyathanawudhiwong *et al*., 2009). Recently, a metabolomic study revealed a new role for AcrB in *Escherichia coli* and *S.* Typhimurium in fatty acid export (Wang-Kan *et al.,* 2021).

RND efflux pumps can also provide protection from host defence mechanisms including antimicrobial peptides and reactive oxygen species (ROS) such as hydrogen peroxide (H_2O_2) and hydroxyl radicals ($HO^{\bullet}$). Antimicrobial peptides can cause membrane disruption and induce stress responses while ROS react with nucleic acids, proteins and lipids to damage cells. By removing these compounds, the bacteria can evade the host's immune response and establish an infection. Examples include MtrCDE in *N. meningitidis* which confers resistance to cationic antimicrobial peptides (Tzeng *et al*., 2005) and MexXY in *P. aeruginosa*, which is induced by oxidative stress leading to increased aminoglycoside resistance (Fraud & Poole, 2011). In addition to evading host mechanisms, they can also modulate the expression of genes involved in virulence. These changes are discussed further in **Section 1.4.7**.

RND pumps can also contribute to the survival in host environments by modulating quorum sensing, a process by which bacteria can sense their population density and coordinate the expression of genes involved in virulence and antibiotic resistance. The contribution of RND efflux pumps to quorum sensing are discussed in more detail in **Section 1.3.2.4**. In *E. coli*, AcrA has recently been associated with another cell-to-cell signalling phenomenon known as necrosignalling. The AcrA protein is released by killed cells within a swarming population following antibiotic-induced cell death, and then interacts with the TolC protein on the surface of live cells to stimulate drug efflux (Bhattacharyya *et al*., 2020).

Finally, RND pumps can also contribute to the formation of biofilms by helping the bacteria to pump out molecules that inhibit biofilm formation, or by pumping out molecules that promote it. These changes are discussed in more detail in **Section 1.5.3**.

1.2.2.1.6 Efflux pump inhibitors as a target to reduce antimicrobial resistance

Efflux pump inhibitors (EPIs) can potentiate the activity of antibiotics which are actively effluxed from the cell, increasing the susceptibility of previously resistant strains. The first EPI to be described was the peptidomimetic molecule phenylalanine-arginine-β-naphthylamide (PAβN) (Renau *et al*., 1999). This dipeptide amide competitively inhibits the active site of multiple RND efflux pumps to increase susceptibility to antibiotic classes including fluoroquinolones and β-lactams (Lamers *et al*., 2013). Alternatively, efflux pumps can be inactivated through the removal of the pumps' energy source such as carbonyl cyanide 3-chlorophenylhydrazone (CCCP), which disrupts the membrane proton gradient by uncoupling oxidative phosphorylation (Heytler, 1963).

Several EPIs have been shown to inhibit MexAB-OprM, MexCD-OprJ and MexEF-OprN (Lomovskaya *et al*., 2001; Watkins *et al*., 2003; Aparna *et al*., 2014; Marshall *et al*., 2020; Yuan *et al*., 2021; Zhang *et al*., 2022) and computational modelling has provided insight into the shared properties of EPIs. Mehla *et al*. (2021) found EPIs interact with Leu674 of MexB while compounds which evade efflux have more interactions with residue Pro668. However, despite these advances no EPIs have been approved for clinical use due to toxicity.

1.3 Gene regulation

The number of genes shared between *P. aeruginosa* strains is known as the core genome and represents only ~ 1% of the total genes (Freschi *et al*., 2019). PAO1-UW has a large genome of approximately 6.3 Mbp (Stover *et al*., 2000) encoding 5,570 genes, of which 690 are regulatory genes (12% of total genes). The virulence regulatory network is complex and includes two-component systems and quorum sensing genes that control secondary metabolism, biofilm formation and other important biological processes.

1.3.1 Two-component systems

Two-component systems (TCS) are typically comprised of a sensor kinase (SK) and a response regulator (RR). The membrane-bound SK or histidine kinase (HK) contains an input domain for signal recognition and a transmitter domain that auto-phosphorylates at a histidine residue upon stimulus detection. The phosphate group is then transferred to an aspartate group in the cytoplasmic RR, activating the DNA-binding sites of the RR to modulate gene expression (**Figure 1.5**).

The *P. aeruginosa* genome encodes 64 SKs and 72 RRs (Rodrigue *et al*., 2000; Stover *et al*., 2000), many of which have been linked to virulence (**Table 1.6**). For example, the GacA/GacS TCS plays a key role in the transition from acute to chronic infections. The SK is encoded by *gacS* and the RR is encoded by *gacA,* which activates the transcription of small RNAs (sRNA) RsmY and RsmZ (Brencic *et al*., 2009). The sRNAs bind to sRNA-binding proteins RsmA (Pessi *et al*., 2001) and RsmN (Morris *et al*., 2013) which regulate the expression of genes involved in T6SS, biofilm formation and pyocyanin production.

Many TCS are implicated in biofilm formation. Cup fimbriae are required for attachment during the initial stages of biofilm formation. CupB and CupC fimbriae are regulated by the Roc network comprising the RocS1 SK, the RocA1 RR and RocR which antagonises RocA1 activity (Kulasekara *et al*., 2005), while CupD fimbriae in PA14 are regulated by PvrS/PvrR and RcsC/RcsB (Mikkelsen *et al*., 2009). Other important TCSs include BfiS/BfiR (Petrova & Sauer, 2009) which regulates the transition to the irreversible-attachment phase, BfmS/BfmS which regulates the transition to maturation 1 stage and MifS/MifS which regulates the transition to maturation 2 stage (Petrova & Sauer, 2009).

Figure 1.5: Two Component Systems in *P. aeruginosa* A) In the classical system the input domain of the histidine kinase (HK) receives the signal and triggers autophosphorylation of a conserved histidine residue in the transmitter domain. The phosphate groups transfers to a conserved aspartate residue known as the receiver domain of the response regulator (RR), triggering DNA-binding sites to promote gene expression B) The unorthodox system contains a second receiver domain and a Hpt domain C) The hybrid system lacks an extended carboxy-terminus in the receiver domain of the RR. Taken from Rodrigue *et al*., (2000).

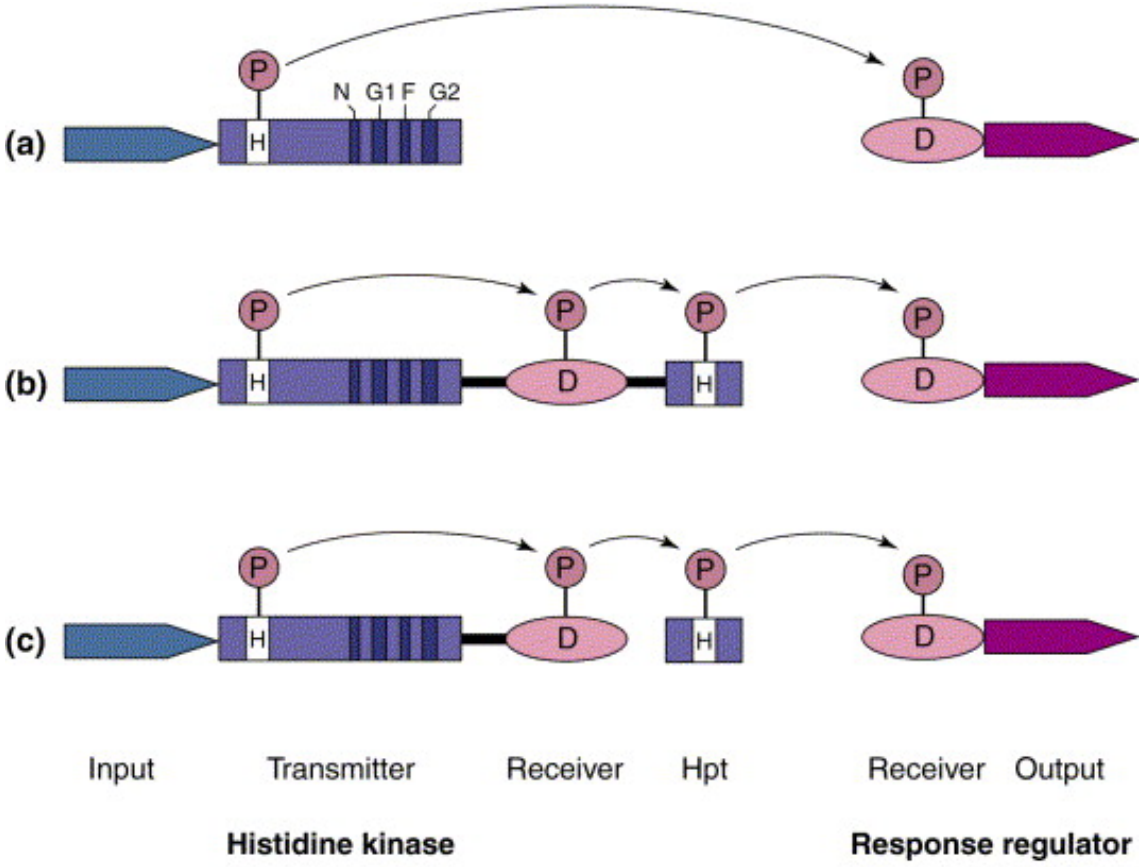


Table 1.6: Two-Component Systems (TCS) regulating virulence and/or biofilm development in *P. aeruginosa*

Sensor kinase	Response regulator	Regulation	Reference
BfiS	BfiR	Biofilm formation; transition to irreversible-attachment phase	Petrova & Sauer, 2009
BfmS	BfmR	Biofilm formation; transition to maturation 1 stage	Petrova & Sauer, 2009
BqsS	BqsR	Biofilm formation; dispersal	Dong *et al*., 2008
CarS	CarR	Biofilm formation; rhamnolipids	Guragain et al., 2016
CbrA	CbrB	Cytotoxins; ExoS and ExoT	Yeung *et al*., 2011
CheA	CheB, CheY	Chemotaxis	Kato *et al*., 1999
ChpA	PilG	Motility; TFP	Bertrand *et al*., 2010
CreC	CreB	Swarming motility	Little *et al*., 2018
FimS	AlgR	Biofilm formation; alginate production, Motility; TFP, pyocyanin production	Whitchurch *et al*., 1996
FleS	FleR	Motility; flagella	Dasgupta *et al*., 2003
GacS	GasA	Siderophore production	Goodman *et al*., 2009
GtrS	GltR	Cytotoxin; ToxA	Daddaoua *et al*., 2010
KinB	AlgB	Biofilm formation; alginate production	Ma *et al*., 1997
MifS	MifR	Biofilm formation; transition to maturation 2 stage	Petrova & Sauer, 2009
ParS	ParR	Antibiotic resistance	Fernández *et al*., 2010
PhoQ	PhoP	OprH, polymyxin B resistance	Macfarlane *et al*., 1999
PhoR	PhoB	Pyocyanin production	Meng *et al*., 2020
PilS	PilR	Motility; TFP	Hobbs *et al*., 1993
PprA	PprB	Biofilm formation; CupE fimbriae	Giraud *et al*., 2011
PvrS	PvrR	Biofilm formation; CupD fimbriae	Mikkelsen *et al*., 2009
RcsC	RcsB	Biofilm formation; CupD fimbriae	Mikkelsen *et al*., 2009

RocS1	RocA1/RocR	Cytotoxins; ExoY and ExoT, Biofilm formation; CupC fimbriae	Kuchma *et al*., 2005; Kulasekara *et al*., 2005
TtsS	TtsR	Cytotoxin; CbpE	Cadoret *et al*., 2014
WspE	WspR	Biofilm formation; c-diGMP	Hickman *et al*., 2005

1.3.2 Quorum sensing

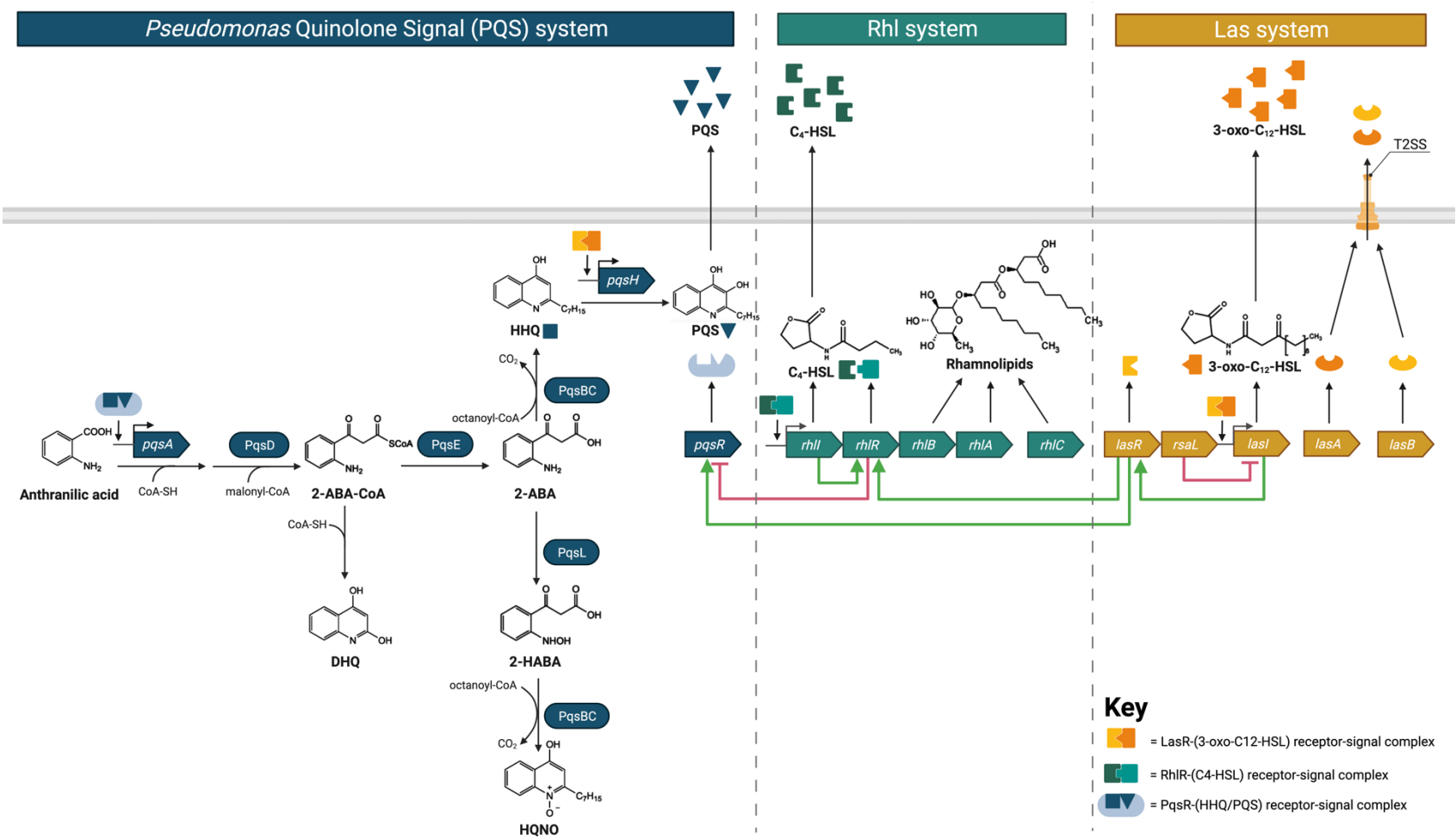
Many bacterial species can control gene regulation in a cell population density-dependent manner known as Quorum Sensing (QS) (Williams and Cámara, 2009). This process is modulated by the production of autoinducers, which are extracellular signalling molecules that increase in concentration as the bacterial population increases. Autoinducers can diffuse back through the cell membrane and bind to their cytoplasmic cognate receptor proteins, usually transcriptional regulators. This in turn modulates the expression of QS-dependent genes. The term QS was first applied to the LuxR-LuxI system in *Vibrio fischeri* (Fuqua *et al*., 1994), although AHL-dependent cell-to-cell communication had been previously described in several Gram-negative bacteria (Bainton *et al*., 1992; Jones *et al*., 1993; Passador *et al*., 1993; Zhang *et al*., 1993).

Many organisms including *P. aeruginosa* have several overlapping QS systems. The three systems of *P. aeruginosa* are interlinked and arranged in a hierarchy with the *las* system regulating the *rhl* and *pqs* systems, and vice versa. An overview of these QS systems is provided in **Figure 1.6** and each is discussed in more detail below. A fourth QS system based around the production of the signalling molecule 2-(2-hydroxyphenyl)- thiazole-4-carbaldehyde (IQS) was hypothesised by Lee *et al*., (2013), but this has since been shown to be an error by our lab and others (Carolina Paiva, PhD thesis; Cornelis, 2020).

1.3.2.1 *las* system

The *las* system is comprised of the *lasI* gene, encoding an AHL synthase to direct the production of the signalling molecule *N*-(3-oxododecanyl)-L-homoserine lactone (3-oxo-C_{12}-HSL) that binds to its cognate transcriptional activator encoded by the *lasR* gene (Seed *et al*., 1995). Production of 3-oxo-C_{12}-HSL creates a positive feedback loop and increases the transcription of *lasI* (Seed *et al*., 1995). The LasR/3-oxo-C_{12}-HSL receptor-signal complex binds to conserved *las* boxes in the promoter regions of target genes, activating the transcription of virulence factors including alkaline protease (Gambello *et al*., 1993), elastase A (Toder *et al*, 1991), elastase B (Gambello *et al*., 1991), PIV, exotoxin A (Gambello *et al*., 1993), haemolysin, and twitching motility (Glessner *et al*., 1999). This complex also activates the transcription of *rhlR* and inhibits the expression of *rhlA* (Latifi *et al*., 1996).

Figure 1.6: The Las, Rhl and PQS quorum sensing systems of *P. aeruginosa*. QS is activated by an increase in cell density or other environmental stimuli. The synthases LasI, RhlI and PqsABCDH produce the autoinducers *N*-(3-oxododecanyl)-L-homoserine lactone (3-oxo-C_{12}-HSL), *N*-butanoyl-L-homoserine lactone (C_4-HSL) and 2-heptyl-3-hydroxy-4(1H)-quinolone (PQS) respectively. Autoinducers bind to the receptors encoded by LasR, RhlR and PqsR, and the receptor-signal complexes regulate group behaviours and the production of QS-regulated products. Green arrows indicate positive gene regulation and red blunted arrows indicate negative gene regulation. Image created using BioRender.



The *las* system is under both positive and negative regulation. The expression of *lasI* is negatively regulated by *rsaL*, a gene located between *lasR* and *lasI* which binds to the *lasI* promoter to negatively regulate QS (Rampioni *et al*., 2006). LasI is also negatively regulated by QscR (Chugani *et al*., 2001), VqsR (Juhas *et al*., 2004), MvaT (Diggle *et al*., 2002), RpoN (Heurlier *et al*., 2003), RsaL (de Kievit *et al*., 1999) and RsmA (Pessi et al., 2001), and positively regulated by VpsR (Juhus *et al*., 2004), and CzcR (Dieppois *et al*., 2012) in addition to LasR. Conversely, the expression of *lasR* is positively regulated by several genes including RelA (Van Delden *et al*., 2001), GacA/GacS (Reimmann *et al*., 1997) and Vfr (Albus *et al*., 1997), and negatively regulated by AlgR2 (Ledgham *et al*., 2003a), QscR (Chugani *et al*., 2001; Ledgham *et al*., 2003b), QslA (Seet and Zhang, 2011), QteE (Siehnel *et al*., 2010), and RpoN (Heurlier *et al*., 2003).

1.3.2.2 *rhl* system

Similar to the *las* system, the *rhl* system also centres around the production of an AHL signal molecule called *N*-butanoyl-L-homoserine lactone (C_4-HSL) (Winson *et al*., 1995). C_4-HSL is produced by the synthase encoded by the *rhlI* gene and binds to its cognate receptor encoded by the *rhlR* gene to autoregulate further production of *rhlI* (Latifi *et al*., 1996). The RhlR/C_4-HSL receptor-signal complex binds to *rhl* boxes (many of which are hybrid *rhl/las* boxes) in the promoter regions of target genes, activating the transcription of virulence factors including elastase A, elastase B, rhamnolipids, hydrogen cyanide, pyocyanin (Brint & Ohman, 1995), and lectins LecA & LecB (Winzer *et al*., 2000). The *rhl* system also controls swarming and twitching motility (Glessner *et al*., 1999; Köhler *et al*., 2000).

The expression of *rhlR* is positively regulated by LasR (Latifi *et al*., 1996), PQS, RelA (Van Delden *et al*., 2001), GacA/GacS (Reimmann *et al*., 1997), Vfr (Albus *et al*., 1997), PA1196 (Liang *et al*., 2009) and PhrD (Malgaonkar & Nair, 2019) and negatively regulated by AlgR2 (Ledgham *et al*., 2003a), QscR (Ledgham *et al*., 2003b), QteE (Siehnel *et al*., 2010), RpoN (Heurlier *et al*., 2003), and BfmR (Cao *et al*., 2014). The expression of *rhlI* is positively regulated by PQS and PA1196 (Liang *et al*., 2009), and negatively regulated by RsmA (Pessi et al., 2001), MvaT (Diggle *et al*., 2002), DksA (Branny *et al*., 2001).

1.3.2.3 *pqs* system

In contrast to the *las* and *rhl* systems, the *pqs* QS system centres around the production of the AQ signalling molecule 2-heptyl-3-hydroxy-4(1H)-quinolone (*Pseudomonas* quinolone signal; PQS) (Pesci *et al*., 1999). The *pqs* system is comprised of several gene clusters including *pqsABCDE*, *pqsR* and neighbouring *phnAB* genes, in addition to *pqsH* and *pqsL* which are distally located on the chromosome. In the first step in PQS biosynthesis, PqsA catalyzes the conversion of anthranilic acid, CoA and ATP to anthraniloyl-CoA (Coleman *et al*., 2008). PqsD then catalyses the condensation of anthraniloyl-CoA and malonyl-CoA to 2-aminobenzoylacetyl-CoA (2-ABA-CoA) (Zhang *et al*., 2008). This unstable intermediate is quickly hydrolysed to 2-aminobenzoylacetate (2-ABA) by PqsE (Drees & Fetzner, 2015). Octanoic acid and 2-ABA can be condensed to form HHQ by the gene products of *pqsB* and *pqsC* which assemble to form a heterodimer (Drees *et al*., 2016). Lastly, PqsH oxidises HHQ to form PQS (Schertzer *et al*., 2010). Alternatively, 2-ABA can also be converted into HQNO in a multi-step process catalysed by PqsL and PqsBC (Lépine *et al*., 2004).

When activated by either HHQ or PQS, the transcriptional regulator PqsR binds to the promoter region of *pqsA* to induce the transcription of *pqsABCDE* (Rampioni *et al*., 2016). This creates a positive feedback loop on the *pqs* system (Cao *et al*., 2001; Xiao *et al*., 2006). While the PqsR-HHQ and PqsR-PQS complexes only activate the *pqsABCDE-phnAB* operon, PQS also acts through a PqsR-independent pathway to regulate 179 other genes (Rampioni *et al*., 2016). These include the sigma factor *pvdS*, protease IV *prpL*, and exoenzyme S biosynthesis genes *exsBCE* in addition to *exoS* (Rampioni *et al*., 2016). PQS also promotes the formation of membrane vesicles (Mashburn & Whiteley, 2005). In addition to a dispensable role in PQS biosynthesis, PqsE activates the transcription of diverse virulence genes including rhamnolipid synthesis genes *rhlAB*, hydrogen cyanide synthesis genes *hcnABC*, phenazine biosynthesis genes *phzC2D2E2F2G2* and *phzH*, lectins *lecAB* and the RND efflux pump *mexGHI-opmD* (Rampioni *et al*., 2016).

The *pqs* system is regulated by both the *las* and *rhl* systems: *lasR* controls the production of PQS through positive regulation of *pqsR*, while *rhlR* negatively regulates *pqsR* expression (Wade *et al*., 2005). The expression of *pqsR* is also negatively regulated by QslA (Seet and Zhang, 2011), PmpR (Liang *et al*., 2008) and CysB (Farrow *et al*., 2015).

1.3.2.4 Quorum sensing and efflux

RND efflux systems are reported to have both direct and indirect involvement in quorum sensing. For example, the *Burkholderia pseudomallei* BpeAB-OprB efflux pump directly exports the quorum sensing signalling molecules (QSSMs) *N*-octanoyl-homoserine lactone (C_8-HSL), *N*-decanoyl-homoserine lactone (C_{10}-HSL), *N*-(3-hydroxy)-octanoyl-homoserine lactone (3-hydroxy-C_8-HSL), *N*-(3-hydroxy)-decanoyl-homoserine lactone (3-hydroxy-C_{10}-HSL), *N*-(3-oxo)-decanoyl-homoserine lactone (3-oxo-C_{10}-HSL), and *N*-(3-oxo)-tetradecanoyl-homoserine lactone (3-oxo-C_{14}-HSL) (Chan *et al*., 2007). While in *E. coli* the links are less clear. The quorum sensing-regulated transcription factor SdiA positively regulates the expression of AcrAB-TolC (Rahmati *et al*., 2002) which may in turn export QSSMs (Yang *et al*., 2006), though further research is needed to elucidate these links.

In *P. aeruginosa*, links between efflux pumps and quorum sensing were first established in *P. aeruginosa* when Evans *et al*., (1998) observed that a strain overexpressing MexAB-OprM produced lower levels of pyocyanin, universal protease and elastase consistent with reduced expression of 3-oxo-C_{12}-HSL. Though it was originally suggested that 3-oxo-C_{12}-HSL was a substrate for MexAB-OprM (Evans *et al*., 1998; Pearson *et al*., 1999; Minagawa *et al*., 2012) recent work has shown this not to be the case (Alcalde-Rico *et al*., 2020). Expression of MexAB-OprM can also be induced by C_4-HSL (Maseda *et al*., 2004; Sawada *et al*., 2004). Other studies have shown that the PQS precursors kynurenine and HHQ are both substrates for MexCD-OprJ and MexEF-OprN (Lamarche and Déziel, 2011; Olivares *et al*., 2012; Alcalde-Rico *et al*., 2018), though while the former favours the extrusion of HHQ (Alcalde-Rico *et al*., 2018) the latter favours kynurenine (Olivares *et al*., 2012).

1.4 Virulence

When *P. aeruginosa* enters the host, the innate immune system recognises outer membrane components such as LPS triggering an infiltration of neutrophils to promote bacterial clearance. Host inflammatory responses including reactive oxygen and nitrogen species, in addition to other environmental stresses such as antibiotics, can induce the expression of gene sets initiating the switch to an acute or chronic strategy. *P. aeruginosa*

produces a host of virulence factors that enable it to adapt to many environments and different extracellular toxins, appendages and proteases are deployed as required (Furukawa *et al*., 2006). A list of virulence factors produced by *P. aeruginosa* is presented in **Table 1.7** and selected virulence factors are discussed in more detail below.

1.4.1 Pyocyanin

Pyocyanin is one of five phenazines produced by *P. aeruginosa* but is of particular importance due to its role as a virulence factor. Pyocyanin is a redox-reactive metabolite that is cytotoxic to host cells due to the production of reactive oxygen species (Britigan et al., 1992; Denning *et al*., 1998; Lau *et al*., 2004). Pyocyanin exists in three different states: oxidised, monovalently reduced and divalently reduced, and is also responsible for the green pigmentation of many strains (Frank and DeMoss, 1959)

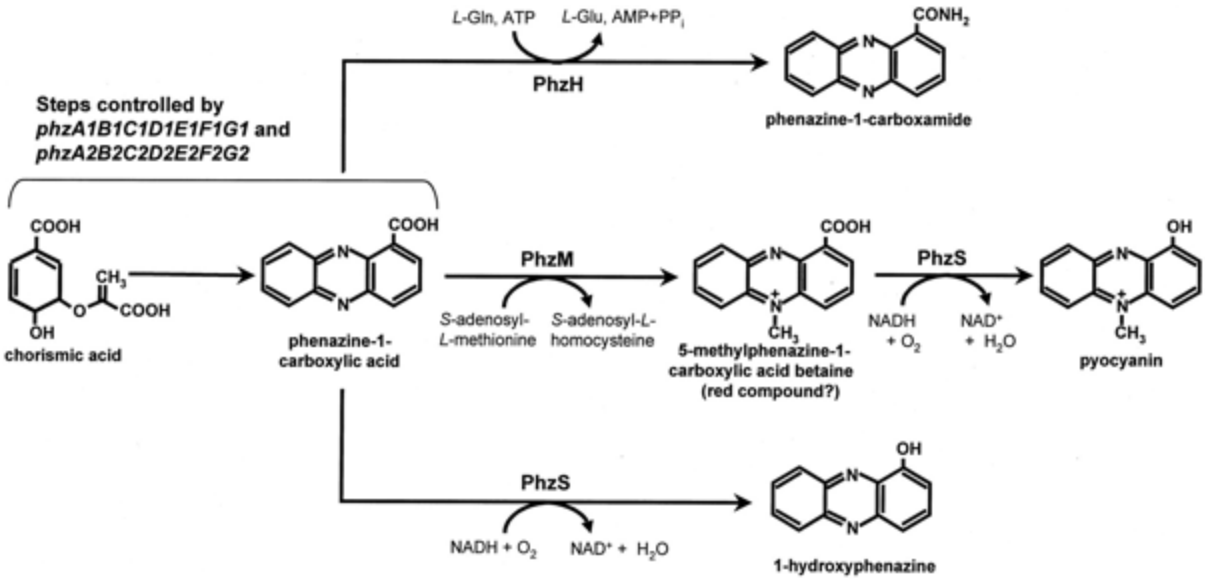
Pyocyanin biosynthesis begins with the conversion of chorismic acid to phenazine-1-carboxylic acid (PCA) by the enzymes encoded by one of two divergent operons: *phzA1B1C1D1E1F1G1* (*phz1*) and *phzA2B2C2D2E2F2G2* (*phz2*). PCA is then converted into 5-methylphenazine-1-carboxylic acid betaine by PhzM, before conversion to pyocyanin by PhzS. The enzymes encoded by PhzH and PhzS can also convert PCA into phenazine-1-carboxamide and 1-hydroxyphenazine respectively (Mavrodi *et al*., 2001) (**Figure 1.7**).

The transcription of both phenazine biosynthesis operons is mediated by quorum sensing, with LasR, RhlR and PqsE required for pyocyanin production (Higgins *et al*., 2018). However, whilst the *phz1* operon is responsible for pyocyanin production in planktonic cultures the *phz2* operon is reserved for pyocyanin production during biofilm formation (Recinos *et al*., 2012). RsaL is a negative regulator of quorum sensing (De Kievit *et al*., 1999) which has also been shown to repress *phz1* and activate *phz2* (Higgins *et al*., 2018).

Table 1.7 Virulence factors produced by *P. aeruginosa*

Virulence factor	Gene(s)	Type	Mechanism
Alginate	*algU*	Exopolysaccharide	Biofilm structure and dynamics
Alkaline protease	*aprA*	Exoenzyme	Immune evasion
Elastase A	*lasA*	Exoenzyme	Immune evasion
Elastase B	*lasB*	Exoenzyme	Immune evasion
Exoenzyme S	*exoS*	Toxin	Cytotoxicity
Exoenzyme T	*exoT*	Toxin	Cytotoxicity
Exoenzyme Y	*exoY*	Toxin	Cytotoxicity
Exotoxin A	*toxA*	Toxin	Cytotoxicity
Flagella	*flgBCDEF and fliCD*	Surface appendage	Motility
Hydrogen cyanide	*hcnABC*	Toxin	Cytotoxicity
Lectin A	*lecA*	Lectin	Biofilm structure and dynamics
Lectin B	*lecB*	Lectin	Biofilm structure and dynamics
Lipase	*lipA*	Exoenzyme	Immune evasion
Phospholipase C	*plcH*	Exoenzyme	Immune evasion
Pili	Multiple	Surface appendage	Motility
Protease IV	*prpL*	Exoenzyme	Immune evasion
Pyochelin	*pchDCBA* and *pchEFGHI*	Siderophore	Iron scavenging
Pyocyanin	*phzA1B1C1D1E1F1G1* (*phz1*), phzM, phzS	Phenazine	Cytotoxicity
	phzA2B2C2D2E2F2G2 (*phz2*)	Phenazine	Cytotoxicity
Pyoverdin	*pvcABCD*	Siderophore	Iron scavenging
Rhamnolipids	*rhlABC*	Surfactant	Biofilm structure and dynamics

Figure 1.7 Pyocyanin biosynthesis and regulation. Taken from Mavrodi *et al*., 2001.



1.4.2 Rhamnolipids

Rhamnolipids are bacterial surfactants produced by the cell that can disrupt tight junctions in the epithelial cell membrane (Zulianello *et al*., 2006), in addition to attacking the host immune response by killing leukocytes and macrophages (Jensen et al., 2007; Van Gennip *et al*., 2009). Rhamnolipids can be further subdivided into mono- or di-rhamnolipids which are comprised of either one or two rhamnose head groups respectively, and a 3-(hydroxyalkanoyloxy)alkanoic acid (HAA) fatty acid tail.

Rhamnolipids are synthesised by the *rhl* operon gene products: RhlA synthesises the HAA, RhlB catalyses the formation of mono-rhamnolipids (Ochsner *et al*., 1994) whilst RhlC catalyses the formation of di-rhamnolipids (Rahim *et al*., 2001). The production of rhamnolipids is regulated by the transcriptional regulator *rhlR* (Medina *et al*., 2003).

1.4.3 Siderophores

Iron is required for many essential bacterial processes including DNA/RNA synthesis, electron transfer and redox reactions. In the host environment, the bioavailability of iron is low due to the production of extracellular iron-binding proteins transferrin and lactoferrin so *P. aeruginosa* secretes ferric iron-chelating compounds known as siderophores. Iron normally binds to Fur (ferric uptake regulator) to inhibit siderophore production, but when iron bioavailability is low Fur is derepressed and the genes involved in the manufacture of siderophores and their associated uptake proteins are transcribed (Cornelis & Dingemens, 2013).

P. aeruginosa secretes two siderophores: pyochelin and pyoverdin. Pyochelin has a lower affinity for binding iron than pyoverdin. The subsequent Fe^{3+}-siderophore complex is recognised by TonB-dependent receptors (TBDR) on the cell's outer membrane and transported into the cytoplasm by ABC transporters (Cornelis & Dingemens, 2013). Ferric iron is then reduced to the ferrous state to enable the non-destructive removal of iron from the siderophore, which has a much lower avidity for Fe^{2+} than Fe^{3+} (Cornelis & Dingemens, 2013) so that the siderophore can be recycled.

Pyochelin is synthesised from chorismate by the *pchDCBA* and *pchEFGHI* operons (Serino *et al*., 1997; Reimmann *et al*., 1998; Reimmann *et al*., 2001), while pyoverdin is synthesised by non-ribosomal peptide synthesis (NRPS) in a complex process involving more than 20 genes. Pyoverdin is then transported across the outer membrane and is secreted into the extracellular environment by the PvdRT-OpmQ efflux pump (Imperi *et al*., 2009). Pyoverdin production is regulated by the sigma factor PvdS, which is in turn regulated by Fur (Cunliffe *et al*., 1995).

1.4.4 Exoproteases

P. aeruginosa secretes at least seven extracellular proteases; elastase A (also known as staphylolysin), elastase B (also known as pseudolysin), alkaline protease (also known as aeruginolysin) (Morihara, 1964), protease IV (Engel *et al*., 1998), PaAP (*P. aeruginosa* aminopeptidase) (Cahan *et al*., 2001), PASP (*P. aeruginosa* small protease) (Marquart *et al*., 2005), and LepA (Large ExoProtease A) (Kida *et al*., 2008). Four exoproteases linked to virulence are discussed in more detail below.

1.4.4.1 Elastase A

Elastase A is encoded by the *lasA* gene and is synthesised as a pre-proenzyme comprising a signal sequence domain, a propeptide domain and a mature enzyme domain. The unusually long 22-kDa signal sequence is removed upon translocation from the inner membrane to the periplasm, before the covalently bonded propeptide-enzyme complex is secreted by the Xcp T2SS (Kessler *et al*., 1998). Following processing to release the 20-kDa metalloprotease, elastase A contributes toward host tissue invasion through the breakdown of the surface proteoglycan syndecan-1 (Park *et al*., 2000). Elastase A is also able to cleave the pentaglycine bridges of *Staphylococcus aureus* peptidoglycan to lyse *S. aureus* in the cystic fibrosis lung (Kessler *et al*., 1993). Elastase A is regulated by the *las* QS system (Toder *et al*., 1991), though the global regulator AmpR has also been shown to negatively regulate LasA levels (Kong *et al*., 2005).

1.4.4.2 Elastase B

Elastase B is synthesised as a 53.4-kDa pre-proenzyme encoded by the *lasB* gene. The signal peptide is removed as the propeptide-enzyme complex translocates across the inner membrane through the Sec pathway. The propeptide is essential for protein folding in the periplasm (Braun *et al*., 1996), and remains noncovalently attached to the mature elastase following autoproteolytic cleavage (McIver *et al*., 1991). This complex is then translocated across the outer membrane by the Xcp T2SS (Kessler *et al*., 1998) where it dissociates to release the 33-kDa metalloprotease. Elastase B degrades host elastin and collagen leading to host tissue damage and has also been shown to degrade immunoglobulin A (IgA) and immunoglobulin G (IgG) (Alcorn *et al*., 2004).

Expression of elastase B is controlled by both the *las* and *rhl* QS systems (Pearson *et al*., 1997) and requires the transcriptional regulator LasR (Gambello & Iglewski, 1991), while the global regulator AmpR has also been shown to positively regulate LasB levels (Kong *et al*., 2005). Activation of the *pqs* QS system through the binding of PQS to the transcriptional regulator PqsR can also lead to transcription of *lasB*.

1.4.4.3 Protease IV

Protease IV (PIV) is synthesised as a 48.2-kDa pre-propeptide encoded by the *prpL* gene. The complex is translocated from the inner membrane to the periplasm by the Sec machinery, where the signal peptide is removed. The propeptide enzyme is then translocated across the outer membrane by the Xcp T2SS to produce the 26 kDa mature PIV (Traidej *et al*., 2003). PIV is a serine protease that degrades various host proteins including fibrinogen, plasminogen and IgG (Engel *et al*., 1998). PIV has also been shown to play an important role in murine keratitis (Marquart & O'Callaghan, 2013). PIV is regulated by the RetS/Rsm pathway which is in turn regulated by the sigma factor PvdS (Wilderman *et al*., 2001; Peng *et al*., 2020). PIV is expressed in iron-limited environments as PvdS is regulated by Fur (Peng *et al*., 2020).

1.4.4.4 Alkaline protease

Alkaline protease is a 50-kDa zinc metalloprotease encoded by the *aprA* gene. Unlike the exoenzymes discussed above, the folded protein is transported directly from the cytoplasm to the extracellular environment by the AprDEF T1SS encoded upstream of *aprA* (Guzzo *et al*., 1991). Following removal of the signal peptide, alkaline protease plays a role in invasion and tissue haemorrhage through the cleavage of laminin (Heck *et al*., 1986), human interferon-γ (IFN-γ), tumour necrosis factor-α (TNF-α) and interleukin-6 (IL-6) (Parmely *et al*., 1990). An alkaline protease inhibitor *aprI* is also encoded downstream of the *aprA* gene which binds to AprA to protect against protein degradation in the periplasm (Bardoel *et al*., 2012). The regulation of *aprA* is not known.

1.4.5 Flagella

P. aeruginosa has a singular polar flagellum which is required for motility, attachment and virulence. Beginning in the inner membrane, the flagellum is comprised of export apparatus, motor switch, MS ring, basal body rod, L ring, P ring, hook, hook filament junction, filament and cap proteins. The filament accounts for more than 95% of the flagellum and is comprised of flagellin proteins (encoded by *fliC*) arranged in a hollow tubular structure that can rotate in both clockwise and counter-clockwise directions (Cai *et al*., 2016). The structural components of the flagella are encoded by the *flgBCDE*, *flgFGHIJKL*, *fliCfleL*, *fliDS* and *fliEFGHIJ* operons. A hierarchy of regulatory systems is required for the assembly and function of the flagellum. These comprise the master regulator FleQ and the alternative sigma factor σ^{28} encoded by *fliA*, the FleSR TCS to positively regulate the assembly of the basal body, rings and flagella export apparatus, FleR and the alternative sigma factor σ^{54} encoded by *rpoN* to regulate the formation of the basal body-rod, ring and hook, and FlgM to regulate expression of *fliA* (Dasgupta *et al*., 2003).

Rotation of the polar flagella is central to two types of coordinated movement: swimming and swarming. Swimming motility is an individual movement through liquid-to-low viscosity media in which cells move in a variety of patterns (Vater *et al.*, 2014) while swarming motility is a multicellular surface movement characterised by the formation of dendrites which produce elaborate patterns. Swarmer cells move in groups known as rafts

(Rashid & Harunur, 2000). The mechanism underlying both motilities and their associated regulation requires further characterisation, though *aefA* has been linked to swimming motility (Li *et al*., 2015) and loss of FleRS inhibits both swimming and swarming motilities (Zhou *et al*., 2021). Although *P. aeruginosa* normally swims with a single flagellum, transitioning from swimming to swarming motility has been shown to increase the number of flagella on the cell surface (Köhler *et al*., 2000).

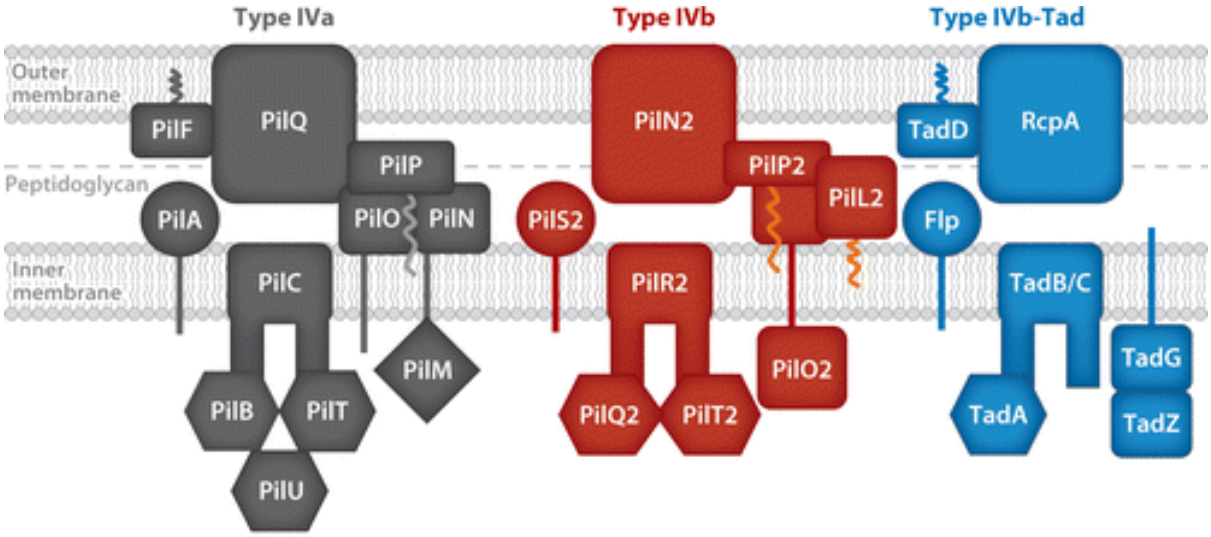
Flagella are required for virulence in mice infection models (Feldman *et al*., 1998; Arora *et al*., 2005), and for inducing host inflammatory responses (Garcia *et al*., 2018). For this reason, flagella proteins have been proposed as *P. aeruginosa* vaccine candidates (Saha *et al*., 2007; Campodónico *et al*., 2010).

1.4.6 Pili

Type IV pili (TFP) are bacterial appendages involved in surface adhesion, colonisation and natural transformation. TFP can be broadly divided into the Type IVa pili (T4aP) and Type IVb pili (T4bP) subfamilies, the latter of which also includes the tight adherence pili subgroup (T4bP-Tad; also known as Flp pili). While T4aP and T4bP-Tad are common to all *P. aeruginosa* strains, T4bP are only found in strains carrying the *P. aeruginosa* pathogenicity island 1 (PAPI-1) such as PA14 (Carter *et al*., 2010). Each system has a unique assembly which is shown in **Figure 1.8**.

TFaP bind eDNA during biofilm formation (Van Schaik *et al*., 2005) and are implicated in several types of motility including walking (Gibiansky *et al*., 2010), slingshot (Jin *et al*., 2011), swarming and twitching motilities. Twitching motility is a “twitchy” movement across a moderately viscose surface that is important for the dispersal of cells from biofilms. Movement results from the extension and retraction of T4aP (Skerker & Berg, 2001) On a 1% agar, this typically presents as a radial twitching zone of approximately 5 cm after 48 h incubation. Regulation of TFaP is complex and involves the PilRS TCS (Hobbs *et al*., 1993), the AlgR-FimS TCS (Whitchurch *et al*., 1996), the alternate sigma factor, RpoN (σ^{54}), the global carbon metabolism regulator Crc (O’Toole *et al*., 2000), and the virulence factor regulator Vfr (Beatson *et al*., 2002a).

Figure 1.8: Organisation and assembly of Type IV pili in *P. aeruginosa*. Taken from Burrows, 2012. The assembly systems are comprised of a major pilin subunit (PilA, PilS2 or Flp), secretin (PilQ, PilN2 or RcpA), putative pilotin (PilF or TadD), putative platform protein (PilC, PilR2 or TadB/TadC), putative pilin polymerase (PilB, PilQ2 or TadA), putative pilin deployerase (PilT, PilU or PilT2), prepilin peptidase (PilD or FppA; not shown), minor pilin (FimU-PilVWXE, PilV2 or TadF; not shown), and other components of unknown function.



Twitching motility is regulated by a chemosensory system encoded by the *pilGHIJKL* (Darzins *et al*., 1993; Darzins *et al*., 1994; Darzins *et al*., 1995), and *chpABCEF* (Whitchurch *et al*., 2004; Bertrand et al., 2010) genes. Twitching motility is not regulated by quorum sensing (Beatson *et al*., 2002b).

TFbP are less well characterised but are conjugative pili that enable the transfer of PAPI-1 to recipient strains (Hong *et al*., 2017). T4bP-Tad are regulated by the PrpAB TCS, which also regulates the assembly of CupE fimbriae (Bernard *et al*., 2009).

1.4.7 Virulence and efflux

None of the virulence factors discussed above are known substrates of RND efflux pumps, yet throughout the Enterobacteriaceae family loss of RND efflux pumps has been shown to attenuate virulence (Buckley *et al*., 2006, Bina *et al*., 2008, Padilla *et al*., 2010, Pérez *et al*., 2012). In *P. aeruginosa*, deletion of *mexAB-oprM* reduced virulence in a mouse model of septicaemia (Hirakata *et al*., 2002) and deletion of *mexEF-oprN* reduced virulence in a murine acute lung infection model (Vaillancourt *et al*., 2021). Aendekerk *et al*., (2005) reported that Δ*mexI* and Δ*opmD* mutants produced less pyocyanin and less elastase B than the parent strain. Disruption of *muxA* has also been shown to decrease virulence in *Drosophila melanogaster* (Yang *et al*., 2011).

At the same time, there is contradictory evidence that mutants overexpressing RND efflux pumps also produce lower amounts of many virulence factors. Strains overexpressing *mexAB-oprM* (*nalB* mutants) produce less pyocyanin, elastase B and 3-oxo-C_{12}-HSL and are less lethal to mice (Evans *et al*., 1998; Vaillancourt *et al*., 2021). Overexpression of *mexCD-oprJ* (*nfxB* mutants) reduces pyocyanin, protease IV, rhamnolipids, elastase B, ExoT, ExoS and PcrV production in addition to abolishing swarming motility (Sánchez *et al*., 2002; Linares *et al*., 2005; Alcalde-Rico *et al*., 2018). The subsequent deletion of *mexD* in an *nfxB* mutant restored elastase, protease IV, pyocyanin, rhamnolipid and swarming phenotypes in line with the parent strain PAO1 (Alcalde-Rico *et al*., 2018). Overexpression of *mexEF-oprN* (*nfxC* mutants) reduces pyocyanin, rhamnolipid, elastase B, ExoT, ExoS and PcrV production (Köhler *et al*., 1997; Köhler *et al*., 2001; Linares *et al*., 2005).

Efflux pumps are also important for the invasion of host cells during the establishment of infection. Despite the association between efflux pumps, MDR infections and poor patient prognosis, Hirakata *et al*., (2002) found strains lacking *mexAB-oprM* or *mexXY* were less effective at penetrating Madin-Darby canine kidney (MDCK) cells than the PAO1 wild-type. While Linares *et al*., (2005) found that strains overexpressing *mexCD-oprJ* and *mexEF-oprN* were less cytotoxic to the macrophage cell line J774 than the parent strain. Strains overexpressing *mexAB-oprM* and *mexCD-oprJ* were less virulent than the wild-type strain in the non-mammalian model organism *C. elegans* (Sánchez *et al*., 2002), while a MexAB-OprM deletion mutant was unable to induce septicaemia in mice indicating this pump is particularly important for invasion (Hirakata *et al*., 2002). A mutant lacking MexCD-OprJ was not involved in cell infection (Hirakata *et al*., 2002). Another study found that MexEF-OprN deletion or MexAB-OprM overexpression reduced mouse survival times in an acute murine infection model (Vaillancourt *et al*., 2021).

1.5 Biofilm formation

A biofilm is an aggregation of cells attached to a surface surrounded by an extracellular polymeric substance (EPS) matrix to enable the exchange of nutrients, gas and waste products. Biofilms are dense, complex and often comprised of several different micro-organisms. *P. aeruginosa* can form biofilms on a range of other surfaces including urinary catheters, contact lenses and water systems.

Bacteria in biofilms show increased tolerance to antibiotics leading to persistent infections that are unresponsive to treatment. Antibiotic tolerance results from limited biofilm penetration; positively charged antibiotics bind to EPS components on the biofilm surface and cannot reach the bacteria within, whereas neutral antibiotics can still pass through the matrix to reach their target (Tseng *et al*., 2013). However, this phenotype is lost when biofilms are dispersed and planktonic cells regain their antibiotic sensitivity (Costerton *et al*., 1999). Biofilms also contain persister cells that evade antimicrobials that target important cellular processes due to their reduced growth and metabolic activity (Lewis, 2010).

1.5.1 Biofilm composition

Bacteria in biofilms are embedded within a self-produced matrix of EPS consisting of exopolysaccharides, LecAB lectins, Cup fimbria, Fap amyloids, CdrA adhesins, nucleic acids, rhamnolipids and proteins (Vallet *et al*., 2001; Tielker *et al*., 2005; Diggle *et al*., 2006; Pamp & Tolker-Nielson, 2007; Borlee *et al*., 2010; Dueholm *et al*., 2013; Rybtke *et al*., 2015). EPS makes up ~ 50-90% of the biofilm and imparts physical and chemical robustness.

P. aeruginosa produces three exopolysaccharides that are important for attachment and cell-to-cell signalling: Psl, Pel and alginate. Psl is a neutral polysaccharide consisting of a repeating pentasaccharide unit, while Pel is a cationic polysaccharide which crosslinks eDNA to maintains biofilm integrity (Jennings *et al*., 2015). The production of Psl and Pel is strain-specific, with PAO1 lineages producing both while PA14 only produces Pel.

Overproduction of the capsular polysaccharide alginate is associated with mucoid strains often found in the lungs of individuals with cystic fibrosis. The expression of the *algD* operon, which encodes the enzymes required for alginate synthesis, is normally antagonized through protein-protein binding of the anti-σ-factor MucA to the alternative RNA polymerase σ-factor σ^{22}, encoded by *algU*. Mucoid isolates overproducing alginate normally carry mutations in *mucA*, leaving σ^{22} free to activate transcription of many genes including those involved in alginate production and the responses to heat shock, osmotic stress and oxidative stress. σ^{22} also negatively regulates several virulence factors, including flagella, TFP, the type III secretion system (T3SS) and rhamnolipids (Folkesson *et al*., 2012).

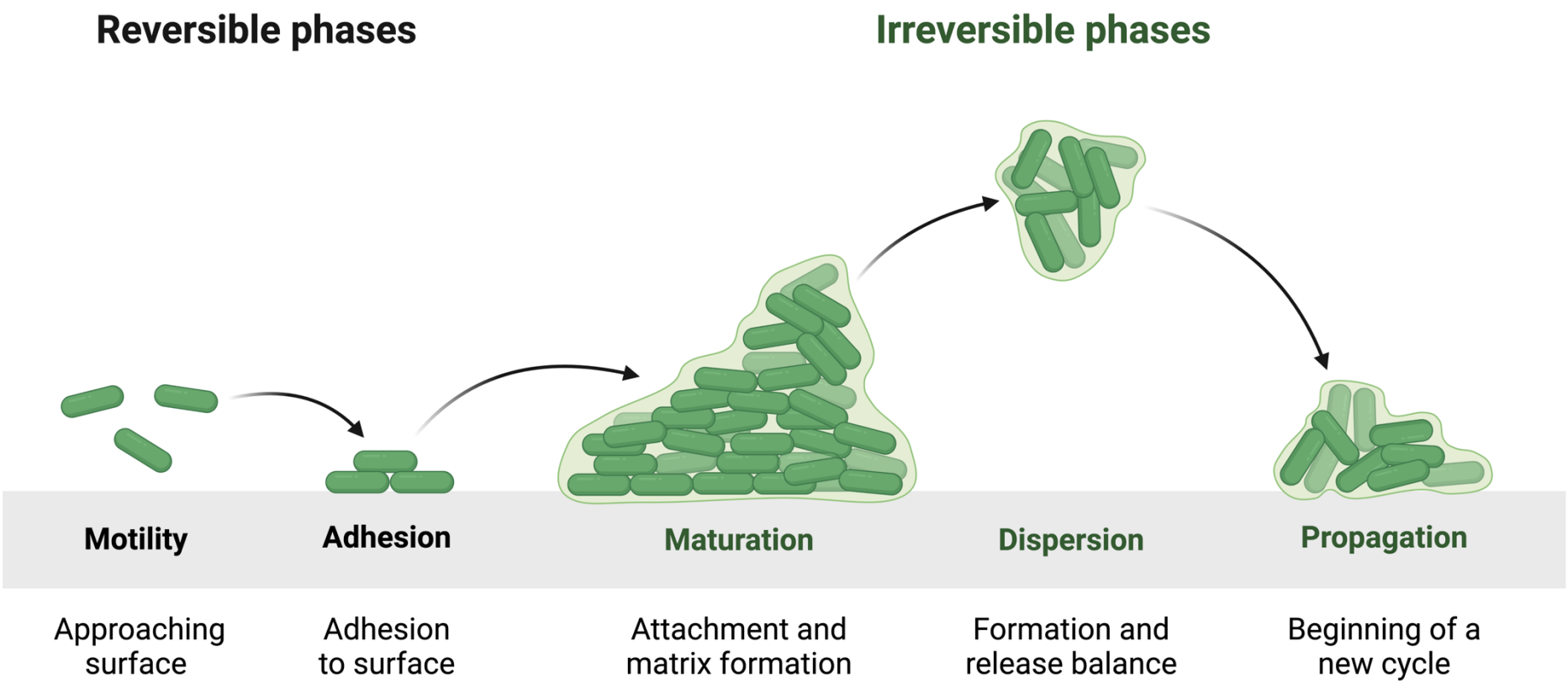
Extracellular DNA is released during cell lysis and is another important component of biofilms (Whitchurch *et al*., 2002; Allesen-Holm *et al*., 2006). In addition to contributing to the biofilm architecture, eDNA has been shown to activate neutrophils (Bass *et al*., 2010), bind positively charged antibiotics such as aminoglycosides and acidify the biofilm environment to increase antimicrobial tolerance (Wilton *et al*., 2016).

1.5.2 Life cycle

The life cycle of a biofilm is separated into five distinct phases (**Figure 1.9**) In the first stage, bacteria moving in a liquid environment sense surfaces using the Pil-Chp chemotaxis-like complex, TFP, PilY1 and mechanosensors (Luo *et al*., 2015; Rodesney *et al*., 2017). Upon surface adhesion, levels of the signalling molecule bis-(3'-5')-cyclic dimeric guanosine monophosphate (c-di-GMP) increase mediating the switch between planktonic and sessile growth. C-di-GMP is synthesized from 2 GTP molecules by diguanylate cyclases (DGCs) and regulates the expression of biofilm initiation genes including the transcription factor *fleQ* to activate the flagella and repress Pel production (Hickman *et al*., 2008), *pelD* to activate Pel production (Lee *et al*., 2007), and Alg44 to activate alginate production (Merighi *et al*., 2007).

In the second stage, cells use TFP to adhere to the surface to enable biofilm formation and the attachment becomes irreversible (Giltner *et al*., 2006). Bacteria can respond to different surfaces, resulting in surface-specific changes to the bacterial proteome (Guilbaud *et al*., 2017) As the cells divide and the biofilm matures (Stage 3), cells within the biofilm have a very different transcriptional profile to planktonic cells. Biofilm dispersal occurs when individual cells separate from the biofilm and return to their free-living form to form new biofilms (Stages 4 & 5). Biofilm dispersal has been linked to changes in environmental cues and signalling molecules including NO, O_2 and c-di-GMP, which are received by regulatory systems including quorum sensing, BdlA, DipA, NicD, and GcbA complex, RbdA system, and MucR-NbdA system (Li *et al*., 2013; Li *et al*., 2014). The BqsS-BqsR TCS has also been shown to modulate biofilm detachment (Dong *et al*., 2008).

Figure 1.9 Lifecycle of a biofilm. Biofilm formation begins when planktonic cells sense and reversibly attach to a surface. The monolayer biofilm irreversibly attaches following the production of the extracellular matrix. The biofilm matures and forms multiple layers with characteristic “mushroom” structures. Eventually, some cells detach and the biofilm disperses. Image created using BioRender.



1.5.3 Biofilms and efflux

It is well-established that bacteria in biofilms are less susceptible to antibiotics than those in planktonic cultures. Ceri *et al.,* (1999) showed that up to 1000 times the antibiotic concentration is required to eradicate bacteria in a biofilm compared to the same species in a planktonic population. Transcriptional studies have shown that efflux pump expression is increased in *E. coli*, *A. baumannii* and *S. aureus* biofilms compared to planktonic cultures which might explain these findings (Schembri *et al.,* 2003; Resch *et al.,* 2005; Rumbo-Feal *et al.,* 2013). Surprisingly, De Kievit *et al*., (2001) found that *P. aeruginosa* biofilms do not exhibit increased expression of *mexAB-oprM*, *mexCD-oprJ*, *mexEF-oprN* or *mexXY*. However, a number of ABC-family and MFS-family efflux pump genes are upregulated in developing biofilms (Waite *et al.,* 2005).

RND efflux pumps have been linked to other changes in *P. aeruginosa* biofilm formation. BrlR is a regulator of biofilm-specific antibiotic tolerance that is also a transcriptional activator of the MexAB-OprM and MexEF-OprN RND efflux pumps (Liao *et al*., 2013) in addition to an ABC transporter encoded by PA1874-PA1877 (Poudyal & Sauer, 2018). Overexpression of *mexAB-oprM* and *mexCD-oprJ* does not impair biofilm formation (Sánchez *et al*., 2002), while overexpression of *mexEF-oprN* has been implicated in reduced biofilm formation in a *qrh* mutant (Ramsey & Whiteley, 2004). The RocA2 response regulator of the Roc2 system, which regulates *cupC* pilus assembly genes has also been shown to repress the expression of MexAB-oprM. (Sivaneson *et al*., 2011). Finally, MexGHI-OpmD exports 5-Me-PCA, which is a phenazine implicated in redox balancing in anoxic environments and which contributes to normal biofilm formation (Sakhtah *et al*., 2016).

1.6 Hypothesis

RND efflux pumps have physiological roles in *P. aeruginosa* PAO1-L beyond antimicrobial resistance.

1.7 Aims

- Construct a set of single and combinatorial RND efflux pump deletion mutants in *P. aeruginosa* PAO1-L
- Determine the phenotypic and transcriptomic changes associated with loss of efflux
- Increase understanding of the physiological roles of RND efflux pumps in *P. aeruginosa* PAO1-L

CHAPTER 2:

Construction of RND efflux pump mutants in *P. aeruginosa* PAO1-L-DS

2. Construction of RND efflux pump mutants in *P. aeruginosa* PAO1-L-DS

2.1 Introduction

Traditionally, organisms with interesting or usual characteristics were studied to identify the genotypes responsible for the phenotypes. Since disrupted cellular processes provide insights into gene function, it is still useful to explore what happens when a gene is overexpressed, interrupted or removed. While both gene interruption/deletion and over-expression mutants can be used for similar types of experiments, such as studying gene function and identifying gene interactions, there are some key differences in the types of experiments for which each method is most useful.

Gene deletion mutants can be used for loss-of-function studies which explore the effects of not having that gene present to infer its function. This method can be used to study the interactions between genes in a biological pathway. For example, genes can be successively deleted from a pathway to tease out their individual functions. While over-expression mutants can be used for gain-of-function studies to explore the effects of having an increased amount of that gene present to infer its function. This can be particularly useful for studying subcellular localisations.

Mutants can be created using many different methods including chemical, radiation and insertional mutagenesis. For example, a Tn5 transposon can be randomly inserted into each bacterium within a population to create a library of individual mutants with insertions spanning the chromosome. Classical genetics can then be combined with whole genome sequencing (WGS) in techniques such as transposon sequencing (Tn-Seq) (Van Opijnen *et al*., 2009) and transposon-directed insertion site sequencing (TraDIS) (Langridge *et al*., 2009) to provide a high-throughput way of linking phenotype to genotype when the mutant library is subjected to stress.

While this approach can be useful for identifying mutants with a phenotype of interest, studying a particular gene or protein requires a more targeted approach. The accessibility of sequencing tools enables the comparison of nucleotide and amino acid sequences to determine if novel sequences are similar to those of known function, or to identify residues involved in key interactions. *In vitro* methods such as site-directed mutagenesis can then be used to mutate a single nucleotide or amino acid to validate *in silico* predictions. A slightly

more crude approach is to create loss-of-function mutants where the gene of interest is interrupted or deleted using methods including homologous recombination, the Red recombinase system and clustered regularly interspaced short palindromic repeats (CRISPR).

Homologous recombination involves the allelic replacement of genetic material. In bacteria, this process is used to repair DNA through two main pathways: the RecBCD pathway repairs double-stranded breaks while the RecF pathway repairs single-stranded breaks. Homologous recombination can also be utilised by researchers to create mutants, traditionally through restriction enzyme cloning although the Red recombination system from bacteriophage λ can also be harnessed to enable restriction-free cloning. This system was first used in *E.coli* (Datsenko and Wanner, 2000), but has since been modified for *P. aeruginosa* (Lesic and Rahme, 2008) and encodes three components: γ binds to endogenous RecBCD and SbcCD nucleases to prevent the digestion of the linear DNA fragments, *exo* is an exonuclease which degrades linear double-stranded DNA and β binds to the single-stranded DNA created by *exo* to promote annealing to a complementary target within the cell.

CRISPR are DNA sequences in prokaryotes originally derived from bacteriophages. The discovery of the CRISPR-associated protein Cas9 (Jinek *et al*., 2012) revolutionised gene editing since the endonuclease makes double-stranded DNA cuts at a location specified by the guide RNA. This system has also been modified for use in *P. aeruginosa* (Chen *et al*., 2018) to provide a cheaper, quicker and more efficient way of creating gene deletions.

A number of *P. aeruginosa* combinatorial RND efflux pump mutants have been described in the literature including a 4-pump mutant (*ΔmexAB-oprM ΔmexCD-oprJ ΔmexEF-OprN ΔmexXY*) (Morita *et al*., 2001), a 5-pump mutant (*ΔmexAB-oprM ΔmexCD-oprJ ΔmexEF-OprN ΔmexJK ΔmexXY*) (Mima *et al*., 2007), a 6-pump mutant (*ΔmexAB-oprM ΔmexCD-oprJ ΔmexEF-OprN ΔmexJKL ΔmexXY ΔtriABC*) (Adamiak *et al*., 2021) and a 9-pump mutant (*ΔmexAB-oprM ΔmexCD-oprJ ΔmexEF-OprN ΔmexJKL ΔmexXY ΔtriABC ΔmexGHI ΔmexVW Δmux*) (Adamiak *et al*., 2021). Our group was previously gifted strain K2733 (PAO1 *ΔmexAB-OprM*, *ΔmexCD-oprJ*, *ΔmexEF-oprN*, *ΔmexXY*) from Professor Keith Poole (Queen's University, Kingston, Canada). This efflux deletion mutant has been well characterised in the literature (Rampioni *et al*., 2017) but the parent strain K2732 was found to have unusually low *pqsA* expression levels as shown in **Appendix AF** (Jess Gray, MRes. Thesis), likely impacting QS.

In light of these findings, a series of single and combinatorial efflux pump deletion mutants were constructed by homologous recombination in PAO1 subline Lausanne (PAO1-L) which has functional quorum sensing. The parent strain will subsequently be referred to as PAO1-L-DS to avoid ambiguity with previously sequenced PAO1-L strains. Deletion of each efflux pump was confirmed by WGS and sequences were assessed for the introduction of unintended single nucleotide polymorphisms (SNPs) and Insertions/deletions (Indels).

2.2 Aims

- Construct a set of *P. aeruginosa* PAO1-L-DS chromosomal deletion mutants lacking each of the 12 RND efflux systems
- Construct a combinatorial series of *P. aeruginosa* PAO1-L-DS chromosomal deletion mutants lacking multiple RND efflux systems

2.3 Construction of a series of isogenic *P. aeruginosa* PAO1-L-DS efflux pump deletion mutants

Chromosomal efflux pump deletion mutants ΔAB, ΔCD, ΔEF, ΔGHI, ΔJK, ΔMN, ΔPQ, ΔXY, Δczc, Δmux and Δtri were constructed using the method described in **Section 6.2.8**, and visualised in **Figure 6.1**. This method utilises the suicide plasmid pEX18Gm, so-called because it can replicate in *E. coli* due to the presence of *ori* (ColE1-derived origin of replication) but not *P. aeruginosa*. The plasmid carries the *gm* gentamicin resistance gene to select for gentamicin resistance during the first recombination step, and the *sacB* levansucrase-encoding gene from *Bacillus subtilis* which is under the control of a sucrose-inducible promoter to select for sucrose resistance during the second recombination step. Attempts to make a ΔVW mutant proved unsuccessful. PCR confirmation of the suicide plasmids and in-frame deletions is provided in **Appendix B** to **Appendix M**.

2.3.1 Construction of pEX18 suicide plasmids and insertion into *E. coli* S17-1λ*pir*

The suicide plasmids were constructed using two approaches. The first approach was used in the construction of the pEX18Gm::*ΔmexEF-oprN* suicide plasmid and used a triple ligation method. A 775 bp fragment upstream of *mexE* which included the first 33 nucleotides of the gene was amplified from PAO1-L-DS template DNA. Similarly, an 815 bp fragment downstream of *oprN* which included the last 51 nucleotides of the gene was amplified. Both fragments and the pEX18Gm vector were similarly digested with restriction enzymes *Eco*RI and *Xba*I and ligated using T4 DNA ligase (New England Biolabs). The mixture was then transformed into *E. coli* S17-1λ*pir* and plated out onto LB agar supplemented with 20 μg/mL gentamicin to select for recombinants. Despite initial success, this method did not work for the construction of other suicide plasmids.

The second approach was used in the construction of all other suicide plasmids and used the commercial HiFi DNA assembly kit (New England Biolabs) which combines an exonuclease, polymerase and DNA ligase to assemble multiple fragments. Primers were designed to contain at least 20 bp homology between the fragments to be assembled. For each efflux pump of interest, regions of approximately 1000 bp immediately upstream and downstream were amplified using PAO1-L-DS template DNA. The pEX18Gm vector was

digested with restriction enzymes and incubated at 50°C with the upstream/ downstream fragments and the HiFi master mix before transformation into *E. coli* S17-1λ*pir* as above. Correct construction of the suicide vectors was confirmed by PCR with the pEX18_fwd primer to bind upstream of the multiple cloning site and the -1000_rev primer specific for the efflux pump of interest (**Table 2.1**). Suicide vectors were successfully constructed for all 12 efflux systems and the sequences were confirmed by Sanger DNA sequencing.

2.3.2 Construction of single *P. aeruginosa* PAO1-L-DS chromosomal efflux pump deletion mutants

The same double homologous recombination method was used to achieve allelic replacement of the wild-type DNA with the deletion variant. The suicide plasmid of interest was first conjugated into PAO1-L-DS and plated onto PIA agar supplemented with 30 μg/mL gentamicin to generate a population of gentamicin-resistant merodiploids during the first crossover event. Plasmid integration was confirmed by PCR using the primers detailed in **Table 2.1** before colonies were streaked onto TYS10 agar containing 10% w/v sucrose to negatively select for cells expressing the *sacB* gene. Sucrose-resistant colonies were screened for gentamicin sensitivity to confirm the second recombination event. The deletion was screened and verified by PCR using the +1000_fwd and -1000_rev primers for the efflux pump of interest (**Table 2.2**). In each case, the size of the fragment amplified from PAO1-L-DS corresponded to the sum of the efflux pump of interest and the flanking regions, while the size of the fragment amplified from the mutant corresponded to the flanking regions only. For additional confirmation, DNA fragments were sent for Sanger sequencing to confirm the absence of any secondary mutations in the flanking regions.

Despite successful construction of the pEX18Gm::*ΔmexVW* suicide plasmid, subsequent attempts to generate a ΔVW mutant proved unsuccessful. The first crossover event generated multiple colonies containing pEX18Gm::*ΔmexVW*, however during selection for the second crossover event all sucrose-resistant colonies reverted to wild-type. The process was repeated using two separate clones of pEX18Gm::*ΔmexVW* and more than 300 sucrose-resistant colonies were screened to no avail. As other studies have generated MexVW deletion mutants (Li *et al*., 2003) loss of this system is not lethal to *P. aeruginosa*.

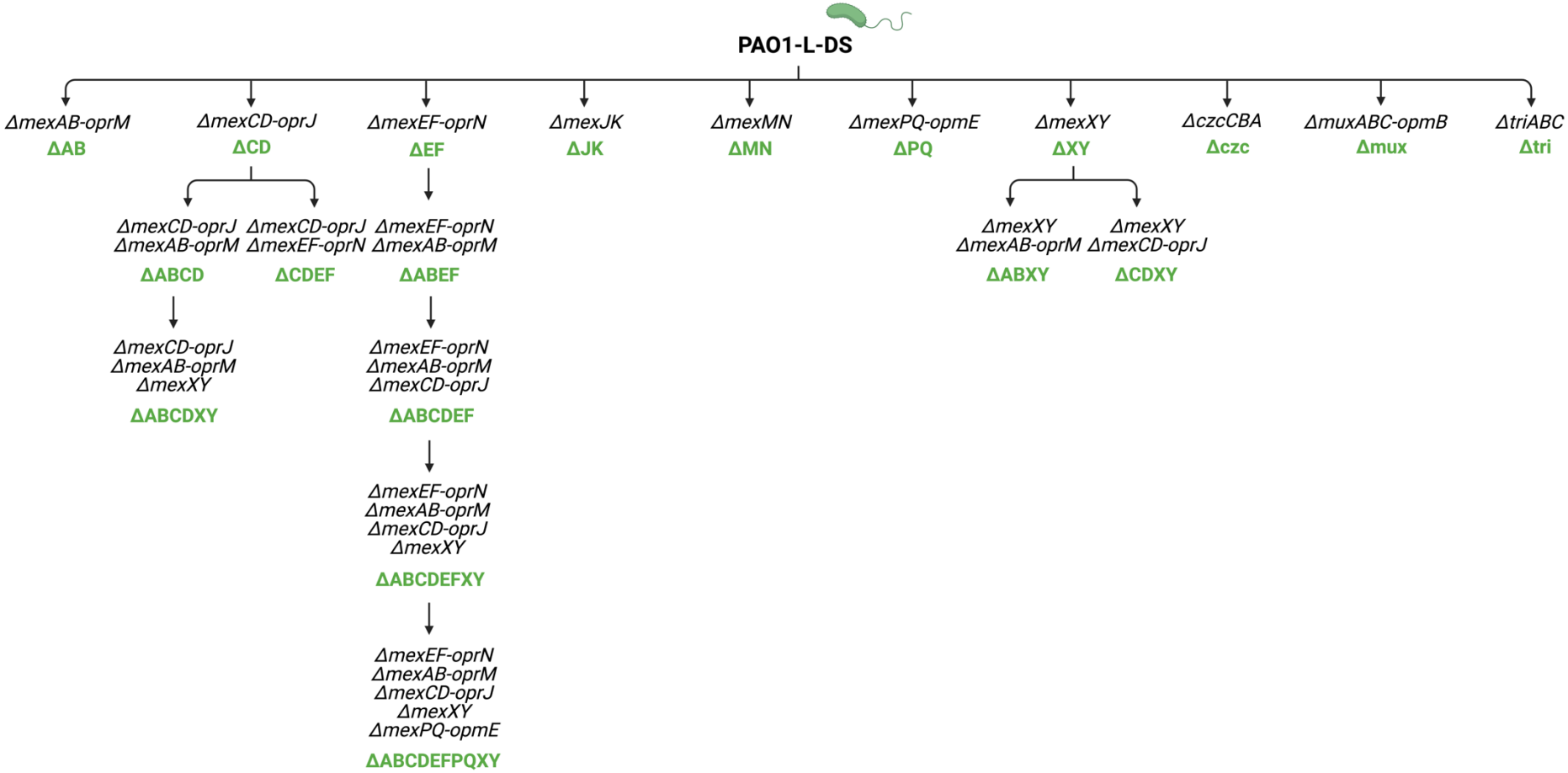
Table 2.1: Expected fragment sizes following the construction of the pEX18Gm suicide vectors

Efflux pump	Forward primer	Reverse primer	Fragment size (bp)
MexAB-OprM	pEX18_fwd	mexAB-oprM_-1000_rev	2,456
MexCD-OprJ	pEX18_fwd	mexCD-oprJ_-1000_rev	2,457
MexEF-OprN	pEX18_fwd	mexEF-oprN_-500_rev	1,590
MexGHI-OpmD	pEX18_fwd	mexGHI-opmD_-1000_rev	2,454
MexJK	pEX18_fwd	mexJK_-1000_rev	2,453
MexMN	pEX18_fwd	mexMN_-1000_rev	2,453
MexPQ-OpmE	pEX18_fwd	mexPQ-opmE_-1000_rev	2,463
MexVW	pEX18_fwd	mexVW_-1000_rev	2,456
MexXY	pEX18_fwd	mexXY_-1000_rev	2,457
CzcCBA	pEX18_fwd	czcCBA_-1000_rev2	2,610
MuxABC-OmpB	pEX18_fwd	muxABC-ompB_-1000_rev	2,453
TriABC	pEX18_fwd	triABC_-1000_rev	2,453

Table 2.2: Expected fragment sizes for second recombination event where upstream integration results in gene deletion and downstream integration reverts to wild-type (WT)

Efflux pump	Forward primer	Reverse primer	WT fragment size (bp)	Mutant fragment size (bp)
MexAB-OprM	mexAB-oprM_+1000_fwd	mexAB-oprM_-1000_rev	7,865	2,098
MexCD-OprJ	mexCD-oprJ_+100_fwd	mexCD-oprJ_-100_rev	5,910	148
MexEF-OprN	mexEF-oprN_+100_fwd	mexEF-oprN_-100_rev	5,981	195
MexGHI-OpmD	mexGHI-opmD_+1000_fwd	mexGHI-opmD_-1000_rev	8,134	2,096
MexJK	mexJK_+1000_fwd	mexJK_-1000_rev	6,192	2,095
MexMN	mexMN_+1000_fwd	mexMN_-1000_rev	6,270	2,095
MexPQ-OpmE	mexPQ-opmE_+1000_fwd	mexPQ-opmE_-1000_rev	7,802	2,105
MexVW	mexVW_+1000_fwd	mexVW_-1000_rev	6,254	2,106
MexXY	mexXY_+100_fwd	mexXY_-100_rev	4,582	244
CzcCBA	czcCBA_+1000_fwd2	czcCBA_-1000_rev2	8,134	2,252
MuxABC-OmpB	muxABC-ompB_+1000_fwd	muxABC-ompB_-1000_rev	11,013	2,095
TriABC	triABC_+1000_fwd	triABC_-1000_rev	7,268	2,095

Figure 2.1: Lineage of the efflux pump deletion mutants. Tree diagram displaying the parent strain PAO1-L-DS and the lineage of subsequent efflux pump deletion mutants. Green text indicates strain designations. Image created using BioRender.



2.3.3 Construction of combinatorial *P. aeruginosa* PAO1-L-DS chromosomal efflux pump deletion mutants

Strains lacking multiple efflux pumps were constructed as above but suicide plasmids were introduced into the efflux pump deletion mutant strains instead of the PAO1-L-DS parent strain. At each stage, the deletion was confirmed by PCR and Sanger sequencing. The lineage of the efflux pump deletion mutants is displayed in **Figure 2.1**.

2.4 Confirmation of efflux pump deletion by whole genome sequencing (WGS)

To confirm the chromosomal efflux pump deletions and determine whether any secondary mutations had occurred in unintended targets, the genomes of the PAO1-L-DS parent strain and the mutants were sequenced.

2.4.1 Assessment of raw read and alignment quality

Following an initial inspection of sequencing output, pre-processing was performed to remove adapter sequences and low-quality bases. Sample level quality was found to be acceptable (**Appendix O** & **Appendix P**). The Illumina short reads were then assembled into contigs and aligned to the PAO1-UW (Stover *et al*., 2000) reference genome in a manner that was tolerant of errors, mismatches, and gaps. PAO1-UW has a large 2.2 Mb inversion not observed in other PAO1 sequences which is a likely computational error, in addition to the loss of the 12 kb RGP42 island (Klockgether *et al*., 2010). Assembly metrics were assessed and found to be acceptable (**Appendix Q** & **Appendix R**).

Multiple genome comparisons were generated to visualise the deletions. The gaps in each chromosome correspond to the location of the appropriate efflux pumps (**Figure 2.2**, **Figure 2.3** & **Figure 2.4**). Mutants ΔGHI and Δczc lack visible gaps in their chromosomes at the locations of MexGHI-OpmD and CzcCBA respectively (**Figure 2.3**). Further inspection of the alignment files found while that Δczc does not have any reads mapped to CzcCBA, ΔGHI has reads mapped across the whole of the *mexGHI-opmD* operon (**Appendix S**). Therefore, despite originally believing a *ΔmexGHI-opmD* mutant had been constructed, WGS identified that this was not the case so this strain is not included in further downstream analysis.

Figure 2.2: Comparative genome assembly of the K2732 (PAO1 WT) and K2733 (Δ*mexAB-oprM* Δ*mexCD-oprJ* Δ*mexEF-oprN* Δ*mexXY* against the PAO1-UW reference genome. Gaps in each ring correspond to regions with no sequence alignment. The location of each of the deleted efflux pumps on the genome is indicated. Image created using BLAST Ring Image Generator (BRIG) (Alikhan *et al*., 2011).

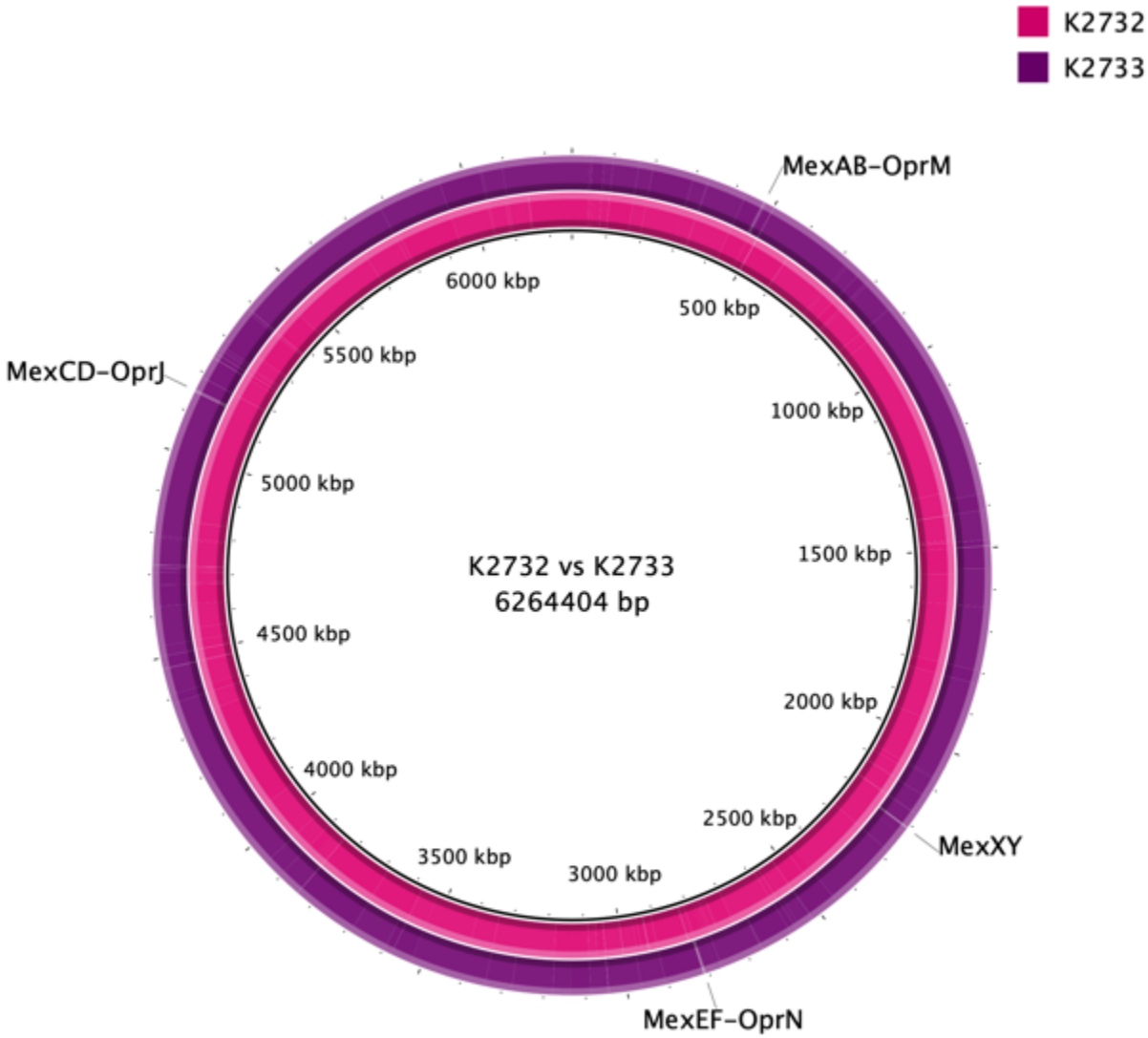


Figure 2.3: Comparative genome assembly of the PAO1-L-DS single efflux pump deletion mutants against PAO1-UW reference genome. Gaps in each ring correspond to regions with no sequence alignment. The location of each of the deleted efflux pumps on the genome is indicated. Image created using BLAST Ring Image Generator (BRIG) (Alikhan *et al*., 2011).

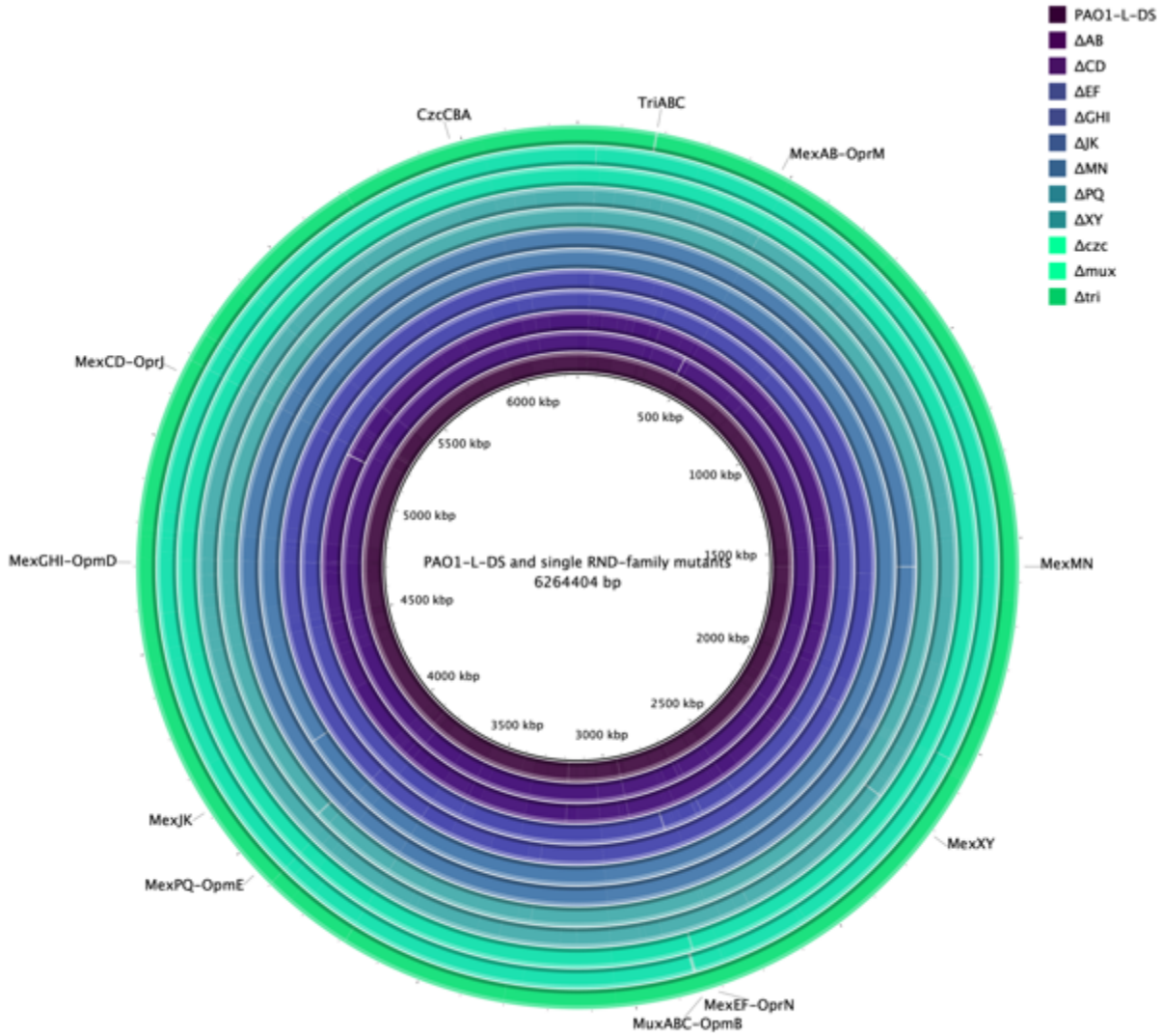
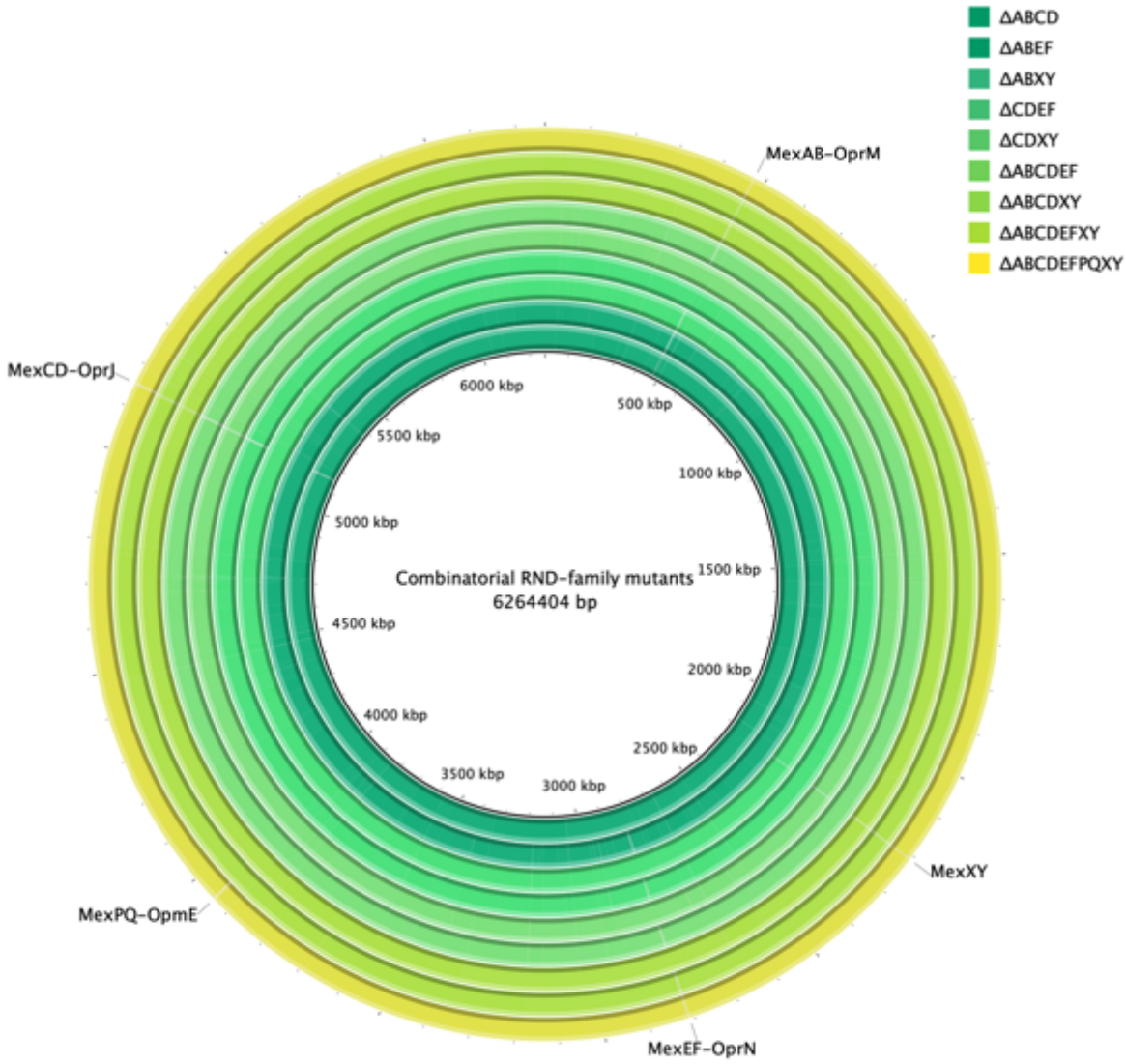


Figure 2.4 Comparative genome assembly of the PAO1-L-DS combinatorial efflux pump deletion mutants against PAO1-UW reference genome. Gaps in each ring correspond to regions with no sequence alignment. The location of each of the deleted efflux pumps on the genome is indicated. Image created using BLAST Ring Image Generator (BRIG) (Alikhan *et al.*, 2011).



2.4.2 Analysis of variants

Variant calling is used to identify differences between the sample reads and the reference genome, and to determine whether these differences are the result of true variants or reads that have been misaligned, had incorrect bases called or contain sequencing artefacts.

2.4.2.1 Identification of variants responsible for QS defects in K2732

Whole genome sequencing of both K2732 and K2733 revealed 6 SNP/Indels which were present in K2732 and absent from PAO1-UW and PAO1-L-DS (**Table 2.3**). These included a GGCCAGCC deletion frequently observed at position 2807693 of the *mexT* gene, which results in a frame shift and the premature termination of the protein. It was originally thought that *nfxC* mutants expressed a functional copy of *mexT*, while wild-type strains produced this truncated version of the MexT protein and did not express MexEF-OprN (Köhler *et al*., 1999; Maseda *et al*., 2000). However, it has since been shown that the *mexT* start site was misannotated in the PAO1-UW reference genome so *nfxC* mutants produce a truncated version of the MexT protein while wild-type strains do not (LoVullo & Schweizer, 2020). Therefore, K2732 does not possess a functional copy of MexT and is unable to express MexEF-OprN.

The functional effect of amino acid substitutions was analysed using the Protein variation effect analyzer (PROVEAN) (Choi and Chan, 2015). The SNP's in PA1611, PA4133 and *fimV* had a PROVEAN score less than -2.5 predicting a deleterious effect on the protein. As two of the genes are uncharacterised and the FimV protein is required for the assembly of TFP, further investigation is required to determine which might be responsible for the effects on the PQS system.

Table 2.3: Single nucleotide polymorphisms, insertions and deletions in K2732 compared to the PAO1-UW reference genome that were not observed in PAO1-L-DS.

Position	Gene ID	Gene name	TYPE	REF	ALT	Reference codon	Mutated codon	Amino acid change	PROVEAN score	Prediction	Effect
1754121	PA1611	-	snp	C	T	GCC	GTC	G481D	-5.401	Deleterious	missense_variant c.1442G>A p.Gly481Asp
2807693	PA2492	*mexT*	del	TCGGC CAGC	T	CCT	CCT	P75P	ND	ND	frameshift_variant c.240_247delGCCGGCCA p.Gln80fs
2807949	PA2492	*mexT*	ins	C	CT	CTG	CTT	L161L	ND	ND	frameshift_variant c.482dupT p.Leu162fs
3497107	PA3115	*fimV*	snp	G	A	CTG	CTA	Q367*	ND	Deleterious	stop_gained c.1099C>T p.Gln367*
4623539	PA4133	-	snp	T	C	GTC	GCC	V243A	-3.817	Deleterious	missense_variant c.728T>C p.Val243Ala
5069340	PA4525	*pilA*	snp	G	T	GCT	TCT	S65R	-0.237	Neutral	missense_variant c.192C>A p.Ser64Arg

2.4.2.2 Comparison of variants found in PAO1-L

The Lausanne (PAO1-L) subline originates from the University of Lausanne, Switzerland and can be differentiated from other sublines commonly used in our lab including Nottingham (PAO1-N) which has a 59 Kb deletion spanning PA4280.5 to the start codon of *toxR* (Dubern *et al*., 2022) and Washington (PAO1-W) by the presence of a C→G SNP at position 4448855 and a G→C SNP at position 4448856 (Hardeep Naghra, PhD Thesis). PAO1-L was previously sequenced in 2015 and this strain will henceforth be referred to as PAO1-L-HN (GenBank accession number: CP099798).

When compared to the PAO1-UW reference genome 49 SNPs and Indels were identified in PAO1-L-DS including the SNPs detailed above, confirming that PAO1-L-DS belongs to the Lausanne subline (**Table 2.4**). Forty-eight of these SNP/Indels were conserved between PAO1-L-DS and PAO1-L-HN, including a T→A substitution at position 4058657 in *mexT* which changes the codon from TTC→ATC. As PAO1-L-DS and PAO1-L-HN do not contain the 8 bp deletion observed in K2732, this data confirms they possess a functional copy of MexT and are able to express MexEF-OprN. All SNP/Indels had a PROVEAN score > -2.5 predicting that the variations would not have a deleterious effect on the protein (**Table 2.5**).

The only SNP/Indel present in PAO1-L-DS which was not identified in PAO1-L-HN was an A→AC insertion at position 891099, and there were 4 SNP/Indels identified in PAO1-L-HN which were not present in PAO1-L-DS (**Table 2.6**). These variations may have occurred spontaneously during routine laboratory culture.

2.4.2.3 Comparison of variants in the RND efflux pump mutants

Ten SNPs were identified in one or more of the mutants, that were not present in the PAO1-L-DS parent strain (**Table 2.7**). Of these, 4 were located in coding regions and PROVEAN analysis predicts that a C→T SNP at position 5069943 of the *pilB* gene of the ΔAB mutant is deleterious to the protein. This changes the codon from CAG→TAG and introduces a stop codon but as this amino acid change was only present in 61/566 reads it is unlikely to be a true SNP (**Table 2.8**). Together, these data did not identify any secondary mutations that might produce phenotypic changes unrelated to the loss of efflux.

Table 2.4: Single nucleotide polymorphisms, insertions and deletions identified in PAO1-L-DS and PAO1-L-HN compared to the PAO1-UW reference genome. Grey shading indicates the presence and white shading indicates the absence of each SNP/indel for each strain

Position	Gene ID	Gene name	TYPE	REF	ALT	PAO1-L-HN	PAO1-L-DS
169283	-	-	del	CG	C		
183697	PA0159	-	snp	T	G		
411125	-	-	del	AC	A		
413850	-	-	snp	T	C		
667028	-	-	ins	G	GC		
721611	-	-	snp	C	T		
721622	-	-	snp	C	T		
721663	-	-	complex	TCCCAGGA	CTCCGGGG		
721718	-	-	snp	A	G		
721725	-	-	snp	C	T		
721740	-	-	snp	C	T		
740419	PA0683	*hxcY*	ins	G	GC		
816529	-	-	ins	G	GC		
891099	-	-	ins	A	AC		
1116213	-	-	ins	G	GC		
1215657	-	-	ins	A	AG		
1275766	PA1174	*napA*	del	GA	G		
1440622	PA1327	-	del	CA	C		
1445357	-	-	ins	A	AG		
1467483	-	-	complex	C	GCG		
1589438	PA1459	-	snp	G	C		
1835045	PA1685	*masA*	ins	G	GC		
2169348	-	-	ins	A	AG		

2186927	-	-	ins	G	GC
2195457	-	-	ins	G	GC
2239547	-	-	snp	T	G
2239555	-	-	ins	A	AG
2342110	-	-	ins	C	CT
2355771	-	-	ins	A	AG
2356681	PA2141	-	del	GC	G
2532046	-	-	ins	G	GC
2669175	PA2400	*pvdJ*	snp	G	C
2753522	-	-	ins	G	GC
2807982	PA2492	*mexT*	snp	T	A
3016844	-	-	ins	G	GC
3083196	-	-	ins	A	AG
3919508	-	-	ins	G	GC
4212201	PA3760	-	snp	A	G
4344266	PA3877	*narK1*	snp	A	G
4448855	-	-	mnp	C	G
4448856	-	-	mnp	G	C
4539468	-	-	ins	G	GC
4869855	PA4341	-	snp	T	G
4888194	-	-	ins	A	AG
4924552	PA4394	-	complex	CG	GC
5033101	PA4496	-	ins	G	GC
5036891	-	-	snp	A	C
5071543	-	-	del	AACTG	A
5472415	-	-	ins	C	CG
5655220	PA5024	-	ins	C	CCGG

5743461	PA5100	*hutU*	mnp	CG	GC	
6079222	PA5399	*dgcB*	snp	A	G	
6098781	PA5418	*soxA*	snp	G	C	
6115455	PA5434	*mtr*	snp	T	G	

snp signifies single nucleotide polymorphism; ins signifies insertion; del signifies deletion

Table 2.5: Predicted impact of single nucleotide polymorphisms, insertions and deletions found in PAO1-L-DS compared to PAO1-UW on the biological function of the protein. If the PROVEAN score is less than, or equal to -2.5 then the variant is predicted to have a deleterious effect.

Position	Gene ID	Gene name	TYPE	REF	ALT	Reference codon	Mutated codon	Amino acid change	PROVEAN score	Prediction (cutoff= -2.5)	Effect
183697	PA0159	-	snp	T	G	TGT	TGG	C310W	4.215	Neutral	missense_variant c.930T>G p.Cys310Trp
740419	PA0683	*hxcY*	ins	G	GC	GTA	GCT	V73A	-0.964	Neutral	frameshift_variant c.217_218insC p.Val73fs
1275766	PA1174	*napA*	del	GA	G	GAA	CGA	F11S	ND	ND	frameshift_variant c.32delT p.Phe11fs
1440622	PA1327	-	del	CA	C	AAA	AAG	K640K	ND	ND	frameshift_variant c.1920delA p.Pro642fs
1589438	PA1459	-	snp	G	C	GGC	GCC	G34A	3.826	Neutral	missense_variant c.101G>C p.Gly34Ala
1835045	PA1685	*masA*	ins	G	GC	AGT	AGC	S218S	0.000	Neutral	frameshift_variant c.653_654insC p.Ser219fs
2356681	PA2141	-	del	GC	G	GCC	GCC	A172A	ND	ND	frameshift_variant c.517delC p.Leu173fs
2669175	PA2400	*pvdJ*	snp	G	C	CGG	CGC	P819A	2.909	Neutral	missense_variant c.2455C>G p.Pro819Ala
2807982	PA2492	*mexT*	snp	T	A	TTC	ATC	F172I	2.431	Neutral	missense_variant c.514T>A p.Phe172Ile

4212201	PA3760	-	snp	A	G	CAC	CGC	H636R	4.896	Neutral	missense_variant c.1907A>G p.His636Arg
4344266	PA3877	*narK1*	snp	A	G	AAG	GAG	L190L	0.000	Neutral	synonymous_variant c.570T>C p.Leu190Leu
4869855	PA4341	-	snp	T	G	TTC	GTC	E158D	-0.071	Neutral	missense_variant c.474A>C p.Glu158Asp
4924552	PA4394	-	complex	CG	GC	CAC, GGG	CAG, CGG	V178L, P177P	-0.128, 0.000	Neutral, Neutral	missense_variant c.531_532delCGinsGC p.Val178Leu
5033101	PA4496	*dppA1*	ins	G	GC	TAG	TAG	*528*	0.000	Neutral	intragenic_variant n.5033101_5033102insC
5655220	PA5024	-	ins	C	CC GG	GCC	GCC	A222A	ND	ND	conservative_inframe_insertion c.673_675dupGGC p.Gly225dup
5743461	PA5100	*hutU*	mnp	CG	GC	CGT	GCT	T431S	0.907	Neutral	missense_variant c.1292_1293delCGinsGC p.Thr431Ser
6079222	PA5399	*dgcB*	snp	A	G	CTA	CTG	L393L	0.000	Neutral	synonymous_variant c.1179A>G p.Leu393Leu
6098781	PA5418	*soxA*	snp	G	C	GGG	GGC	G586G	0.000	Neutral	synonymous_variant c.1758G>C p.Gly586Gly
6115455	PA5434	*mtr*	snp	T	G	TTT	GTT	K286N	1.152	Neutral	missense_variant c.858A>C p.Lys286Asn

Table 2.6 Single nucleotide polymorphisms, insertions and deletions present in PAO1-L-HN but not PAO1-L-DS, when compared to the PAO1-UW reference genome.

Position	Gene ID	Gene name	TYPE	REF	ALT
721718	-	-	snp	A	G
721725	-	-	snp	C	T
721740	-	-	snp	C	T
727254	PA0668.5	-	ins	T	TCC
727257	-	-	del	T	-
740420	PA0683	*hxcY*	ins	T	TC
816533	PA0748	-	ins	G	GC
891101	-	-	ins	G	GC
1116214	PA1029	-	Ins	T	TC
1215660	PA1122	-	Ins	A	AG
1275769	PA1174	*napA*	del	T	-
1440626	PA1327	-	del	G	-
1445358	-	-	Ins	C	CG
1835046	PA1685	*masA*	ins	T	TC
2169351	-	-	ins	A	AG
2186928	-	-	Ins	G	GC
2195463	-	-	Ins	T	TG
2239556	-	-	Ins	C	CG
2342112	-	-	Ins	C	CT
2355772	PA2139	-	ins	C	CG
2356685	PA2141	-	del	T	-
2532047	-	-	Ins	T	TC
2753523	PA2452	-	ins	T	TC
3016846	PA2668	-	ins	A	AC

3083197	PA2727	-	ins	C	CG
3919509	-	-	ins	G	GC
4539470	PA4059	-	ins	G	GC
4888194	PA4360	-	Ins	A	AG
5230036	-	-	Ins	C	CA
5234824	PA4666	*hemA*	del	T	-
5242101	PA4673.1	-	del	C	-
5655220	PA5024	*ytnM*	ins	C	CCGG

snp signifies single nucleotide polymorphism; ins signifies insertion; del signifies deletion

Table 2.7 Single nucleotide polymorphisms, insertions and deletions in the efflux pump deletion mutants compared to the PAO1-L-DS parent strain. Grey shading indicates the presence and white shading indicates the absence of each SNP/indel for each of the sequenced RND efflux mutants

Position (*)	Gene ID	Gene name	TYPE	REF	ALT	ΔAB	ΔCD	ΔEF	ΔJK	ΔMN	ΔPQ	ΔXY	Δczc	Δmux	Δtri	ΔABCD	ΔABEF	ΔABXY	ΔCDEF	ΔCDXY	ΔABCDEF	ΔABCDXY	ΔABCDEFXY	ΔABCDEFPQXY
721718	-	-	snp	A	G	■	■	■	■	■			■	■	■	■		■	■		■	■		
721725	-	-	snp	C	T	■	■	■		■			■	■	■	■		■				■		
721740	-	-	snp	C	T					■			■		■	■		■				■		
1725926	PA1585	*sucA*	snp	C	T					■														
1844903	PA1695	*pscP*	ins	T	TGTTGGC																	■		
2186927	-	-	ins	G	GC	■		■								■		■	■		■	■	■	
2814749	-	-	snp	G	A			■									■		■		■		■	■
5069943	PA4526	*pilB*	snp	C	T	■																		
5096219	PA4547	*pilR*	snp	A	C		■									■			■			■		

Table 2.8: Predicted impact of single nucleotide polymorphisms, insertions and deletions in the efflux pump deletion mutants compared to PAO1-L-DS on the biological function of the protein. If the PROVEAN score is less than, or equal to -2.5 then the variant is predicted to have a deleterious effect.

Position	Gene ID	Gene name	TYPE	REF	ALT	Reference codon	Mutated codon	Amino acid change	PROVEAN score	Prediction	Effect
1725926	PA1585	*sucA*	snp	C	T	ACC	ACT	T561T	0.000	Neutral	synonymous_variant c.1683C>T p.Thr561Thr
1844903	PA1695	*pscP*	ins	T	TGTTGGC	ACT	ACT	T117T	-0.017	Neutral	disruptive_inframe_insertion c.345_350dupGCCAAC p.Thr117_Val118insProThr
5069943	PA4526	*pilB*	snp	C	T	CAG	TAG	Q61*	ND	Deleterious	stop_gained c.181C>T p.Gln61*
5096219	PA4547	*pilR*	snp	A	C	CAG	CCG	Q412P	-2.490	Neutral	missense_variant c.1235A>C p.Gln412Pro

2.5 Discussion

Using homologous recombination, single mutants lacking 10 of the 12 RND efflux pumps were successfully constructed and confirmed by WGS, including the first MexMN deletion mutant to be described. Mutants lacking different combinations of RND efflux pumps were also constructed, culminating in a 5-pump chromosomal deletion mutant (PAO1-L-DS *ΔmexAB-oprM ΔmexCD-oprJ ΔmexEF-OprN ΔmexPQ-opmE ΔmexXY*). Though attempts to construct a *ΔmexVW* mutant failed, a *ΔmexGHI-opmD* mutant was believed to have been successfully constructed until WGS unexpectedly revealed reads mapping to the *mexGHI-opmD* operon. Subsequent amplification of the region by PCR confirmed the presence of the MexGHI-OpmD efflux pump therefore this was not a sequencing error and is likely to be the result of a strain mix-up.

It is important to note that the whole *mexAB-oprM* operon was deleted including the *oprM* gene. This gene encodes the outer membrane component OprM which associates with several RND components in addition to MexB including MexK, MexN, MexW and MexY. MexXY has been shown to associate with OprA in addition to OprM (Morita *et al*., 2012), while MexVW may also be able to associate with other OMPs (Li *et al*., 2003). MexJK does not require an OMP for the efflux of triclosan (Chuanchuen *et al*., 2002), but MexMN can only associate with OprM (Mima *et al*., 2005) so single and combinatorial mutants lacking MexAB-OprM are unlikely to have functional copies of all of the other efflux pumps. This is an important consideration for future studies.

Traditionally, once a gene has been mutated or deleted a copy of the native gene located on an expression vector is inserted into the bacterium to produce a complementation mutant. These mutants are then used to confirm that any changes in phenotype are due to the deleted gene. However, previous studies have noted that the phenotypes of efflux pump mutants are not always fully restored in complementation mutants (Köhler *et al*., 1997; Nehme *et al*., 2004; Vogne *et al*., 2004; Minagawa *et al*., 2012). Complementation plasmids do not always replicate native protein expression levels or the timing of expression as they are usually introduced on plasmids with strong constitutive promoters. For this reason, each chromosomal mutant was sent for whole genome sequencing to confirm the deletions and also to determine whether any secondary mutations had occurred. Compared to the parental PAO1-L-DS strain, 10 SNPs and Indels

were observed in the isogenic mutants. None were predicted to have a deleterious effect on the protein except one SNP in the *pilB* gene of the ΔAB mutant. As this SNP was observed in less than 11% of reads it is likely to be an incorrect base call rather than a genuine variant. Sanger sequencing of the *pilB* gene could be used to confirm the nucleotide sequence.

The large number of *P. aeruginosa* combinatorial RND family efflux pump mutants constructed during this study and others (Morita *et al*., 2001; Mima *et al*., 2007; Adamiak *et al*., 2021) suggests the loss of a large number of efflux pumps is not lethal. A recent study in *E. coli* K12 supports this hypothesis, where the inactivation of 35 efflux pumps resulted in a strain with impaired fitness but which was still viable (Teelucksingh *et al*., 2022). It would be interesting to introduce subsequent deletions into ΔABCDEFPQXY to determine whether efflux pumps are essential for viability in *P. aeruginosa*.

Finally, it has been suggested that deletion mutants are a poor model for the study of efflux pumps as any phenotypic changes might be due to changes in the membrane structure resulting from the loss of large proteins rather than the absence of efflux itself (Wang-Kan *et al*., 2017). Mutants could be reconstructed using site-directed mutagenesis of key residues and compared with the deletion mutants. Alternatively, changes to cell morphology could be observed using scanning electron microscopy, and changes to the cell wall could be visualised using transmission electron microscopy. To determine whether cell permeability increased following deletion of the efflux pump proteins, the leakage of intracellular ions (eg. K^+ and Ca^{2+}) from cell supernatants could be measured using an inductively coupled plasma mass spectrometer. Intracellular ATP could also be quantified using an ATP determination kit to determine whether loss of efflux alters energy metabolism.

2.6 Summary of key findings

- Individual mutants lacking 10 out of the 12 RND efflux pumps were successfully obtained
- Mutants lacking different combinations of RND efflux pumps were constructed, culminating in a mutant lacking 5 RND efflux pumps
- Whole genome sequencing confirms that efflux pump deletion has not resulted in any deleterious downstream SNP/Indels

2.7 Future work

- Construct *ΔmexGHI-opmD* and *ΔmexVW* single mutants
- Continue to introduce subsequent deletions to determine whether efflux pumps are essential for *P. aeruginosa* viability
- Create loss-of-function mutants and compare results
- Determine whether the absence of the efflux pump proteins results in any structural changes to the cell envelope
- Determine whether the absence of the efflux pump proteins results in any changes to the integrity of the cytoplasmic membrane

CHAPTER 3:

Transcriptomic changes caused by loss of MexAB-OprM, MexCD-OprJ, MexEF-OpN and MexXY in *P. aeruginosa* PAO1-L-DS

3. Transcriptomic changes caused by loss of MexAB-OprM, MexCD-OprJ, MexEF-OprN and MexXY in *P. aeruginosa* PAO1-L-DS

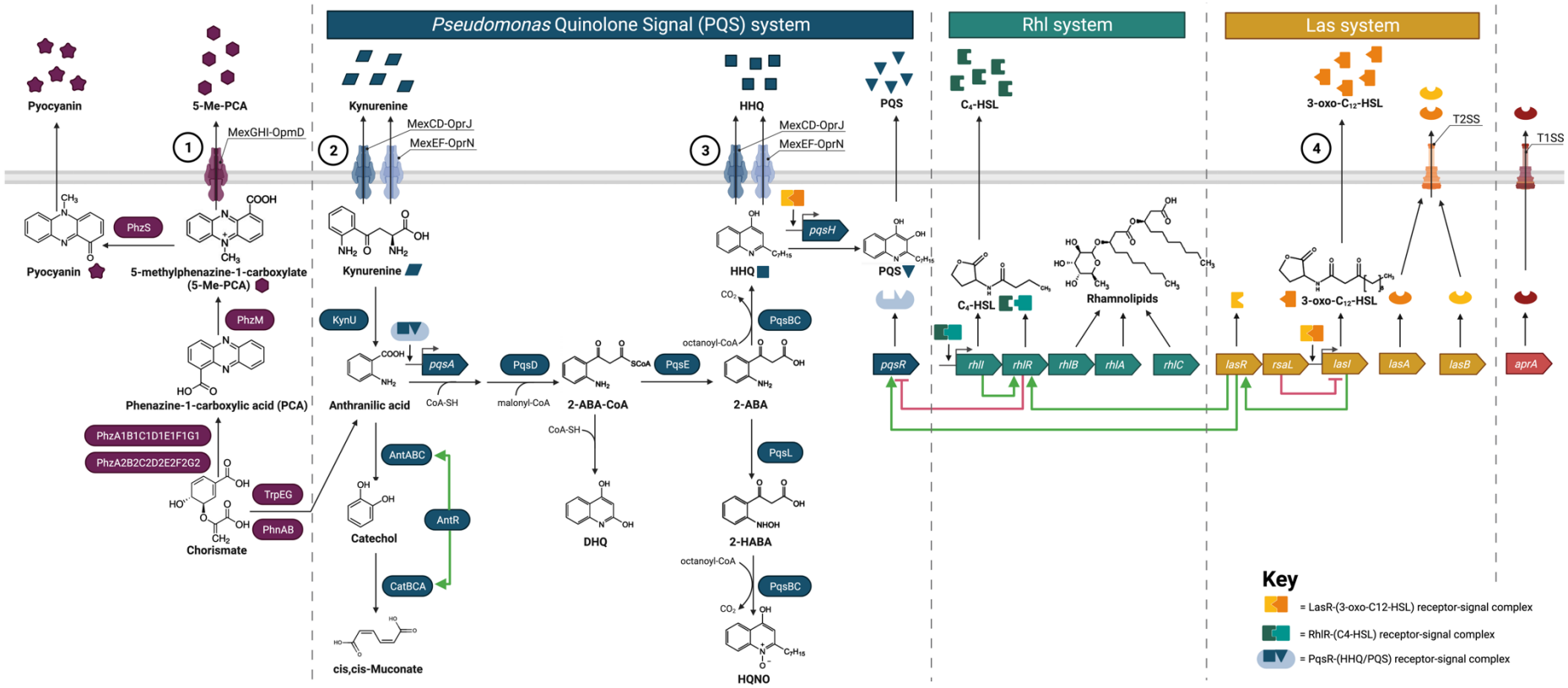
3.1 Background

P. aeruginosa infections are difficult to treat due to intrinsic, acquired and adaptive mechanisms of antimicrobial resistance. The MexAB-OprM, MexCD-OprJ, MexEF-OprN and MexXY-OprM multi-drug efflux pumps are important resistance determinants and extrude structurally diverse antibiotics such as aminoglycosides, β-lactams and fluoroquinolones (Poole, 2007). These four pumps also export a wide range of other toxic compounds across the cytoplasmic membrane including dyes, heavy metals and biocides. Members of the Resistance-Nodulation-Division family, as their name might suggest, are known to have additional functions within the cell (Piddock, 2006; Blanco *et al*., 2016) and have been linked to changes in quorum sensing and metabolism.

The *P. aeruginosa* quorum sensing regulatory network controls the production of many virulence factors, metabolites and biofilm development in a cell density-dependent manner. The *lasRI* and *rhlRI* quorum sensing systems produce the autoinducers 3-oxo-C_{12}-HSL and C_4-HSL respectively, while the *pqsABCDE/pqsH/pqsR* system produces HHQ and PQS (Williams and Cámara, 2009). The known links between quorum sensing and efflux in *P. aeruginosa* are summarised in **Figure 3.1**, however little is known about the mechanisms underlying these associations.

To further study the contribution of RND efflux pumps to the lifestyle of *P. aeruginosa*, the transcriptomes of *P. aeruginosa* PAO1-L-DS and a mutant lacking the four RND efflux pumps linked to antimicrobial resistance: MexAB-OprM, MexCD-OprJ, MexEF-OprN and MexXY, were evaluated using RNA-Seq. Several other groups have used transcriptomics as a tool to study efflux pumps in *P.aeruginosa*. Wang *et al*. (2013) first used RNA-Seq to identify the ParS/ParR TCS as a regulator of MexEF-OprN in addition to the Rhl and Pqs quorum sensing systems. Olivares *et al*., (2012) characterised a MexEF-OprN overexpressing mutant and found that PQS-regulated genes were downregulated. Alcalde-Rico *et al*., (2020) characterised the changes associated with overexpression of *mexR* and found that attenuation of quorum sensing in this mutant was due to reduced availability of octanoate

Figure 3.1 Summary of known links between RND efflux pumps and bacterial physiology in *P. aeruginosa* 1) 5-Me-PCA is exported by MexGHI-OpmD (Sakhtah *et al*., 2016) 2) Kynurenine is exported by MexCD-OprJ and MexEF-OprN (Olivares *et al*., 2012; Alcalde-Rico *et al*., 2018) 3) HHQ is exported by MexCD-OprJ and MexEF-OprN (Lamarche and Déziel, 2011; Alcalde-Rico *et al*., 2018) 4) 3-oxo-C_{12}-HSL is not exported by MexAB-OprM (Alcalde-Rico *et al*., 2020). Green arrows indicate positive gene regulation and red blunted arrows indicate negative gene regulation. Image created using BioRender.



impacting AQ biosynthesis. Most recently, Adamiak *et al*., (2021) characterised the transcriptome of a PAO1 strain lacking MexAB-OprM, MexCD-OprJ, MexEF-OprN, MexJKL, MexXY and TriABC. Here we present the first study characterising the transcriptome of a mutant lacking the MexAB-OprM, MexCD-OprJ, MexEF-OprN and MexXY efflux pumps.

Following transcriptome sequencing, differentially expressed genes (DEG) were validated using a combination of transcriptional reporters and *in vitro* assays. In addition, AHL and AQ levels were measured from whole cell and culture supernatants by LC-MS to quantify changes in the intracellular and extracellular concentrations of quorum sensing signalling molecules.

3.2 Aims

- Explore the transcriptomic changes arising due to loss of the MexAB-OprM, MexCD-OprJ, MexEF-OprN and MexXY efflux pumps in *P. aeruginosa* PAO1-L-DS by RNA sequencing
- Confirm changes in gene expression
- Identify the phenotypes associated with changes in the transcriptome

3.3 Hypothesis

- Loss of MexAB-OprM, MexCD-OprJ, MexEF-OprN and MexXY changes the transcriptome of *P. aeruginosa* PAO1-L-DS
- Loss of MexAB-OprM, MexCD-OprJ, MexEF-OprN and MexXY alters *P. aeruginosa* PAO1-L-DS physiology

3.4 Transcriptomic changes arising from loss of MexAB-OprM, MexCD-OprJ, MexEF-OprN and MexXY in *P. aeruginosa* PAO1-L-DS

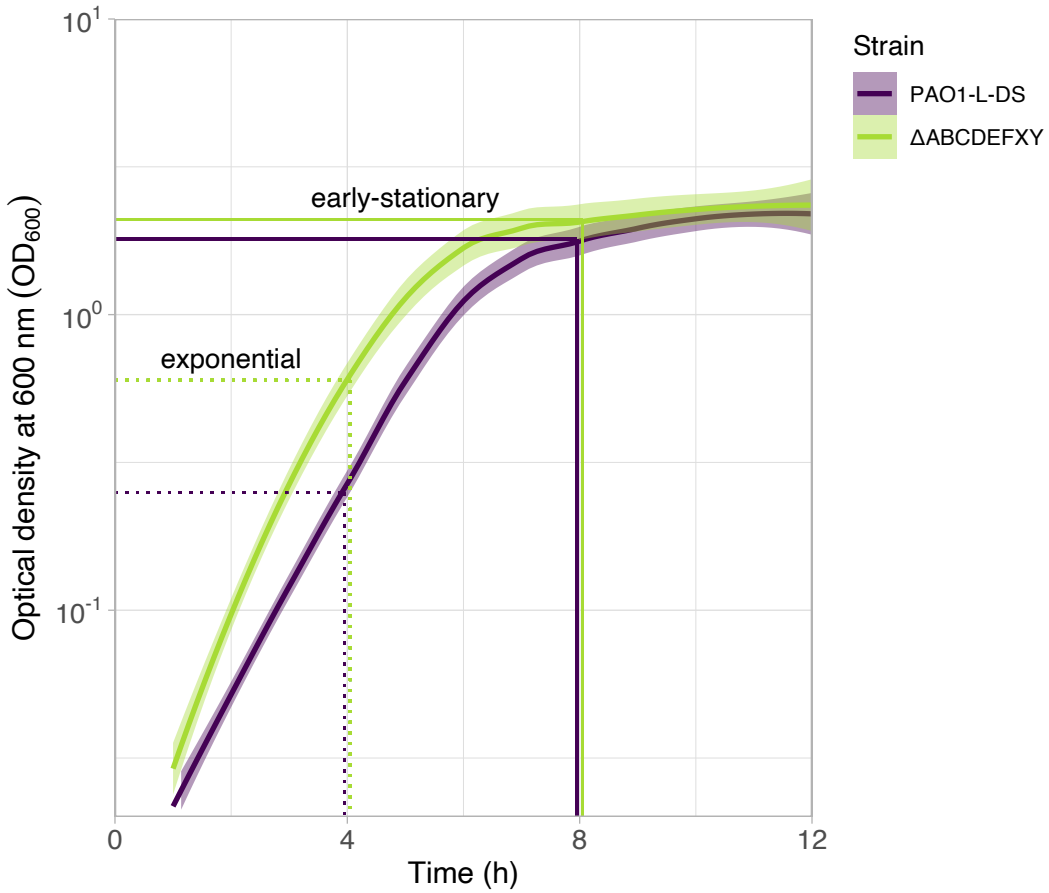
To assess the impact of MexAB-OprM, MexCD-OprJ, MexEF-OprN and MexXY deletion on gene expression in *P. aeruginosa*, the transcriptomes of PAO1-L-DS and the ΔABCDEFXY mutant were compared. Strains were grown in a rich medium (LB) without the addition of antimicrobial agents to explore the biological processes affected by efflux in the absence of stress.

The growth profiles of each strain in LB were defined (**Figure 3.2A**) and three biological replicates of each strain were grown to either exponential phase (OD_{600} 0.6 – 0.8) or early stationary phase (OD_{600} 1.5 - 2). These two distinct phases were chosen as the expression of some efflux pumps is growth-phase dependent, including MexAB-OprM whose expression increases with cell growth and peaks at early stationary phase when population density reaches OD_{600} 1.5 (Evans & Poole, 1999; Maseda *et al*., 2004). It is also known that the majority of quorum sensing controlled genes are expressed in cultures with an OD_{600} greater than 2.0, but not at all at an OD_{600} less than 0.8 (Schuster *et al*., 2003). As quorum sensing and efflux are interlinked, we wanted to compare the changes caused by loss of efflux before and after these systems are switched on.

Strains were grown for either 4 h (exponential phase) or 8 h (early stationary phase), and the optical density of each strain is detailed in **Figure 3.2B**. Cultures were centrifuged before the supernatant was discarded and the whole cell pellets were shipped on dry ice to Novogene (Cambridge, UK) where RNA extraction, quality control evaluation and sequencing were performed (**Appendix U, Appendix V** & **Appendix W**).

Figure 3.2. Selection of samples for RNA-Seq A) Overnight cultures of PAO1-L-DS and the ΔABCDEFXY mutant were standardized to OD_{600} 0.01 and grown in LB at 37°C with shaking at 200 rpm for 12 h. The optical density of each culture was measured every hour at a wavelength of 600 nm B) The OD_{600} of each sample sent for RNA extraction and sequencing

A



B

Sample	OD_{600}
PAO1-L-DS_exponential_1	0.66
PAO1-L-DS_exponential_2	0.68
PAO1-L-DS_exponential_3	0.6
ΔABCDEFXY_exponential_1	0.621
ΔABCDEFXY_exponential_2	0.598
ΔABCDEFXY_exponential_3	0.561
PAO1-L-DS_stationary_1	1.59
PAO1-L-DS_stationary_1	1.68
PAO1-L-DS_stationary_1	1.6
ΔABCDEFXY_stationary_1	1.44
ΔABCDEFXY_stationary_1	1.71
ΔABCDEFXY_stationary_1	1.73

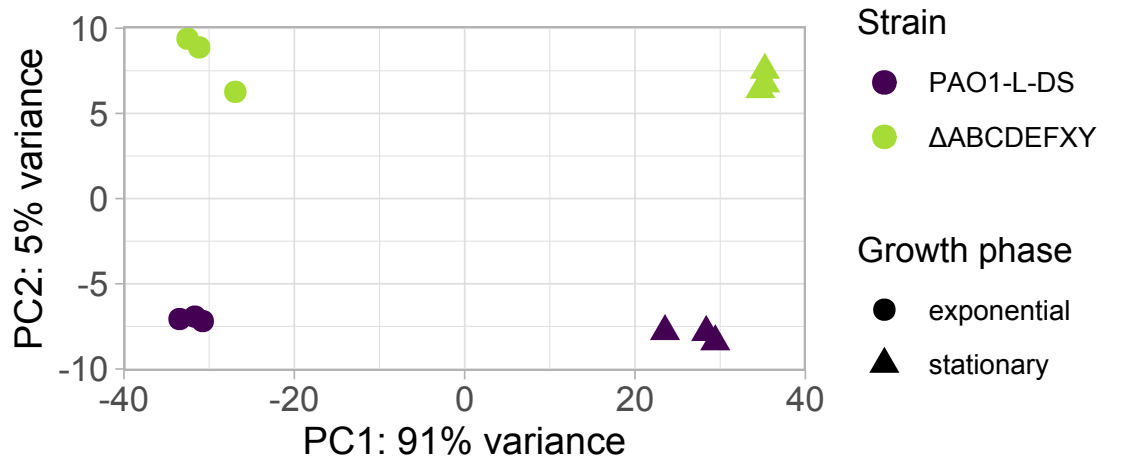
3.4.1 Quality control of RNA-Seq results

The initial assessment of raw read quality was found to be acceptable (**Appendix Y**). Reads were aligned to a PAO1-UW reference genome corrected for the large inversion between rRNA operons *rrnA* and *rrnB* and 12 kb RGP42 deletion (Klockgether *et al.*, 2010). Samples typically had total mapping rates > 97% with the exception of ΔABCDEFXY_stationary_1 and ΔABCDEFXY_stationary_2 which had rates of 65.44% and 71.72% respectively. A total mapping rate < 70% suggests contamination samples were re-sequenced by Novogene and subsequent mapping rates increased to 98.67% and 98.31% (**Appendix Z**). The number of reads mapped to each gene was counted and normalized to account for gene length (DEseq2's median of ratios). Gene-level differential expression analysis was found to be acceptable (**Appendix AA**).

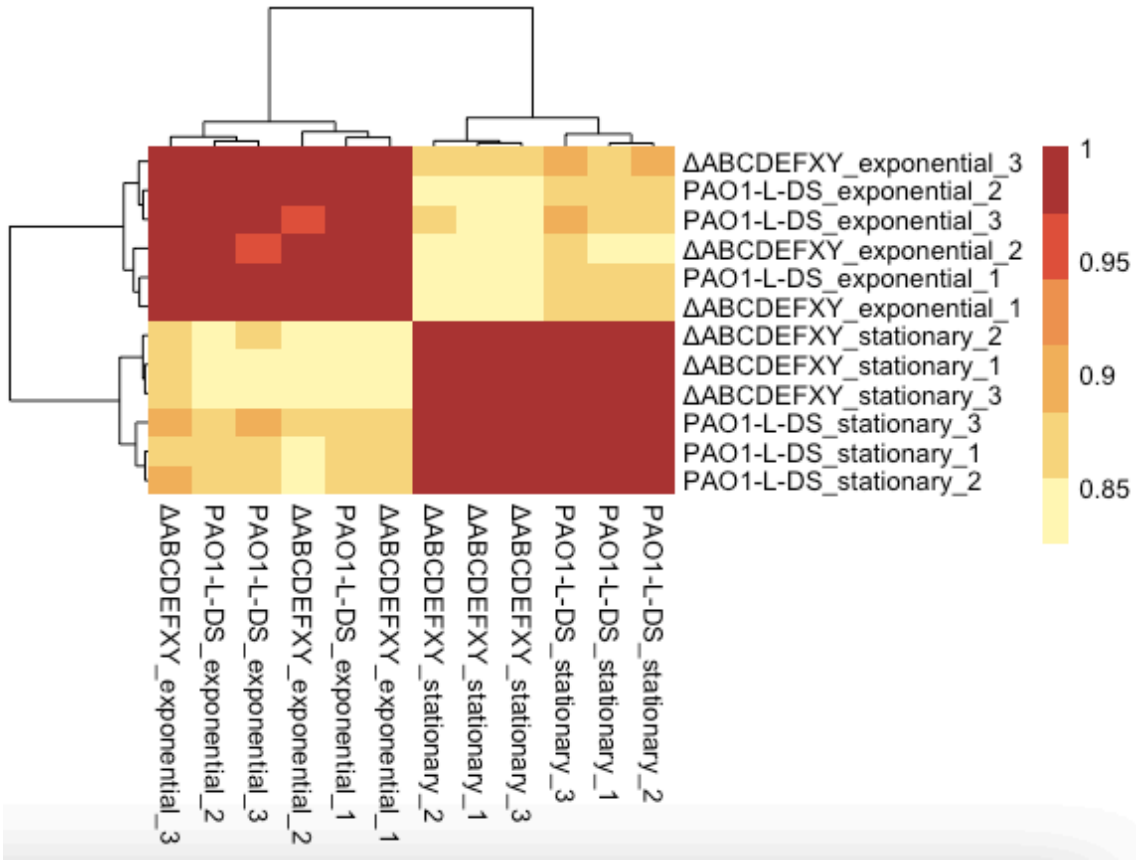
Principal Component Analysis (PCA) was used to assess the similarity between biological replicates and identify any potential outliers in the dataset. The PCA shows a strong correlation between replicates of each strain and time-point for principal components 1 and 2, which contribute to 96% of the total variance (**Figure 3.3A**). Hierarchal clustering was used to calculate the pairwise distance between data points and identify positive relationships between samples. The majority of genes were not differentially expressed so all pairwise combinations of samples have an R^2 value > 0.8, rising to > 0.95 for biological replicates (**Figure 3.3B**). As no outliers were observed in either analysis, the data confirms the different strains and time points are the main sources of variation within the dataset.

Figure 3.3: Unsupervised clustering analysis of RNA-Seq results indicates a strong correlation between replicates of each strain and time-point. A) Principal Component Analysis. Figure created using the R package [ggplot2]. B) Pearson correlation between samples. Samples with greater similarity have a correlation coefficient (R^2) closer to 1. Figure created using the R package [pheatmap].

A.



B.



3.4.2 Analysis of differentially expressed genes identified by RNA-Seq

Using an adjusted *p*-value < 0.05, 176 genes at exponential phase and 435 genes at early-stationary phase were defined as having significant changes in gene expression in the ΔABCDEFXY mutant compared to PAO1-L-DS. The fold-change describes the ratio of gene expression between strains and is displayed on a log2 scale to reduce the dynamic range. A log2 fold-change less than -1 or greater than 1, equating to an absolute fold-change of 2 was arbitrarily applied to select the significant genes with the greatest changes in expression. Of the 5570 open reading frames in *P. aeruginosa* PAO1-UW (Stover *et al*., 2000), only 59 genes were significantly up- or down-regulated at exponential phase (1.06% of genome), and 48 at early-stationary phase (0.86% of genome) (**Figure 3.4**).

Differentially transcribed genes at exponential phase included efflux pumps (*mexGHI-opmD*, *mexJK*, PA1131, PA1316), pyocyanin synthesis genes (*phzA1*, *phzB1*, *phzD1*, *phzF1*, *phzM, phzD2*, *phzF2*), rhamnolipid synthesis genes (*rhlA*), elastase synthesis genes (*lasB*) anthranilate synthesis genes (*phnA*, *phnB*) and exoenzymes (*aprA*). The most upregulated gene was the hypothetical protein PA2358, whose function is unknown. Downregulated genes in ΔABCDEFXY included those involved in zinc uptake (*zur*), SDS hydrolysis (*sdsA1*) and nitrate reduction (*narJ*). The most downregulated gene was the Psl and pyoverdine regulator *ppyR* with a log2 fold-change of -1.75 (**Table 3.1**). Conversely, significantly upregulated genes at early-stationary phase included anthranilate degradation (*antA*, *antB*, *antC*, *antR*), glycerol metabolism (*glpD*, *glpF*, *glpK*), T6SS proteins (*hcpA*, *hcpC*) and sarcosine oxidation genes (*soxA*, *soxB*, *soxD*). The gene with the largest log2 fold-change (2.8) was the alkyl hyperoxide reductase protein *ahpB*. Thirteen tRNAs were downregulated in addition to the 30S ribosomal protein *rpsT* (**Table 3.2**).

Between-sample variation in gene expression was visualized on a heatmap. Values were normalized to prevent genes with high expression values from dominating (**Figure 3.5**). The heatmap displays clustering between the 3 replicates of each condition despite between-sample differences in gene expression. At exponential phase, samples PAO1-L-DS_exponential_3 and ABCDEFXY_exponential_3 showed increased expression of several DEGs compared to the other replicates (**Figure 3.5A**). At stationary phase, the expression profile of PAO1-L-DS_stationary_3 also displayed an increased DEG expression compared to the other two PAO1-L-DS samples (**Figure 3.5B**).

Figure 3.4: Volcano plots displaying differentially expressed genes (DEGs) in the ΔABCDEFXY mutant compared to PAO1-L-DS A) DEGs at exponential growth phase B) DEGs at early-stationary growth phase. The x-axis shows the log2 fold change and the y-axis shows the –log10 adjusted *p*-value. Orange dots indicate genes with upregulated expression (defined as a log2 fold change less than -1.0 and an adjusted *p*-value less than 0.05), pink dots indicate genes with downregulated expression (defined as a log2 fold change greater than 1.0 and an adjusted *p*-value less than 0.05), and grey dots indicate genes with non-significant changes in expression. Selected differentially expressed genes are labelled.

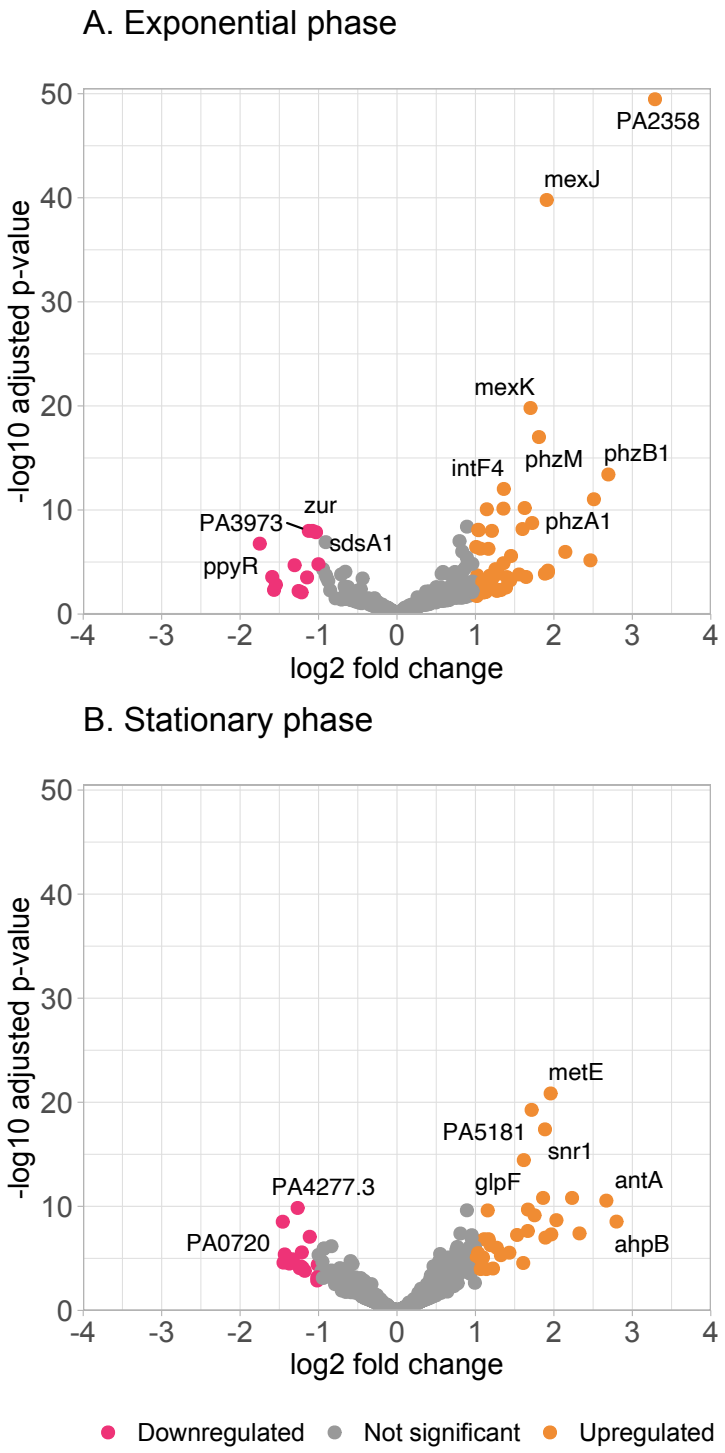


Table 3.1: Differentially expressed genes in the ΔABCDEFXY mutant compared to PAO1-L-DS at exponential growth phase growth. DEGs are defined as a log2 fold changes less than -1.0 or greater than 1.0, and an adjusted *p*-value less than 0.05.

Gene	Name	p-value	padj	log2FoldChange	Description
PA2358	PA2358	2.98e-53	3.39e-50	↑ 3.29	hypothetical protein
PA4211	phzB1	8.19e-17	3.87e-14	↑ 2.69	probable phenazine biosynthesis protein
PA4210	phzA1	2.62e-14	9.29e-12	↑ 2.51	probable phenazine biosynthesis protein
PA4206	mexH	4.97e-08	6.88e-06	↑ 2.47	Resistance-Nodulation-Cell Division (RND) multidrug efflux membrane fusion protein
PA4208	opmD	7.14e-09	1.07e-06	↑ 2.15	Multidrug efflux outer membrane protein
PA4205	mexG	5.99e-07	6.66e-05	↑ 1.92	Resistance-Nodulation-Cell Division (RND) multidrug efflux transporter
PA4207	mexI	1.00e-06	1.03e-04	↑ 1.92	Resistance-Nodulation-Cell Division (RND) multidrug efflux transporter
PA3677	mexJ	1.73e-43	1.63e-40	↑ 1.91	Resistance-Nodulation-Cell Division (RND) multidrug efflux membrane fusion protein
PA2357	msuE	1.34e-06	1.31e-04	↑ 1.89	NADH-dependent FMN reductase MsuE
PA4209	phzM	1.56e-20	9.82e-18	↑ 1.81	probable phenazine-specific methyltransferase
PA1316	PA1316	6.92e-12	1.78e-09	↑ 1.72	probable major facilitator superfamily (MFS) transporter
PA3676	mexK	2.23e-23	1.58e-20	↑ 1.7	Resistance-Nodulation-Cell Division (RND) multidrug efflux transporter
PA2356	msuD	3.18e-06	2.74e-04	↑ 1.65	methanesulfonate sulfonatase MsuD
PA3479	rhlA	2.16e-13	6.46e-11	↑ 1.63	rhamnosyltransferase chain A
PA1249	aprA	2.86e-11	6.75e-09	↑ 1.6	alkaline metalloproteinase precursor
PA1904	phzF2	1.63e-06	1.57e-04	↑ 1.56	probable phenazine biosynthesis protein
PA0806	PA0806	1.81e-08	2.63e-06	↑ 1.45	hypothetical protein
PA3329	PA3329	7.28e-06	5.58e-04	↑ 1.44	hypothetical protein
PA3330	PA3330	4.63e-06	3.75e-04	↑ 1.42	probable short chain dehydrogenase
PA3327	PA3327	3.29e-06	2.79e-04	↑ 1.4	probable non-ribosomal peptide synthetase
PA3328	PA3328	4.45e-05	2.81e-03	↑ 1.39	probable FAD-dependent monooxygenase
PA0728	intF4	2.34e-15	9.50e-13	↑ 1.36	probable bacteriophage integrase
PA3724	lasB	9.83e-08	1.30e-05	↑ 1.36	elastase lasB
PA1797	PA1797	2.61e-13	7.39e-11	↑ 1.36	hypothetical protein
PA1902	phzD2	8.20e-05	4.84e-03	↑ 1.32	phenazine biosynthesis protein PhzD
PA4213	phzD1	8.28e-05	4.84e-03	↑ 1.3	phenazine biosynthesis protein PhzD
PA2069	PA2069	1.34e-06	1.31e-04	↑ 1.29	probable carbamoyl transferase
PA2411	PA2411	1.13e-04	5.99e-03	↑ 1.27	probable thioesterase
PA1869	acp1	4.08e-07	4.83e-05	↑ 1.26	Probable acyl carrier protein
PA0547	PA0547	5.23e-06	4.06e-04	↑ 1.21	probable transcriptional regulator
PA1245	aprX	5.20e-11	1.02e-08	↑ 1.21	Apr type I secretion system, aprX
PA1002	phnB	2.32e-06	2.06e-04	↑ 1.18	anthranilate synthase component II
PA4142	PA4142	3.43e-09	5.40e-07	↑ 1.16	probable secretion protein
PA3331	PA3331	3.94e-05	2.57e-03	↑ 1.14	cytochrome P450
PA0715	PA0715	3.15e-13	8.50e-11	↑ 1.14	hypothetical protein
PA3333	fabH2	1.53e-04	7.49e-03	↑ 1.13	3-oxoacyl-[acyl-carrier-protein] synthase III
PA4215	phzF1	1.46e-04	7.19e-03	↑ 1.12	probable phenazine biosynthesis protein
PA1001	phnA	1.77e-04	8.24e-03	↑ 1.11	anthranilate synthase component I
PA1000	pqsE	1.73e-04	8.16e-03	↑ 1.1	Quinolone signal response protein
PA4139	PA4139	1.11e-05	8.10e-04	↑ 1.09	hypothetical protein
PA2588	PA2588	3.23e-09	5.23e-07	↑ 1.06	Probable transcriptional regulator
PA3335	PA3335	1.23e-04	6.38e-03	↑ 1.06	hypothetical protein
PA4600	nfxB	4.00e-11	8.74e-09	↑ 1.04	transcriptional regulator NfxB
PA1131	PA1131	3.50e-11	7.93e-09	↑ 1.04	probable major facilitator superfamily (MFS) transporter
PA0852	cbpD	2.14e-06	1.92e-04	↑ 1.02	chitin-binding protein CbpD precursor

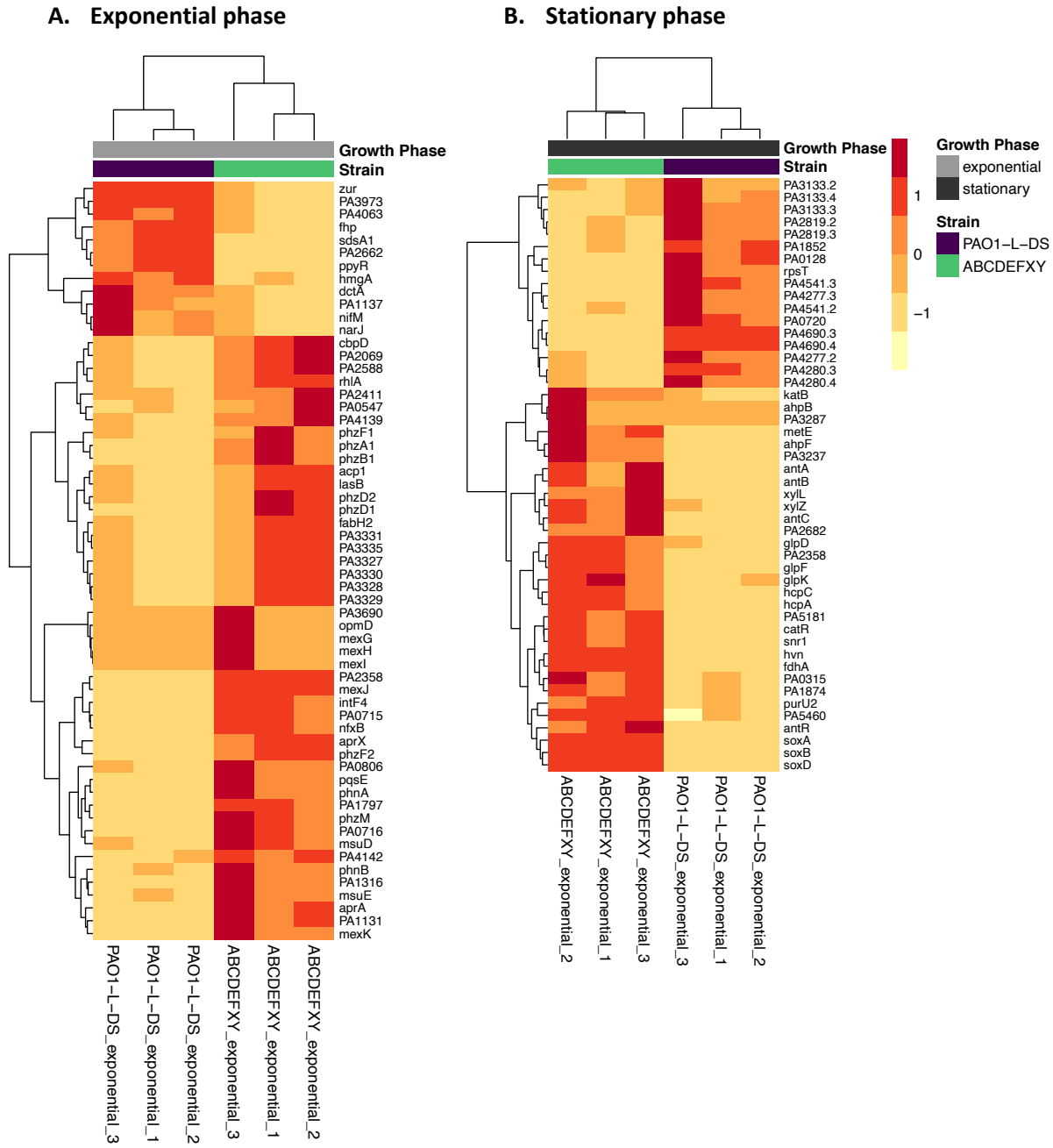
PA3690	PA3690	4.38e-04	1.85e-02	↑ 1.02	probable metal-transporting P-type ATPase
PA0716	PA0716	2.14e-09	3.57e-07	↑ 1.01	hypothetical protein
PA2662	PA2662	1.29e-07	1.62e-05	↓ -1	conserved hypothetical protein
PA0740	sdsA1	7.24e-11	1.37e-08	↓ -1.03	SDS hydrolase SdsA1
PA5499	zur	4.85e-11	1.02e-08	↓ -1.08	zinc uptake regulator, Zur
PA3973	PA3973	5.09e-11	1.02e-08	↓ -1.12	probable transcriptional regulator
PA2009	hmgA	3.66e-06	3.01e-04	↓ -1.15	homogentisate 1,2-dioxygenase
PA3873	narJ	1.76e-04	8.24e-03	↓ -1.22	respiratory nitrate reductase delta chain
PA3871	nifM	1.16e-04	6.08e-03	↓ -1.25	probable peptidyl-prolyl cis-trans isomerase, PpiC-type
PA4063	PA4063	1.64e-07	2.02e-05	↓ -1.31	hypothetical protein
PA1137	PA1137	2.14e-05	1.50e-03	↓ -1.54	probable oxidoreductase
PA2664	fhp	7.96e-05	4.76e-03	↓ -1.57	flavohemoprotein
PA1183	dctA	3.16e-06	2.74e-04	↓ -1.59	C4-dicarboxylate transport protein
PA2663	ppyR	9.99e-10	1.72e-07	↓ -1.75	psl and pyoverdine operon regulator, PpyR

Table 3.2: Differentially expressed genes in the ΔABCDEFXY mutant compared to PAO1-L-DS at early stationary growth phase growth. DEGs are defined as a log2 fold changes less than -1.0 or greater than 1.0, and an adjusted *p*-value less than 0.05.

Gene	Name	p-value	padj	log2FoldChange	Description
PA0848	ahpB	1.29e-11	2.93e-09	↑ 2.8	alkyl hydroperoxide reductase
PA2512	antA	8.30e-14	2.83e-11	↑ 2.67	anthranilate dioxygenase large subunit
PA3287	PA3287	1.97e-10	3.99e-08	↑ 2.33	conserved hypothetical protein
PA3237	PA3237	4.29e-14	1.56e-11	↑ 2.23	hypothetical protein
PA2515	xylL	8.99e-12	2.13e-09	↑ 2.03	cis-1,2-dihydroxycyclohexa-3,4-diene carboxylate dehydrogenase
PA3584	glpD	2.64e-10	4.96e-08	↑ 1.97	glycerol-3-phosphate dehydrogenase
PA1927	metE	1.57e-24	1.42e-21	↑ 1.96	5-methyltetrahydropteroyltriglutamate-homocysteine S-methyltransferase
PA2513	antB	6.15e-10	1.02e-07	↑ 1.89	anthranilate dioxygenase small subunit
PA3032	snr1	5.86e-21	4.00e-18	↑ 1.89	cytochrome c Snr1
PA1914	hvn	3.99e-14	1.55e-11	↑ 1.86	conserved hypothetical protein
PA3582	glpK	2.93e-12	7.27e-10	↑ 1.75	glycerol kinase
PA5181	PA5181	6.91e-23	5.38e-20	↑ 1.72	probable oxidoreductase
PA2511	antR	7.11e-13	2.04e-10	↑ 1.67	anthranilate regulator
PA2514	antC	1.11e-10	2.33e-08	↑ 1.67	anthranilate dioxygenase reductase
PA3581	glpF	6.63e-18	3.62e-15	↑ 1.62	glycerol uptake facilitator protein
PA2516	xylZ	3.42e-07	2.78e-05	↑ 1.61	toluate 1,2-dioxygenase electron transfer component
PA0263	hcpC	3.11e-10	5.65e-08	↑ 1.53	secreted protein Hcp
PA1512	hcpA	2.46e-08	2.85e-06	↑ 1.43	secreted protein Hcp
PA2358	PA2358	4.79e-08	4.92e-06	↑ 1.32	hypothetical protein
PA0140	ahpF	7.30e-09	9.48e-07	↑ 1.27	alkyl hydroperoxide reductase subunit F
PA5460	PA5460	1.52e-06	9.41e-05	↑ 1.22	hypothetical protein
PA5421	fdhA	3.65e-09	5.38e-07	↑ 1.19	glutathione-independent formaldehyde dehydrogenase
PA5418	soxA	9.45e-10	1.43e-07	↑ 1.17	sarcosine oxidase alpha subunit
PA2682	PA2682	9.51e-13	2.47e-10	↑ 1.16	conserved hypothetical protein
PA5417	soxD	1.79e-06	1.07e-04	↑ 1.14	sarcosine oxidase delta subunit
PA1874	PA1874	9.47e-10	1.43e-07	↑ 1.11	hypothetical protein
PA0315	PA0315	8.57e-08	8.19e-06	↑ 1.1	hypothetical protein
PA5416	soxB	1.76e-06	1.07e-04	↑ 1.07	sarcosine oxidase beta subunit
PA5420	purU2	2.76e-08	3.14e-06	↑ 1.03	formyltetrahydrofolate deformylase
PA4613	katB	1.01e-06	6.85e-05	↑ 1.03	Catalase
PA2510	catR	6.67e-08	6.73e-06	↑ 1.02	transcriptional regulator CatR
PA0128	PA0128	5.35e-07	4.05e-05	↓ -1.01	conserved hypothetical protein
PA4280.4	PA4280.4	1.70e-05	7.24e-04	↓ -1.01	tRNA-Ile
PA4280.3	PA4280.3	1.50e-05	6.67e-04	↓ -1.01	tRNA-Ala
PA3133.2	PA3133.2	3.48e-05	1.34e-03	↓ -1.02	tRNA-Ala
PA4277.2	PA4277.2	4.93e-10	8.40e-08	↓ -1.11	tRNA-Gly
PA3133.3	PA3133.3	2.82e-06	1.57e-04	↓ -1.18	tRNA-Glu
PA4690.4	PA4690.4	1.21e-06	7.90e-05	↓ -1.2	tRNA-Ile
PA1852	PA1852	2.25e-08	2.66e-06	↓ -1.21	hypothetical protein
PA4690.3	PA4690.3	8.54e-07	5.97e-05	↓ -1.23	tRNA-Ala
PA3133.4	PA3133.4	1.37e-06	8.68e-05	↓ -1.24	tRNA-Ala
PA4277.3	PA4277.3	4.72e-13	1.43e-10	↓ -1.27	tRNA-Tyr
PA4563	rpsT	1.35e-07	1.22e-05	↓ -1.33	30S ribosomal protein S20
PA4541.3	PA4541.3	4.00e-07	3.16e-05	↓ -1.37	tRNA-Asn

PA2819.3	PA2819.3	8.19e-08	8.12e-06	↓ -1.41	tRNA-Glu
PA2819.2	PA2819.2	3.88e-08	4.15e-06	↓ -1.43	tRNA-Gly
PA4541.2	PA4541.2	3.10e-07	2.56e-05	↓ -1.45	tRNA-Pro
PA0720	PA0720	1.38e-11	3.01e-09	↓ -1.46	helix destabilizing protein of bacteriophage Pf1

Figure 3.5: Visualization of gene expression between samples. Heatmap displaying normalised values of DEGs at A) Exponential and B) Early-stationary phases of growth. Figure created using the R package [pheatmap].



3.4.3 Enrichment analysis of RNA-Seq results

DEGs were assigned Gene Ontology (GO) classifications which are divided into biological, cellular and molecular processes. At exponential phase, overrepresented biological classes include “phenazine biosynthetic process” and “transmembrane transport” owing to the number of pyocyanin biosynthesis (*phzA1*, *phzB1*, *phzD1*, *phzF1*, *phzM, phzD2*, *phzF2, phnA, phnB*) and efflux pump genes (*mexH, mexI, opmD*, *mexJ, mexK*, PA1131, PA1316, *glpF*) that were upregulated. Downregulated biological classes were predominately related to the role of dicarboxylate transport proteins such as “Dicarboxylic acid transport” and “Oxidation-reduction process” (**Figure 3.6A**).

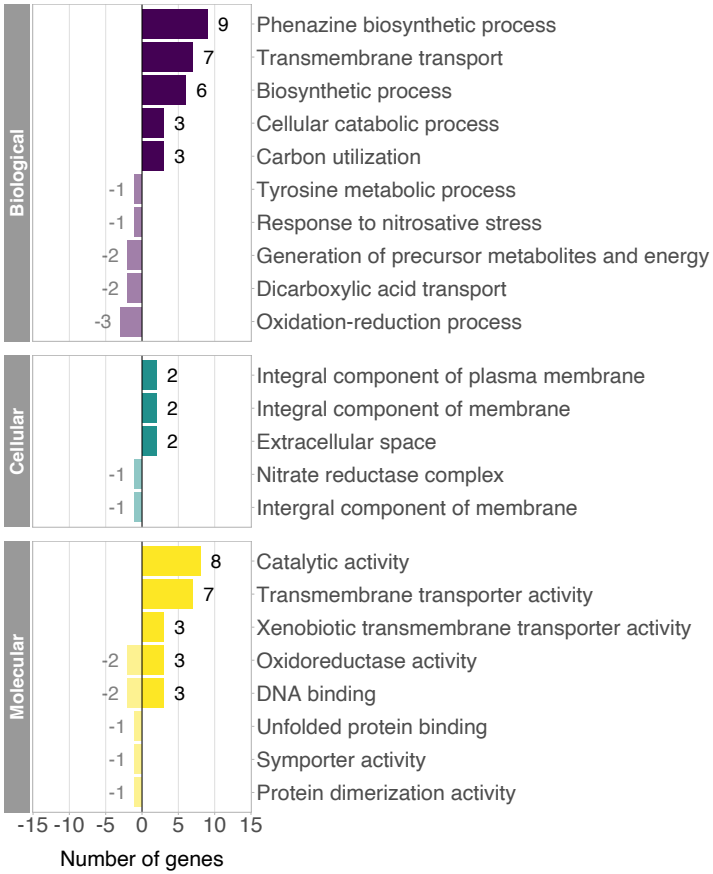
Conversely, in early-stationary phase, the largest biological class was the “Oxidation-reduction process” owing to the number of genes upregulated genes in the oxidative stress response (*katB*, *ahpB*, *ahpF*), sarcosine metabolism (*soxA*, *soxB*), and anthranilate degradation (*antA*, *antB*, *antC*). Other biological classes in which transcription increased include “Cellular catabolic process”, “Carbon utilization” and “Aromatic compound catabolic process” (**Figure 3.6B**). The only downregulated biological process was “Translation” due to the 30S ribosomal protein encoded by *rpsT*. It was not possible to assign GO classifications to the 13 downregulated tRNA’s.

3.5 Validation of transcriptomic changes associated with loss of MexAB-OprM, MexCD-OprJ, MexEF-OprN and MexXY in *P. aeruginosa* PAO1-L-DS

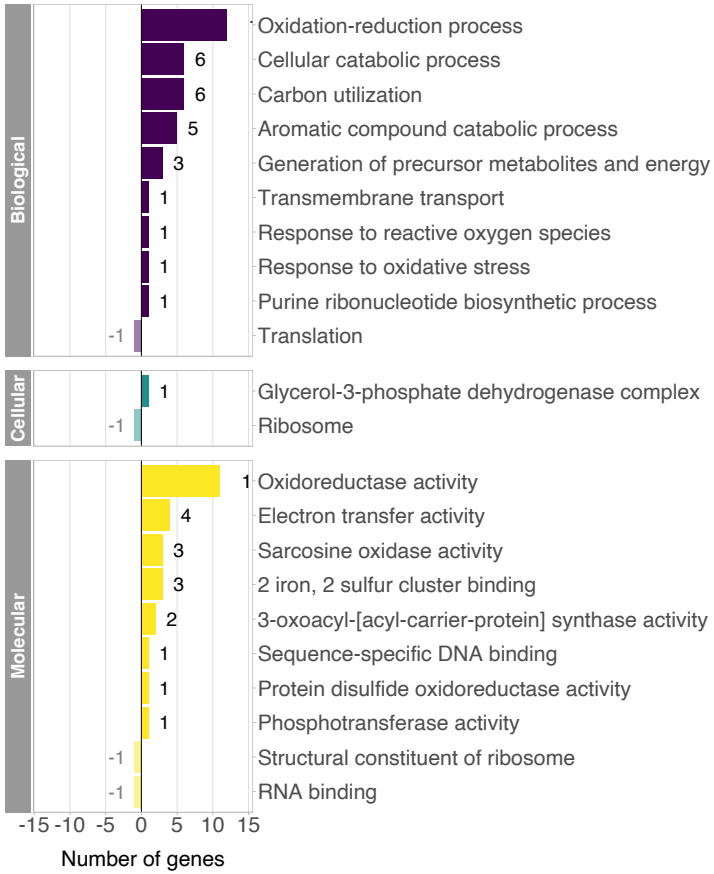
A selection of differentially expressed genes identified by RNA-Seq, in addition to some which were not, were validated using a combination of phenotypic assays, LC-MS/MS quantification of metabolites and transcriptional promoter fusions comprising the promoter region of the gene of interest cloned upstream of the *luxCDABE* operon from *Xenorhabdus luminescens* (Becher & Schweizer, 2000). Transcriptional reporters enable the visualisation of changes in gene expression over time, as opposed to other popular techniques such as RT-PCR which only provide a snapshot of transcription levels at a given timepoint (as with RNA-Seq).

Figure 3.6: Gene Ontology classification of differentially expressed gene products in the ΔABCDEFXY mutant compared to PAO1-L-DS at A) exponential and B) stationary growth phases. Gene products which contribute to biological processes are coloured purple, cellular components are teal and those with a molecular function are yellow. For each GO term, a negative number indicates the number of gene products downregulated and a positive number indicates the number of gene products upregulated. The top 10 GO terms for each process are displayed (where applicable).

A



B



Promoter activation was quantified by measuring the light output at 490 nm every 30 min over a 24 h period and correcting for growth. Assays were performed in black plastic 96-well plates to prevent light from leaching into other wells. To confirm reporters were working effectively, strains were also tagged with the empty pMiniCTX::*lux* backbone and a transcriptional reporter for the P*tac* promoter which is constitutively expressed (**Appendix AB**).

3.5.1 Differential transcription of the alkaline protease gene *aprA*

Alkaline protease is a 50-kDa metalloprotease encoded by the *aprA* gene which is responsible for host tissue damage. The *aprA* gene had a log2 fold-change of 1.6 at exponential phase. To further explore the effect of efflux pump deletion on alkaline protease production, strains were stabbed into 13% skimmed milk agar plates and incubated for 24 h. Clear zones around the culture indicate casein hydrolysis, which is a semiquantitative measure of alkaline protease activity.

In contrast to the RNA-Seq data, we observed smaller proteolytic zones around ΔABCDEFXY compared to PAO1-L-DS (**Figure 3.7**). As AprA (Duong *et al*., 1992) and AprX (Duong *et al*., 2001) are secreted by the AprDEF T1SS, these results indicate a reduction in the production or secretion of alkaline protease despite increased gene expression.

3.5.3 Differential transcription of the rhamnolipid synthesis gene *rhlA*

The expression of *rhlA* was significantly higher in the ΔABCDEFXY mutant than in PAO1-L-DS at exponential phase. The *rhlA* gene encodes one of the two proteins required for the production of rhamnosyltransferase 1, an enzyme involved in rhamnolipid biosynthesis. The expression of *rhlA* is normally regulated by the *rhlRI* QS-system and though these genes were not differentially expressed at either growth phase, their expression was highest during exponential phase (**Figure 3.8A**). This was unexpected given that previous studies have found expression of both *rhlI* and *rhlR* increases with cell density, reaching maximal expression levels during stationary phase (Schuster *et al*., 2003).

Figure 3.7: Loss of MexAB-OprM, MexCD-OprJ, MexEF-OprN and MexXY decreases alkaline protease production. Overnight cultures of PAO1-L-DS and the ΔABCDEFXY mutant were standardized to OD_{600} 1.0 and 1 µL was used to inoculate each plate using the stabbing method. Plates were incubated at 37°C for 24 h. Plate pictures are representative of at least three biological and three technical replicates.



PAO1-L-DS



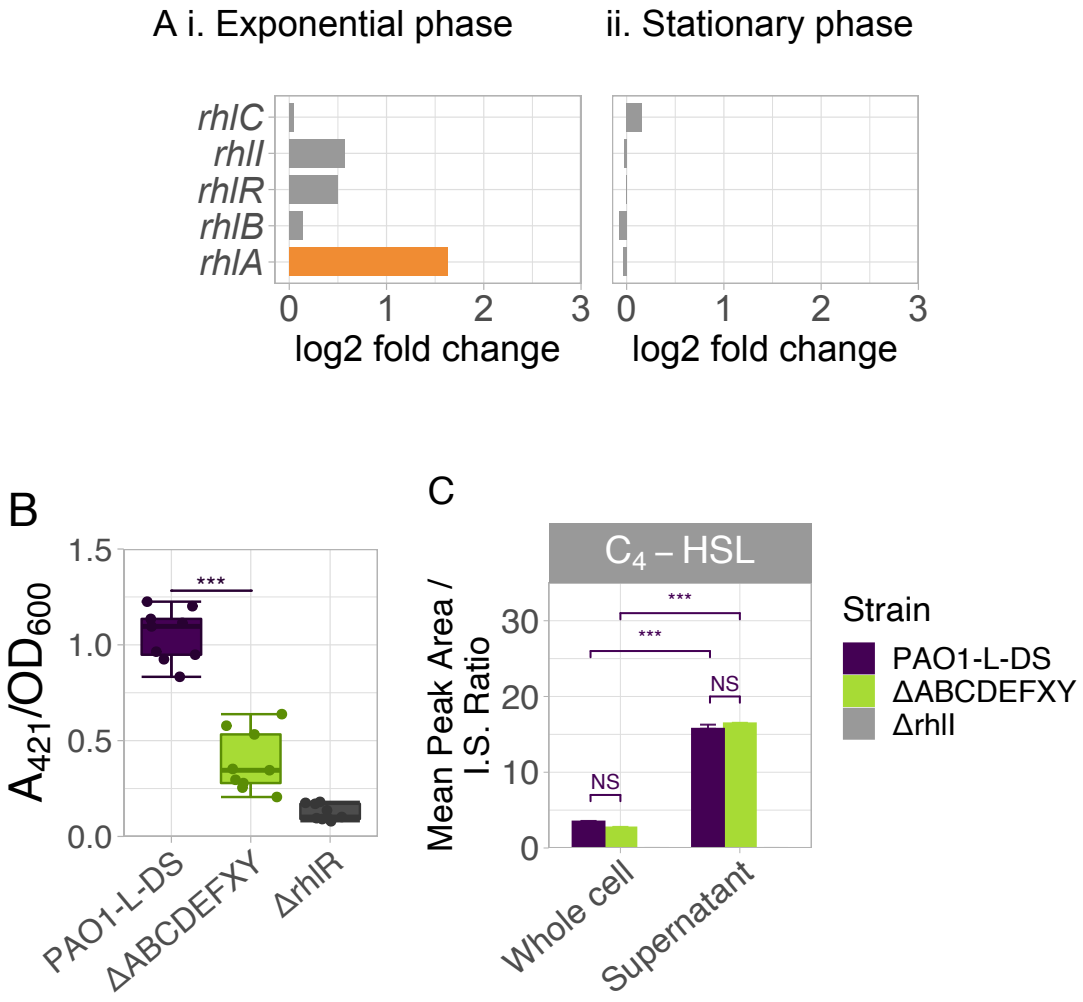
ΔABCDEFXY

To validate the transcriptomic results PAO1-L-DS and ΔABCDEFXY were tagged with either *rhlA::lux* or *rhlI::lux* promoter fusions and gene expression was profiled over a 24 h period (**Figure 3.8Di**). In line with the transcriptomic data, *rhlA* was expressed earlier in ΔABCDEFXY than PAO1-L-DS, though the maximal expression of *rhlA* occurred at approximately 8 h in the ΔABCDEFXY mutant compared to 20 h in PAO1-L-DS (**Figure 3.8Di**). Conversely, the transcriptomic data shows an increase in gene expression at 4 h (exponential phase) rather than 8 h (early stationary). This is likely explained by the differences in population densities as the starting concentration of the TECAN cultures was OD_{600} 0.006 compared to OD_{600} 0.01 for the RNA-Seq samples. Looking at the overall data trend, the maximal expression levels of *rhlA* were significantly higher in ΔABCDEFXY compared to PAO1-L-DS while there was no change in the expression of *rhlI* between the two strains. These results align with the RNA-Seq data (**Figure 3.8Dii**).

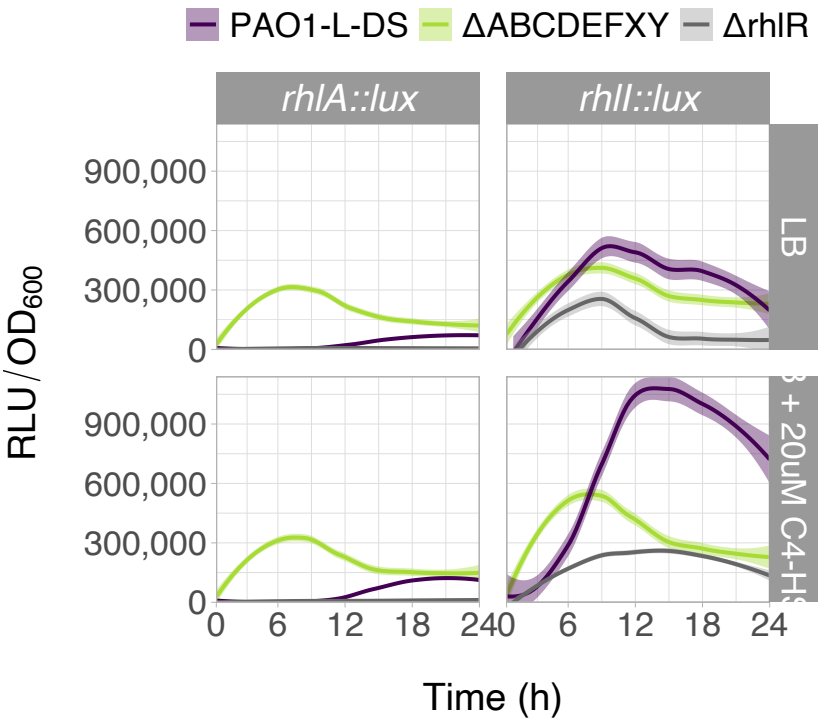
To confirm that the *rhlA::lux* and *rhlI::lux* reporters were working effectively, they were conjugated into a Δ*rhlR* control strain lacking the transcriptional regulator of the *rhl* quorum sensing system. As expected, the Δ*rhlR* mutant had a negligible expression of *rhlA* while maximal *rhlI* expression levels were comparable with PAO1-L-DS (**Figure 3.8Dii**). As *rhlI* expression is also regulated by LasR, it is unsurprising that expression of *rhlI* was observed in the absence of *rhlR* (Latifi *et al*., 1996).

Previous work has shown that expression of *rhlA* increases with the addition of C_4-HSL (Schuster *et al*., 2003), so to confirm these results we added 20 μM exogenous C_4-HSL to cultures. In contrast, the expression of *rhlA* did not alter with the cognate signal molecule in either PAO1-L-DS or ΔABCDEFXY (**Figure 3.8Di**). However in line with Schuster *et al*., (2003), *rhlI* expression increased significantly in PAO1-L-DS following the addition of C_4-HSL compared to the ΔABCDEFXY mutant where expression only slightly increased (**Figure 3.8Di**). As PAO1-L-DS and ΔABCDEFXY differed in their response to the addition of the signaling molecule, we used LC-MS/MS to investigate whether loss of efflux altered the levels of C_4-HSL signalling molecule in the whole cell and supernatant cultures during late exponential phase (6 h) (**Figure 3.8C**). While there was no significant difference in C_4-HSL levels between the strains in each sample group, higher levels of C_4-HSL were observed in the extracellular environment compared to the whole cell pellets.

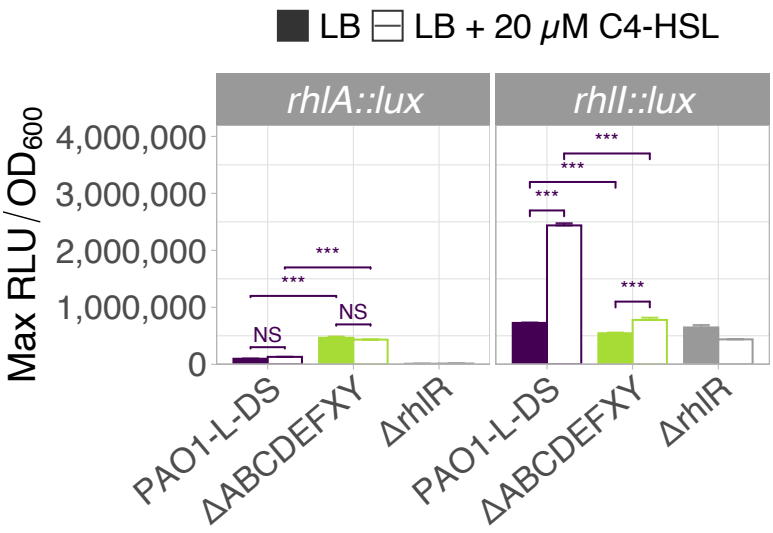
Figure 3.8: Rhamnolipid production decreases with loss of MexAB-OprM, MexCD-OprJ, MexEF-OprN and MexXY A) Log2 fold-change of *rhl* genes at i) exponential and ii) early-stationary phase. DEGs with a log2 fold-change > 1 are shown in orange B) Strains tagged with *rhlA::lux* or *rhlI::lux* were grown in LB alone or with the addition of 20 μM C_4-HSL at 37°C i) Light output (RLU) and OD_{600} readings were taken every 30 min for 24 h. The dark line for each strain represents the normalized mean (RLU/OD_{600}) while lighter shading represents ± 1SD ii) Maximum gene expression normalized for growth ($Max\ RLU/OD_{600}$) ± 1SD C) LC-MS/MS quantification of C_4-HSL from whole cell and culture supernatants of PAO1-L-DS, ΔABCDEFXY and Δ*rhlI* grown in LB for 6 h at 37°C D) Rhamnolipid concentration at 421 nm from culture supernatants of PAO1-L-DS and ΔABCDEFXY grown in LB for 24 h at 37°C. Figures are representative of at least 3 biological and 3 technical replicates. $p \geq 0.05$ (NS; not significant), $p \leq 0.05$ (*), $p \leq 0.01$ (**), $p \leq 0.001$ (***).



D i.


PAO1-L-DS
ΔABCDEFXY
ΔrhlR
rhlA::lux
rhlI::lux
LB
+ 20uM C4-HS
RLU/OD600
900,000
600,000
300,000
0
0
6
12
18
24
Time (h)

ii.


LB
LB + 20 μM C4-HSL
rhlA::lux
rhlI::lux
Max RLU/OD600
4,000,000
3,000,000
2,000,000
1,000,000
0
NS
NS
***
***
***
***
***
PAO1-L-DS
ΔABCDEFXY
ΔrhlR
PAO1-L-DS
ΔABCDEFXY
ΔrhlR

To determine whether increased expression of *rhlA* in the ΔABCDEFXY mutant translated to an increase in rhamnolipid production, exogenous rhamnolipid levels were indirectly quantified using an orcinol rhamnolipid assay (**Figure 3.8B**). The absorbance of each strain was measured at 421 nm and revealed that ΔABCDEFXY produced significantly less biosurfactant compared to the parent strain. Together this data indicate that loss of MexAB-OprM, MexCD-OprJ, MexEF-OprN and MexXY increases the expression of *rhlA* and not *rhlI*, but this does not translate to an increase in extracellular rhamnolipid production.

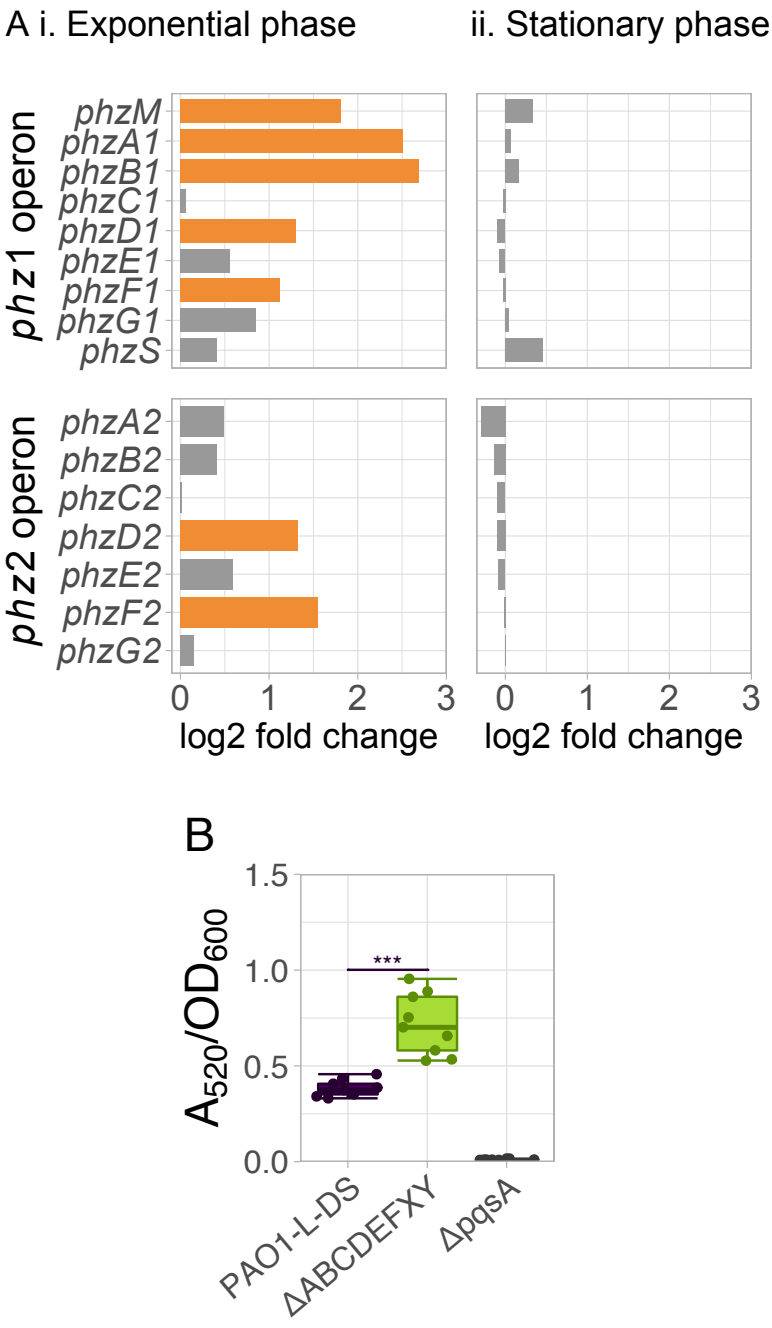
3.5.4 Differential transcription of the pyocyanin synthesis gene *phzA1*

The expression of several pyocyanin synthesis genes (*phzA1*, *phzB1*, *phzD1*, *phzF1*, *phzM, phzD2*, *phzF2*) was upregulated in the ΔABCDEFXY mutant at exponential phase (**Figure 3.9A**). Two distant operons produce pyocyanin: the enzymes encoded by *phz1* (*phzA1B1C1D1E1F1G1*) and *phz2* (*phzA2B2C2D2E2F2G2*) catalyse the conversion of chorismic acid to phenazine-carboxylic acid (PCA), which is then converted to 5-methylphenazine-1-carboxylic acid betaine by PhzM before conversion to pyocyanin by PhzS (Mavrodi *et al*., 2001).

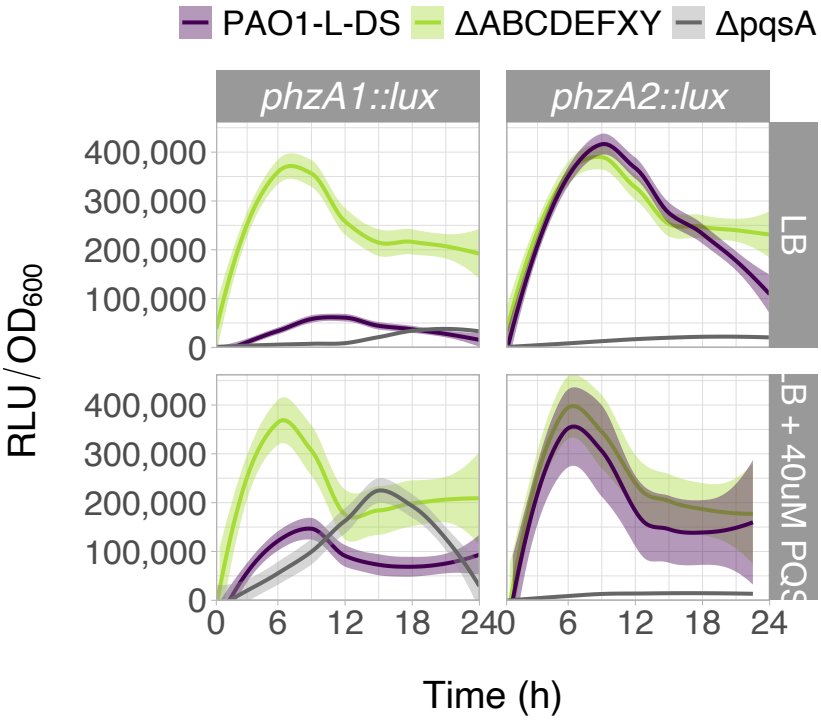
To confirm these changes in gene expression, PAO1-L-DS and ΔABCDEFXY were tagged with transcriptional reporters for *phzA1* which was differentially expressed, or *phzA2* which was not (**Figure 3.9Ci**). Consistent with the transcriptomic data the expression of *phzA1* was significantly upregulated in ΔABCDEFXY while the expression of *phzA2* did not differ significantly between the strains (**Figure 3.9Cii**). The addition of 40 μM exogenous PQS induced the expression of *phzA1*, but not *phzA2*, in all strains (**Figure 3.9Ci**). This data is consistent with the finding that *phz1* is responsible for phenazine production during planktonic growth, while *phz2* is reserved for biofilm formation (Recinos *et al*., 2012).

Finally, to determine whether increased expression of *phzA1* and *pqsA* increased pyocyanin production, exogenous pyocyanin levels were quantified using the solvent extraction method (**Figure 3.9B**). In line with our previous results, ΔABCDEFXY produced 2-fold more pyocyanin than PAO1-L-DS. Together this data indicate that loss of MexAB-OprM, MexCD-OprJ, MexEF-OprN and MexXY increases pyocyanin production by upregulating the expression of *phzA1* but not *phzA2*, as a consequence of increased PQS production.

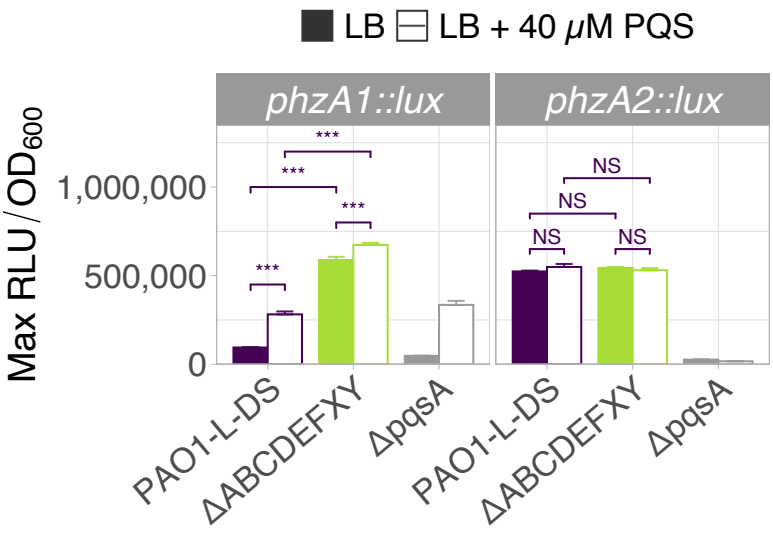
Figure 3.9: Pyocyanin production increases with loss of MexAB-OprM, MexCD-OprJ, MexEF-OprN and MexXY. A) Log2 fold-change of genes in the *phz1*, and *phz2* operons at i) exponential and ii) early-stationary phase. DEGs with a log2 fold-change > 1 are shown in orange. B) Strains tagged with *phzA1::lux* or *phzA2::lux* were grown in LB alone or with the addition of 40 μM PQS at 37°C. i) Light output (RLU) and OD_{600} readings were taken every 30 min for 24 h. The dark line for each strain represents the normalized mean (RLU/OD_{600}) while lighter shading represents ± 1SD ii) Maximum gene expression normalized for growth (Max RLU/OD600) ± 1SD C) Pyocyanin concentration at 520 nm from culture supernatants of PAO1-L-DS and ΔABCDEFXY grown in LB for 24 h at 37°C. Figures are representative of at least 3 biological and 3 technical replicates. $p \geq 0.05$ (NS; not significant), $p \leq 0.05$ (*), $p \leq 0.01$ (**), $p \leq 0.001$ (***).



C i.


PAO1-L-DS
ΔABCDEFXY
ΔpqsA
phzA1::lux
phzA2::lux
LB
LB + 40uM PQS
RLU/OD600
400,000
300,000
200,000
100,000
0
0
6
12
18
24
Time (h)

ii.


LB
LB + 40 μM PQS
phzA1::lux
phzA2::lux
Max RLU/OD600
1,000,000
500,000
0
***
NS
PAO1-L-DS
ΔABCDEFXY
ΔpqsA

3.5.4 Differential transcription of the *pqs* quorum sensing system

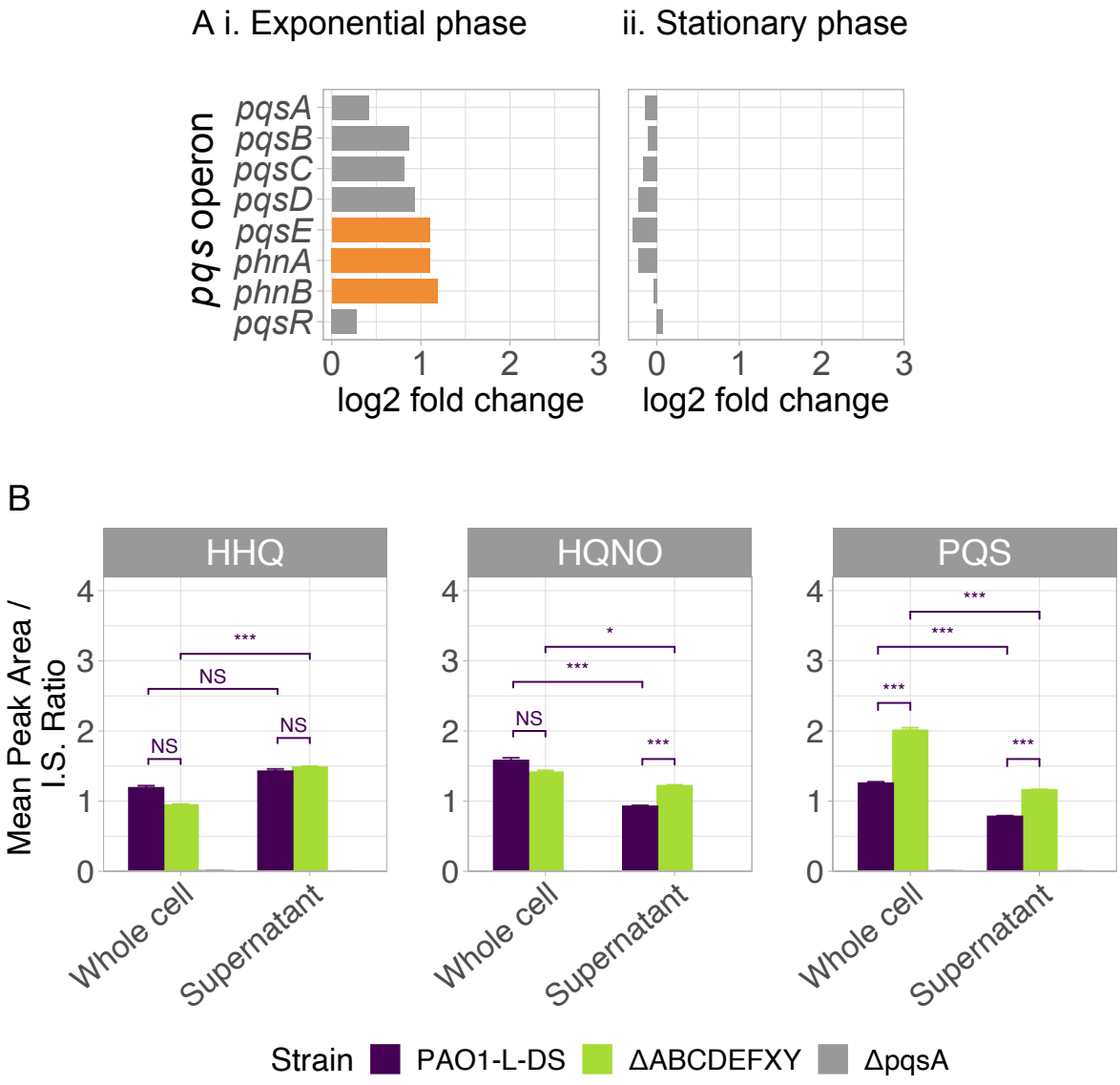
Pyocyanin biosynthesis is regulated by both the *rhl* and the *pqs* QS-systems. As we did not observe differences in *rhlI* expression in the experiments above, we hypothesized that the *pqs* system was upregulated. Several genes from the *pqs* operon were upregulated at exponential phase including *phnA*, *phnB* and *pqsE* (**Figure 3.10A**). *P. aeruginosa* possesses two anthranilate synthases encoded by *phnAB* and *trpEG* to catalyse the conversion of chorismate to anthranilate. TrpEG-generated anthranilate is generated at low cell densities for PQS biosynthesis, while PhnAB-generated anthranilate is generated at high cell densities for tryptophan biosynthesis (Palmer *et al*., 2013). Anthranilate synthesis genes *phnA* and *phnB* were upregulated in ΔABCDEFXY at exponential phase, which was unexpected as these genes are normally activated at high cell densities.

Until recently the function of *pqsE* in PQS biosynthesis was not known as Δ*pqsE* mutants can produce PQS (Gallagher *et al*., 2002) however, Drees & Fetzner, (2015) showed that PqsE hydrolyses 2-aminobenzoylacetyl-coenzyme A to 2-aminobenzoylacetate (2-ABA). PqsE has been shown to activate the transcription of a large number of genes including *phnAB*, *mexGHI-opmD* and *phzC2D2E2F2G2* (Rampioni *et al*., 2010; Rampioni *et al*., 2016) by binding directly to RhlR to activate the Rhl system (Taylor *et al*., 2021; Simanek *et al*., 2022).

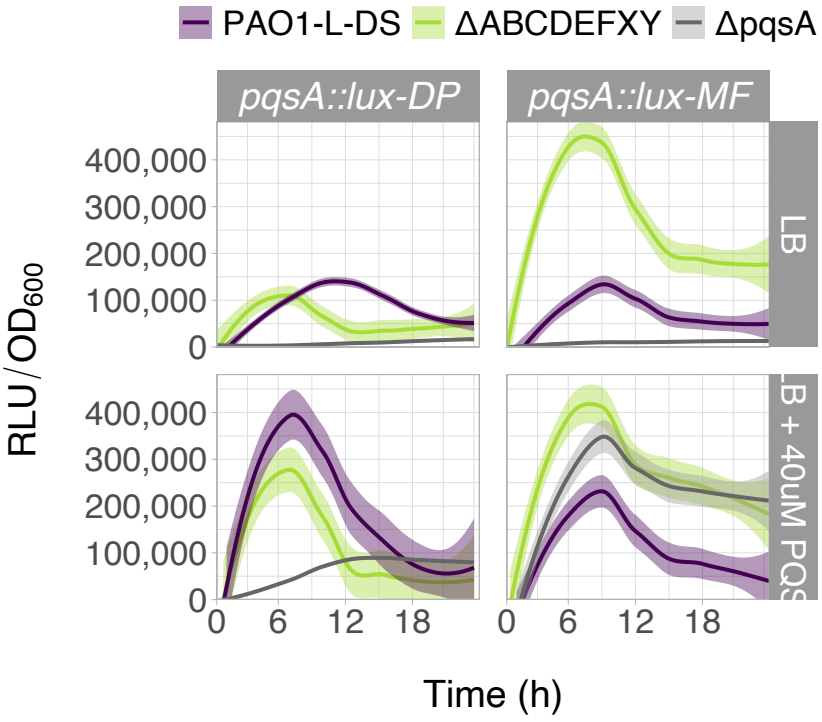
To measure the impact of increased *pqsE* expression on the production of PQS, strains were tagged with a *pqsA* promoter fusion which either contained (*pqsA::lux-DP*) or lacked (*pqsA::lux-MF*) the *las/rhl* binding box centred at -311 bp upstream of the *pqsA* transcriptional initiation site. Both transcriptional reporters contain the PqsR binding site centred at -45 bp upstream of the *pqsA* transcriptional initiation site for *pqsABCDE* transcription. The reporters were also introduced into a Δ*pqsA* control strain.

Although *pqsA* was not differentially expressed, we observed earlier expression of *pqsA-DP* in ΔABCDEFXY compared to the parent strain in line with the transcriptomic data. RhlR normally binds to the las/rhl box to repress *pqsA* transcription, so higher levels of *pqsA* expression were observed in ΔABCDEFXY carrying *pqsA::lux-MF* compared to *pqsA::lux-DP*. Levels of *pqsA::lux-MF* were significantly higher in ΔABCDEFXY than PAO1-L-DS. The addition of 40 μM exogenous PQS to the media significantly increased *pqsA* expression in PAO1-L-DS, and to a lesser extent ΔABCDEFXY with both reporters (**Figure 3.10C**).

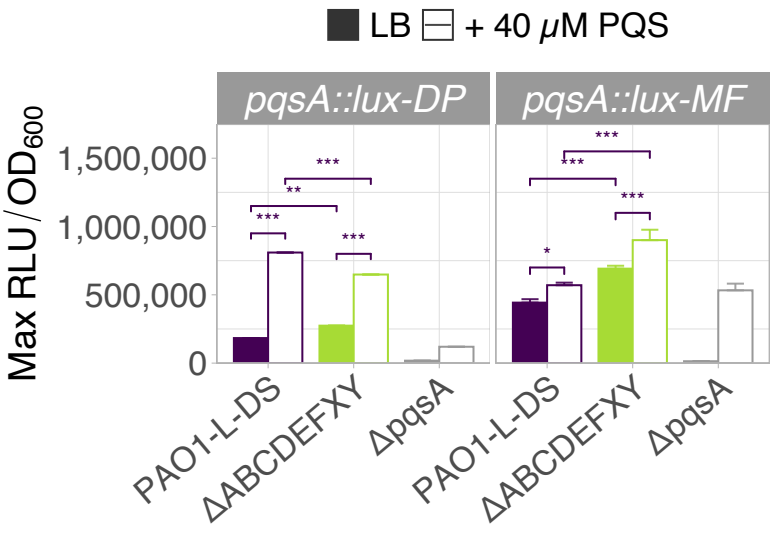
Figure 3.10: PQS production increases with loss of MexAB-OprM, MexCD-OprJ, MexEF-OprN and MexXY. A) Log2 fold-change of genes in the *pqs* operon at i) exponential and ii) early-stationary phase. DEGs with a log2 fold-change > 1 are shown in orange. B) Strains tagged with *pqsA::lux-MF or pqsA::lux-DP* were grown in LB alone or with 40 µM PQS at 37°C. i) Light output (RLU) and OD_{600} readings were taken every 30 min for 24 h. The dark line for each strain represents the normalized mean (RLU/OD_{600}) while lighter shading represents ± 1SD ii) Maximum gene expression normalized for growth (Max RLU/OD600) ± 1SD C) LC-MS/MS quantification of HHQ, HQNO and PQS from whole cell and supernatants of PAO1-L-DS, ΔABCDEFXY and Δ*pqsA* grown in LB for 6 h at 37°C. Figures are representative of at least 3 biological and 3 technical replicates. $p \geq 0.05$ (NS; not significant), $p \leq 0.05$ (*), $p \leq 0.01$ (**), $p \leq 0.001$ (***).



C i.


PAO1-L-DS
ΔABCDEFXY
ΔpqsA
pqsA::lux-DP
pqsA::lux-MF
LB
LB + 40uM PQS
RLU/OD600
400,000
300,000
200,000
100,000
0
0
6
12
18
Time (h)

ii.


LB
+ 40 μM PQS
pqsA::lux-DP
pqsA::lux-MF
Max RLU/OD600
1,500,000
1,000,000
500,000
0
***
**
*
PAO1-L-DS
ΔABCDEFXY
ΔpqsA

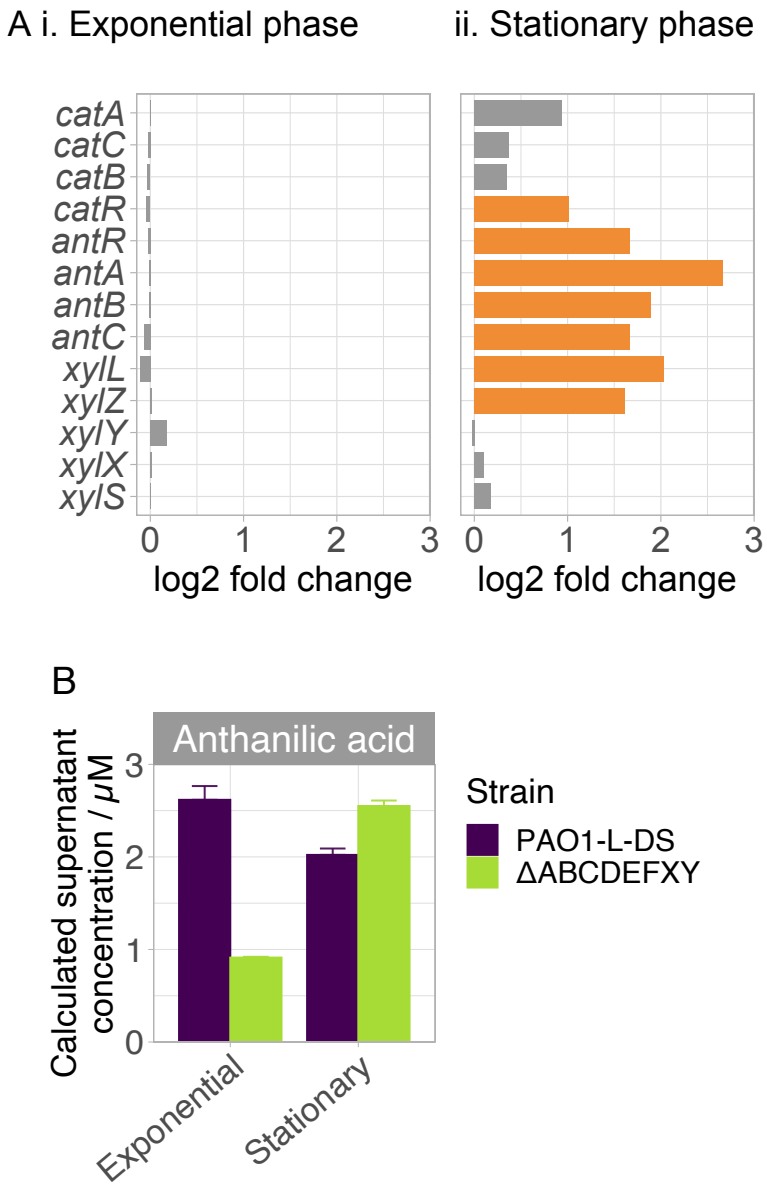
The levels of AQs HHQ, HQNO and PQS were also quantified by LC-MS/MS to determine whether the increased transcription of *pqsA* and *pqsE* in ΔABCDEFXY was attributable to an increase in either HHQ or PQS production, which are both able to bind to PqsR and activate transcription of *pqsABCDE* (Xiao *et al*., 2006) (**Figure 3.10B**). A Δ*pqsA* strain which does not produce AQs was used as a control. The ΔABCDEFXY mutant produced significantly more PQS than the parent strain from both whole cell and supernatant cultures, and while slight differences in HHQ and HQNO were observed the only significant result between strains was an increase in extracellular HQNO. These results confirm that increased expression of the *pqsABCDE* operon is due to an increase in PQS and not HHQ.

3.5.5 Differential transcription of the anthranilate degradation genes *antA* and *antR*

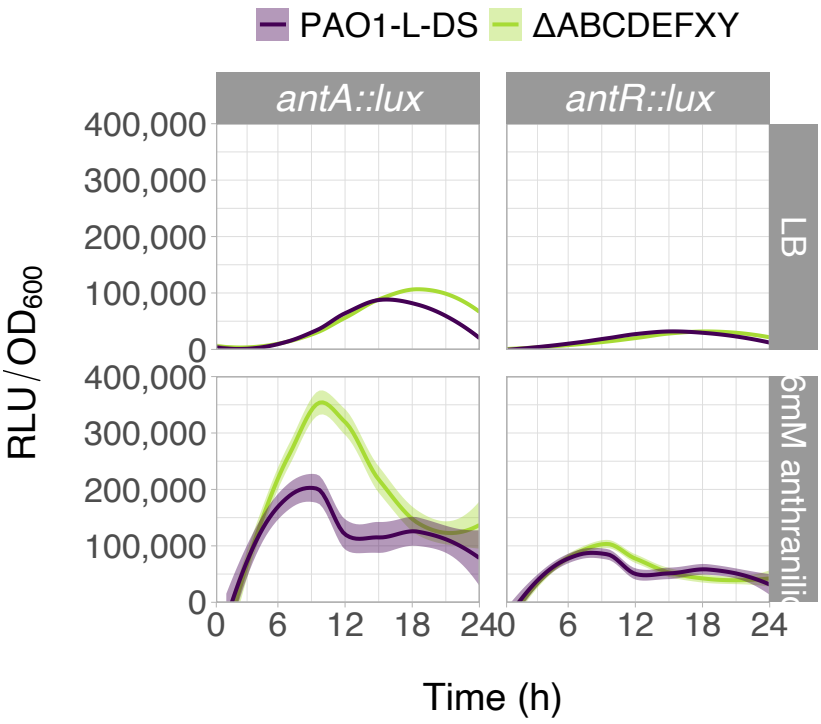
In addition to upregulation of the anthranilate synthase genes *phnAB* at exponential phase, we observed significant upregulation of the anthranilate degradation genes *antABC* and the bidirectional transcriptional activator *antR* in early-stationary phase (**Figure 3.11A**). Choi *et al*., (2011) found that *antA* is repressed by LasR during exponential phase and activated by RhlR in late stationary phase in agreement with these results. The enzymes encoded by *antABC* convert anthranilate into catechol, which can be further converted into tricarboxylic acid cycle intermediates by the *cat* operon and feed into the TCA cycle. The regulator c*atR*, and neighbouring genes *xylL* and *xylZ* which encode enzymes involved in the degradation of toxic intermediates produced during aerobic catabolism were also upregulated at early-stationary phase.

To validate changes in *antA* and *antR* expression, transcriptional fusions for each of the respective genes were conjugated into PAO1-L-DS and ΔABCDEFXY (**Figure 3.11Ci**). Though expression of *antA* occurs slightly later in the ΔABCDEFXY mutant compared to the parent strain, expression patterns and maximum expression levels of both *antA* and *antR* did not differ significantly between the strains (**Figure 3.11Cii**). The addition of 6 mM anthranilic acid induced expression of both *antA* and *antR* in both strains. Though maximum expression levels did not differ significantly between the strains, the mean expression of *antA* was higher in the ΔABCDEFXY mutant than in PAO1-L-DS (**Figure 3.11Ci**). These data do not support the RNA-Seq results.

Figure 3.11: Anthranilate metabolism changes with loss of MexAB-OprM, MexCD-OprJ, MexEF-OprN and MexXY A) Log2 fold-change of genes in the *cat*/*ant*/*xyl* operons at i) exponential and ii) early-stationary phase. DEGs with a log2 fold-change > 1 are shown in orange B) Strains tagged with *antA::lux or antR::lux* were grown in LB alone or with 6 mM anthranilic acid at 37°C i) Light output (RLU) and OD_{600} readings were taken every 30 min for 24 h. The dark line for each strain represents the normalized mean (RLU/OD_{600}) while lighter shading represents ± 1SD ii) Maximum gene expression normalized for growth (Max RLU/OD600) ± 1SD C) LC-MS/MS quantification of anthranilic acid from supernatants of PAO1-L-DS and ΔABCDEFXY grown in LB at 37°C to exponential or stationary phase. Figures are representative of at least 3 biological and 3 technical replicates. $p \geq 0.05$ (NS), $p \leq 0.05$ (*), $p \leq 0.01$ (**), $p \leq 0.001$ (***).

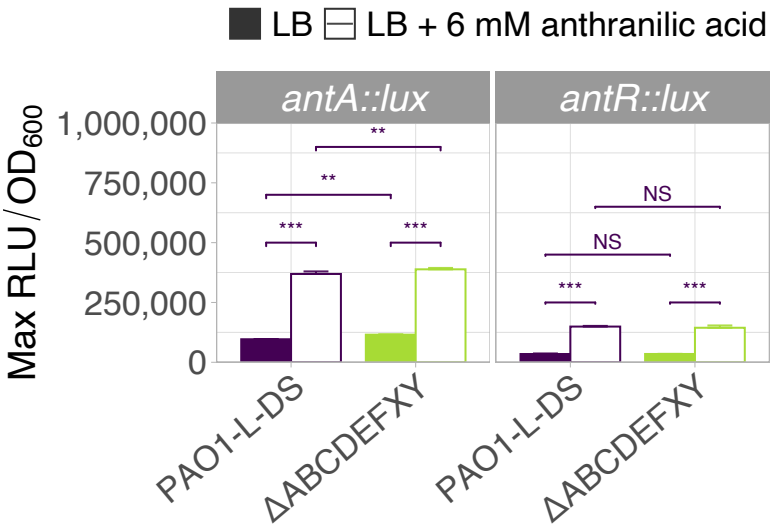


C i.


PAO1-L-DS
ΔABCDEFXY
antA::lux
antR::lux
LB
6mM anthranili
RLU/OD600
400,000
300,000
200,000
100,000
0
0
6
12
18
24
Time (h)

ii.

ii.


LB
LB + 6 mM anthranilic acid
antA::lux
antR::lux
Max RLU/OD600
1,000,000
750,000
500,000
250,000
0
**
**
***
***
NS
NS
***
***
PAO1-L-DS
ΔABCDEFXY
PAO1-L-DS
ΔABCDEFXY

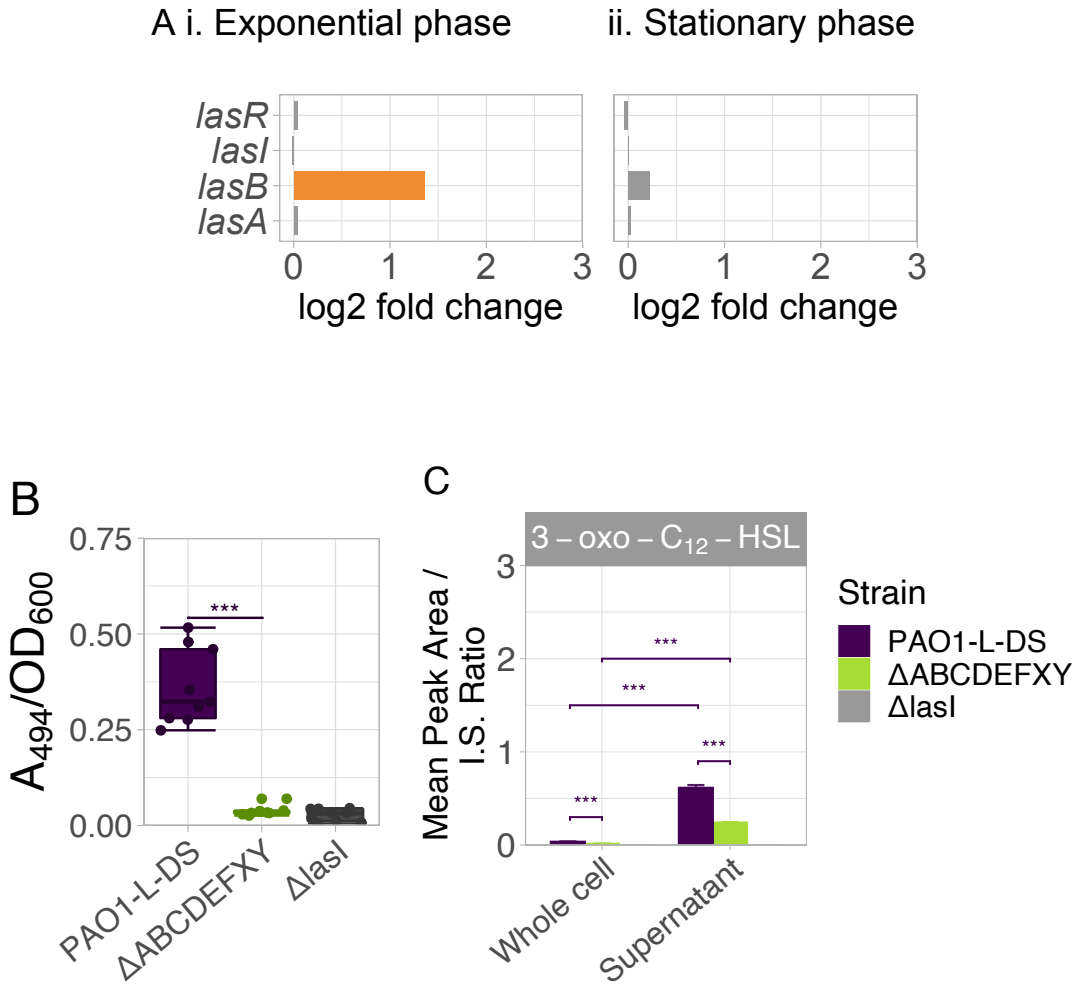
It has also been speculated that anthranilate may be exported by the MexGHI-OpmD efflux pump (Aendekerk *et al*., 2005) which was upregulated in the ΔABCDEFXY mutant at exponential phase. Anthranilate levels were quantified from culture supernatants at both growth phases using LC-MS/MS and show that at exponential phase there was significantly less anthranilate in the ΔABCDEFXY supernatant compared to PAO1-L-DS, but no significant difference between the strains at stationary phase (**Figure 3.11B**). As upregulation of MexGHI-OpmD in the ΔABCDEFXY mutant increased pyocyanin levels in culture supernatants but not anthranilate, the results support those of Sakhtah *et al*., (2016) who found that MexGHI-OpmD is involved in the export of the pyocyanin precursor 5-Me-PCA and not anthranilate.

3.5.6 Elastase production decreases with the loss of MexAB-OprM, MexCD-OprJ, MexEF-OprN and MexXY in *P. aeruginosa* PAO1-L-DS

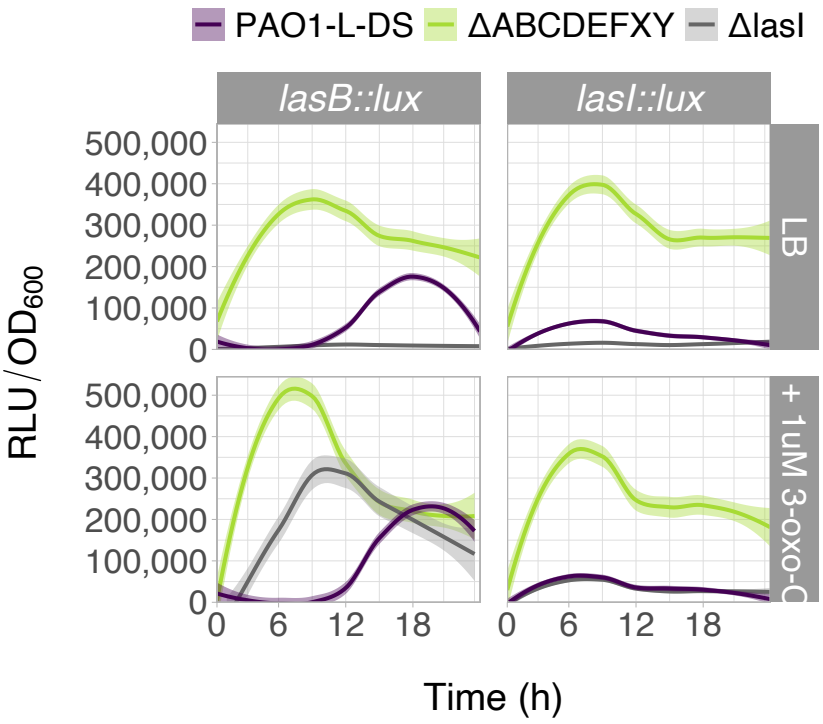
The RNA-Seq data revealed that the expression of quorum sensing controlled genes was upregulated in the ΔABCDEFXY mutant compared to the wild-type strain. Our earlier experiments indicate that the *pqs* system was upregulated through increased expression of *pqsA* and increased production of PQS, while expression of the *rhlI* from the *rhl* system was not. As the *P. aeruginosa* quorum sensing systems are arranged in a hierarchy with the *las* system regulating both the *rhl* and *pqs* systems we investigated whether the transcriptomic changes we observed were ultimately attributable to the upregulation of the *las* quorum sensing system.

To test this hypothesis, transcriptional reporters for *lasB* which was differentially expressed and *lasI* which was not (**Figure 3.12A**) were conjugated into PAO1-L-DS and ΔABCDEFXY in addition to a Δ*lasI* control strain which is unable to produce 3-oxo-C_{12}-HSL. Our results show ΔABCDEFXY shows increased expression of both *lasB* and *lasI* compared to PAO1-L-DS (**Figure 3.12Di**), with maximal expression levels of *lasI* 2-fold greater than those of PAO1-L-DS (**Figure 3.12Dii**). The Δ*lasI* mutant showed minimal expression of both genes.

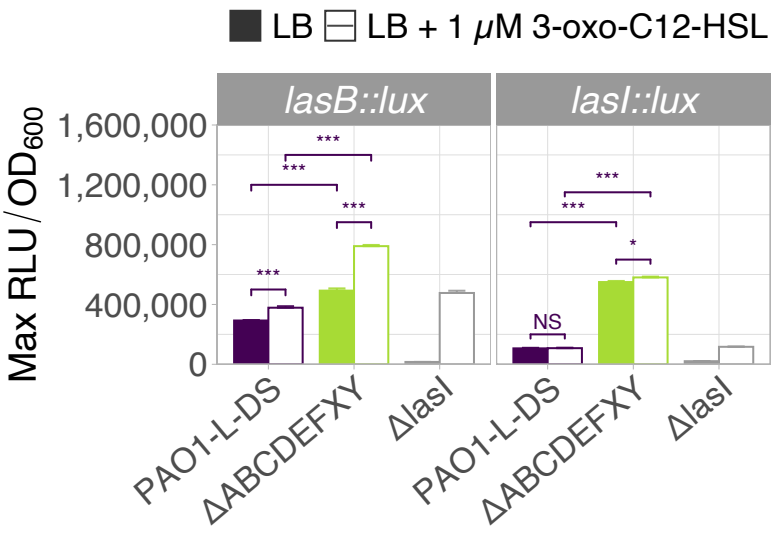
Figure 3.12: Elastase production decreases with loss of MexAB-OprM, MexCD-OprJ, MexEF-OprN and MexXY A) Log2 fold-change of genes in the *las* operon at i) exponential and ii) early-stationary phase. DEGs with a log2 fold-change > 1 are shown in orange. B) Strains tagged with *lasB::lux or lasI::lux* were grown in LB alone or with the addition of 1 μM 3-oxo-C_{12}-HSL at 37°C. i) Light output (RLU) and OD_{600} readings were taken every 30 min for 24 h. The dark line for each strain represents the normalized mean (RLU/OD_{600}) while lighter shading represents ± 1SD ii) Maximum gene expression normalized for growth (Max RLU/OD600) ± 1SD C) LC-MS/MS quantification of 3-oxo-C_{12}-HSL from the whole cell and culture supernatants of PAO1-L-DS, ΔABCDEFXY and Δ*lasI* grown in LB for 6 h at 37°C. D) Elastase B concentration at 495 nm from culture supernatants of PAO1-L-DS and ΔABCDEFXY grown in LB for 24 h at 37°C. Figures are representative of at least 3 biological and 3 technical replicates. $p \geq 0.05$ (NS; not significant), $p \leq 0.05$ (*), $p \leq 0.01$ (**), $p \leq 0.001$ (***).



D i.


PAO1-L-DS
ΔABCDEFXY
ΔlasI
lasB::lux
lasI::lux
LB
+ 1uM 3-oxo-C
RLU/OD600
500,000
400,000
300,000
200,000
100,000
0
0
6
12
18
Time (h)

ii.


LB
LB + 1 μM 3-oxo-C12-HSL
lasB::lux
lasI::lux
Max RLU/OD600
1,600,000
1,200,000
800,000
400,000
0
***
NS
*
PAO1-L-DS
ΔABCDEFXY
ΔlasI

Expression of *lasB* can be induced with the addition of 3-oxo-C_{12}-HSL, and to a lesser extent C_4-HSL (Schuster *et al*., 2003) so to validate our reporters 1 μM exogenous 3-oxo-C_{12}-HSL was added to all cultures, significantly increasing the expression of *lasB* in all three strains. As transcription of *lasI* is activated by the LasR/3-oxo-C_{12}-HSL receptor-signal complex we expected an increase in *lasI* expression in PAO1-L-DS. However, *lasI* expression levels were unaffected by the addition of 3-oxo-C_{12}-HSL with the exception of the Δ*lasI* control strain carrying the *lasI::lux* reporter (**Figure 3.12Di**).

To determine whether increased expression of *lasI* in the ΔABCDEFXY mutant resulted in increased 3-oxo-C_{12}-HSL production, levels of the quorum sensing signaling molecules were measured using LC-MS/MS (**Figure 3.12C**). We expected to isolate more 3-oxo-C_{12}-HSL from whole cell cultures given that 3-oxo-C_{12}-HSL gets stuck in the cell envelope, however levels of 3-oxo-C_{12}-HSL from whole cell cultures were lower than those of supernatants in both strains. In addition, the ΔABCDEFXY mutant showed reduced production of 3-oxo-C_{12}-HSL in both whole cell and culture supernatants compared to PAO1-L-DS.

An elastin Congo-Red assay was also performed to determine the overall effect of differential transcription on the ability of the strains to produce elastase (**Figure 3.12B**). In contrast to the increased expression of *lasB*, we observed a significant decrease in elastase production in the ΔABCDEFXY culture supernatants compared to PAO1-L-DS. LasB is secreted by the Xcp T2SS, but as none of the 12 *xcp* genes were differentially regulated the differences are likely to be due to changes in quorum sensing as the secretion system is regulated by both the *las* and *rhl* QS systems (Chapon-Hervé *et al*., 1997). Together these results indicate that although the expression of *lasB* and *lasI* increases in the ΔABCDEFXY mutant, lower levels of both 3-oxo-C_{12}-HSL and the LasB exoenzyme are found in the extracellular environment. Therefore, increased expression of the *pqs* quorum sensing system does not lead to increased 3-oxo-C_{12}-HSL production.

3.6 Discussion

Efflux pumps are evolutionarily ancient and highly conserved between bacterial species (Saier *et al*., 1998). Their existence predates the introduction of antibiotics, so their role in antimicrobial resistance is likely to be an advantageous by-product of their primary physiological function. In support of this theory is the observation that bacteria have multiple chromosomally encoded efflux systems with overlapping substrate profiles. It is therefore anticipated that they evolved to survive in hostile environments, or in response to toxins produced by competing organisms.

To gain further insight into the biological functions of RND efflux systems we took a transcriptomic approach to identify the genes that were differentially expressed when MexAB-OprM, MexCD-OprJ, MexEF-OprN and MexXY (ΔABCDEFXY) were chromosomally deleted. A small subset of differentially expressed genes was identified using an adjusted *p*-value < 0.05 and a log2 fold change greater than 1. These included 59 genes at exponential and 48 genes at stationary phase. The majority of DEGs at exponential phase were quorum sensing genes or QS-controlled virulence genes, while DEGs at stationary phase were mainly involved in oxidation-reduction processes. A summary of the differently expressed genes validated at exponential phase is provided In **Figure 3.13**, and the differently expressed genes validated at early-stationary phase in **Figure 3.14**.

At exponential phase genes from the *las*, *rhl* and *pqs* QS-systems were upregulated. The *pqsE* gene was the only gene from the *pqsABCDE* operon upregulated by a log2 fold-change of 1.1. We also observed increased *pqsA* expression in ΔABCDEFXY using a transcriptional promoter fusion despite this gene not being identified as differentially expressed from the RNA-Seq data. It is important to note that changes in gene expression do not always equate to biological impact. Enzymes such as the thioesterase encoded by *pqsE* are relatively stable so small changes in gene expression can lead to large changes in activity. In support of this hypothesis, we also observed an increase in the expression of many *pqsE* regulated genes including *rhlA*, *mexGHI-opmD* and *phzD2F2* (Rampioni *et al*., 2016).

We also observed an increase in the intracellular and extracellular levels of PQS in ΔABCDEFXY, but not HQNO or HHQ. As HHQ is exported by the MexCD-OprJ and MexEF-OprN efflux systems, we expected to see lower levels of this AQ in the ΔABCDEFXY culture supernatant which does not possess either of these pumps. These results suggest that HHQ

Figure 3.13: Summary of changes in gene expression and virulence caused by loss of MexAB-OprM, MexCD-OprJ, MexEF-OprN and MexXY at exponential phase. Upregulated genes and gene products are shown in green, while downregulated genes and gene products are shown in red. Image created using BioRender.

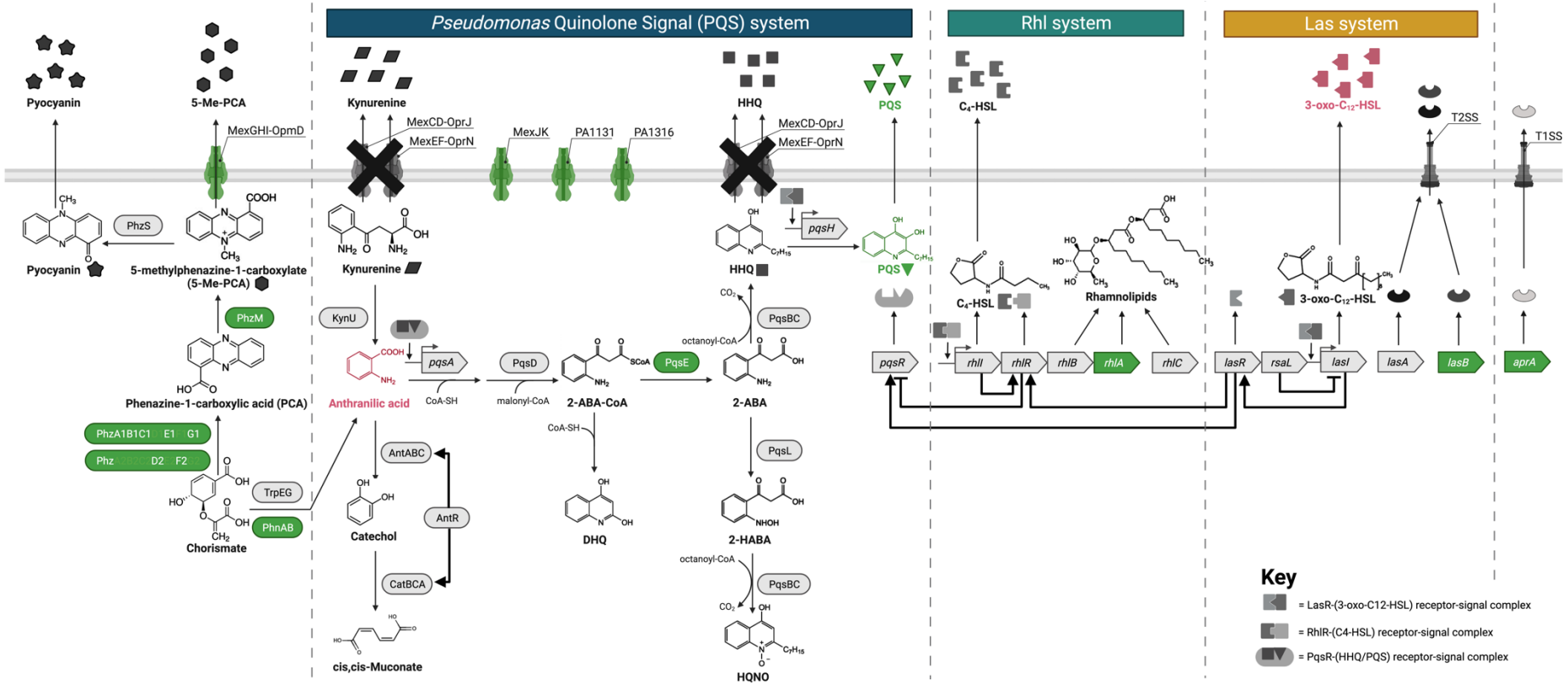
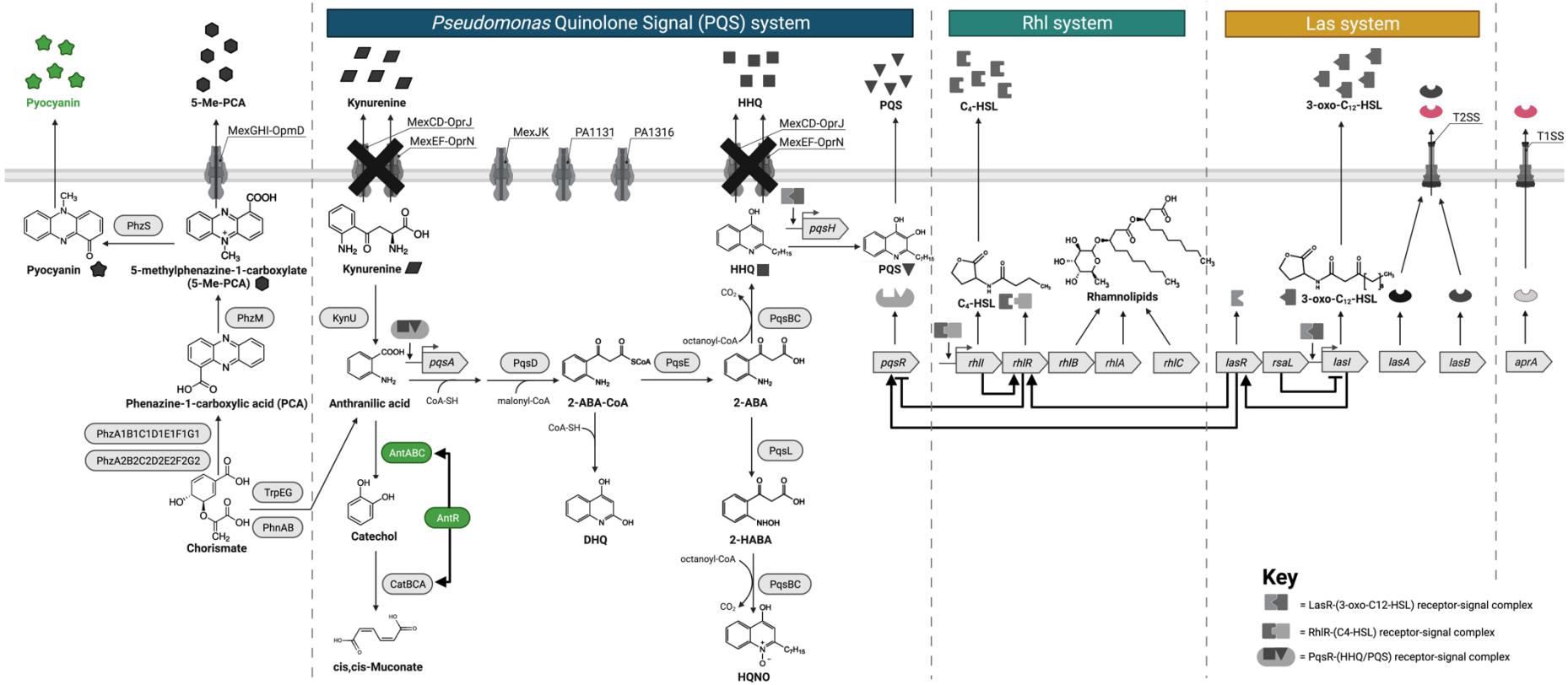


Figure 3.14: Summary of changes in gene expression and virulence caused by loss of MexAB-OprM, MexCD-OprJ, MexEF-OprN and MexXY at stationary phase. Upregulated genes and gene products are shown in green, while downregulated genes and gene products are shown in red. Image created using BioRender.



might also be exported by another system. Given the increase in PQS levels, it is not surprising that genes linked to PQS biosynthesis (*phnA, phnB, pqsE*) and PQS-controlled genes (*phzA1*, *phzB1*, *phzD1*, *phzF1*, *phzM, phzD2*, *phzF2*) were also upregulated. These results are consistent with other RNA-Seq studies reporting the upregulation of the *pqsABCDE* operon and phenazine biosynthesis genes as a consequence of efflux pump deletion or the addition of the EPI PAβN (Rampioni *et al*., 2017; Adamiak *et al*., 2021).

Genes encoding the RND efflux pumps MexGHI-OpmD and MexJK, the putative MFS family transporters PA1131 and PA1316 and the local repressor of the MexCD-OprJ efflux pump nfxB were upregulated during exponential phase. Given the upregulation of so many efflux systems in the ΔABCDEFXY mutant, it would be useful to determine the intake and efflux of ethidium bromide to establish the efflux pump function of the mutants (Blair & Piddock, 2016). When combined with flow cytometry, accumulation within single cells can determine the diversity within a bacterial population (Whittle *et al*., 2019).

MexGHI-OpmD exports the pyocyanin intermediate 5-methylphenazine-1-carboxylate (5-Me-PCA) (Sakhtah *et al*., 2016), but is also interlinked with the *pqs* system as HHQ, PQS, and pyocyanin have all been shown to bind to MexG and upregulate expression of *mexGHI-opmD* (Dietrich *et al*., 2006; Hodgkinson *et al*., 2016; Wolloscheck *et al*., 2018). Though we did not observe upregulation of *soxR* which positively regulates transcription of the MexGHI-OpmD efflux pump (Palma *et al*., 2005), several other genes in the sarcosine-catabolic operon (*soxA*, *soxB* and *soxD*) were upregulated at early stationary phase. Expression of *mexGHI-opmD* has also been shown to increase with the addition of C_4-HSL, particularly *mexG* and *mexH*, while *mexJK* responds to the addition 3-oxo-C_{12}-HSL. PA1131 and PA1316 are not known to be responsive to the addition of QSSMs (Schuster *et al*., 2003). As no differences were observed in the levels of these QSSMs, the upregulation of these efflux pumps is most likely attributable to the increase in PQS.

In addition to these main findings, we also found that in the absence of these efflux systems, genes encoding proteins exported by other active transport systems were differentially transcribed at exponential phase. Namely, increased expression of both *lasB* and the chitin-binding protein *cbpD* which are both exported by the Xcp T2SS. We also saw upregulation of *aprA* and *aprX* proteins which are exported by the Apr T1SS, and the probable secretion protein PA4142. This data contradicts other studies reporting that QS-

regulated genes are not induced until cells reach stationary phase (Schuster *et al*., 2003). Increases in gene expression did not translate to increased enzymic activity *in vitro* as we observed lower levels of both alkaline protease and elastase B in the ΔABCDEFXY mutant compared to PAO1-L-DS. This suggests an impact on translation, post-translational modifications such as removal of the signal peptide from the pre-proenzyme encoded by *lasB,* or regulation of the secretion systems themselves. The majority of secretion systems are regulated by QS (Pena *et al*., 2019) including AprA (Hentzer *et al*., 2003; Schuster *et al*., 2003; Wagner *et al*., 2003), while PqsR can directly bind to *xcp* genes and induce expression of the Xcp T2SS (Maura *et al*., 2016).

Though the majority of the RNA-Seq results were confirmed, *antA::lux* and *antR::lux* transcriptional reporter fusions did not confirm differences in gene expression between the strains. While the samples collected for RNA-Seq were grown in shaking flasks, the promoter fusion experiments were performed in a TECAN plate reader. A gas permeable membrane was applied to each plate but it is possible that oxygen limitation impacted the results. There is also growing evidence to suggest *P. aeruginosa* can sense light and switch on bacterial responses in the absence of light (Mukherjee *et al*., 2019; Kahl *et al*., 2020) resulting in clinical strains with increased virulence (Mesquite *et al*., 2021). The TECAN experiments were performed in the dark while the shaking flasks were grown with light exposure, which may also impact the results.

Due to time constraints, it was only possible to validate a subset of the RNA-Seq results. Other interesting results include the 13 genes with oxidoreductase activity which were upregulated at stationary phase (*ahpB*, *ahpF*, *antA*, *antC*, *fdhA*, *fhp*, *glpD*, *soxA*, *soxB*, *xylL*, *xlyZ*, PA3331, PA5181). NADP+/NADPH and NAD+/NADH assays could be performed to determine the cellular redox state of the strains. Detection of the fluorescent redox probe diacetyldichlorofluorescein (DCFH-DA) could also be used to determine the intracellular levels of reactive oxygen species (ROS). Gene expression and phenotypic assays could also be repeated under anaerobic conditions to determine whether the efflux pump mutants have a fitness advantage in hypoxic environments, which is a hallmark of infection.

3.7 Summary of key findings

- Loss of MexAB-OprM, MexCD-OprJ, MexEF-OprN and MexXY upregulates genes related to quorum sensing, pyocyanin biosynthesis and other RND family efflux pumps at exponential phase.
- Most of the up-regulated genes at stationary phase were involved with anthranilate degradation and glycerol metabolism
- Independent validation of results supports the RNA-Seq data

3.8 Future work

- Quantify the efflux activity of PAO1-L-DS and ΔABCDEFXY using ethidium bromide accumulation and efflux assays
- Determine whether the cellular redox state is altered between PAO1-L-DS and ΔABCDEFXY

CHAPTER 4:

Phenotypic changes caused by loss of RND efflux pumps in *P. aeruginosa* PAO1-L-DS

4. Phenotypic changes caused by loss of efflux

4.1 Background

P. aeruginosa produces a host of virulence factors to facilitate colonisation and evasion of the host immune response, nutrient acquisition and biofilm formation. These include surface appendages (flagella, TFP) for motility and surface attachment in addition to the secretion of toxins (exotoxin A, hydrogen cyanide), enzymes (elastase A, elastase B, protease IV, alkaline protease) and siderophores (pyoverdine, pyochelin) into the extracellular environment. Deletion or overexpression of RND efflux systems, particularly MexAB-OprM, MexCD-OprJ, MexEF-OprN and MexXY, has been shown to alter the production of many virulence factors despite not being directly involved in their export from the cell (Köhler *et al*., 1997; Evans *et al*., 1998; Köhler *et al*., 2001; Hirakata *et al*., 2002; Sánchez *et al*., 2002; Aendekerk *et al*., 2005; Linares *et al*., 2005; Alcalde-Rico *et al*., 2018; Vaillancourt *et al*., 2021).

Furthermore, *P. aeruginosa* has several denitrification enzymes that enable anaerobic respiration in anoxic environments such as the cystic fibrosis lung. In the first step in the denitrification pathway nitrate (NO_3^-) is reduced to nitrite (NO_2^-) by either the inner-membrane bound nitrate reductase enzyme encoded by *narGHJI* (Fewson & Nicholas, 1961) or the periplasmic nitrate reductase encoded by *napAB*. Nitrite is then reduced to nitric oxide (NO) by the nitrite reductase encoded by *nirS* (Silvestrini *et al*., 1989). Nitric oxide is further reduced to nitrous oxide (N_2O) by the nitric oxide reductase encoded by *norCB* (Arai *et al*., 1995) and in the final step, nitrous oxide is reduced to dinitrogen (N_2) by the nitrous oxide reductase encoded by *nosZ* (Zumft *et al*., 1992). The global regulator MexT, which also activates MexEF-OprN, has been shown to activate the nitrate respiratory chain (Tian *et al*., 2009a; Tian *et al*., 2009b). While overexpression of MexAB-OprM, MexCD-OprJ, MexEF-OprN and MexXY has also been shown to increase the expression of *nirQ*, *norB*, *nosZ* and *fhp*, but not *narJ* (Olivares *et al*., 2014; Olivares Pacheco *et al*., 2017).

In the previous chapter, we established that the combined loss of MexAB-OprM, MexCD-OprJ, MexEF-OprN and MexXY resulted in the differential expression of virulence genes related to quorum sensing, rhamnolipid and pyocyanin production. To determine the

efflux pump or combination of efflux pumps responsible for these changes, we characterised the phenotypes of the RND efflux pump mutants constructed in chapter 2. Phenotypic assays were used to quantify pyocyanin, rhamnolipid and exoenzyme production, while plate assays were used to screen for changes in motility. Metabolic profiles were characterised using Biolog phenotypic assays, changes to biofilm structure were visualised using confocal microscopy and *Galleria mellonella* and murine infection models were used to determine how these phenotypic changes impact virulence.

4.2 Aims

- Characterise the phenotypic changes associated with loss of efflux

4.3 Hypotheses

- Loss of efflux alters phenotypes in *P. aeruginosa* PAO1-L-DS
- Loss of efflux alters biofilm formation in *P. aeruginosa* PAO1-L-DS
- Loss of efflux alters the virulence of *P. aeruginosa* PAO1-L-DS in *G. mellonella* and murine infection models

4.4 Phenotypic characterisation of the *P. aeruginosa* PAO1-L-DS efflux pump deletion mutants

4.4.1 Growth profiles

The growth profiles of the RND efflux pump mutants were compared with PAO1-L-DS in both rich (LB) (**Figure 4.1**) and minimal (M9) (**Figure 4.2**) media to determine whether loss of efflux impacted growth. Strains were grown in plastic 96-well plates and the optical density of each strain was measured at 600 nm (OD_{600}) every 30 min. In LB, all mutants except Δczc and Δmux reached higher optical densities than PAO1-L-DS after 24 h. The same pattern was observed in M9, though the optical densities were lower overall. These results suggest that loss of all efflux pumps except CzcCBA and MuxAB-OpmB increases the fitness of the mutants.

Figure 4.1: Growth profiles of PAO1-L-DS and the RND efflux system mutants in LB. Overnight cultures were standardized to OD_{600} 0.006 and grown at 37°C for 24 h. The OD_{600} of each culture was measured every 30 min on the TECAN Infinite F200Pro.

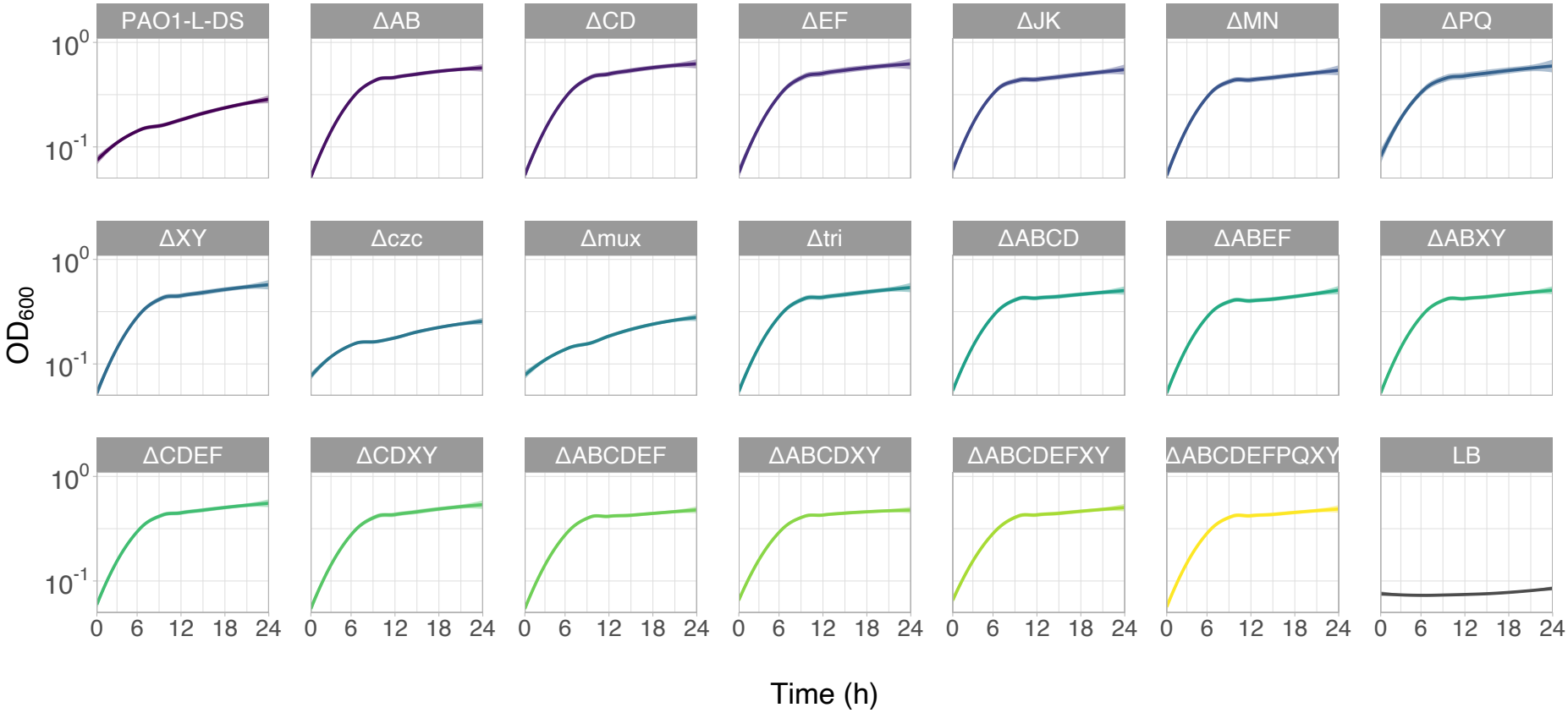


Figure 4.2: Growth profiles of PAO1-L-DS and the RND efflux system mutants in M9. Overnight cultures were standardized to OD_{600} 0.006 and grown at 37°C for 24 h. The OD_{600} of each culture was measured every 30 min on the TECAN Infinite F200Pro.

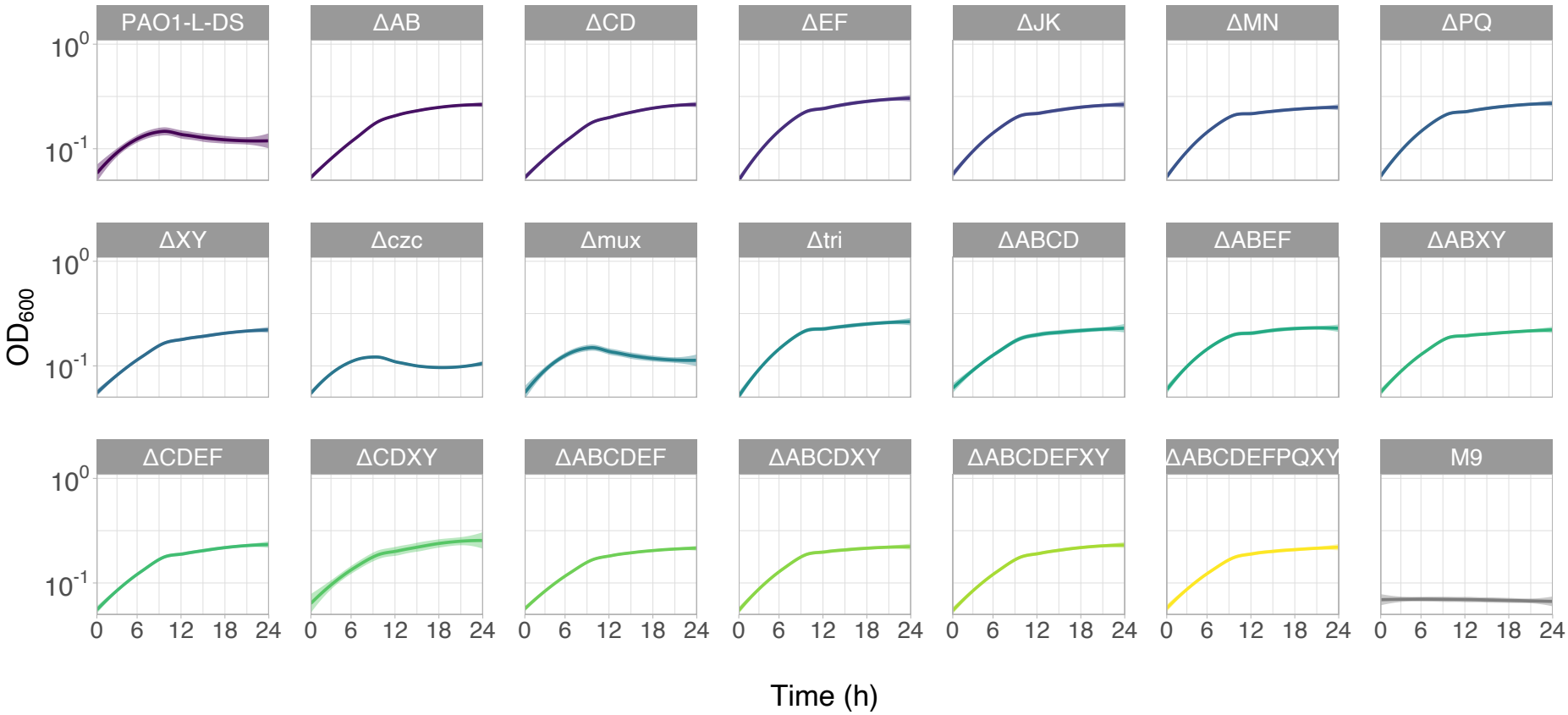


Table 4.1: Minimum inhibitory concentrations of antibiotics for PAO1-L-DS and the efflux pump mutants.

Strain	MIC[a] (μg/mL)						
	AZ	CEF	CHL	ERY	GEN	NOR	TET
ATCC 27853	8	2	128	512	2	2	128
PAO1-L-DS	16	4	128	512	4	2	128
ΔAB	4	2	16	256	2	≤ 0.5	2
ΔCD	8	2	128	512	4	1	128
ΔEF	8	2	128	512	4	2	64
ΔJK	8	1	256	512	4	2	128
ΔMN	8	2	128	512	4	2	128
ΔPQ	8	2	128	512	4	2	128
ΔXY	8	2	256	128	≤ 0.5	1	16
Δczc	4	2	128	512	4	2	128
Δmux	8	2	128	512	4	2	64
Δtri	8	2	128	512	4	2	128
ΔABCD	2	1	8	128	2	≤ 0.5	2
ΔABEF	4	2	16	128	2	≤ 0.5	2
ΔABXY	2	≤ 0.5	8	32	≤ 0.5	≤ 0.5	≤ 0.5
ΔCDEF	4	1	16	512	4	1	64
ΔCDXY	2	1	32	256	4	1	16
ΔABCDEF	2	1	4	32	2	≤ 0.5	2
ΔABCDXY	1	≤ 0.5	4	16	≤ 0.5	≤ 0.5	1
ΔABCDEFXY	≤ 0.5	≤ 0.5	4	16	1	≤ 0.5	1
ΔABCDEFPQXY	≤ 0.5	≤ 0.5	4	32	≤ 0.5	≤ 0.5	1

[a]AZ, aztreonam; CEF, cefepime; CHL, chloramphenicol; ERY, erythromycin; GEN, gentamicin; NOR, norfloxacin; TET, tetracycline. Broth MICs were repeated at least three times and the modal value is displayed. Grey shading represents more than a twofold change in MIC

4.4.2 Antimicrobial susceptibility of the RND efflux pump mutants

Clinically relevant antibiotics were selected from the literature including known RND efflux pump substrates. The minimum inhibitory concentration (MIC) of each antibiotic was determined using the British Society for Antimicrobial Chemotherapy (BSAC) macrodilution method in iso-sensitest broth (Andrews, 2001). MIC values for each strain are detailed in **Table 4.1**. Where reference MICs were available, the MICs for PAO1-L-DS fell within one doubling dilution of the control strain ATCC 27853 so results were deemed valid.

Aztreonam and cefepime belong to the monobactam and fourth-generation cephalosporin classes of β-lactams respectively, which are exported by multiple efflux pumps including MexAB-OprM, MexCD-OprJ, MexXY and CzcCBA (Li *et al*., 1995; Masuda *et al*., 2000; Perron *et al*., 2004) however, the loss of each individual efflux pump did not significantly reduce the MIC of either antibiotic. Similarly, the macrolide erythromycin is exported by MexAB-OprM, MexCD-OprJ, MexJK, MexPQ-OpmE, MexVW, MexXY and MuxABC-OpmB (Li *et al*., 1995; Masuda *et al*., 2000; Chuanchuen *et al*., 2002; Li *et al*., 2003; Mima *et al*., 2005; Mima *et al*., 2009), but no significant decrease in MIC was observed in the single pump mutants. Chloramphenicol is known to be exported by the MexAB-OprM, MexCD-OprJ, MexEF-OprN, MexMN, MexVW and MexXY efflux systems (Köhler *et al*., 1997; Masuda *et al*., 2000; Li *et al*., 2003; Mima *et al*., 2005;) however a significant reduction in MIC was only observed in the ΔAB mutant. Norfloxacin is a fluroquinolone which is exported by MexAB-OprM, MexCD-OprJ, MexEF-OprN, MexGHI-OpmD, MexPQ-OpmE, MexVW, MexXY and MuxABC-OpmB (Köhler *et al*., 1997; Masuda *et al*., 2000; Li *et al*., 2003; Sekiya *et al*., 2003; Mima *et al*., 2005; Mima *et al*., 2009) however a significant reduction in MIC was only observed in the ΔAB mutant. Tetracycline is exported by MexAB-OprM, MexCD-OprJ, MexEF-OprN, MexGHI-OpmD, MexJK, MexVW, MexXY and MuxABC-OpmB (Köhler *et al*., 1997; Masuda *et al*., 2000; Chuanchuen *et al*., 2002; Li *et al*., 2003; Aendekerk *et al*., 2005; Mima *et al*., 2009) however a significant reduction in MIC was only observed in the ΔAB and ΔXY mutants. Lastly, gentamicin is an aminoglycoside which mainly exported by MexXY, but also MexAB-OprM to a lesser extent (Masuda *et al*., 2000). In line with the expected results we only observed a significant reduction in MIC in the ΔXY mutant.

For each of the antibiotics tested, the loss of multiple efflux pumps resulted in a greater fold reduction in the MIC than the loss of any one individual system. The largest reductions were observed for the combinatorial loss of both MexAB-OprM and MexXY. This is likely due to functional redundancy, whereby antibiotics are exported by several different efflux systems so in the absence of one pump the strain can still survive by relying on other pumps to remove the antibiotic from the cell. However, simultaneously deleting multiple efflux systems results in an inability to remove the antibiotic from the cell so the strain becomes susceptible. Interestingly, for each antibiotic tested the maximum reduction in MIC peaked with the loss of three efflux systems, and the deletion of additional pumps did not result in any further reductions to the MIC.

Some of the observed MICs differ from previously reported results. The ΔABCDEFXY mutant had a MIC of 0.5 µg/mL norfloxacin, which is greater than the 0.06 µg/mL observed by Li *et al*., (2003) for similar efflux pump deletion strain YM64 (Δ*mexAB-oprM* Δ*mexCD-oprJ* Δ*mexEF-oprN* Δ*mexXY*). As 0.5 µg/mL was the lowest antibiotic concentration tested for aztreonam, cefepime, gentamicin, norfloxacin and tetracycline the actual MICs were likely lower. Unlike the other antibiotics which are exported by multiple efflux pumps, aminoglycosides are uniquely exported by MexXY, and to a lesser extent MexAB-OprM (Masuda *et al*., 2000). In line with previous research, we found that only loss of MexXY significantly reduced the MIC of gentamicin. These results confirm that loss of efflux increases antibiotic sensitivity and that efflux pump inhibition is an attractive target for overcoming antimicrobial resistance.

4.4.3 Changes in motility

Previous studies suggest a clear link between RND efflux pumps and motility. Loss of MexAB or overexpression caused by loss of MexR decreases swarming ability (Vaillancourt *et al*., 2021). Alcalde-Rico *et al*., (2018) found a strain over-expressing MexCD-OprJ had reduced swarming motility which was complemented by loss of MexD. Overexpression of MexEF-OprN decreases swarming ability (Köhler *et al*., 2001), while loss of MexEF increases swarming ability (Vaillancourt *et al*., 2021). Rampioni *et al*., (2017) found a 4-pump mutant lacking MexAB-OprM, MexCD-OprJ, MexEF-OprN and MexXY had reduced swimming,

swarming and twitching motilities compared to the PAO1 parent strain. The addition of the EPI PAβN to the WT strain also reduced motility in a dose-dependent manner suggesting these results are due to inhibition of the efflux pumps. Aendekerk *et al*., (2002) found strains lacking MexI or OmpD had reduced swarming capabilities compared to PAO1, and complementation restored normal swimming behaviour. Yang *et al*., (2011) found interruption of *muxA* decreased twitching motility. Most recently, Amieva *et al*., (2022) found overexpression of MexJK caused by loss of MexL increased swimming and swarming motilities, while loss of MexK reduced motility compared to PAO1.

To further explore the link between efflux pump deletion and swimming, swarming and twitching motility phenotypes, plate assays were carried out. Swimming motility was measured by the ability of the bacteria to move through a low-viscosity agar (**Figure 4.3**). The swimming diameters of the ΔAB, ΔCD, ΔEF, ΔPQ, ΔXY, Δtri, ΔABCD, ΔABXY and ΔABCDXY mutants were larger than PAO1-L-DS while those of ΔABEF, ΔABCDEFXY and ΔABCDEFPQXY were smaller. The ΔJK mutant was not less motile than the parent strain.

The ability of each strain to swarm across the surface of semi-solid agar was also measured (**Figure 4.4**). The formation of dendritic structures is dependent on functional flagella and TFP (Köhler *et al*., 2000), in addition to rhamnolipids which reduce the surface tension (Caiazza *et al*., 2005). The loss of MexAB-OprM reduced the swarming ability of both the single mutant and all combinatorial mutants lacking this efflux pump, particularly the ΔABEF mutant which was unable to produce any dendrites. Conversely, loss of MexCD-OprJ or MexXY resulted in an over-swarming phenotype as indicated by the thicker dendrites in both the single mutants and the ΔCDXY mutant lacking both efflux pumps. These results are consistent with the work of others except we did not observe an increase in the swarming ability of ΔEF or a decrease in the swarming ability of ΔJK.

Twitching motility is also dependent on the rapid assembly and disassembly of TFP, enabling the cells to migrate across a solid surface (**Figure 4.5**). Deletion of MexAB-OprM, MexCD-OprJ or MexXY resulted in the abolition of twitching motility in both single and combinatorial mutants. The twitching zone of the Δczc mutant was comparable with PAO1-L-DS. Together, these results indicate that MexAB-OprM, MexCD-OprJ and MexXY are required for normal motility.

Figure 4.3: Swimming motility of PAO1-L-DS and the RND efflux system mutants. The inoculum was stabbed in the centre of the swimming agar and plates were incubated at 37°C for 8 h. Images are representative of at least 3 technical and 3 biological replicates.

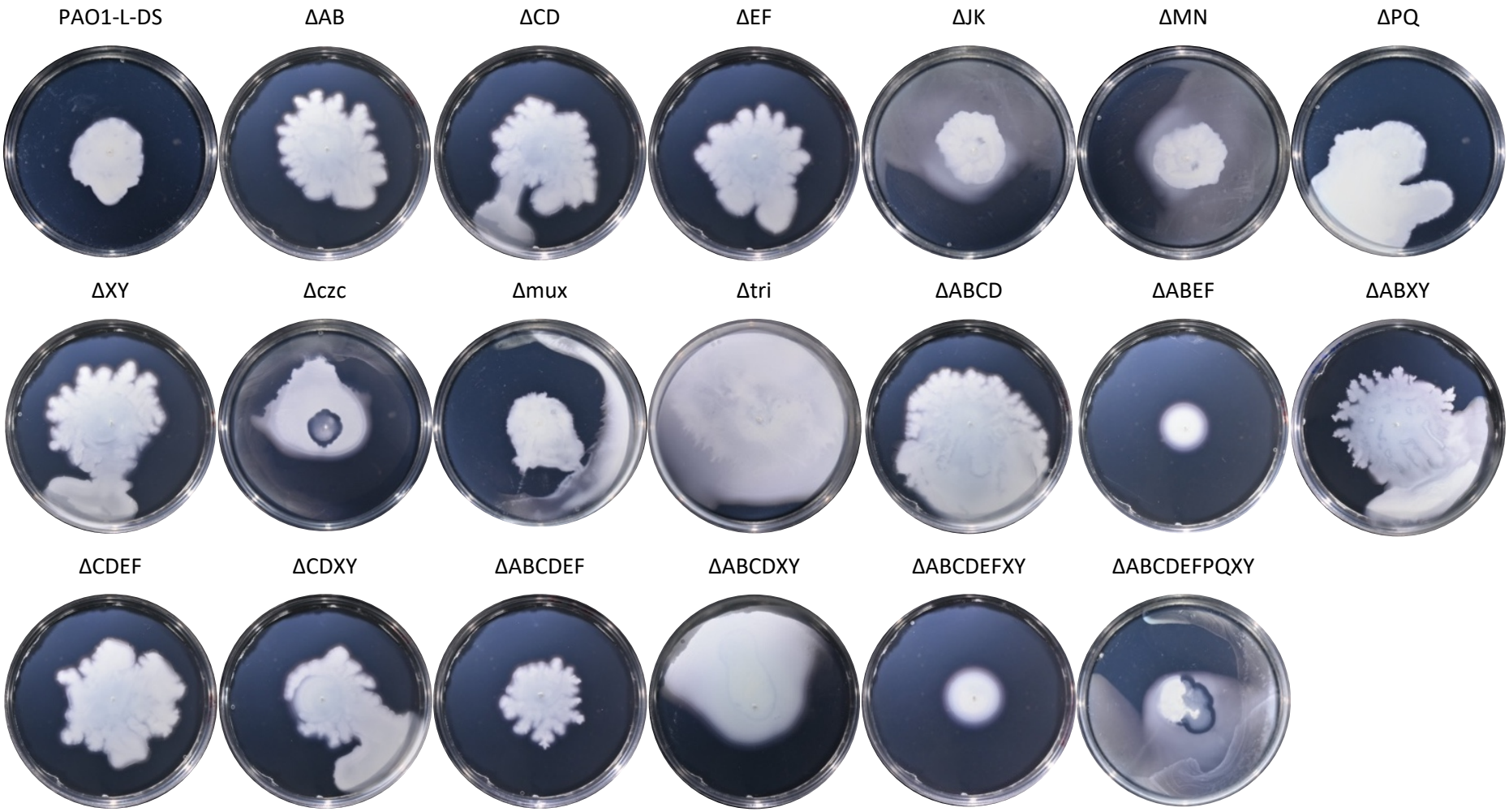


Figure 4.4: Swarming motility of PAO1-L-DS and the RND efflux system mutants. The inoculum was placed on the surface of the swarming agar and plates were incubated at 37°C for 16 h. Images are representative of at least 3 technical and 3 biological replicates.

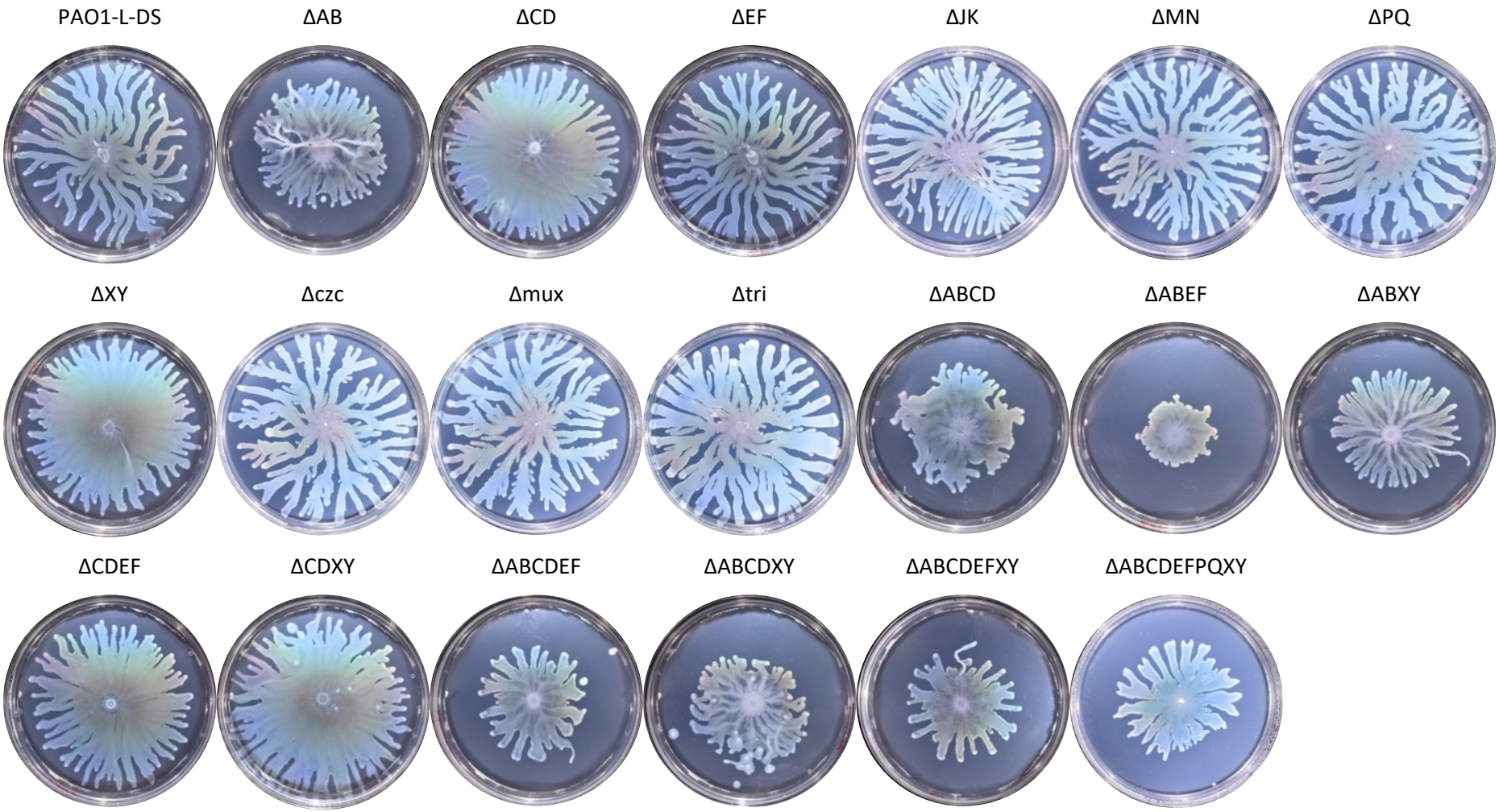
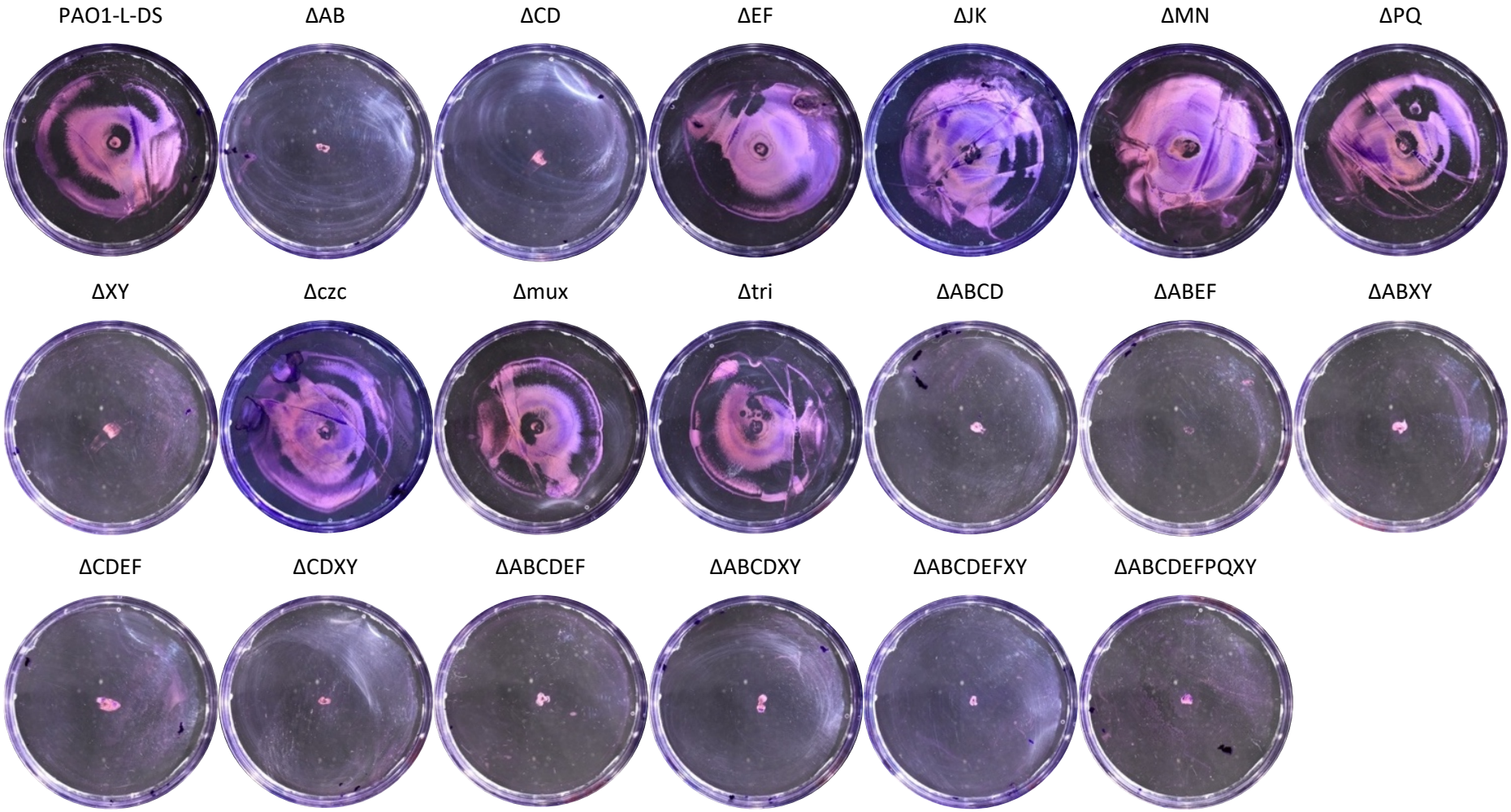


Figure 4.5: Twitching motility of PAO1-L-DS and the RND efflux system mutants. The inoculum was placed on the surface of the swarming agar and plates were incubated at 37°C for 16 h. The media was then removed and the twitching zone was stained with crystal violet. Images are representative of at least 3 technical and 3 biological replicates.



4.4.4 Changes in pyocyanin production

In the previous chapter, we observed an increase in the pyocyanin production of the ΔABCDEFXY mutant so the pyocyanin production of the remaining mutants was characterized to determine which efflux pumps were responsible for these differences. As the production of virulence factors is cumulative, supernatants were collected from strains grown to stationary phase (**Figure 4.6A**). Quorum sensing mutants were used as controls.

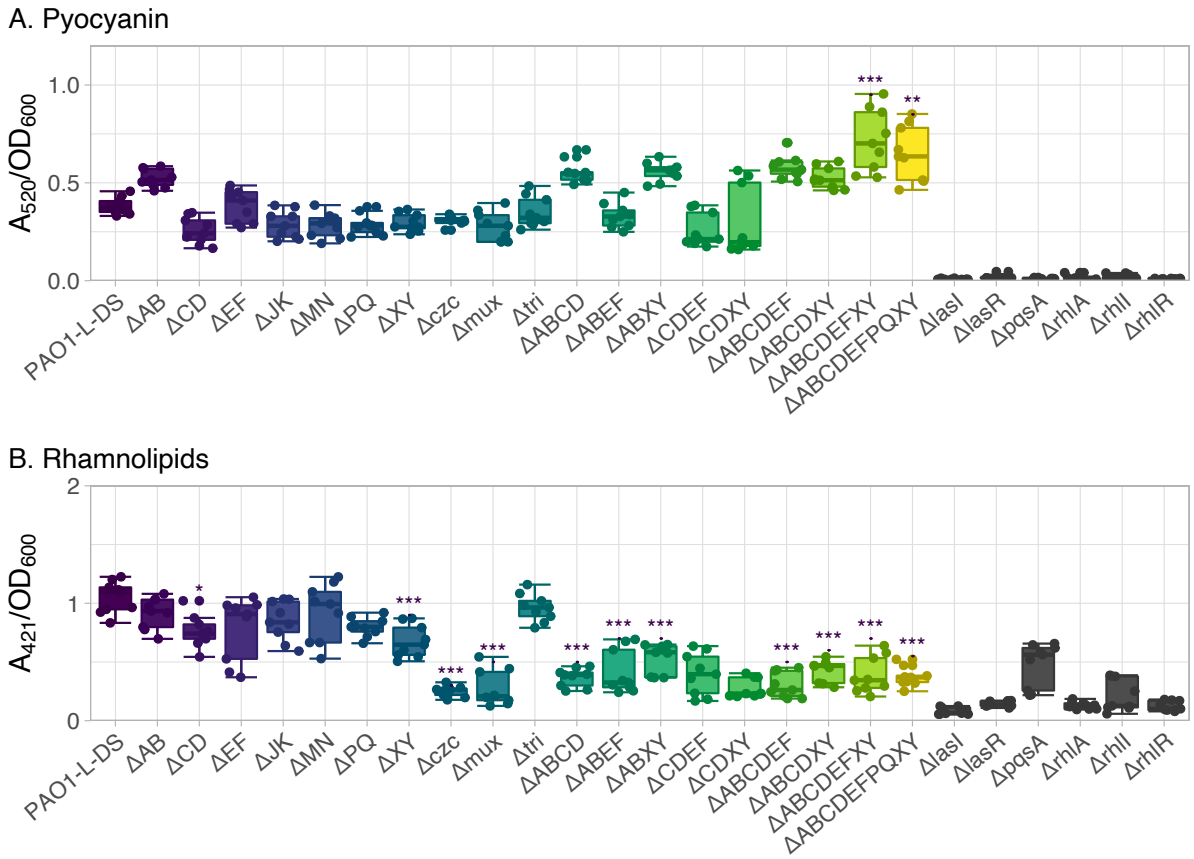
We observed significant increases in pyocyanin production for the ΔABCDEFXY and ΔABCDEFPQXY mutants. In contrast to Amieva *et al*., (2022) we did not observe a difference in pyocyanin production for the ΔJK mutant.

4.4.5 Changes in rhamnolipid production

We also found ΔABCDEFXY produced fewer rhamnolipids than the parent strain. Köhler *et al*., (2000) established a link between rhamnolipid production and swarming motility when they found a *rhlA* mutant was unable to swarm. Rhamnolipids reduce the surface tension which aids swarming motility (Glick *et al*., 2010). The ΔABCDEFXY mutant is also impaired in its ability to swarm so we hypothesised that all of the efflux pump mutants with impaired swarming motility would produce fewer rhamnolipids than PAO1-L-DS.

The rhamnolipid production of the single and combinatorial mutants was indirectly quantified using the orcinol method on 16 h supernatants (**Figure 4.6B**). Though we observed a significant decrease in rhamnolipid production for all of the combinatorial mutants, we did not observe a significant decrease for ΔAB, or increase for the ΔCD and ΔXY mutants in line with the swarming assay results. Unexpectedly, we also observed decreases in rhamnolipid production for the Δczc and Δmux mutants which is the first time CzcCBA and MuxABC-OpmB have been linked to changes in rhamnolipid production. In contrast to Amieva *et al*., (2022) we did not find loss of MexJK altered rhamnolipid production.

Figure 4.6: Pyocyanin and rhamnolipid production of PAO1-L-DS and the RND efflux system mutants A) Pyocyanin production at 520 nm B) Rhamnolipid production at 421 nm. Assays were performed using culture supernatants of strains grown in LB medium for 16 h at 37°C. Results were divided by the starting OD_{600} to normalize for growth. Figures are representative of at least 3 biological and 3 technical replicates. $p \leq 0.05$ (*), $p \leq 0.01$ (**), $p \leq 0.001$ (***).



4.4.6 Changes in protease production

Pseudomonas aeruginosa secretes several proteases into host cells including alkaline protease, elastase A, elastase B and protease IV which cleave peptide bonds and degrade the host immune response. Alkaline protease is secreted by the Apr T1SS, while elastase A, elastase B and protease IV are secreted by the T2SS. In the previous chapter, we found the ΔABCDEFXY mutant produced less alkaline protease and elastase B than PAO1-L-DS so the exoprotease phenotypes of the mutant library were determined.

A universal protease assay was used to determine whether efflux pump deletion altered the production of exoenzymes (**Figure 4.7A**). Azocasein is used as a substrate for this fluorescence-based assay where casein hydrolysis is quantified by the release of the azo dye, which is detected at 400 nm. We observed a significant reduction in protease activity with loss of MexAB-OprM, MexCD-OprM and MexEF-OprN (ΔABCDEF), and subsequent deletions (ΔABCDEFXY and ΔABCDEFPQXY)

As the universal protease assay is non-specific we were unable to determine whether the changes were caused by a reduction in one or a combination of proteases, so individual proteases were quantified. An elastin Congo-Red assay was used to quantify elastase B activity (**Figure 4.7B**). Elastase B hydrolyses elastin and releases the Congo-Red dye which is detectable at 495 nm. In accordance with the universal protease assay, we observed a significant reduction in elastin hydrolysis for the ΔABCDEF, ΔABCDXY, ΔABCDEFXY and ΔABCDEFPQXY mutants. Unexpectedly, we also observed a decrease in elastase B production for the Δczc mutant.

Protease IV production was quantified using the chromogenic substrate Chromozym PL, which is cleaved by plasmin to produce a residual peptide and 4-nitraniline whose absorbance is measured at 410 nm (**Figure 4.7C**). A significant increase in protease IV production was only observed in the ΔXY mutant.

Elastase A activity was measured by combining *P. aeruginosa* supernatants with heat-inactivated *S. aureus* and measuring the reduction in turbidity over 90 mins (**Figure 4.8**: Elastase A production of PAO1-L-DS and the RND efflux system mutants. *S. aureus* SH1000 was heated to 100°C for 10 mins and standardized to OD600 1.0. Assays were performed using culture supernatants of strains grown in LB medium for 16 h at 37°C. The elastase A activity of each culture

was measured at OD595 every 1 min for 90 mins on a TECAN Spark 10 M. Figures are representative of at least 3 biological and 3 technical replicates.

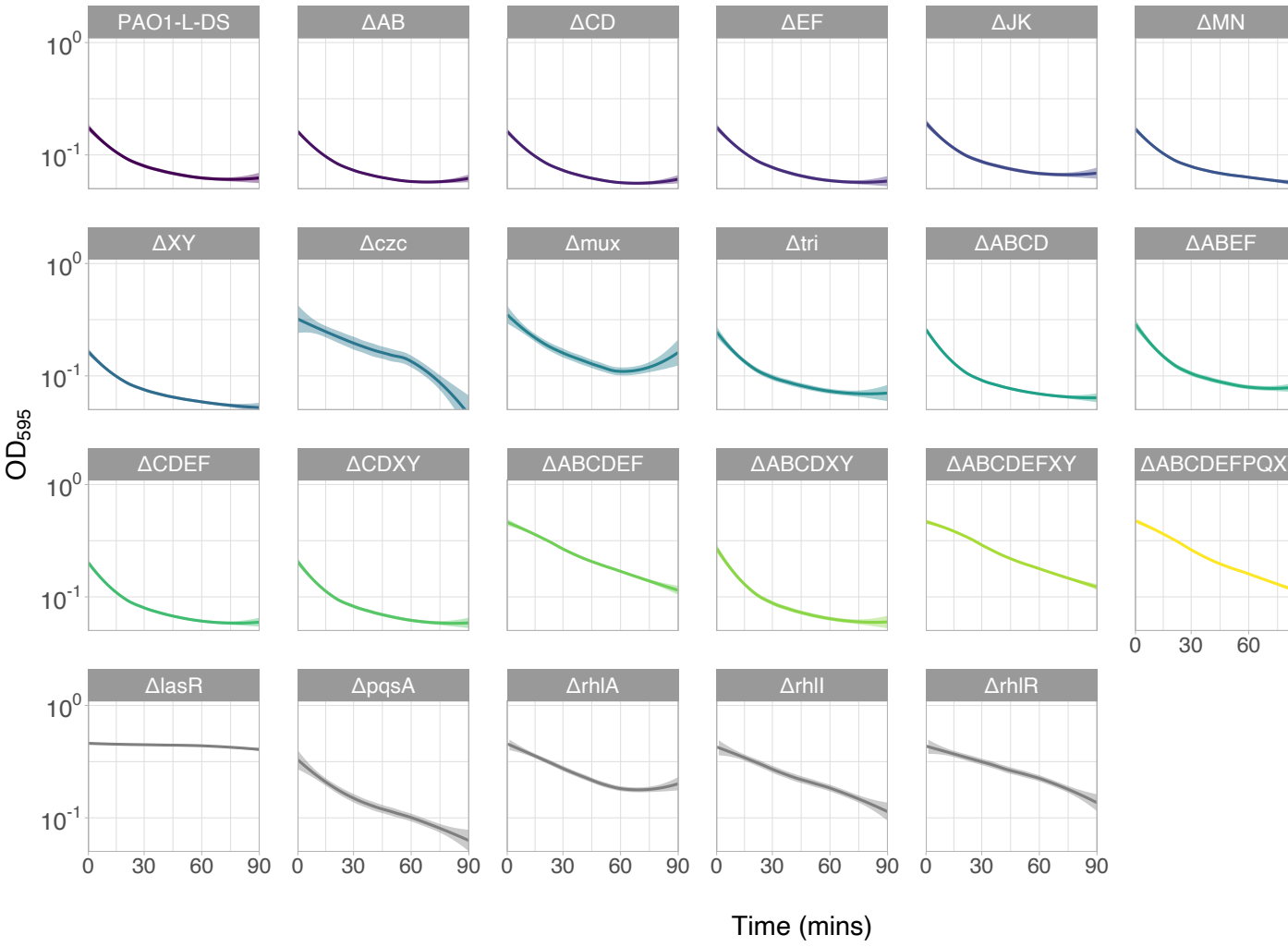


Figure 4.9). As reductions in OD_{595} correlate with increased elastase A activity, smaller decreases indicate less enzyme production. A reduction in the rate of *S. aureus* hydrolysis was observed in the Δczc, ΔABCDEF, ΔABCDEFXY and ΔABCDEFPQXY mutants.

Figure 4.7: Universal protease, Elastase B and Protease IV production of PAO1-L-DS and the RND efflux system mutants A) Universal protease activity at 400 nm B) Elastase B activity at 495 nm C) Protease IV activity at 410 nm. Assays were performed using culture supernatants of strains grown in LB medium for 16 h at 37°C. Results were divided by the starting OD_{600} to normalize for growth. Figures are representative of at least 3 biological and 3 technical replicates. $p \leq 0.05$ (*), $p \leq 0.01$ (**), $p \leq 0.001$ (***).

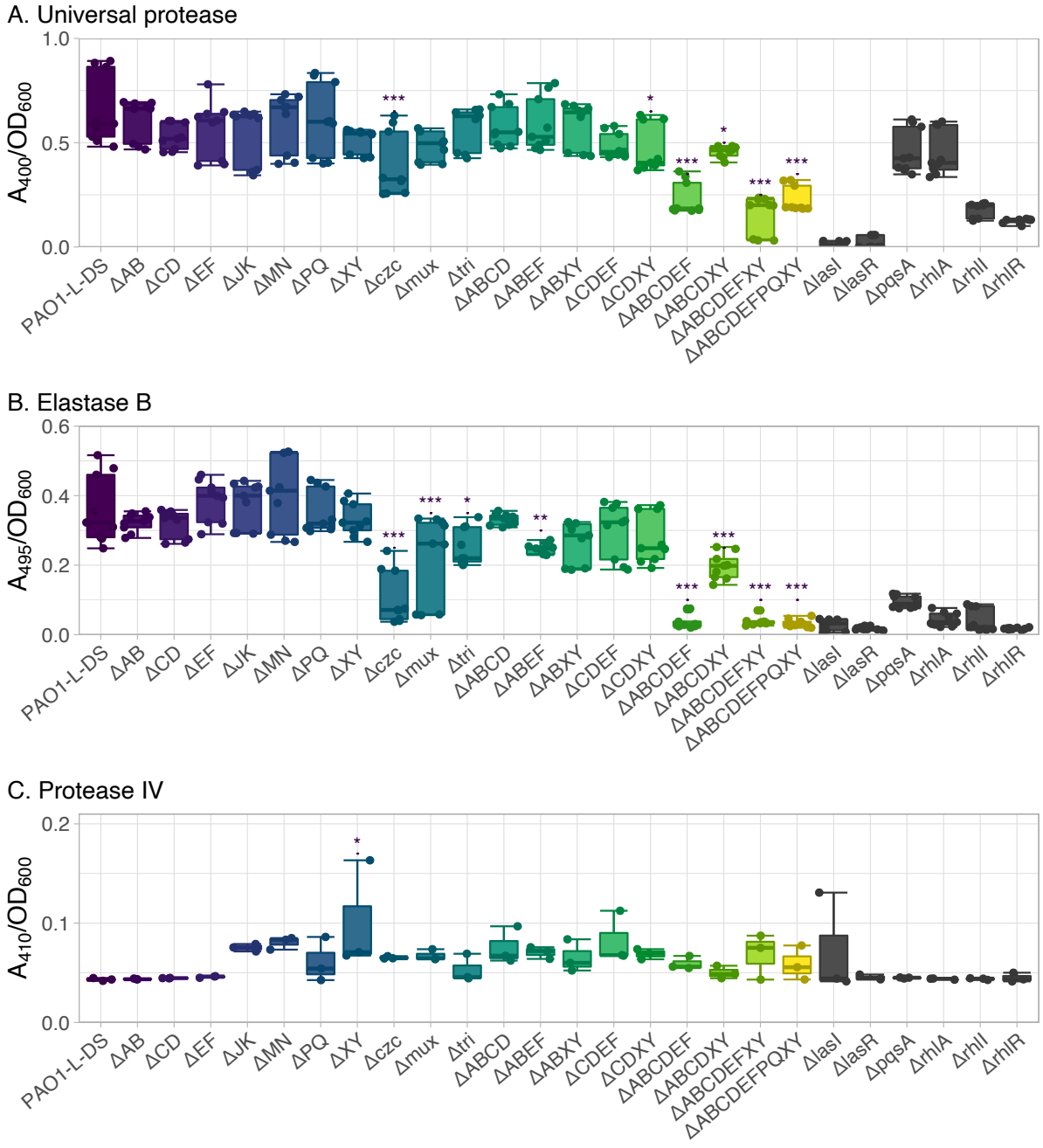


Figure 4.8: Elastase A production of PAO1-L-DS and the RND efflux system mutants. *S. aureus* SH1000 was heated to 100°C for 10 mins and standardized to OD_{600} 1.0. Assays were performed using culture supernatants of strains grown in LB medium for 16 h at 37°C. The elastase A activity of each culture was measured at OD_{595} every 1 min for 90 mins on a TECAN Spark 10 M. Figures are representative of at least 3 biological and 3 technical replicates.

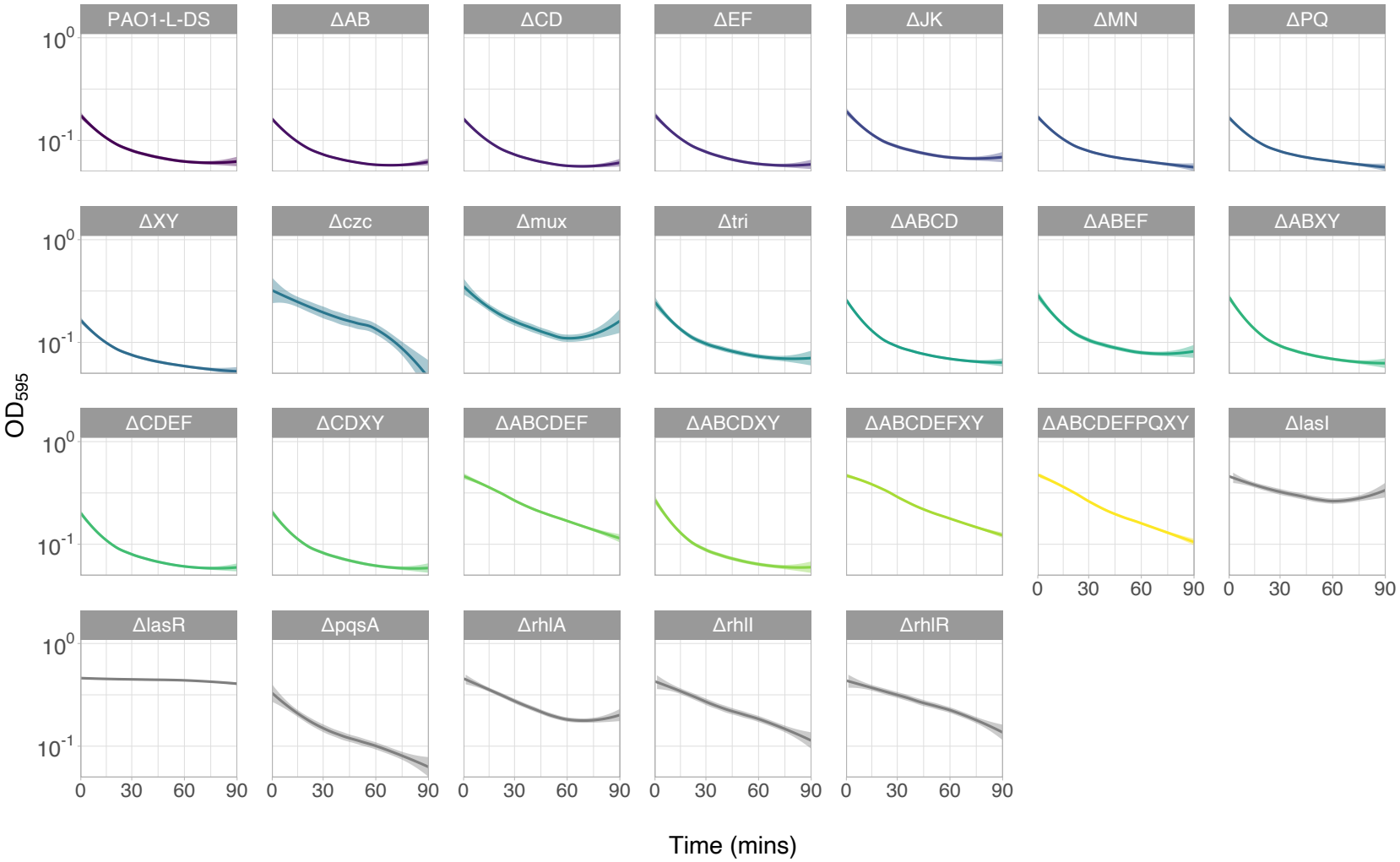
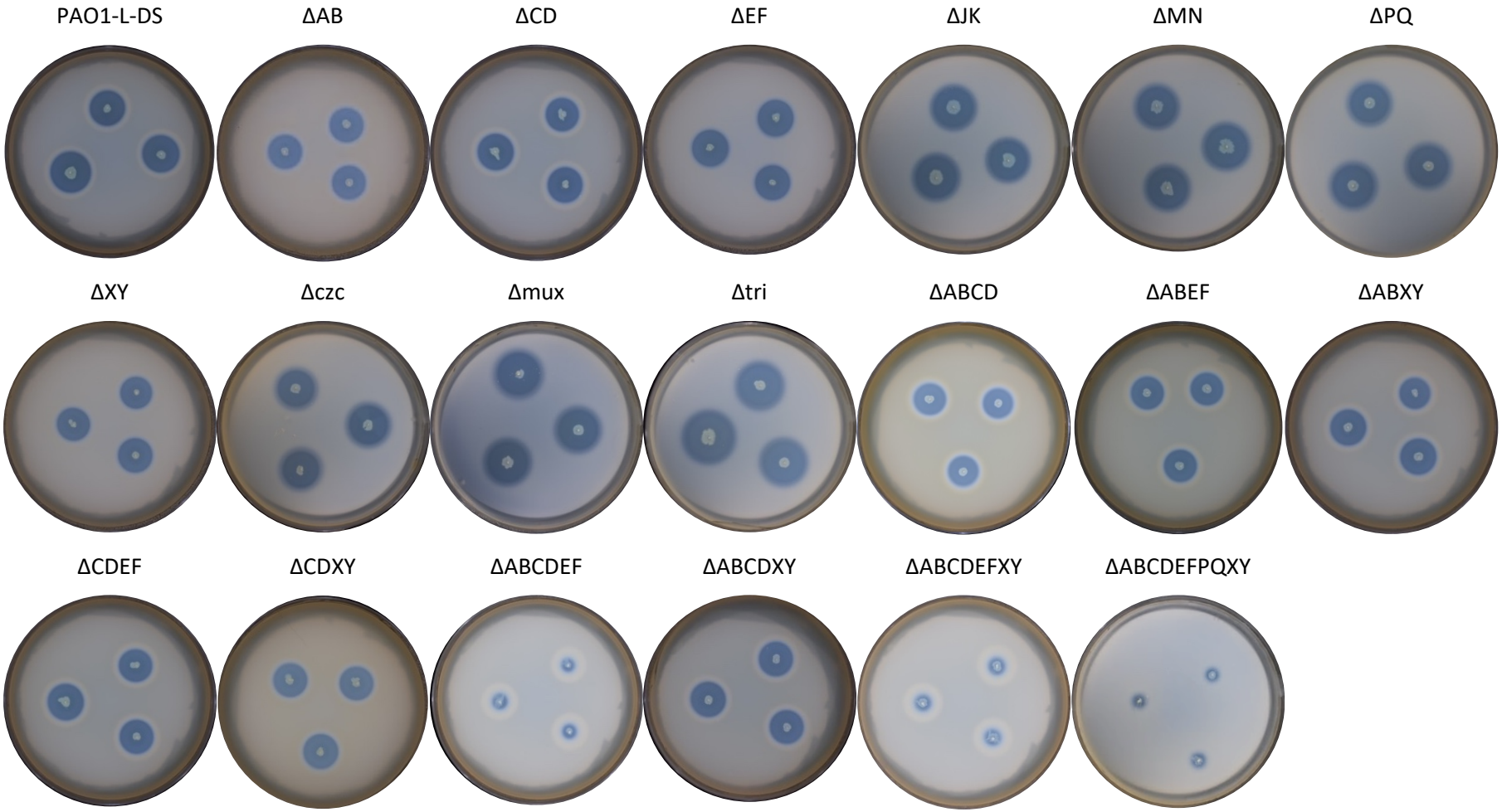


Figure 4.9: Alkaline protease production of PAO1-L-DS and the RND efflux system mutants. The inoculum was stabbed in the center of the skimmed milk agar, and plates were incubated at 37°C for 24 h. Images are representative of at least 3 technical and 3 biological replicates.



Lastly, alkaline protease activity was visualised on skimmed milk agar plates (**Figure 4.9**). Though casein is also the main protein in milk, the agar was adjusted to pH 10.0 to select for alkaline protease. The results follow the same pattern with strains ΔABCDEF, ΔABCDEFXY and ΔABCDEFPQXY displaying a loss of alkaline protease production.

4.5 Metabolic profiling

P. aeruginosa employs various catabolic pathways to utilise different nutrient (eg. carbon, nitrogen, phosphorus and sulphur) sources. Metabolic versatility enables the organism to adapt to a variety of environments including those with nutrient limitations. To further explore the effect of loss of efflux on metabolism, we compared the metabolic profiles of PAO1-L-DS, ΔABCDEFXY and ΔABCDEFPQXY using Biolog phenotypic microarrays. Tetrazolium dye reduction was measured at 590 nm every 15 mins for 24 h (**Appendix AC**, **Appendix AD** & **Appendix AE**). The area under the curve (AUC) was calculated for each strain and the percentage change in AUC from PAO1-L-DS was considered to be significant if it was greater than 50 %. Compounds with an AUC < 1000 for all three strains were removed to avoid small changes in AUC producing large percentage changes that would make the compound seem more significant than it was (**Figure 4.10**).

P. aeruginosa can utilise a variety of carbon sources for bacterial growth. Of the 95 carbon sources tested, all three strains were unable to metabolise 57 compounds including simple sugars (eg. L-arabinose, D-ribose), polysaccharides (eg. sucrose, maltotriose) and carboxylic acids (eg. formic acid, glyoxylic acid). All strains were able to utilise tricarboxylic acid (TCA) cycle intermediates (pyruvic acid, citric acid, α-Keto-Glutaric Acid, succinic acid and fumaric acid) however, while the strains were able to utilise D,L-Malic Acid and L-Malic Acid, none of the strains were able to utilise D-Malic Acid. There was also a reduction in α-Keto-Glutaric acid and L-Malic Acid metabolism in the ΔABCDEFPQXY mutants compared to PAO1-L-DS and ΔABCDEFXY. Uniquely, the AUC of the ΔABCDEFXY mutant with adenosine as the carbon source was 245% greater than PAO1-L-DS (**Figure 4.10A**).

Figure 4.10: Carbon, nitrogen, phosphorus and sulphur utilisation of PAO1-L-DS, ΔABCDEFXY and ΔABCDEFPQXY. Biolog PM1, PM3B and PM4A microplates were inoculated with each strain and incubated at 37°C for 24 h. Readings were taken every 15 min and respiration was measured in OmniLog units. Results were normalized relative to the negative control well on each plate. The area under the curve (AUC) was calculated for each strain using the R package [pracma] and compounds with AUC < 1000 for all three strains were removed. The percentage change in AUC from PAO1-L-DS was calculated for A) Carbon B) Nitrogen C) Phosphorus and D) Sulphur sources. Positive numbers represent an increase in AUC and negative numbers represent a decrease in AUC compared to PAO1-L-DS. Only metabolites with a > 50% increase in AUC (pink) or > 50% reduction in AUC (orange) for at least one of the mutants are shown. Tables generated using the R package [formattable].

A.

Carbon source	ΔABCDEFXY	ΔABCDEFPQXY
Adenosine	245	37.6

B.

Nitrogen source	ΔABCDEFXY	ΔABCDEFPQXY
Xanthine	-115.2	-124.1
Ala-Thr	-25.6	-82.7
Ala-Asp	9.0	-73.4
N-Acetyl-D- Galactosamine	-19.3	-69.5
D-Valine	-29.1	-65.1
Alloxan	-22.3	-62.9
Ala-Leu	-10.5	-61.2
Gly-Gln	-5.0	-60.3
D,L-Lactamide	-2.9	-58.8
Guanine	-32.8	-57.7
Ala-Gly	-13.4	-55.9
Ala-Glu	3.7	-55.7
ß-Phenylethylamine	15.6	-50.9

C.

Phosphorus source	ΔABCDEFXY	ΔABCDEFPQXY
D-Glucose-6- Phosphate	-33.3	-110.5
Adenosine-2'- monophosphate	-62.0	-77.2
Adenosine-3'- monophosphate	-58.3	-72.7
Thymidine-3'- monophosphate	-61.0	-72.6
Cytidine-5'- monophosphate	-53.9	-71.5
Uridine-5'- monophosphate	-53.4	-68.8
Thymidine-5'- monophosphate	-55.1	-67.4
Adenosine-5'- monophosphate	-51.1	-63.5
Cytidine-2'- monophosphate	-45.7	-63.0
Cytidine-2',3'-cyclic monophosphate	-47.7	-61.1
Guanosine-5'- monophosphate	-50.7	-59.9
Thymidine-3-,5'-cyclic monophosphate	-42.2	-56.0
Guanosine-2',3'-cyclic monophosphate	-45.3	-55.3
Uridine-2'- monophosphate	-41.0	-52.9
Guanosine-2'- monophosphate	-47.4	-51.4
Guanosine-3',5'-cyclic monophosphate	-40.8	-51.1
Uridine-2',3'-cyclic monophosphate	-47.0	-50.8

D.

Sulphur source	ΔABCDEFXY	ΔABCDEFPQXY
Lanthionine	-55.7	-52.3

In the previous chapter, the transcriptomic analysis revealed the nitrate reductase *narJ* and flavohemoglobin *fhp* were downregulated 1.22 and 1.57 fold respectfully at exponential phase in the ΔABCDEFXY mutant compared to PAO1-L-DS. Several other studies have also reported the altered expression of nitrate metabolism genes in efflux pump mutants (Olivares *et al*., 2014; Olivares Pacheco *et al*., 2017; Rampioni *et al*. 2017; Adamiak *et al*. 2021). We compared the utilisation of 95 nitrogen sources including amino acids and dipeptides. The mutants were unable to metabolise 15 compounds including amino acids (L-cysteine, D-aspartic acid or L-Homoserine), amines (N-amylamine, N-butylamine ethylamine, methylamine) purines and pyrimidines (thymidine). The biggest reduction in AUC was seen with xanthine (**Figure 4.10B**). We observed poor utilization of many dipeptide nitrogen sources by the ΔABCDEFXY mutant, which were amplified in the ΔABCDEFPQXY mutant which grew poorly on all dipeptides except Ala-Gln, Ala-His and Gly-Asn.

Phosphate is an essential component of nucleic acids, phospholipids and other biomolecules. Phosphate limitation is sensed by the PhoBR TCS (Filloux *et al*., 1988) leading to the activation of phosphate acquisition genes such as *plcB*, *plcH* and *plcR* (Bains *et al*., 2012). Phosphate starvation has also been associated with changes in quorum sensing and swarming motility (Bains *et al*., 2012) as PhoB activates the expression of *rhlR*, *pqsA*, *pqsR* and *lasI* (Meng *et al*., 2020). The three strains were grown on 59 phosphorus sources including inorganic phosphates and phosphorylated amino acids. The strains were unable to utilise trethyl phosphate, hypophosphite, cytidine-3'-monophosphate, phosphono acetic acid or methylene disphosphonic acid. Of the remaining 54 phosphorous sources tested, the ΔABCDEFXY and ΔABCDEFPQXY mutants had decreased metabolic activity on nucleotides and cyclic nucleotides containing adenosine, cytidine, guanosine and thymidine compared to PAO1-L-DS (**Figure 4.10C**).

Sulphur is another important element required for the formation of proteins, enzymes and enzyme co-factors. Genes from the sulphur-regulated *msu* operon (*msuD*, *msuE*) were upregulated in the ΔABCDEFXY at exponential phase. Of the 35 sulphur sources tested, the strains were only unable to utilise N-acetyl-L-cysteine and tetramethylene sulfone. The only sulphur compound with a > 50% change in AUC was Lanthionine: ΔABCDEFXY and ΔABCDEFPQXY had decreases of 55.7% and 52.3% respectively compared to PAO1-L-DS (**Figure 4.10D**)

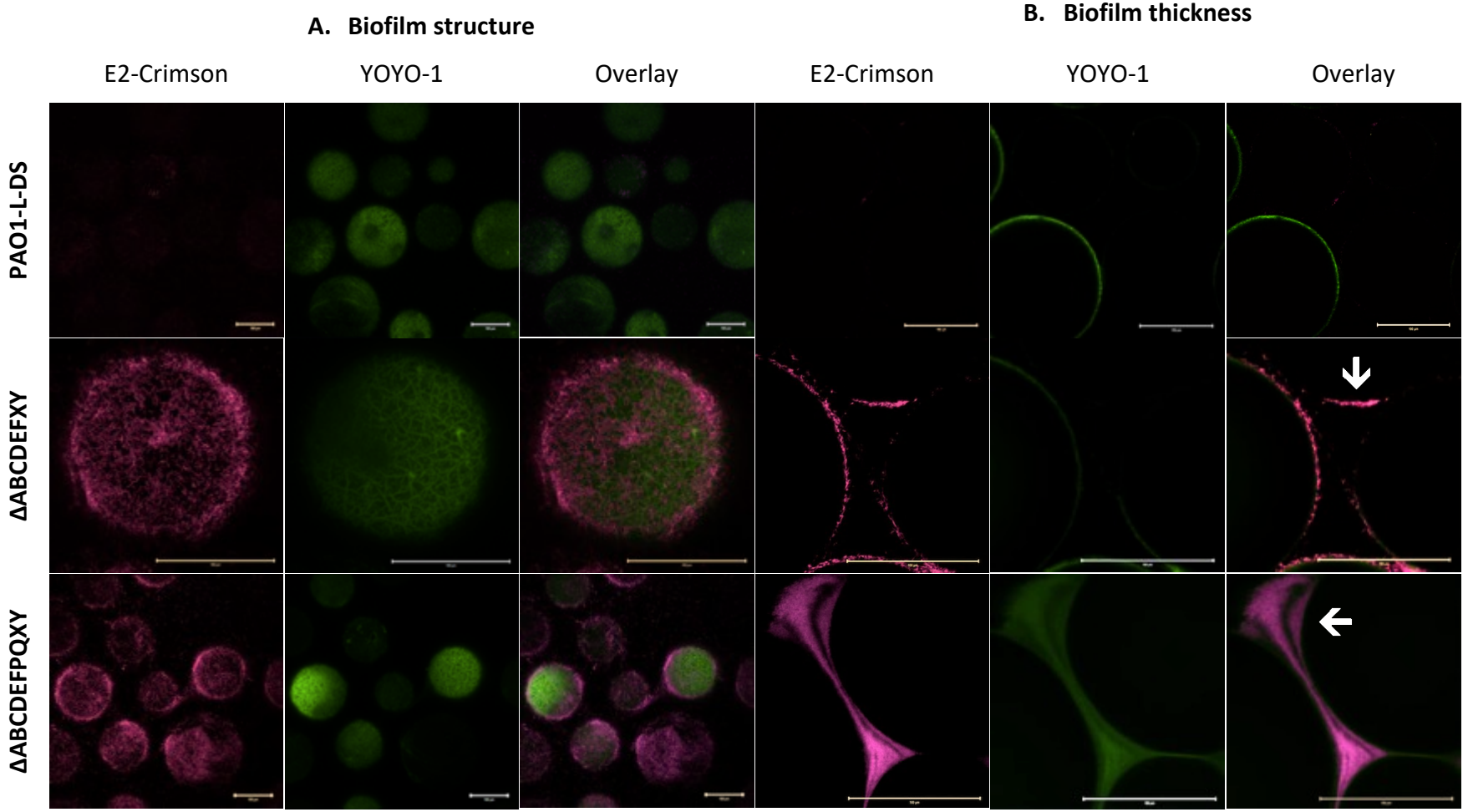
4.6 Biofilm formation

In the previous chapter, RNA sequencing of the ΔABCDEFXY mutant indicated that several genes involved in biofilm formation were differentially expressed. These included upregulation of the genes encoding the MexGHI-OpmD efflux pump at exponential growth phase as a substrate of this pump, 5-Me-PCA, has been linked to biofilm development (Sakhtah *et al*., 2016). One of the few downregulated genes in the ΔABCDEFXY mutant was the Psl and pyoverdine operon regulator *ppyR*, which had a log2 fold-change of -1.75 at exponential phase. This gene positively regulates the production of the siderophore pyoverdine and the extracellular polysaccharide matrix component Psl, which is important for biofilm initiation and maturation (Ma *et al*., 2007). Inactivation of *ppyR* has been shown to reduce biofilm formation (Attila *et al*., 2008). Hcp proteins encoded by *hcpA* and *hcpC* were also upregulated at stationary phase and the H2-T6SS has been linked to biofilm formation (Chen *et al*., 2020).

The RNA-seq results suggest that biofilm formation may be altered in the ΔABCDEFXY mutant. To test this hypothesis PAO1-L-DS, ΔABCDEFXY and ΔABCDEFPQXY tagged with the constitutively fluorescent protein E2-Crimson were grown on cytodex beads in M9 for 48 h at 37°C. Extracellular DNA (eDNA) is a major structural component of the biofilm matrix, so to investigate whether the differences in biofilm formation were the result of changes to eDNA production, biofilms were also stained with the nucleic acid binding stain YOYO-1. Qualitative fluorescent images were taken with a confocal microscope (**Figure 4.11**).

The lack of visible E2-Crimson for PAO1-L-DS indicates the absence of bacteria. However, the presence of YOYO-1 staining contradicts this finding and suggests the bacteria have lysed. Overall, the images suggest eDNA from all three strains formed a clear lattice structure on the bead surface similar to that described for other bacteria (Devaraj *et al*., 2019), and while ΔABCDEFXY tended to form threads between beads ΔABCDEFPQXY formed streamers (indicated by white arrows on images). Further biological repeats and quantitative analysis are required to confirm these findings.

Figure 4.11: Confocal microscopy of PAO1-L-DS, ΔABCDEFXY and ΔABCDEFPQXY biofilm production on cytodex beads. Strains tagged with the fluorescent protein E2-Crimson (magenta) were grown on cytodex beads in M9 for 48 h at 37°C. Biofilms were imaged using a confocal microscope at 20 x magnification. Extracellular DNA fibres in the biofilm matrix are illustrated by nucleic acid straining with YOYO-1 (green). A) Biofilm structure B) Biofilm thickness. Differences in biofilm structure are indicated with white arrows. Images were analysed using ZEN software. Scale bars represent 100 µm.



4.7 Virulence

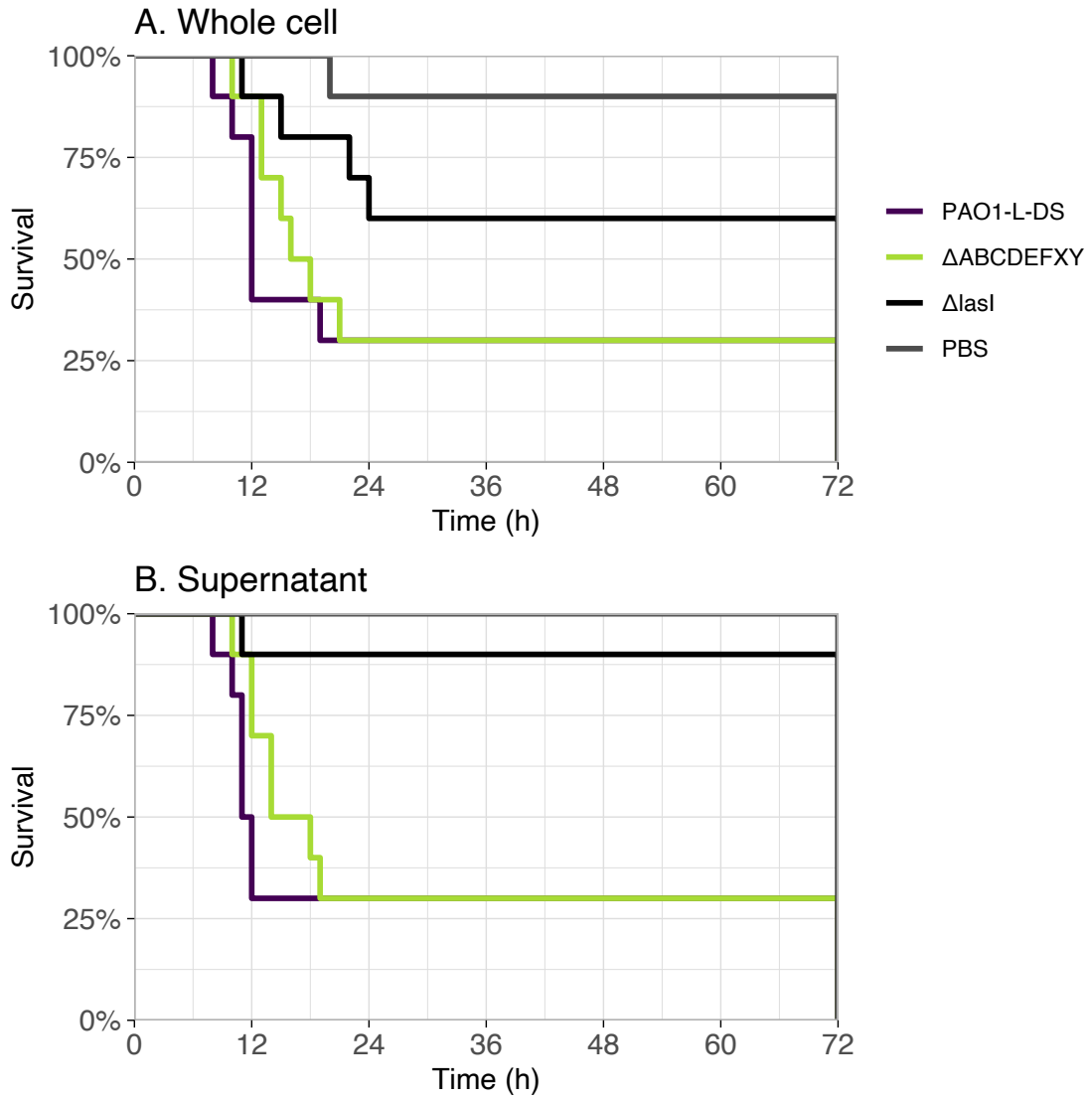
4.7.1 *Galleria mellonella* infection

Like mammals, the waxworm larvae of *G. mellonella* has an innate immune system comprising both cellular and humoral responses. The cellular response is mediated by haemocytes, which play a similar role to mammalian phagocytes while the humoral response includes the production of antimicrobial peptides and melanisation. In mammals, melanisation protects against UV radiation while in insects melanin is used to encapsulate pathogens and heal wounds. Melanin production is triggered by pathogen-associated molecular patterns (PAMPs) which activate the phenoloxidase cascade. This process is tightly regulated as melanin overproduction is toxic, and complete melanisation correlates with death. *G. mellonella* larvae are also cheap and easy to inoculate making them a suitable infection model.

Previous research found that loss of MexAB-OprM, MexCD-OprJ, MexEF-OprN and MexXY increased *G. mellonella* survival (Rampioni *et al*., 2017). These results were also replicated by the addition of 50 μM PAβN to the PAO1 parent strain (Rampioni *et al*., 2017). To confirm these findings, *G. mellonella* larvae were infected with PAO1-L-DS or ΔABCDEFXY tagged with the fluorescent protein E2-Crimson and constitutively expressing *lux*. Larvae were incubated at 37°C and checked for survival every h.

The median survival times for larvae injected with whole cell cultures of PAO1-L-DS and ΔABCDEFXY were 12 and 17 h (**Figure 4.12A**). Median survival times for bacterial supernatants were 11.5 and 16 h respectively (**Figure 4.12B**). Although PAO1-L-DS whole cell and supernatant cultures appeared to kill larvae quicker than ΔABCDEFXY, these results were not found to be statistically significant (**Figure 4.12C**). The median survival times for control larvae injected with Δ*lasI* and PBS were 72 h for both whole cell cultures and supernatants. The results of this experiment are unclear so in the absence of further biological repeats no conclusions can be drawn.

Figure 4.12: *G. mellonella* infection with PAO1-L-DS and ΔABCDEFXY. Kaplan-Meier survival plots of *G. mellonella* larvae injected with A) 10 µL OD_{600} 0.05 or B) 10 µL bacterial supernatants of PAO1-L-DS or ΔABCDEFXY constitutively expressing *lux* and the fluorescent protein E2-Crimson. Larvae were also injected with Δ*lasI* and PBS as controls. Ten larvae were injected for each condition and the % survival over 72 h is shown C) The median survival times of *G. mellonella* larvae injected with each strain were compared using a log-rank test. $p \leq 0.05$ (*), $p \leq 0.01$ (**), $p \leq 0.001$ (***).



C.

Whole cell

	PAO1-L-DS	**ΔABCDEFXY**	**Δ*lasI***
ΔABCDEFXY	0.604	-	-
Δ*lasI*	0.160	0.160	-
PBS	0.014*	0.014*	0.160

Supernatant

	PAO1-L-DS	**ΔABCDEFXY**	**Δ*lasI***
ΔABCDEFXY	0.4448	-	-
Δ*lasI*	0.0146*	0.0162*	-
PBS	0.0039**	0.0039**	0.3808

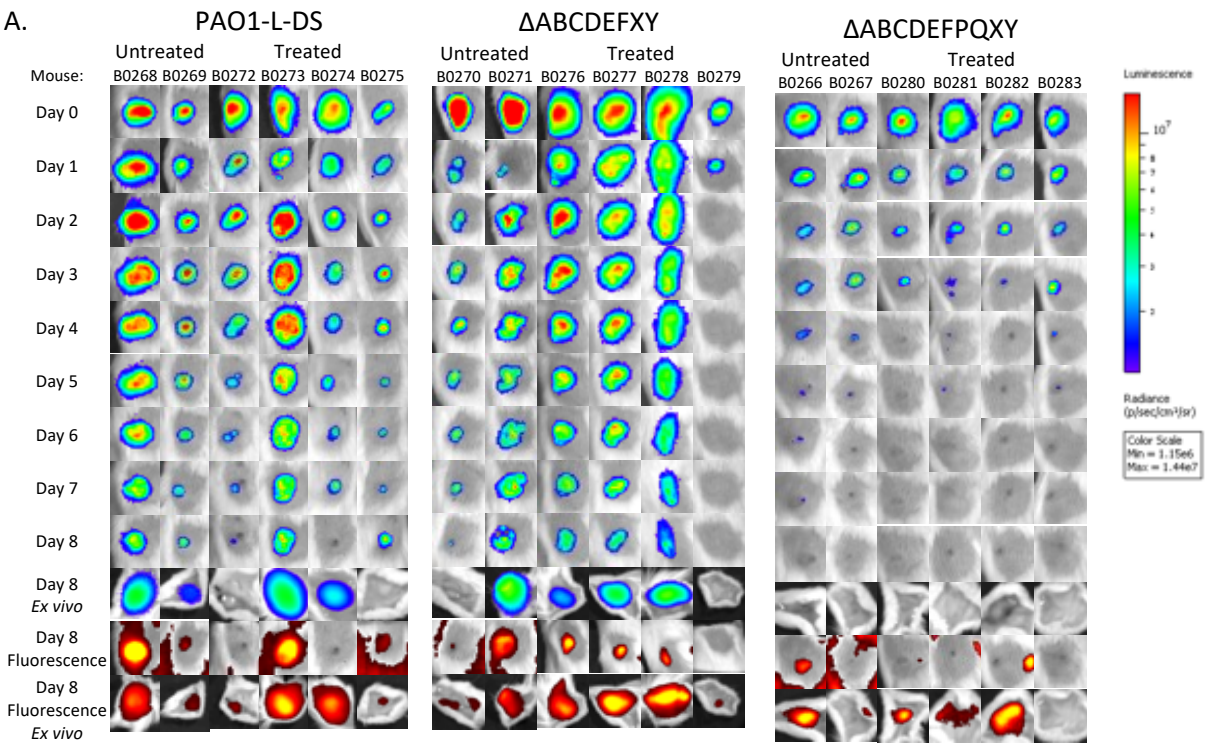
4.7.2 Murine infection

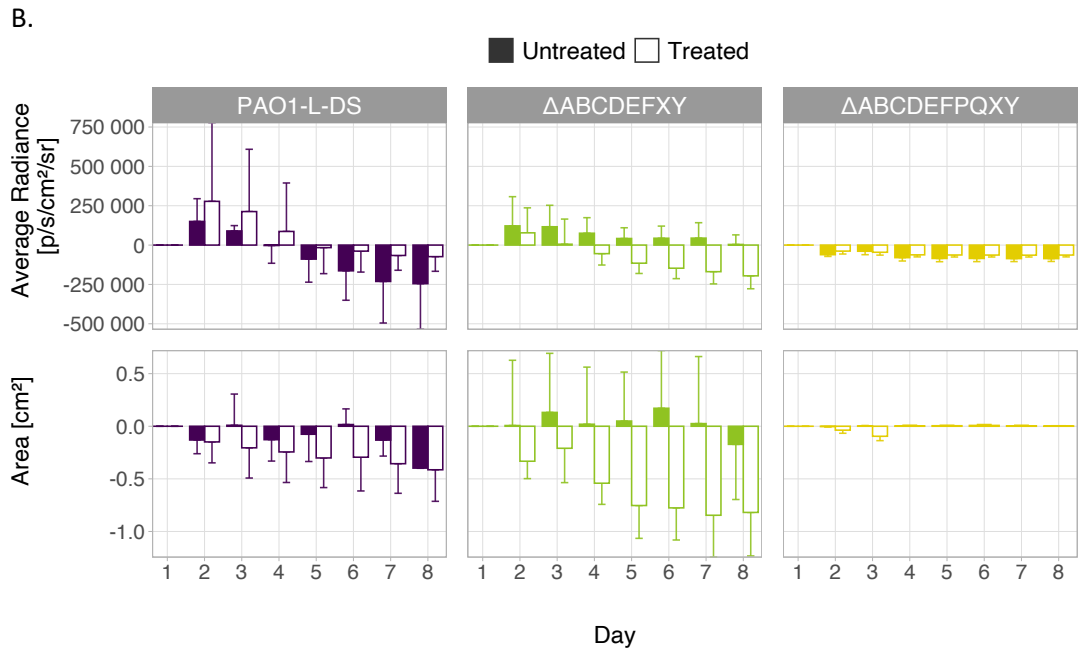
Though we didn't observe any clear differences in virulence between the strains in a *G. mellonella* infection model, insects lack the adaptive immune response possessed by mammals. Mice are a common mammalian model used for studying infection due to the high genetic similarity between mice and mammals. We hypothesised that both the ΔABCDEFXY and ΔABCDEFPQXY mutants would be less virulent than PAO1-L-DS. Since many mouse models are highly invasive, ethically challenging and carry a high mortality rate a chronic ulcer model was chosen for this experiment.

To test this hypothesis, mice were subcutaneously injected with 1 x 10^5 CFU PAO1-L-DS (n = 6), ΔABCDEFXY (n = 6) or ΔABCDEFPQXY (n = 6) on cytodex beads to prevent rapid host clearance. Genetically identical BALB/c mice were chosen to limit the impact of host genetics on the infection response and to enable comparison across treatment groups. All three strains induced clinical signs of local infection including a raised lump and dermonecrosis around the injection site. No mice died during the experiment and *ex vivo* examination confirmed the absence of dissemination to the lymph nodes or other organs. Strains were tagged with P*tac*::*lux*, so the bacterial infection was also tracked in real-time using bioluminescence as a measure of metabolic activity (**Figure 4.13A**). Despite standardising the starting inoculum (day 0), the ΔABCDEFXY mutant had a higher starting bioluminescence than the other strains, resulting in a greater established infection (days 1 - 8). This could be attributable to increased *lux* expression in this strain as opposed to a greater number of bacteria. However, as the infection response was highly variable among mice in all treatment groups further optimisation of this method is required.

We predicted that the efflux pump mutants would be more sensitive to antibiotic treatment than the parent strain due to the accumulation of antibiotics within the cell. Four mice from each strain group were treated with a sub-inhibitory dose of gentamicin. On day 1, day 2 and day 3 post-infection, mice in the treatment group were intraperitoneally injected with 0.4 mg/kg gentamicin. Gentamicin was chosen as a clinically relevant antibiotic which is known to be exported by MexXY (Masuda *et al*., 2000) and to a lesser extent MexAB-OprM (Masuda *et al*., 2000) and MexPQ-OpmE (Mima *et al*., 2005). In the absence of significant changes to the infection sites, the gentamicin concentration was increased to 4 mg/kg on day 4 and at subsequent 24 h intervals until day 8.

Figure 4.13: Murine infection with PAO1-L-DS, ΔABCDEFXY and ΔABCDEFPQXY A) Luminescence images with overlaid brightfield of mice over 8 days following inoculation with 1 x10^5 bacteria. Untreated mice (n = 2) did not receive any gentamicin, while treated mice (n = 4) were intraperitoneally injected with 0.4 mg/kg gentamicin on days 1 - 3, and with 4 mg/kg gentamicin on days 4 - 8. Bioluminescence was measured 10 minutes following inoculation (day 0), at subsequent 24 h intervals and following euthanasia. Fluorescence was measured on day 8 and following euthanasia B) Change in radiance and area of the infection site over 8 days. B0279 was removed as an outlier and bioluminescence was normalised to the output on day 1. Data represents the mean change from day 1 at each time point ± 1SD.





The total radiance and area of the infections were compared between the treated and untreated groups (**Figure 4.13B**). Though we observed an increase in the mean radiance of PAO1-L-DS in the treated group compared with the untreated group, we saw an overall reduction in the size of the infection site. This suggests that rather than an increase in the total number of bacteria following gentamicin treatment, the bacteria within the infection site are stressed and therefore more metabolically active. Conversely, we saw a reduction in both the mean radiance and area of the infection site of ΔABCDEFXY in the treated group compared to the untreated group. The ΔABCDEFPQXY mutant did not have a strong response to the antibiotic treatment, but the infection sites were much smaller in both the treated and untreated groups. As it is unclear whether this mutant is less able to establish infection than ΔABCDEFXY or whether there were differences in the starting inoculum, further biological repeats are needed.

Strains were also tagged with the constitutively fluorescent protein E2-Crimson to visualise the total number of bacteria present at the end of the infection (**Figure 4.13A**). A fluorescent signal was detected in all mice following dispatch except B0267 (ΔABCDEFPQXY untreated) and B0283 (ΔABCDEFPQXY treated), including those where no bioluminescent signal was detected. This pilot confirmed all strains were able to establish an infection in a murine chronic ulcer model and in the absence of antibiotic treatment ΔABCDEFPQXY is cleared more rapidly than PAO1-L-DS. Due to the uncertainty with light output, it is difficult to draw a conclusion for the ΔABCDEFXY mutant.

4.8 Discussion

There is a growing body of evidence to suggest that the deletion of efflux pump genes and their regulators alters the virulence phenotypes and *in vivo* host interactions of *P. aeruginosa*. In agreement with previous studies, we found the deletion of individual and combinatorial efflux systems from PAO1-L-DS altered motility, pyocyanin, rhamnolipid and exoprotease production. Our data also suggests that loss of 4 (ΔABCDEFXY) and 5 (ΔABCDEFPQXY) efflux systems increases biofilm formation and alters the metabolic profile of the mutants.

In agreement with previous studies, we found swarming and twitching motility were particularly impacted by the loss of MexAB-OprM, MexCD-OprJ and MexXY. However, some of the mutants did not display the same motility phenotypes reported by other groups. We did not observe an increase in swarming for the ΔEF mutant as reported by Vaillancourt *et al*., (2021). These differences could be attributable to different sublines used as their mutants were created in a Washington subline (PAO1-W) which is unable to swarm. However, Amieva *et al*., (2022) generated a Δ*mexK* mutant in a PAO1-L background and found reductions in swimming and swarming motility not seen in our ΔJK mutant suggesting that method variations might be the most likely explanation as all studies used different agar recipes. These results highlight the difficulty in assigning phenotypes under laboratory conditions.

Motility is mediated by surface appendages so it remains unclear why the loss of efflux impacts motility. One widely accepted theory is that a decrease in swarming motility correlates with a decrease in rhamnolipid production. A total rhamnolipid assay was performed to measure extracellular rhamnolipids but as changes to swarming motility did not correlate with changes to rhamnolipid production our results do not support this hypothesis. Other studies have also reported increased *rhlA* expression in efflux pump mutants with both normal and increased swarming ability (Vaillancourt *et al*., 2021). We found similar increases in *rhlA* expression of the ΔABCDEFXY mutant from the previous chapter did not correlate with an increase in rhamnolipid production. These results suggest that increases in rhamnolipid production might be correlational rather than causational. Quantification of individual rhamnolipids by LC-MS/MS might reveal more subtle differences in the type or ratio of rhamnolipids produced.

We observed the complete abolition of alkaline protease and elastase B production in the ΔABCDEF, ΔABCDEFXY and ΔABCDEFPQXY mutants, which was not replicated with elastase A or protease IV production. Alkaline protease and elastase B are exported by the T1SS and T2SS respectively. One possibility is that the absence of efflux pump proteins causes membrane perturbation which prevents the normal assembly and function of other secretion systems, but as production of the T2SS substrate elastase A was not significantly altered in 18/19 of the mutants this is unlikely.

Some of the mutants did not display altered phenotypes under any of the conditions tested. These results indicate that MexJK, MexMN, MexPQ-OpmE and TriABC do not play a role in motility, antimicrobial resistance or the production of the virulence factors examined in this study.

The ΔABCDEFXY and ΔABCDEFPQXY combinatorial mutants were selected for further metabolic profiling and virulence studies: ΔABCDEFXY to build upon the findings of the RNA-seq results in Chapter 3, and ΔABCDEFPQXY as the mutant with the greatest number of combinatorial efflux pump deletions at the end of the study. These mutants differ by the presence or absence of MexPQ-OpmE: all suicide plasmids were introduced into ΔABCDEFXY and this was the first deletion to be confirmed.

The metabolic profiles of PAO1-L-DS, ΔABCDEFXY and ΔABCDEFPQXY were characterized for a total of 284 carbon, nitrogen, phosphorus and sulphur sources. Our findings indicate that the mutants are unable to utilise many nucleotide and cyclic nucleotide phosphate sources compared to PAO1-L-DS. Many nucleotides including adenosine 3’5’-cyclic monophosphate (cAMP) and guanosine 3’,5’-cyclic monophosphate (cGMP) are important secondary messengers. Nucleotides are hydrolysed by phosphodiesterases suggesting that there might be a reduction in the production or secretion of these enzymes, though this wasn’t apparent from the RNA-Seq data. It might also be interesting to explore the effects of changes in aeration, pH and temperature and aeration on efflux pump deletion given overexpressing mutants have increased oxygen consumption and a decrease in intracellular pH (Olivares Pacheco *et al*., 2017).

As much of the work on *P. aeruginosa* efflux pumps has focused on antimicrobial resistance, the metabolites exported by the different efflux systems remain poorly understood. Adamiak *et al*., (2021) performed a small targeted metabolomic study on PAO1 and a 6 pump mutant (*ΔmexAB-oprM ΔmexCD-oprJ ΔmexEF-OprN ΔmexJKL ΔmexXY ΔtriABC*) at exponential and stationary phase. They found the mutant produced more quinolones and acylhomoserine lactones at both growth phases. They also found the mutant produced more pyochelin than the parent strain at stationary phase. Future studies should include an untargeted metabolomics approach. In this way, Wang-Kan *et al.,* (2021) recently determined the substrate profile of AcrB in *E. coli* and *S.* Typhimurium. The study identified oxidised fatty acids as substrates of AcrAB-TolC in both species, but as the

proteins share 95% homology it is somewhat surprising that the exometabolomes of AcrB differed so much. It is important to consider that these results may not be a true reflection of the metabolites exported by AcrB given the overlapping substrate profiles of many efflux systems. It is possible some substrates are exported by other pumps in the absence of AcrB. To tease out the individual role of each efflux system, Goetz *et al.,* (2022) overexpressed different combination of efflux pumps in an efflux deficient strain of *E. coli*. It would be interesting to delete the remaining efflux pumps in *P. aeruginosa* to create a similar genetic background for the exploration of functional interplay.

We also investigated whether the loss of efflux altered virulence in *G. mellonella* and murine infection models. The finding that the ΔABCDEFXY mutant was not significantly more virulent than PAO1-L-DS in a *G. mellonella* infection model contradicts previous research. This inconstancy could be attributable to the effect of carrying two plasmids, so future studies should include the unlabelled strains as a control.

The only murine studies using efflux pump mutants in *P. aeruginosa* have used acute infection models (Hirakata *et al*., 2002; Vaillancourt *et al*., 2021) so the impact loss of efflux had in a chronic wound infection model was investigated. Strains were tagged with a luciferase from *Xenorhabdus luminescens* (Becher & Schweizer, 2000) which requires oxygen to produce light. Bioluminescence was used as a measure of metabolic activity however as *P. aeruginosa* can also respire anaerobically lower levels of bioluminescence might also result in a hypoxic environment. A high-density infection might also produce a similar effect. Alternative luciferases such as nanoLuc do not require oxygen but instead require the addition of an alternative substrate (Hall *et al*., 2012), and are not ideal for *in vivo* studies due to emission at 460 nm. To visualise the total number of bacteria present within the infection site, strains were also fluorescently labelled, but this does not enable differentiation between live and dead cells. To determine the number of live cells within the infection site, future studies should include the recovery and quantification of the bacterial burden.

We predicted that the efflux pump mutants would be more susceptible to antibiotic treatment than the parent strain, but a subinhibitory concentration of gentamicin only had a modest impact on the infection sites of all strains. Gentamicin is an aminoglycoside that sterically blocks tRNA binding sites to inhibit protein synthesis. These results might be

explained by the downregulation of the 30S ribosomal protein *rpsT* and 13 tRNAs in the ΔABCDEFXY mutant at stationary phase. Another possible explanation is that gentamicin was not available to bacteria at the infection site using IP delivery. Other studies have directly injected gentamicin into the infection site (Pletzer *et al*., 2017) or used nanoparticles for gentamicin delivery (Abdelghany *et al*., 2012) with greater effect and should be considered for future studies.

One hypothesis is that the acquisition of antimicrobial resistance comes at a fitness cost to the organism as these genetic changes often impact other areas of bacterial physiology such as growth rate (Andersson & Levin, 1999). Indeed, we found that loss of all of the efflux systems except Δczc and Δmux enables the strains to grow to higher optical densities than PAO1-L-DS in both rich and minimal media. Though the presence of antibiotics favours the persistence of AMR strains, in the absence of selective pressure susceptible bacteria may have a competitive advantage.To further explore the fitness of the mutants, competition experiments could be performed in conjunction with PAO1-L-DS (Popat *et al*., 2012).

4.9 Summary of key findings

- Mutants lacking all efflux systems except CzcCBA and MuxABC-OpmB grew better than PAO1-L-DS in rich and minimal media
- Loss of MexAB-OprM or MexXY had the biggest effect on antimicrobial susceptibility
- The combinatorial mutants had attenuated motility, pyocyanin, rhamnolipid and exoprotease production
- Loss of MexJK, MexMN, MexPQ-OpmE or TriABC was not associated with any phenotypes.

4.10 Future work

- Competition experiments in conjunction with the wild-type strain to determine whether loss of efflux provides a fitness advantage
- Untargeted metabolomics of the efflux pump mutants to determine the metabolites exported by each of the different efflux systems

CHAPTER 5:

Overall discussion

5. Overall discussion

Four of the twelve RND efflux pumps in *P. aeruginosa* are primarily responsible for innate and acquired resistance to a diverse range of antibiotic substrates: MexAB-OprM, MexCD-OprJ, MexEF-OprN and MexXY (Blair *et al*., 2014). None of these systems is constitutively expressed under laboratory conditions, except MexAB-OprM, and their substrate profiles overlap. As protein production is a tightly regulated energy-intensive process, it is likely that efflux pumps have a secondary role within the cell in the face of so much redundancy. In support of this hypothesis, deletion of these systems has been shown to produce strains that are less virulent. The mechanisms underlying these effects are not known.

During a previous project exploring the physiology of a 4-pump mutant (K2733), it was observed that the PAO1 parent strain (K2732) had low *pqsA* expression compared to other PAO1 strains (Jessica Grey, MRes. Thesis). This study began by reconstructing this efflux pump deletion mutant in a PAO1-L background whose quorum sensing systems have been well characterised by our lab and others. In doing so, a library of 10 individual RND pump mutants and 9 combinatorial mutants lacking different combinations of these systems was generated by homologous recombination in Chapter 2, culminating in a 5-pump deletion mutant lacking MexAB-OprM, MexCD-OprJ, MexEF-OprN, MexPQ-OpmE and MexXY (ΔABCDEFPQXY).

Whole genome sequencing of the 19 mutants, in addition to K2732 and K2733, confirmed the deletions and the absence of any detrimental secondary mutations. Of the 10 SNPs and Indels present in the mutants which were not identified in PAO1-L-DS, only one SNP in the *pilB* gene of the ΔAB mutant was predicted to be deleterious, but this was likely to be an incorrect base call. However, it is interesting that both ΔAB and PilB mutants are unable to twitch (Chiang *et al*., 2005).

Six SNPs and Indels identified in K2732 were not present in PAO1-UW or PAO1-L-DS, though it is unclear which of these was responsible for the reduction in *pqsA* expression. It is possible there was an issue with the *pqsA*::*lux* reporter, which could be confirmed using an alternative measure of gene expression such as RT-PCR.

To understand the contribution of RND efflux pumps to virulence and bacterial physiology, the transcriptome of a mutant lacking MexAB-OprM, MexCD-OprJ, MexEF-OprN and MexXY (ΔABCDEFXY) was characterised in Chapter 3. RNA-Seq revealed that quorum sensing, pyocyanin synthesis, and efflux genes were upregulated at exponential phase, while the nitrate reductase *narJ* and the Psl and pyoverdine operon regulator *ppyR* were downregulated. Anthranilate degradation, T6SS proteins (*hcpA*, *hcpC*) and sarcosine oxidase genes were amongst the most upregulated at stationary phase, while the 30S ribosomal protein *rpsT* and 13 tRNAs were downregulated. The downregulation of tRNA's was also observed in *S.* Typhimurium AcrB mutant (Wang-Kan *et al*., 2017). This study highlighted the impact RND efflux pumps have on *P. aeruginosa* physiology in the absence of antimicrobial or metabolic stresses.

Several aspects of the RNA-Seq require further investigation. Firstly, an interesting observation was that despite increased expression of the *aprA*, *lasB* and *rhlA* genes, phenotypic assays revealed the mutant produced less alkaline protease, elastase B and rhamnolipids than PAO1-L-DS. Additional phenotypic assays in Chapter 4 revealed that ΔABCDEFXY also produced less protease IV but not less elastase A. To determine whether these results are due to the absence of a compound directly exported by the efflux systems, the assays could be repeated with PAO1-L-DS in the presence of an EPI.

Secondly, the link between loss of efflux and the anaerobic nitrate respiratory chain. Other studies have reported the increased expression of nitrate metabolism genes in overexpressing mutants (Olivares *et al*., 2014; Olivares Pacheco *et al*., 2017) and in agreement with these results, we observed the downregulation of *nirJ* and *fhp* at the exponential phase. We also observed a decrease in the utilisation of 13 nitrogen sources, including 7 dipeptides. Growth and virulence factor production under anaerobic conditions was not explored during this study but should be included in future work.

The ability of PAO1-L-DS, ΔABCDEFXY and ΔABCDEFPQXY mutant to form biofilms on Cytodex beads was explored. As the mutants appeared to form better biofilms than the parent strain, the clinical relevance of these results could be assessed by analysing biofilm formation on medical devices such as catheters. RNA-Seq also identified the regulator of Psl and pyoverdine (*ppyR*) was downregulated at exponential phase, so the levels of individual

exopolysaccharides could be quantified using stains to determine whether loss of efflux affects EPS composition.

One of the main limitations of this data is that the outer membrane channel OprM was removed with the deletion of the *mexAB-oprM* operon. This means that any of the pumps that associate with this pump are likely to be non-functional in any of the mutants lacking the MexAB-OprM efflux system. In these mutants, the OprM gene could be reintroduced on a complementation plasmid and determine whether that affected the results. A previous study compared the antimicrobial susceptibility of a Δ*mexAB-oprM* Δ*mexCD-oprJ* Δ*mexEF-oprN* Δ*mexXY* mutant (YM64) with that of a Δ*mexAB* Δ*mexCD-oprJ* Δ*mexEF-oprN* Δ*mexXY* mutant (YM44) and found that loss of OprM resulted in lower MICs to erythromycin and tetracycline (Li *et al*., 2003).

Another limitation is that most of the work was performed in LB medium which was chosen to look at the effects when the bacteria were not stressed. However, the clinical relevance of this medium is limited and alternatives such as an artificial sputum medium or artificial urine medium would mimic growth during CF and UTI infections respectively. Similarly, experiments were performed with each mutant in isolation. *P. aeruginosa* is commonly isolated from chronic infections with other bacterial and fungal species including *Candida albicans*, which has been shown to increase meropenem tolerance (Alam *et al*., 2020). To truly understand the physiological relevance of efflux pumps we need to mimic the complexity of nature.

In conclusion, the RND efflux pump mutants generated during this study should be considered a starting point for the generation of additional combinatorial mutants in a PAO1-L background. The mutant library should also be used to build upon the experiments in this study and further our understanding of efflux pumps on bacterial physiology.

CHAPTER 6:

Materials and methods

6. Materials and Methods

6.1 Strains and culture conditions

6.1.1 Bacterial strains and growth conditions

The strains used in this study are detailed in **Table 6.1**.

Unless otherwise stated, frozen aliquots of *P. aeruginosa*, *E. coli* and *S. aureus* strains were streaked onto solid agar plates supplemented with antibiotics as appropriate using a sterile inoculation loop. Agar plates were incubated overnight at 37°C under static conditions.

Overnight bacterial cultures were prepared by inoculating a 50 mL falcon tube containing 10 mL sterile LB with a single bacterial colony from a solid agar plate using a sterile inoculation loop. Cultures were incubated overnight at 37°C in a shaking incubator at 200 rpm.

Filter-sterilised culture supernatants were prepared by diluting an overnight bacterial culture to a starting OD_{600} 0.05 in a 150 mL conical flask containing 25 mL sterile LB and incubating at 37°C with shaking at 200 rpm for 16 h. Cultures were centrifuged at 6000 rpm for 2 min before the supernatant was passed through a 0.22 μm filter (Fisher Scientific).

6.1.2 Plasmids

The plasmids used in this study are detailed in **Table 6.2**.

Plasmid DNA was extracted from a 4.5 mL overnight bacterial culture using the GenElute Plasmid DNA Miniprep kit (Merck, UK). The culture was centrifuged at 3,000 x *g* for 2 min and the plasmid was extracted from the pellet following the manufacturer's instructions with the exception that all plasmids were eluted in 50 μL nuclease-free water.

6.1.3 Media

The growth media used in this study are detailed in **Table 6.3**. Media were prepared using water distilled by reverse osmosis, and sterilised for 15 min at 121°C prior to use. Where appropriate, media were supplemented with filter-sterilized antibiotics as per **Table 6.4**.

6.1.4 Antibiotic selection

The antibiotics used in this study are detailed in **Table 6.4**.

6.1.5 Storage

Bacterial stocks were prepared from an agar plate containing the appropriate strain. An overnight culture was prepared and 750 µL of this culture was mixed with 750 µL 80% (v/v) glycerol solution in a 2 mL cryo tube (Sarsteadt) and stored at -80°C until required.

6.1.6 Growth curves

Bacterial growth over time was determined by diluting overnight bacterial cultures to a starting OD_{600} 0.006 in either LB or M9 and 300 µL of each sample was transferred to a UV-sterilised flat-bottomed transparent 96-well plate (Greiner). Plates were sealed with gas permeable adhesive film (4titude, product code: 4ti-0516/96). The OD_{600} was measured at 30 min intervals over a 24 h period on the TECAN Infinite F200Pro (TECAN).

To determine the appropriate timepoints for RNA sequencing, overnight bacterial cultures were diluted to a starting OD_{600} 0.01 in a 250 mL conical flask containing 50 mL sterile LB. Strains were incubated at 37°C with shaking at 200 rpm and the OD_{600} of each culture was measured every h for 12 h. Uninoculated LB medium was used as a negative control.

Table 6.1: Bacterial strains used in this study

Designation	Species	Genotype	Antibiotic resistance	Reference
ATCC 27853	*P. aeruginosa*	wild type	None	ATCC*
PAO1-L-DS	*P. aeruginosa*	PAO1-L wild-type, Lausanne subline	None	B. Holloway via D. Haas
ΔAB	*P. aeruginosa*	PAO1-L Δ*mexAB-oprM*	None	This study
ΔCD	*P. aeruginosa*	PAO1-L Δ*mexCD-oprJ*	None	This study
ΔEF	*P. aeruginosa*	PAO1-L Δ*mexEF-oprN*	None	This study
ΔGHI	*P. aeruginosa*	PAO1-L Δ*mexGHI-opmD*	None	This study
ΔJK	*P. aeruginosa*	PAO1-L Δ*mexJK*	None	This study
ΔMN	*P. aeruginosa*	PAO1-L Δ*mexMN*	None	This study
ΔPQ	*P. aeruginosa*	PAO1-L Δ*mexPQ-opmE*	None	This study
ΔXY	*P. aeruginosa*	PAO1-L Δ*mexXY*	None	This study
Δczc	*P. aeruginosa*	PAO1-L Δ*czcCBA*	None	This study
Δmux	*P. aeruginosa*	PAO1-L Δ*muxABC-opmB*	None	This study
Δtri	*P. aeruginosa*	PAO1-L Δ*triABC*	None	This study
ΔABCD	*P. aeruginosa*	PAO1-L Δ*mexAB-oprM* Δ*mexCD-oprJ*	None	This study

ΔABEF	*P. aeruginosa*	PAO1-L Δ*mexAB-oprM* Δ*mexEF-oprN*	None	This study
ΔABXY	*P. aeruginosa*	PAO1-L Δ*mexAB-oprM* Δ*mexXY*	None	This study
ΔCDEF	*P. aeruginosa*	PAO1-L Δ*mexCD-oprJ* Δ*mexEF-oprN*	None	This study
ΔCDXY	*P. aeruginosa*	PAO1-L Δ*mexCD-oprJ* Δ*mexXY*	None	This study
ΔABCDEF	*P. aeruginosa*	PAO1-L Δ*mexAB-oprM* Δ*mexCD-oprJ* Δ*mexEF-oprN*	None	This study
ΔABCDXY	*P. aeruginosa*	PAO1-L Δ*mexAB-oprM* Δ*mexCD-oprJ* Δ*mexXY*	None	This study
ΔABCDEFXY	*P. aeruginosa*	PAO1-L Δ*mexAB-oprM* Δ*mexCD-oprJ* Δ*mexEF-oprN* Δ*mexXY*	None	This study
ΔABCDEFPQXY	*P. aeruginosa*	PAO1-L Δ*mexAB-oprM* Δ*mexCD-oprJ* Δ*mexEF-oprN* Δ*mexPQ-opmE* Δ*mexXY*	None	This study
ΔlasI	*P. aeruginosa*	PAO1-L Δ*lasI*	None	Constructed by Dr Matthew Fletcher
ΔlasR	*P. aeruginosa*	PAO1-L Δ*lasR*	None	Constructed by Dr Matthew Fletcher
ΔpqsA	*P. aeruginosa*	PAO1-L Δ*pqsA*	None	Constructed by Dr Matthew Fletcher
ΔrhlA	*P. aeruginosa*	PAO1-L Δ*rhlA*	None	Constructed by Dr Matthew Fletcher
ΔrhlI	*P. aeruginosa*	PAO1-L Δ*rhlI*	None	Constructed by Dr Matthew Fletcher

ΔrhlR	*P. aeruginosa*	PAO1-L Δ*rhlR*	None	Constructed by Dr Matthew Fletcher
S17-1λ*pir*	*E. coli*	*recA thi pro hsdR*$^{-}$ *M*$^{+}$ RP4::2-Tc::Mu::Km Tn7 Tp^{R} Sm^{R} λ*pir*	None	De Lorenzo *et al*., 1993
SH1000	*S. aureus*	SH1000 wild-type	None	Horsburgh *et al*., 2002

*ATCC refers to the American Type Culture Collection (USA)

Table 6.2: Plasmids

Plasmid	Description	Ab Resistance	Reference
pEX18Gm	*oriT*$^{+}$ *sacB*$^{+}$ suicide vector with MCS from pUC18	Gm^{R}	Hoang *et al*., 1998
pEX18Gm-Δ*mexAB-oprM*	pEX18Gm containing the 1047 bp region upstream of *mexA* and the 1051 bp region downstream of *oprM*	Gm^{R}	This study
pEX18Gm-Δ*mexCD-oprJ*	pEX18Gm containing the 1026 bp region upstream of *mexC* and the 1073 bp region downstream of *oprJ*	Gm^{R}	This study
pEX18Gm-Δ*mexEF-oprN*	pEX18Gm containing the 1004 bp region upstream of *mexE* and the 1064 bp region downstream of *oprN*	Gm^{R}	This study
pEX18Gm-Δ*mexGHI-opmD*	pEX18Gm containing the 1050 bp region upstream of *mexG* and the 1046 bp region downstream of *opmD*	Gm^{R}	This study
pEX18Gm-Δ*mexJK*	pEX18Gm containing the 1047 bp region upstream of *mexJ* and the 1048 bp region downstream of *mexK*	Gm^{R}	This study
pEX18Gm-Δ*mexMN*	pEX18Gm containing the 1049 bp region upstream of *mexM* and the 1046 bp region downstream of *mexN*	Gm^{R}	This study
pEX18Gm-Δ*mexPQ-opmE*	pEX18Gm containing the 1050 bp region upstream of *mexP* and the 1055 bp region downstream of *opmE*	Gm^{R}	This study
pEX18Gm-Δ*mexXY*	pEX18Gm containing the 1093 bp region upstream of *mexX* and the 1006 bp region downstream of *mexY*	Gm^{R}	This study

pEX18Gm-Δ*czcCBA*	pEX18Gm containing the 1132 bp region upstream of *czcC* and the 1120 bp region downstream of *czcA*	Gm^R	This study
pEX18Gm-Δ*muxABC-opmB*	pEX18Gm containing the 1049 bp region upstream of *muxA* and the 1046 bp region downstream of *opmB*	Gm^R	This study
pEX18Gm-Δ*triABC*	pEX18Gm containing the 1049 bp region upstream of *triA* and the 1046 bp region downstream of *triC*	Gm^R	This study
pFLP2	Site-specific excision vector for removal of gentamicin resistance cassette from pMiniCTX-*lux*(Gm)	Cb^R	Hoang *et al*., 1998
pMiniCTX-*lux*(Gm)	pMiniCTX-*lux* plasmid, with *lecA*::*luxCDABE* inserted into BamHI site. Tc^R cassette replaced by *aacC1* gene for gentamicin resistance	Gm^R	Constructed by Dr Matthew Fletcher
pMiniCTX-*lux*(Gm)::P*antA*	Transcriptional reporter containing the promoter region of *antA*	Gm^R	Constructed by Dr Frances Smith
pMiniCTX-*lux*(Gm)::P*antR*	Transcriptional reporter containing the promoter region of *antR*	Gm^R	Constructed by Dr Frances Smith
pMiniCTX-*lux*(Gm)::P*lasB*	Transcriptional reporter containing the promoter region of *lasB*	Gm^R	Constructed by Dr Matthew Fletcher
pMiniCTX-*lux*(Gm)::P*lasI*	Transcriptional reporter containing the promoter region of *lasI*	Gm^R	Constructed by Dr Matthew Fletcher
pMiniCTX-*lux*(Gm)::P*phzA1*	Transcriptional reporter containing the promoter region of *phzA1*	Gm^R	Higgins *et al*., 2018
pMiniCTX-*lux*(Gm)::P*phzA2*	Transcriptional reporter containing the promoter region of *phzA2*	Gm^R	Higgins *et al*., 2018
pMiniCTX-*lux*(Gm)::P*tac*	Transcriptional reporter containing the promoter region of *ptac*	Gm^R	Constructed by Dr Matthew Fletcher

pMiniCTX-*lux*(Gm)::P*pqsA*	Transcriptional reporter containing the promoter region of *pqsA*	Gm^R	Constructed by Dimitra Panagiotopoulou
pMiniCTX-*lux*(Gm)::P*rhlA*	Transcriptional reporter containing the promoter region of *rhlA*	Gm^R	Constructed by Dr Matthew Fletcher
pMiniCTX-*lux*(Gm)::P*rhlI*	Transcriptional reporter containing the promoter region of *rhlI*	Gm^R	Constructed by Dr Matthew Fletcher
pSW002-PpsbA-E2-Crimson	Bacterial expression vector with constitutive PsbA promoter and E2-Crimson fluorescent protein	Tet^R	Wilton *et al*., 2018

Cb^R indicates resistance to 300 μg/mL carbenicillin for *P. aeruginosa* strains.. Gm^R indicates resistance to 20 μg/mL gentamicin for *P. aeruginosa* strains and 10 μg/mL gentamicin for *E. coli* strains. Tet^R indicates resistance to 125 μg/mL tetracycline for *P. aeruginosa* strains.

Table 6.3: Media composition

Media	Description	Reference
Iso-Sensitest broth	23.4 g/L [11 g/L hydrolysed casein, 3 g/L peptones, 2 g/L glucose, 3 g/L NaCl, 1 g/L soluble starch, 2 g/L Na_2HPO_4, 1 g/L (w/v) $C_2H_3NaO_2$, 0.2 g/L $C_3H_7MgO_6P$, 0.1 g/L $C_{12}H_{22}CaO_{14}$, 0.001 g/L $CoSO_4$, 0.001 g/L $CuSO_4$, 0.001 g/L $ZnSO_4$, 0.001 g/L $FeSO_4$, 0.002 g/L $MnCl_2$, 0.001 g/L menadione, 0.001 g/L cyanocobalamin, 0.02 g/L L-cysteine hydrochloride, 0.02 g/L (w/v) L-trytophan, 0.003 g/L pyridoxine, 0.003 g/L pantothenate, 0.003 g/L nicotinamide, 0.0003 g/L biotin, 0.00004 g/L thiamine, 0.01 g/L adenine, 0.01 g/L guanine, 0.01 g/L xanthine, and 0.01 g/L uracil] (Oxoid, cat. No CM0473)	NA
Lysogeny broth (LB)	10 g/L Tryptone (Oxoid), 5 g/L Yeast extract (Oxoid), 5 g/L NaCl (Merk), buffered to a pH of 7.0 $\pm$ 15 g/L Bacto Agar (Difco) if required	Lennox, 1955
M9	240.7 mg/L $MgSO_4$, 11.098 mg/L $CaCl_2$ and D-glucose at 0.4 %. A 5x stock solution of M9 salts was prepared for a final concentration of: 1 g/L NH_4Cl, 6.78 g/L Na_2HPO_4, 3 g/L KH_2PO_4 and 0.5 g/L NaCl.	NA
Pseudomonas isolation agar (PIA)	[1.4 g/L $MgCl_2$, 20 g/L Peptone, 10 g/L K_2SO_4, 0.025 g/L Triclosan, 13.6 g/L agar] (Oxoid). Following sterilization 2 % (v/v) glycerol (Merck) was added to the medium	NA
Skimmed milk agar	1 g/L peptone, 5 g/L NaCl, 8 g/L Technical agar No. 3 (Oxoid) buffered to a pH of 10.0. Following sterilization 13 % UHT skimmed milk was added to the medium	Chu, 2007
Swimming agar	10 g/L NaCl (Merck), 10 g/L Tryptone (Oxoid), 3 g/L Bacto agar (Difco)	Rashid & Kornberg, 2000
Swarming agar	8 g/L Nutrient broth N°2 (Oxoid), 5 g/L Bacto agar (Difco). Following sterilization 5 g/L D-glucose (Merck) was added to the medium	Rashid & Kornberg, 2000
Twitching agar	10 g/L Agar grade 1 (Oxoid), 10 g/L Tryptone (Oxoid), 5 g/L Yeast extract (Oxoid), 10 g/L NaCl (Merck)	Rashid & Kornberg, 2000
Tryptone, yeast extract and sucrose (TYS10) agar	10 g/L Tryptone (Oxoid), 5 g/L yeast extract (Oxoid), 100 g/L sucrose (Merck), 15 g/L Technical agar No. 3 (Oxoid)	Huang & Wilks, 2017

Table 6.4: Antibiotics used in this study

Antibiotic	Abbreviation	Antibiotic class	Solvent	Stock concentration (mg/mL)
Aztreonam	Az	β-lactam	DMSO	1
Carbenicillin	Cb	β-lactam	Water	100
Cefepime	Cef	β-lactam	Methanol	1
Chloramphenicol	Chl	Chloramphenicol	Ethanol	10
Erythromycin	Ery	Macrolide	2M HCl	10
Gentamicin	Gm	Aminoglycoside	Water	10
Norfloxacin	Nor	Fluoroquinolone	HOAc	1
Tetracycline	Tet	Tetracycline	Ethanol	100

All antibiotics were purchased from Merck, UK

6.1.7 Transcriptional promoter fusion assays

Previously constructed transcriptional reporter fusions pMiniCTX-*lux*(Gm)::P*antA*, pMiniCTX-*lux*(Gm)::P*antR*, pMiniCTX-*lux*(Gm)::P*lasB*, pMiniCTX-*lux*(Gm)::P*lasI*, pMiniCTX-*lux*(Gm)::P*phzA1*, pMiniCTX-*lux*(Gm)::P*phzA2*, pMiniCTX-*lux*(Gm)::P*pqsA-DP*, pMiniCTX-*lux*(Gm)::P*pqsA-MF*, pMiniCTX-*lux*(Gm)::P*rhlA* and pMiniCTX-*lux*(Gm)::P*rhlI* were conjugated into PAO1-L-DS and the ΔABCDEFXY mutant.

Overnight bacterial cultures were diluted to a starting OD_{600} 0.006 and 300 µL of each sample was transferred to a UV-sterilised flat black transparent bottom 96-well plate (Greiner). Plates were sealed with gas permeable adhesive film (4titude, product code: 4ti-0516/96). The OD_{600} and bioluminescence (Relative Light Units) at 490 nm were measured using the TECAN Infinite F200Pro (TECAN). Measurements were taken at 30 min intervals over a 24 h period. The median RLU at each timepoint was calculated for each strain and corrected for growth, in addition to the maximum RLU for each strain. Results are representative of at least three biological and three technical replicates. Strains carrying the pMiniCTX-*lux*(Gm)::P*tac* plasmid containing the constitutive promoter P*tac* were used as positive controls, while strains carrying the pMiniCTX-*lux*(Gm) empty vector were used as negative controls.

6.1.8 Antimicrobial susceptibility testing

The minimum inhibitory concentration (MIC) of *P. aeruginosa* parent and mutants for a range of antimicrobial agents was determined using the British Society for Antimicrobial Chemotherapy (BSAC) macrodilution method in Iso-sensitest broth (Andrews, 2001). Overnight bacterial cultures grown in Iso-sensitest broth were incubated with the appropriate concentration of antibiotics in a UV-sterilised flat transparent bottom 96-well plate (Greiner) for 16 h at 37°C. The MIC was defined as the lowest concentration of an antibiotic at which no growth was visible. Results were acceptable if the MIC of the quality control strain *P. aeruginosa* ATCC 27853 fell within one doubling dilution of previously published values (where applicable). Significant increases in microbial susceptibility were defined as a two-fold or greater reduction in MIC.

6.2 General molecular techniques

6.2.1 Primers

The oligonucleotides used in this study were synthesised by Merck and are detailed in **Table 6.5**. Where applicable, restriction endonucleases recognition sites are underlined. Dried primers were reconstituted to a concentration of 100 μM in nuclease-free water and working stocks of each primer were prepared by further diluting primers 1:10 in nuclease-free water. Primers were stored at -20°C until use.

6.2.2 Polymerase chain reaction

Polymerase chain reactions (PCR) were prepared in PCR tubes using premade 'Master Mixes', and performed in a thermocycler. Q5® High-Fidelity 2X Master Mix (New England Biolabs) was used for the construction of chromosomal deletion mutants and a general 50 μL reaction comprised 25 μL master mix, 2.5 μL each of forward and reverse primer stocks a concentration of 10 μM, 2 μL template DNA and 18 μL nuclease-free water. The generic thermocycling conditions are detailed in **Table 6.6**

The 2X GoTaq® 2X Green Master Mix (Promega) was used for all other PCR reactions and a general 25 μL reaction comprised 12.5 μL master mix, 1.25 μL each of forward and reverse primer stocks a concentration of 10 μM, 1 μL template DNA and 9 μL nuclease-free water. The generic thermocycling conditions are detailed in **Table 6.7**

Table 6.5: Primers used in this study

Name	5' - 3' sequence*	Restriction site	Description
mexAB-oprM_+1000_fwd	aagcttgcatgcctgcaggtcgactctagACCTTCGAATCCACCGAAGTGAAGG	*Xba*I	Primers used to amplify 1047 bp upstream of *mexA*
mexAB-oprM_+1000_rev	cggaaggcgatcaCATAGCGTTGTCCTCATGAGCGAAAG	NA	
mexAB-oprM_-1000_fwd	ggacaacgctatgTGATCGCCTTCCGCGCCATGCAAGA	NA	Primers used to amplify 1051 bp downstream of *oprM*
mexAB-oprM_-1000_rev	ggaaacagctatgaccatgattacgaattCTATGTCCACCGCATCGGCCGTACC	*Eco*RI	
mexCD-oprJ_+1000_fwd	cgttgtaaaacgacggccagtgccaagcttACGGTCAGTGGGTCGCCGGCGGGAG	*Hin*dIII	
mexCD-oprJ_+1000_rev	gtttacccgctcaCATGACACACCCGACCGTTGATTGAAAACGGATCGAATGGTAC TTTTTCGAGC	NA	Primers used to amplify 1026 bp upstream of *mexC*
mexCD-oprJ_-1000_fwd	cgggtgtgtcatgTGAGCGGGTAAACGTGTGGGAAACG	NA	Primers used to amplify 1073 bp downstream of *oprJ*
mexCD-oprJ_-1000_rev	ttcgagctcggtacccggggatcctctagaCTGAGCCAAAACGAGCACCTCATGAAG	*Xba*I	
mexCD-oprJ_+100_fwd	AAAACTGGCCTCGCGTCCAAAG	NA	Primers used to amplify 5910 bp fragment in PAO1-L-DS and 148 bp in *⊿mexCD-oprJ*
mexCD-oprJ_-100_rev	CACCGTTTCCCACACGTTTACC	NA	
mexEF-oprN_+500_fwd	TATGAATTCGCGCCAACTATCTAT	*Eco*RI	Primers used to amplify 775 bp upstream of *mexE*
mexEF-oprN_+500_rev	GTAGCGCCAGGAGAA	NA	
mexEF-oprN_-500_fwd	TTCTCCTGGCGCTACATCGTGGCGATCTAC	NA	Primers used to amplify 815 bp downstream of *oprN*
mexEF-oprN_-500_rev	TATTCTAGAGATGCACGCCTGGAA	*Xba*I	

mexEF-oprN_+100_fwd	CCAATCCCGAAAAACCGAC	NA	Primers used to amplify 5981 bp fragment in PAO1-L-DS and 195 bp in *⊿mexEF-oprN*
mexEF-oprN_-100_rev	ATAAAAAAGCCCCGCGAC	NA	
mexGHI-opmD_+1000_fwd	cgttgtaaaacgacggccagtgccaagcttCACGACCTGGCGCCTGCCGGCTTCC	*Hin*dIII	Primers used to amplify 1050 bp upstream of *mexG*
mexGHI-opmD_+1000_rev	atcggaactttcaCATGGGTCGTTCCTTGTGCTGGTCGCCATC	NA	
mexGHI-opmD_-1000_fwd	gaacgacccatgTGAAAGTTCCGATTCAGGCCCTGGC	NA	Primers used to amplify 1046 bp downstream of *opmD*
mexGHI-opmD_-1000_rev	ttcgagctcggtacccggggatcctctagaTCTTGCTGCTGCGCGTAATTTGATAC	*Xba*I	
mexJK_+1000_fwd	aagcttgcatgcctgcaggtcgactctaGATCCCCGTTGGTTCGAGGCGCCGC	*Xba*I	Primers used to amplify 1047 bp upstream of *mexJ*
mexJK_+1000_rev	cttctcccgtcaCATGTGACACCTTCCGCAAACTGCGTTCGAG	NA	
mexJK_-1000_fwd	aaggtgtcacatgTGACGGGAGAAGGGACGGGGCGATC	NA	Primers used to amplify 1048 bp downstream of *mexK*
mexJK_-1000_rev	ggaaacagctatgaccatgattacgaattcAGGTCAAGCCGGGCCACAGCTATGC	*Eco*RI	
mexMN_+1000_fwd	cgttgtaaaacgacggccagtgcc*aagct*TGGCCGCGCAACTGCTCGCGGGAGT	*Hin*dIII	Primers used to amplify 1049 bp upstream of *mexM*
mexMN_+1000_rev	ccgttacgcctcaCATCTGTCCACCTTTCCCAGTAGCCGGCCTCG	NA	
mexMN_-1000_fwd	ggtggacagatgTGAGGCGTAACGGACGCGGCTTTCCTGGACG	NA	Primers used to amplify 1046 bp downstream of *mexN*
mexMN_-1000_rev	ttcgagctcggtacccggggatcct*ctaga*GCCCTGCAGGTGCGGCCAGCGCTCG	*Xba*I	
mexPQ-opmE_+1000_fwd	cgttgtaaaacgacggccagtgcc*aagctt*CGCAAGTCCGACGACTCGCTGTTCG	*Hin*dIII	Primers used to amplify 1050 bp upstream of *mexP*
mexPQ-opmE_+1000_rev	cggcggctgatcaCATTGTTGTGCCTTCCTGGTCTGAGC	NA	
mexPQ-opmE_-1000_fwd	ggcacaacaatgTGATCAGCCGCCGGCGGCTTCCGGC	NA	

mexPQ-opmE_-1000_rev	ttcgagctcggtacccggggatcct*ctaga*CGGAGAATAACTTTTAGGGTTTCCTGTCAG CGCCTCTTTCCGTTCACATAACTGTCACC	*Xba*I	Primers used to amplify 1055 bp downstream of *opmE*
mexVW_+1000_fwd	cgttgtaaaacgacggccagtgcc*aagctt*AAGCTACCTGATCGACCTGAACGAC	*Hin*dIII	
mexVW_+1000_rev	ccgtttccgatcaCATAATCCTGGTCCCTGGTATGCCG	NA	Primers used to amplify 1093 bp upstream of *mexV*
mexVW_-1000_fwd	accaggattatgTGATCGGAAACGGCGGACAGCGACAAC	NA	
mexVW_-1000_rev	ttcgagctcggtacccggggatcct*ctag*AATGGGTCGCCCGAGTCGTGGCGGA	*Xba*I	Primers used to amplify 1006 bp downstream of *mexW*
mexXY_+1000_fwd	cgttgtaaaacgacggccagtgccaagctTGACAGAACCCGCGCGGATGCCCGG	*Hin*dIII	
mexXY_+1000_rev	gctaggggcatcaCATGGGTGTCCCTCGATTCGTGAACTCGCG	NA	Primers used to amplify 1093 bp upstream of *mexX*
mexXY_-1000_fwd	agggacacccatgTGATGCCCCTAGCGAAACTCTCGCT	NA	
mexXY_-1000_rev	ttcgagctcggtacccggggatcctctagaCTATCGGGTCGATATCGAAGCCCGC	*Xba*I	Primers used to amplify 1006 bp downstream of *mexY*
mexXY_+100_fwd	GATTATATGCTACTGTCGCGCC	NA	Primers used to amplify 4582 bp fragment in PAO1-L-DS and 244 bp in *ΔmexXY*
mexXY_-100_rev	AACTGCTGTTGCCAGTCGTC	NA	
czcCBA_+1000_fwd2	cgttgtaaaacgacggccagtgccaagcttACTTCCACCACGTTGGAGTCGTTGTC	*Hin*dIII	
czcCBA_+1000_rev2	gcgcccgcttcaCATGTTCCGCTCCTCGTCTGCTGAT	NA	Primers used to amplify 1132 bp upstream of *czcC*
czcCBA_-1000_fwd2	ggagcggaacatgTGAAGCGGGCGCGCAAGCGGGCCGG	NA	
czcCBA_-1000_rev2	ttcgagctcggtacccggggatcctctagAAGTCCAGGGCCAGTTCGGTGAGGTTGCGT ACCCG	*Xba*I	Primers used to amplify 1120 bp downstream of *czcA*
muxABC-ompB_+1000_fwd	cgttgtaaaacgacggccagtgcc*aagctt*CGATCGACTCGTGGATCTGCAGGAT	*Hin*dIII	

muxABC-ompB_+1000_rev	gagaagaactcaCATGGTTCTTCTTCAGGCTTAGAACGG	NA	Primer used to amplify 1049 bp upstream of *muxA*
muxABC-ompB_-1000_fwd	aagaagaaccatgTGAGTTCTTCTCGCTGCCTGTTCCTGAC	NA	Primers used to amplify 1046 bp downstream of *ompB*
muxABC-ompB_-1000_rev	ttcgagctcggtacccggggatcct*ctaga*CTGCAACCTGCTGGTGCGCAACCAG	*Xba*I	
triABC_+1000_fwd	cgttgtaaaacgacggccagtgcc*aagctt*GCCCGAACGTCCATGAGCGAACTCC	*Hin*dIII	Primers used to amplify 1049 bp upstream of *triA*
triABC_+1000_rev	acgccgcgctcaCATGCCTTCCCCTTCGCGATCCATAC	NA	
triABC_-1000_fwd	aggggaaggcatgTGAGCGCGGCGTAAGGGGAAGGGGG	NA	Primer used to amplify 1046 bp downstream of *triC*
triABC_-1000_rev	ttcgagctcggtacccggggatcct*ctag*ATGGTCCGCTGGTGCATGGCATGGC	*Xba*I	
pEX18_fwd	CCCACACTACCATCGGCGC	NA	Used to sequence inserts within the MCS of pEX18Gm
pEX18_rev	TTAGGCACCCCAGGCTTTA	NA	

Table 6.6: Generic PCR thermocycling condition using Q5® High-Fidelity Master Mix

Step	Temperature	Duration (*min*:*sec*)	Number of cycles
Initial denaturation	98 °C	00:30	1
Denaturation	98 °C	00:10	30
Annealing	* °C	00:30	
Extension	72 °C	30 seconds per kb of amplicon	
Final extension	72 °C	02:00	1

* Primer annealing temperatures were calculated using the NEB T_m Calculator (http://tmcalculator.neb.com)

Table 6.7: Generic PCR thermocycling condition using GoTaq® Master Mix

Step	Temperature	Duration (*min*:*sec*)	Number of cycles
Initial denaturation	95 °C	02:00	1
Denaturation	95 °C	00:30	
Annealing	* °C	00:30	30
Extension	72 °C	1 minute per kb of amplicon	
Final extension	72 °C	05:00	1

* Primer annealing temperatures were calculated using the NEB T_m Calculator (http://tmcalculator.neb.com)

6.2.3 Gel electrophoresis and extraction

DNA fragments were separated on agarose gels (1% (w/v) agarose, 1X TAE buffer [40 mM Tris, 20 mM HOAc, 1 mM EDTA]) with 0.01% (v/v) SYBR Safe DNA Gel Stain (ThermoFisher Scientific). Where required, samples were mixed with 6X Gel Loading Dye Blue (New England Biolabs) and run alongside a 1 kb Plus DNA ladder (New England Biolabs) to determine fragment size.

Electrophoresis was performed in a horizontal gel apparatus (BioRad) containing 1X TAE buffer at 110 V for 45 min. DNA fragments were visualised on a UV-transilluminator (UVP) or ChemiDoc XRS+ gel documentation system (BioRad). Where applicable, bands of the appropriate size were excised and purified using the Wizard SV Gel and PCR Clean-Up System (Promega) as per manufacturer's instructions.

6.2.4 Restriction digests

Single or double restriction digests were performed using High-fidelity restriction endonucleases (New England Biolabs) following the manufacturer's instructions. Digests were incubated at 37°C for 1 h.

6.2.5 Ligation

Digested fragments and vectors were ligated using T4 DNA ligase (Promega) in a 2:1 ratio. Reactions were incubated overnight at 4°C.

6.2.6 Bacterial transformation

6.2.6.1 *E.coli* electro-competent cells

An overnight culture of *E. coli* S17-1λ*pir* was diluted 1:100 in a 150 mL conical flask containing 25 mL sterile LB. The culture was incubated at 37°C with shaking at 200 rpm until an OD_{600} of 0.6 – 0.8 was reached. It was then split between 8 x 50 mL falcon tubes and cells were pelleted at 6000 rpm for 20 min at 4°C. The supernatant from each tube was carefully

discarded and the pellet was resuspended in 40 mL ice-cold dH_2O. This process was repeated for three more washes before the pellet was resuspended in 1 mL of ice-cold 10 % glycerol and transferred to a 1.5 mL microcentrifuge tube (Greiner). After a final centrifugation step at 6000 rpm for 10 min at 4°C, electro-competent cells were stored in 50 µL aliquots at -80°C until use.

6.2.6.2 *P. aeruginosa* electro-competent cells

P. aeruginosa competent cells were prepared using the method described by Choi *et al*. (2006). Overnight bacterial cultures of *P. aeruginosa* strains were grown at 37°C with shaking at 200 rpm. For each strain, two x 1.5 mL cultures were centrifuged at 6000 rpm for 2 min at room temperature and the supernatant discarded. Cell pellets were resuspended in 1 mL of a 300 mM sucrose solution. After another centrifugation step the pellet was resuspended in a 30 µL 300 mM sucrose solution and used immediately.

6.2.6.3 Electroporation

Competent cells were transferred to a 2 mm gap width electroporation cuvette (BioRad) and mixed with plasmid DNA. As a negative control, an additional cuvette was prepared for each strain containing electrocompetent bacteria only. Electroporation was carried out in a BioRad Micropulser at 12.5 kV/cm. Cells were immediately resuspended in 1mL LB and transferred to a 50 mL falcon tube where they were left to recover for between 1 and 3 h at 37°C with shaking at 200 rpm. A 100 µL aliquot of the transformed cells was plated onto LB agar supplemented with antibiotics to select for transformants. Another 100 µL aliquot was plated onto LB agar alone to ensure cell viability. Plates were incubated at 37°C for 24 – 72 h.

6.2.6.3 Conjugation

Overnight cultures of *E. coli* S17-1λ*pir* donor strains were grown in LB at 37°C with shaking at 200 rpm, while *P. aeruginosa* recipient strains were grown in LB at 42°C with shaking at

200 rpm to inactivate endogenous restriction endonucleases. Cells were mixed together in a 3:1 ratio of donor to recipient cells in a 1.5 mL microcentrifuge tube (Greiner). The mixtures were centrifuged at 6000 rpm for 2 minutes, washed in 1 mL LB and resuspended in 50 μL LB. The conjugation mixture was then spotted onto a dry LB plate and incubated for 6 hours at 30°C to allow the conjugation event to take place. Bacterial cells were harvested with a sterile 1000 μL pipette tip and resuspended in 1 mL LB, of which 50 μL was plated onto PIA agar supplemented with the appropriate antibiotics to select for the uptake of the plasmid.

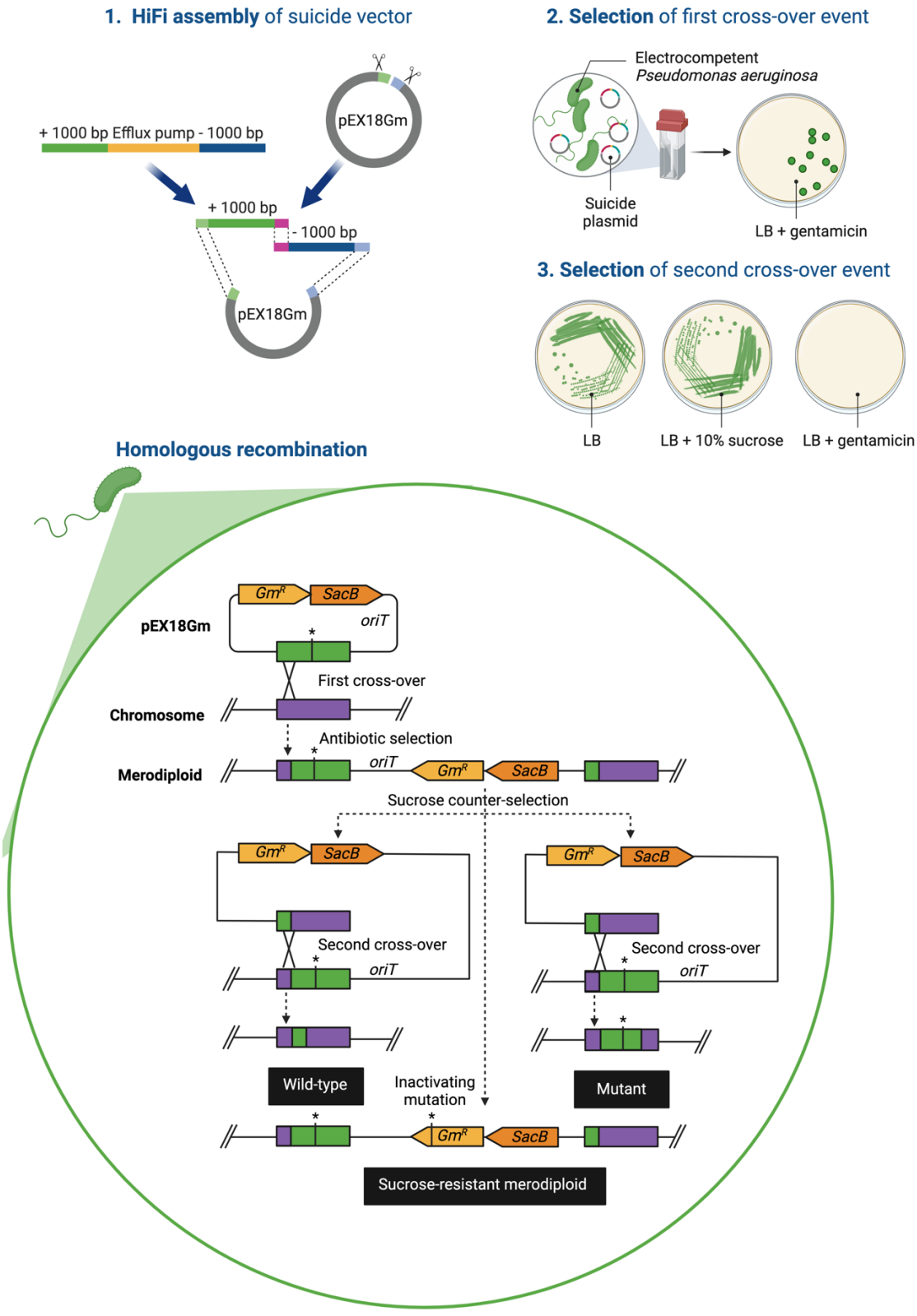
6.2.7 DNA extraction

Chromosomal DNA was extracted from 1 mL overnight bacterial culture using the GenElute Bacterial Genomic DNA kit (Merck). The culture was centrifuged at 3,000 x *g* for 2 min and chromosomal DNA was extracted from the pellet following the manufacturer's instructions with the exception that all chromosomal DNA was eluted in 50 μL nuclease-free water.

6.2.8 Construction of a series of RND efflux pump mutants

An overview of the two-step method used to construct a series of chromosomal deletion mutants lacking individual and combinations of RND efflux pumps in *P. aeruginosa* PAO1-L-DS is shown in **Figure 6.1**. Firstly, a suicide vector was constructed comprising the upstream and downstream regions of the efflux pump of interest cloned into the pEX18Gm backbone. The pEX18Gm suicide vector contains *oriT* for conjugation-based plasmid transfer, *aacC1* for gentamicin resistance to select for recombinants during the first homologous recombination step, and *sacB* to counter select for loss of the plasmid during the second recombination step. Secondly, the wild-type loci was replaced with the deletion variant by allelic replacement.

Figure 6.1: Overview of the construction of a series of RND efflux pump mutants 1) Suicide vectors were constructed by amplifying the upstream and downstream regions of the efflux pump of interest and cloning into a previously digested pEX18Gm backbone using the HiFi system 2) Suicide vectors were conjugated into PAO1-L-DS and plated onto LB + 20 μg/mL gentamicin to select for the first cross-over event 3) Gentamicin resistant colonies were patched onto LB + 10% sucrose (TYS10) to select for the second cross-over event. Figure adapted from Hmelo *et al.,* (2015)



6.2.8.1 Construction of a series of suicide vectors

Primers were designed using the NEBuilder Assembly Tool version 2.5.6 (nebuilder.neb.com) and contained at least 20 bp homology to facilitate the repair of the double stranded break during the second recombination step. The upstream region of each efflux pump of interest was amplified using the +1000_fwd/+1000_rev respective primer pair, and the downstream region was amplified using the -1000_fwd/-1000_rev primer pair. Fragments were amplified with Q5 high-fidelity polymerase. To confirm the correct fragment size following amplification, 3 μL of each DNA fragment was visualised on an agarose gel and a PCR clean-up of the remaining mixture was performed using the Wizard SV Gel and PCR Clean-Up System (Promega) as per manufacturer's instructions.

Between 50 and 100 ng of the previously digested pEX18Gm vector was combined with a 2-fold excess of each upstream and downstream DNA fragment, 10 μL HiFi DNA Assembly Master Mix (New England Biolabs, catalogue number: E2621S) and nuclease-free water to a final reaction volume of 20 μL. The reaction mixture was incubated in a thermocycler at 50°C for 1 h. The resultant suicide plasmids pEX18Gm-Δ*mexAB-oprM,* pEX18Gm-Δ*mexCD-oprJ,* pEX18Gm-Δ*mexEF-oprN,* pEX18Gm-Δ*mexGHI-opmD,* pEX18Gm-Δ*mexJK,* pEX18Gm-Δ*mexMN,* pEX18Gm-Δ*mexPQ-opmE,* pEX18Gm-Δ*mexVW,* pEX18Gm-Δ*czcCBA,* pEX18Gm-Δ*muxABC-opmB,* and pEX18Gm-Δ*triABC* were transformed into *E. coli* S17-1λ*pir* and plated onto LB agar supplemented with 10 μg/mL gentamicin to select for the uptake of the plasmid. To confirm the correct sequence, plasmids were extracted and Sanger sequenced.

6.2.8.2 Allelic replacement of the wild-type loci with the deletion variant in *P. aeruginosa* PAO1-L-DS

E. coli S17-1λ*pir* strains carrying the suicide plasmid of interest were conjugated with PAO1-L-DS. Resultant merodiploids were screened by PCR to confirm the presence of the plasmid using the pEX18_fwd primer and the -1000_rev primer specific to the relevant efflux pump. Colonies were then patched onto successive LB agar, LB agar supplemented with 20 μg/mL gentamicin and TYS10 agar plates with a 24 h at 37°C incubation step in between. Colonies were then patched onto concurrent LB agar supplemented with 20 μg/mL gentamicin, TYS10 agar and LB agar plates to confirm the loss of the plasmid. Colonies that did not grow

on LB agar supplemented with 20 μg/mL gentamicin were screened by PCR using the +1000_fwd/-1000_rev primer pair to confirm the absence of the efflux pump, and PCR fragments were sent for Sanger sequencing to confirm the correct sequence.

Resultant strains PAO1-L-DS Δ*mexAB-oprM,* Δ*mexCD-oprJ,* Δ*mexEF-oprN,* Δ*mexGHI-opmD,* Δ*mexJK,* Δ*mexMN,* Δ*mexPQ-opmE,* Δ*mexVW,* Δ*czcCBA,* Δ*muxABC-opmB,* and Δ*triABC* were sent for whole genome sequencing to confirm the absence of any secondary mutations.

6.2.8.3 Allelic replacement of the wild-type loci with the deletion variant in previously constructed RND efflux pump mutants

To create strains lacking combinations of efflux pumps, suicide plasmids were conjugated into previously constructed mutants to create strains ΔABCD, ΔABEF, ΔABXY, ΔCDEF, ΔCDXY, ΔABCDEF, ΔABCDXY, ΔABCDEFXY and ΔABCDEFPQXY. At each stage, mutants were confirmed by PCR and Sanger sequencing

6.3 Phenotypic assays

6.3.1 Rhamnolipids

Rhamnolipids were indirectly quantified using an adapted version of the method described by Wilhelm *et al*. (2007). In a fresh 1.5 mL microcentrifuge tube (Sarstedt), 500 µL of a 16 h filter-sterilized culture supernatant was mixed with 500 µL acidified ethyl acetate. After vortexing, the organic phase was transferred to a separate 1.5mL microcentrifuge tube (Sarstedt) and the extraction process was repeated twice more. The organic phase was evaporated and the dried samples were resuspended in 100 µL of 1.6 % (w/v) orcinol monohydrate (Merck) in dH_20 plus 800 µL of 60 % (v/v) H_2SO_4 in dH_20. The mixture was heated for 30 mins at 80°C with mixing every 10 minutes, and allowed to cool to room temperature. The absorbance of the solution was measured at 421 nm and divided by the OD_{600} to standardise for growth. Results are representative of at least three biological and three technical replicates for each strain. Un-inoculated growth medium was used as a negative control.

6.3.2 Pyocyanin

Pyocyanin levels were measured in culture supernatants using an adapted version of the method described by Essar *et al*. (1990). In a fresh 15 mL tube, 7.5 mL of a 16 h filter-sterilised culture supernatant was mixed with 4.5 mL chloroform and centrifuged at 10,000 x *g* for 20 min. 3 mL of the blue organic phase was transferred to a fresh 15 mL tube containing 1.5 mL of 0.2 M HCl. Samples were vortexed and centrifuged at 10,000 x *g* for 2 min at 4°C, and the absorbance of the pink aqueous phase was measured at 520 nm and pyocyanin concentration was calculated by multiplying the A_{520nm} by 17.072. Results were then divided by the OD_{600} to standardise for growth. Results are representative of at least three biological and three technical replicates for each strain. Un-inoculated growth medium was used as a negative control.

6.3.3 Exoenzyme activity assays

6.3.3.1 Universal protease

Non-specific protease activity was determined by mixing 100 µL of a 16 h filter-sterilised culture supernatant with 900 µL of 5 mg/mL Azocasein (Merck) diluted in ECR buffer (100 mM Tris, 1 mM $CaCl_2$, pH 7.5). The mixture was incubated at 37°C for 15 min with shaking at 200 rpm. To stop the reaction, 500 µL of 10% trichloroacetic acid was added to each sample prior to centrifugation at 13,000 x *g* for 3 min. The A_{400} of the supernatant was measured and divided by the starting OD_{600} to standardise for growth. Results are representative of at least three biological and three technical replicates for each strain. Un-inoculated growth medium was used as a negative control.

6.3.3.2 Alkaline protease

Following sterilisation, the cooled skimmed milk agar base was adjusted to pH 10 prior to the addition of 13 % (v/v) UHT skimmed milk. Fresh 20 mL plates were prepared for each assay and dried in a laminar flow cabinet for 30 min prior to use. Overnight bacterial cultures were diluted to a starting OD_{600} 1 and 3 µL of this culture was inoculated onto the

agar surface. Plates were incubated at 37°C for 24 h and pictures are representative of at least three biological and three technical replicates.

6.3.3.3 Elastase A

Staphylolytic activity of the strains was estimated using an adapted version of the method described by Caballero *et al*. (2001). An overnight culture of *S. aureus* SH1000 was centrifuged for 10 min at 10,000 x *g*. The supernatant was discarded and the pellet was resuspended in 250 µL of a 25 mM diethanolamine buffer (Acros Organics), pH 9.5. The mixture was boiled for 10 min at 100°C and diluted to an OD_{595} 1.0 in additional diethanolamine buffer. In each well of a UV-sterilised 96-well plate (Greiner), 200 µL of the heat-treated bacterial suspension was mixed with 40 µL diethanolamine buffer and 10 µL of a 16 h filter-sterilised *P. aeruginosa* culture supernatant. Staphylolytic activity was determined in a Tecan Spark 10 M microplate reader (Tecan) by measuring the change in OD_{595} every 1 min over a 90-min period at 37°C. Results are representative of at least three biological and three technical replicates for each strain. Un-inoculated growth medium was used as a negative control.

6.3.3.4 Elastase B

Elastase B activity was determined by mixing 100 µL of a 16 h filter-sterilised culture supernatant with 900 µL of 5 mg/mL elastin-Congo red (Merck) diluted in ECR buffer (100 mM Tris, 1 mM $CaCl_2$, pH 7.5). The mixture was incubated at 37°C for 4 h with shaking at 200 rpm. Samples were centrifuged at 13,000 x *g* for 3 min. The A_{495} of the supernatant measured and divided by the starting OD_{600} to standardise for growth. Results are representative of at least three biological and three technical replicates for each strain. Un-inoculated growth medium was used as a negative control.

6.3.3.5 Protease IV

Protease IV activity of the strains was estimated using an adapted version of the method described by Andrejko *et al*. (2013). In a UV-sterilised 96-well plate, 10 µL of a 16 h filter-sterilised culture supernatant was mixed with 200 µL of an 80 mg/mL Chromozym PL (tosyl-Gly-Pro-Lys-p- nitroanilide, Merck) in a buffer consisting of 50 mM Tris/HCl, 150 mM NaCl, pH 8.0, with or without the addition of 2 mM tosyl-L-lysine chloromethylketone (Merck). Proteolytic activity was quantified using a Tecan Spark 10 M microplate reader (Tecan) by measuring the change in A_{410} every 5 min over a 30-min period at 37°C. Results are presented as the final A_{410} divided by the starting OD_{600} to standardise for growth, and are representative of at least three biological and three technical replicates for each strain. Un-inoculated growth medium was used as a negative control.

6.3 Motility assays

6.3.4.1 Swimming

Fresh 20 mL swimming plates (**Table 6.3**) were prepared for each assay and dried in a laminar flow cabinet for 15 min prior to use. Overnight bacterial cultures were diluted to a starting OD_{600} 1 and 1 µL of this culture was stabbed to an agar depth of approximately 50 %, taking care to avoid touching the bottom of the petri dish. Plates were incubated at 37°C for 8 h and the pictures taken are representative of at least three biological and three technical replicates.

6.3.4.2 Swarming

Following sterilisation, 0.5 % (w/v) filter-sterilised D-glucose solution was added to the cooled swarming agar (**Table 6.3**). Fresh 20 mL plates were prepared for each assay and thoroughly dried in a laminar flow cabinet for 30 min prior to use. Overnight bacterial cultures were diluted to a starting OD_{600} 1 and 3 µL of this culture was inoculated onto the agar surface. Plates were incubated at 37°C for 16 h and images are representative of at least three biological and three technical replicates.

6.3.4.3 Twitching

Fresh 10 mL twitching plates (**Table 6.3**) were prepared for each assay and thoroughly dried in a laminar flow cabinet for 30 mins prior to use. Overnight bacterial cultures were diluted to a starting OD_{600} 1 and 1 µL of this culture was stabbed through the agar touching the bottom of the petri dish. Plates were incubated at 37°C with high humidity for 48 h and pictures taken are representative of at least 3 biological replicates. Following incubation, the agar was removed and the petri dish was stained with 20 % (v/v) crystal violet solution to visualise the twitching motility. Plate pictures are representative of at least three biological and three technical replicates.

6.3.5 LC-MS/MS analysis

6.3.5.1 AHL and AQ quantification

AHL's and AQ's were quantified from filter-sterilised culture supernatants or whole cell pellets by Nigel Halliday (Biodiscovery Institute, University of Nottingham) using the method described by Otori *et al*. (2011).

6.3.5.2 Anthranilate quantification

Anthranilate quantification was performed by Nigel Halliday (Biodiscovery Institute, University of Nottingham)

6.3.6 Biolog phenotype assays

PM1, PM3B and PM4B microplates (Biolog) were prepared and run by Dr Adriano Gigante (School of Veterinary Medicine and Science, University of Nottingham) according to the "PM Procedures for *E. coli* and other GN Bacteria" protocol with the exception that succinic acid was used as the carbon source instead of sodium succinate. Cell suspensions were prepared for each strain by transferring cells from an agar plate into a sterile tube containing 16 mL IF-0 (Biolog). The turbidity of the suspension was measured in a Turbidimeter (Biolog) and additional cells were added until the solution reached 42% transmittance. 15 mL of this

solution was transferred to a vial containing 75 mL of a 1:5 dilution of IF-0 and tetrazolium dye to reach a final cell density of 85% transmittance. For PM01, 100 µL of the cell suspension was transferred to each well. For PM03B and PM04B, 680 µL of a 20 mM succinic acid/2 µM ferric citrate was added to 68 mL cell suspension and 100 µL of this solution was transferred to each well. Plates were incubated in the OmniLog ID system (Biolog) for 24 h at 37°C.

6.4 Biofilm formation

6.4.1 Biofilm formation on glass beads

Overnight bacterial cultures tagged with the fluorescent protein E2-Crimson (excitation/emission - 611/646 nm) were diluted to a starting OD_{600} 0.01 in M9 medium and 1 mL of this culture was mixed with 20 µL sterile glass bead solution (0.5 g of 50 – 100 µm Cytodex beads (Sigma) in 10 mL PBS) in a 1.5 mL microcentrifuge tube (Greiner) and incubated at 37°C for 1 h. After seeding, planktonic growth was carefully removed and 1 mL fresh M9 medium was added. The beads were carefully transferred to a glass bottomed 8-well µ-Slide (Ibidi) and incubated at 37°C for 48 h under static conditions. After incubation, planktonic growth was removed and the beads were examined for biofilm formation.

6.4.2 Biofilm imaging

Biofilms were visualised using a LSM70 inverted confocal laser scanning fluorescent microscope (ZEISS) at a 20X magnification and ZEN imaging software (ZEISS). Extracellular DNA was stained with 0.1 µM YOYO-1 (ThermoFisher) (excitation/emission – 491/509 nm).

6.5 Sequencing

6.5.1 Sanger sequencing

PCR fragments were purified prior to sequencing using the Wizard SV Gel and PCR Clean-Up System (Promega). DNA concentrations were quantified on a Nanodrop spectrophotometer (Thermo Scientific, UK). PCR products at a concentration of 10 ng/µL in nuclease-free water

and the appropriate sequencing primers at a concentration of 3.2 pmol/μL in nuclease-free water were sequenced by Source BioScience. The nucleotide sequences were aligned to the reference sequence using Benching (Benchling, 2021).

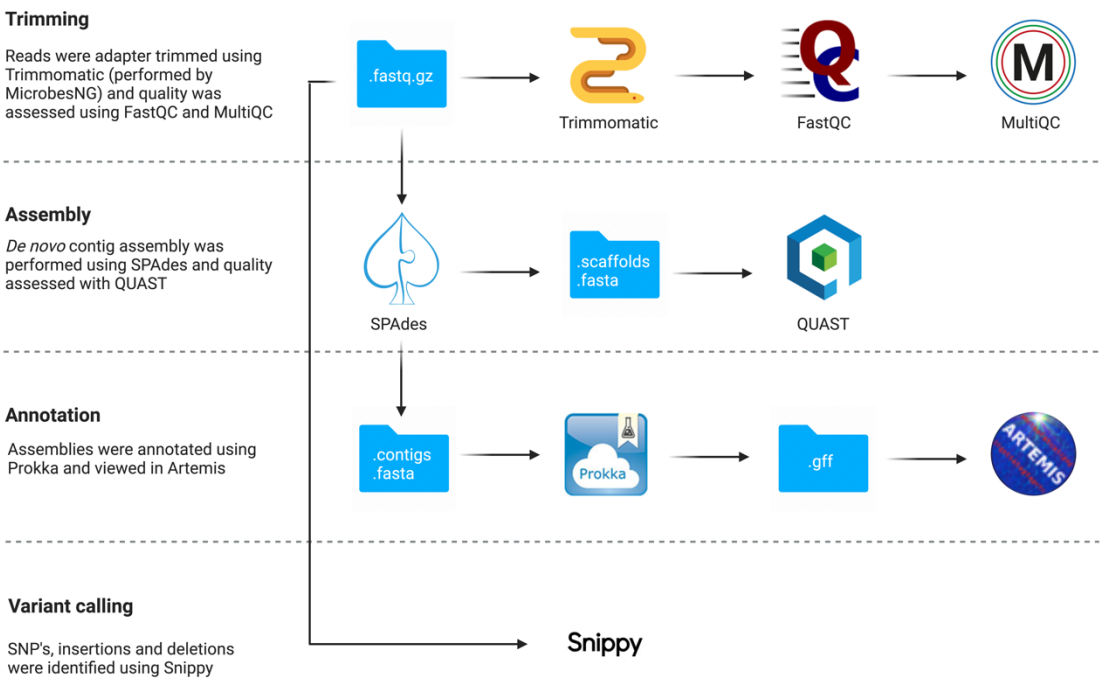
6.5.2 Whole genome sequencing and data analysis

Overnight cultures of each strain were diluted to OD_{600} 1 and 10 mL of this culture was centrifuged at 10,000 rpm for 2 min. The supernatant was discarded and the cell pellet was resuspended in 500 μL 1x DNA/RNA Shield buffer (provided by MicrobesNG). Strains were streaked onto LB agar prior to shipping to confirm the absence of contamination.

WGS was performed by MicrobesNG (Birmingham, UK). Briefly, genomic DNA libraries were prepared using Nextera XT Library Prep Kit (Illumina, San Diego, USA) following the manufacturer's protocol with the following modifications: 2 ng of DNA was used as input instead of 1 ng, and PCR elongation time was increased from 30 s to 1 min. Pooled libraries were quantified using the Kapa Biosystems Library Quantification Kit for Illumina on a Roche light cycler 96 qPCR machine. Libraries were sequenced on the Illumina HiSeq using a 250 bp paired end protocol to a minimum 30x coverage. Reads were adapter trimmed using Trimmomatic version 0.30 (Bolger *et al*., 2014) with a sliding window quality cut-off of Q15.

The data processing pipeline used to assemble, annotate and compare genomes is shown in **Figure 6.2**. The quality of the Illumina genome sequencing reads was assessed using FastQC version 0.11.9 and MultiQC version 1.9 (Ewels *et al*., 2016). *De novo* genome assemblies were performed using SPAdes version 3.15.0 (Prjibelski *et al*., 2020) under the default settings with the inclusion of the careful flag. The quality of the assemblies was assessed using QUAST version 5.0.2 (Mikheeko *et al*., 2018) before annotation with Prokka version 1.14.5 (Seemann, 2014) under default conditions. Prokka-annotated genomes were manually inspected in Artemis version 18.2.0 (Carver *et al*., 2011) to confirm the efflux pump deletions. Variant calling was performed using Snippy version 4.6.0. Circular genome comparisons were created using BLAST Ring Image Generator (BRIG) version 0.95 (Alikhan *et al*., 2011). The complete script used for genome sequencing analysis is detailed in **Appendix N**.

Figure 6.2: WGS data analysis pipeline. Blue folders indicate the input and output file formats for each step.

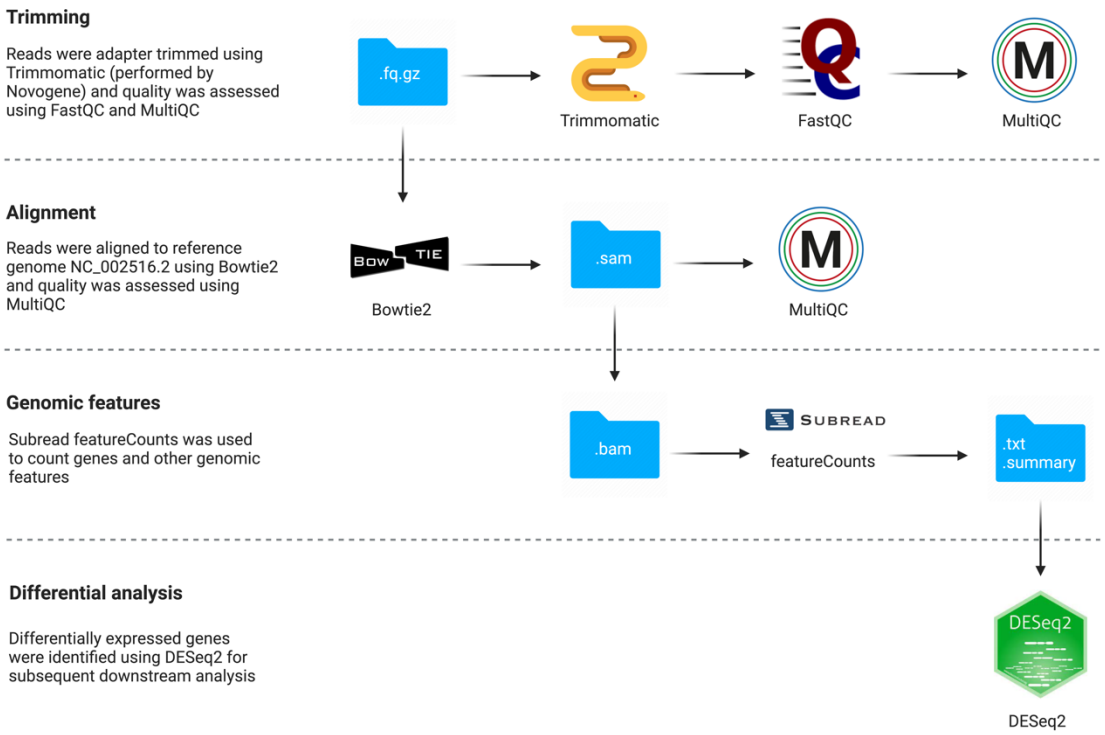


6.5.3 Transcriptome sequencing and data analysis

Overnight bacterial cultures were diluted to a starting OD_{600} 0.01 in a 150 mL conical flask containing 25 mL sterile LB. 1 mL of each culture was transferred to a 1.5 mL microcentrifuge tube (Greiner) centrifuged at 6000 rpm for 2 min. The supernatant was discarded and the cell pellets were shipped on dry ice to Novogene (Cambridge, UK) for RNA extraction and sequencing. RNA quantity for each sample was quantified using a Nanodrop, sample integrity was confirmed using an Agilent 2100, and sample purity was confirmed by agarose gel electrophoresis (**Appendix U**, **Appendix V** & **Appendix W**). All samples met the quality control criteria and were sequenced on Illumina NovoSeq 6000 sequencing system.

The data processing pipeline used to align reads, count genomic features and identify differentially expressed genes is shown in **Figure 6.3**. Paired end 150 bp reads were assessed using FastQC version 0.11.9 and MultiQC version 1.9 (Ewels *et al*., 2016) and adapter trimmed using Trimmomatic version 0.30 (Bolger *et al*., 2014) with a sliding window quality cut-off of Q15. Reads were aligned to a PAO1-UW reference genome using Bowtie2 version 2.4.2 (Langmead and Salzberg, 2012) under default settings, and alignment quality was checked using MultiQC. Alignment files were converted into BAM format using SAMtools version 1.12 (Li *et al*., 2009) and genomic features were counted using Subread FeatureCounts version 2.0.1 (Liao *et al*., 2019).The R package DESeq2 version 3.14 (Love *et al*., 2014) was used to map the number of reads to each gene, and identify differentially expressed genes between PAO1-L-DS and the ΔABCDEFXY mutant at exponential and early-stationary phases of growth using a corrected P-value (Padj) of 0.005 and a log10 fold-change of 1 as the threshold. Gene Ontology (GO) enrichment analysis was performed using information from pseudomonas.com. The complete script used for RNA-seq data analysis is detailed in the **Appendix X**.

Figure 6.3: RNA-Seq data analysis pipeline. Blue folders indicate the input and output file formats for each step.



6.6 *In vivo* infection models

In vivo infection assays were performed using strains PAO1-L, ΔABCDEFXY and ΔABCDEFPQXY tagged with pMiniCTX-*lux*::P*tac* and pSW002-PpsbA-E2-Crimson

6.6.1 Excision of gentamicin resistance cassette

The pFLP2 plasmid was transformed into electrocompetent PAO1-L, ΔABCDEFXY and ΔABCDEFPQXY strains carrying pMiniCTX-*lux*(Gm)::P*tac* and plated onto LB agar supplemented with 300 μg/mL carbenicillin. Resultant colonies were streaked onto LB agar supplemented with either 20 μg/mL gentamicin or 300 μg/mL carbenicillin to select for the loss of the gentamicin resistance cassette. Colonies which did not grow on LB agar supplemented with 20 μg/mL gentamicin were streaked onto TYS10 agar plates to select for the loss of pFLP2. Sucrose resistant colonies were patched onto concurrent LB agar supplemented with 20 μg/mL gentamicin, LB agar supplemented with 300 μg/mL carbenicillin and LB agar plates to confirm loss of both the gentamicin resistance cassette and pFLP2 to create resultant strains PAO1-L pMiniCTX-*lux*::P*tac,* ΔABCDEFXY pMiniCTX-*lux*::P*tac* and ΔABCDEFPQXY pMiniCTX-*lux*::P*tac*.

6.6.2 *Galleria mellonella* infection model

A batch of *G. mellonella* larvae (Live Food UK) were sorted according to size and any larvae showing signs of early or late pupation, sickness or melanisation were removed. Healthy larvae weighing 0.2 – 0.29 g were acclimatised at 37°C under static conditions for 24 h prior to infection (Andrea *et al*., 2019).

G. mellonella larvae were inoculated using an adapted version of the method described by Desbois and Coote (2001). Ten larvae per condition were injected in the last left proleg using a 50 μL Hamilton syringe with a 30 G sterile Agani needle (Terumo). Larvae were transferred to a transparent 12-well plate (Greiner) and incubated at 37°C under static conditions. Larvae were monitored every h for survival. Larvae injected with 10 μL PBS were used as a negative control.

6.6.3 Murine infection model

Mouse infection assays were performed by Dr Jeni Luckett (Biodiscovery Institute, University of Nottingham) under U.K Home Office licence PP5768261. Eighteen female BALB/c mice, 19 – 22 g (Charles River) were allowed to recover for 24 h with observation prior to anaesthesia with 2% isoflurane. The hair on one flank was shaved and mice were subcutaneously injected with 50 µL PBS containing 1 x 10^5 CFU *P. aeruginosa* on cytodex beads. Mice were imaged 10 mins post-inoculation to determine background luminescence using an IVIS spectrum camera (Caliper), and at subsequent 24 h intervals to track the infection. Four mice in each group were intraperitoneally injected with 0.4 mg/kg gentamicin 16 h post-infection, and at subsequent 24 h intervals on day 2-3, increasing to 4 mg/kg gentamicin on days 4 - 8. The weight and condition of the mice was recorded every 12 h. On day 8 the mice were humanely euthanised, the infection site was harvested and *ex vivo* bioluminescence and fluorescence was determined.

6.7 Statistical analysis

Statistical analysis and visualisation was performed using R software version 4.1 (R Core Team, 2021). Multiple groups were compared using a two-way ANOVA. Significant results were followed up using Tukey's honestly significant difference (HSD) post hoc test to identify where the differences occurred between groups. Kaplan-Meier survival plots were generated for the *G. mellonella* infection assay using the R package [survminer]. Median survival times were calculated for each strain and condition, and compared using a log-rank test. For all tests, a *p*-value < 0.05 was considered to be significant and a *p*-value > 0.05 was considered not significant (NS). Significant *p*-values are presented as P ≤ 0.05 (*), P ≤ 0.01 (**), P ≤ 0.001 (***).

Unless otherwise stated, all data visualisations were generated using the R packages [ggplot2] (Wickham, 2016), [dplyr] version 1.0.7 (Wickham *et al*., 2022), [patchwork] version 1.1.1 (Lin Pederson, 2020), [scales] version 1.2.0 (Wickham & Seidel, 2022), and [ggsignif] (Ahlmann-Eltze & Patil, 2021).

References

Abraham, E.P. and Chain, E., 1988. An enzyme from bacteria able to destroy penicillin. 1940. *Reviews of infectious diseases*, 10(4), pp.677-678.

Abdelghany, S.M., Quinn, D.J., Ingram, R.J., Gilmore, B.F., Donnelly, R.F., Taggart, C.C. and Scott, C.J., 2012. Gentamicin-loaded nanoparticles show improved antimicrobial effects towards *Pseudomonas aeruginosa* infection. *International journal of nanomedicine*, 7, p.4053.

Adamiak, J.W., Jhawar, V., Bonifay, V., Chandler, C.E., Leus, I.V., Ernst, R.K., Schweizer, H.P. and Zgurskaya, H.I., 2021. Loss of RND-Type Multidrug Efflux Pumps Triggers Iron Starvation and Lipid A Modifications in *Pseudomonas aeruginosa. Antimicrobial Agents and Chemotherapy*, 65(10), pp.e00592-21.

Aendekerk, S., Ghysels, B., Cornelis, P. and Baysse, C., 2002. Characterization of a new efflux pump, MexGHI-OpmD, from *Pseudomonas aeruginosa* that confers resistance to vanadium. *Microbiology*, 148(8), pp.2371-2381.

Aendekerk, S., Diggle, S.P., Song, Z., Høiby, N., Cornelis, P., Williams, P. and Cámara, M., 2005. The MexGHI-OpmD multidrug efflux pump controls growth, antibiotic susceptibility and virulence in *Pseudomonas aeruginosa* via 4-quinolone-dependent cell-to-cell communication. *Microbiology*, 151(4), pp.1113-1125.

Ahlmann-Eltze, C., & Patil, I. (2021). ggsignif: R Package for Displaying Significance Brackets for 'ggplot2'. *PsyArxiv*. doi:10.31234/osf.io/7awm6

Alam, F., Catlow, D., Di Maio, A., Blair, J.M. and Hall, R.A., 2020. Candida albicans enhances meropenem tolerance of *Pseudomonas aeruginosa* in a dual-species biofilm. *Journal of Antimicrobial Chemotherapy*, 75(4), pp.925-935.

Albus, A.M., Pesci, E.C., Runyen-Janecky, L.J., West, S.E. and Iglewski, B.H., 1997. Vfr controls quorum sensing in *Pseudomonas aeruginosa*. *Journal of Bacteriology*, 179(12), pp.3928-3935.

Alcalde-Rico, M., Olivares-Pacheco, J., Alvarez-Ortega, C., Cámara, M. and Martínez, J.L., 2018. Role of the multidrug resistance efflux pump MexCD-OprJ in the *Pseudomonas aeruginosa* quorum sensing response. *Frontiers in Microbiology*, p.2752.

Alcalde-Rico, M., Olivares-Pacheco, J., Halliday, N., Cámara, M. and Martínez, J.L., 2020. The impaired quorum sensing response of *Pseudomonas aeruginosa* MexAB-OprM efflux pump overexpressing mutants is not due to non-physiological efflux of 3-oxo-C12-HSL. *Environmental Microbiology*, 22(12), pp.5167-5188.

Alav, I., Bavro, V.N. and Blair, J., 2022. A role for the periplasmic adaptor protein AcrA in vetting substrate access to the RND efflux transporter AcrB. *Scientific reports*, 12(1), pp.1-13.

Alikhan, N.F., Petty, N.K., Ben Zakour, N.L. and Beatson, S.A., 2011. BLAST Ring Image Generator (BRIG): simple prokaryote genome comparisons. *BMC genomics*, 12(1), pp.1-10.

Allesen-Holm, M., Barken, K.B., Yang, L., Klausen, M., Webb, J.S., Kjelleberg, S., Molin, S., Givskov, M. and Tolker-Nielsen, T., 2006. A characterization of DNA release in *Pseudomonas aeruginosa* cultures and biofilms. *Molecular microbiology*, 59(4), pp.1114-1128.

Amieva, R., Gil-Gil, T., Martínez, J.L. and Alcalde-Rico, M., 2022. The MexJK Multidrug Efflux Pump Is Not Involved in Acquired or Intrinsic Antibiotic Resistance in *Pseudomonas aeruginosa*, but Modulates the Bacterial Quorum Sensing Response. *International Journal of Molecular Sciences*, 23(14), p.7492.

Andersson DI and Levin BR. 1999. The biological cost of antibiotic resistance. *Curr Opin Microbiol* 2:489–493.

Andrea, A., Krogfelt, K.A. and Jenssen, H., 2019. Methods and challenges of using the greater wax moth (*Galleria mellonella*) as a model organism in antimicrobial compound discovery. *Microorganisms*, 7(3), p.85.

Andrejko, M., Zdybicka-Barabas, A., Janczarek, M. and Cytryńska, M., 2013. Three *Pseudomonas aeruginosa* strains with different protease profiles. *Acta Biochimica Polonica*, 60(1).

Andrews, J.M., 2001. Determination of minimum inhibitory concentrations. *Journal of antimicrobial Chemotherapy*, 48(suppl_1), pp.5-16.

Arai, H., Igarashi, Y. and Kodama, T., 1995. The structural genes for nitric oxide reductase from *Pseudomonas aeruginosa. Biochimica et Biophysica Acta (BBA)-Gene Structure and Expression*, 1261(2), pp.279-284.

Aparna, V., Dineshkumar, K., Mohanalakshmi, N., Velmurugan, D. and Hopper, W., 2014. Identification of natural compound inhibitors for multidrug efflux pumps of *Escherichia coli* and *Pseudomonas aeruginosa* using in silico high-throughput virtual screening and in vitro validation. *PloS one*, 9(7), p.e101840.

Arora, S.K., Neely, A.N., Blair, B., Lory, S. and Ramphal, R., 2005. Role of motility and flagellin glycosylation in the pathogenesis of *Pseudomonas aeruginosa* burn wound infections. *Infection and immunity*, 73(7), pp.4395-4398.

Attila, C., Ueda, A. and Wood, T.K., 2008. PA2663 (PpyR) increases biofilm formation in *Pseudomonas aeruginosa* PAO1 through the psl operon and stimulates virulence and quorum-sensing phenotypes. *Applied microbiology and biotechnology*, 78(2), pp.293-307.

Bains, M., Fernández, L. and Hancock, R.E., 2012. Phosphate starvation promotes swarming motility and cytotoxicity of *Pseudomonas aeruginosa. Applied and environmental microbiology*, 78(18), pp.6762-6768.

Bainton, N.J., Bycroft, B.W., Chhabra, S.R., Stead, P., Gledhill, L., Hill, P.J., Rees, C.E., Winson, M.K., Salmond, G.P., Stewart, G.S. and Williams, P., 1992. A general role for the *lux* autoinducer in bacterial cell signalling: control of antibiotic biosynthesis in *Erwinia. Gene*, 116(1), pp.87-91.

Balasubramanian, D., Schneper, L., Merighi, M., Smith, R., Narasimhan, G., Lory, S. and Mathee, K., 2012. The regulatory repertoire of *Pseudomonas aeruginosa* AmpC ß-lactamase regulator AmpR includes virulence genes. *PloS one*, 7(3), p.e34067.

Balasubramanian, D., Schneper, L., Kumari, H. and Mathee, K., 2013. A dynamic and intricate regulatory network determines *Pseudomonas aeruginosa* virulence. *Nucleic acids research*, 41(1), pp.1-20.

Bardoel, B.W., van Kessel, K.P., van Strijp, J.A. and Milder, F.J., 2012. Inhibition of *Pseudomonas aeruginosa* virulence: characterization of the AprA–AprI interface and species selectivity. *Journal of molecular biology*, 415(3), pp.573-583.

Bass, J.I.F., Russo, D.M., Gabelloni, M.L., Geffner, J.R., Giordano, M., Catalano, M., Zorreguieta, Á. and Trevani, A.S., 2010. Extracellular DNA: a major proinflammatory component of *Pseudomonas aeruginosa* biofilms. *Journal of Immunology*, 184(11), pp.6386-6395.

Bassetti, M., Vena, A., Croxatto, A., Righi, E. and Guery, B., 2018. How to manage *Pseudomonas aeruginosa* infections. *Drugs in context*, *7*.

Beatson, S.A., Whitchurch, C.B., Sargent, J.L., Levesque, R.C. and Mattick, J.S., 2002a. Differential regulation of twitching motility and elastase production by Vfr in *Pseudomonas aeruginosa*. *Journal of bacteriology*, 184(13), pp.3605-3613.

Beatson, S.A., Whitchurch, C.B., Semmler, A.B. and Mattick, J.S., 2002b. Quorum sensing is not required for twitching motility in *Pseudomonas aeruginosa. Journal of bacteriology*, 184(13), pp.3598-3604.

Becher, A. and Schweizer, H.P., 2000. Integration-proficient *Pseudomonas aeruginosa* vectors for isolation of single-copy chromosomal *lacZ* and *lux* gene fusions. *Biotechniques*, 29(5), pp.948-952.

Benchling [Biology Software]. (2021). Retrieved from https://benchling.com.

Bernard, C.S., Bordi, C., Termine, E., Filloux, A. and de Bentzmann, S., 2009. Organization and PprB-dependent control of the *Pseudomonas aeruginosa tad* Locus, involved in Flp pilus biology. *Journal of bacteriology*, 191(6), pp.1961-1973.

Bernat, B.A., Laughlin, L.T. and Armstrong, R.N., 1997. Fosfomycin resistance protein (FosA) is a manganese metalloglutathione transferase related to glyoxalase I and the extradiol dioxygenases. *Biochemistry*, 36(11), pp.3050-3055.

Bertrand, J.J., West, J.T. and Engel, J.N., 2010. Genetic analysis of the regulation of type IV pilus function by the Chp chemosensory system of *Pseudomonas aeruginosa. Journal of bacteriology*, 192(4), pp.994-1010.

Bhattacharyya, S., Walker, D.M. and Harshey, R.M., 2020. Dead cells release a 'necrosignal' that activates antibiotic survival pathways in bacterial swarms. *Nature communications*, 11(1), pp.1-12.

Bina, X.R., Provenzano, D., Nguyen, N. and Bina, J.E., 2008. *Vibrio cholerae* RND family efflux systems are required for antimicrobial resistance, optimal virulence factor production, and colonization of the infant mouse small intestine. *Infection and immunity*, 76(8), pp.3595-3605.

Blair, J.M., Richmond, G.E. and Piddock, L.J., 2014. Multidrug efflux pumps in Gram-negative bacteria and their role in antibiotic resistance. *Future microbiology*, 9(10), pp.1165-1177.

Blair, J.M. and Piddock, L.J., 2016. How to measure export via bacterial multidrug resistance efflux pumps. *MBio*, 7(4), pp.e00840-16.

Blanco, P., Hernando-Amado, S., Reales-Calderon, J.A., Corona, F., Lira, F., Alcalde-Rico, M., Bernardini, A., Sanchez, M.B. and Martinez, J.L., 2016. Bacterial multidrug efflux pumps: much more than antibiotic resistance determinants. *Microorganisms*, 4(1), p.14.

Bolger, A.M., Lohse, M. and Usadel, B., 2014. Trimmomatic: a flexible trimmer for Illumina sequence data. *Bioinformatics*, 30(15), pp.2114-2120.

Borlee, B.R., Goldman, A.D., Murakami, K., Samudrala, R., Wozniak, D.J. and Parsek, M.R., 2010. *Pseudomonas aeruginosa* uses a cyclic-di-GMP-regulated adhesin to reinforce the biofilm extracellular matrix. *Molecular microbiology*, 75(4), pp.827-842.

Branny, P., Pearson, J.P., Pesci, E.C., Köhler, T., Iglewski, B.H. and Van Delden, C., 2001. Inhibition of quorum sensing by a *Pseudomonas aeruginosa dksA* homologue. *Journal of bacteriology*, 183(5), pp.1531-1539.

Braun, P., Tommassen, J. and Filloux, A., 1996. Role of the propeptide in folding and secretion of elastase of *Pseudomonas aeruginosa. Molecular microbiology*, 19(2), pp.297-306.

Braun, P., de Groot, A., Bitter, W. and Tommassen, J., 1998. Secretion of elastinolytic enzymes and their propeptides by *Pseudomonas aeruginosa. Journal of bacteriology*, 180(13), pp.3467-3469.

Brencic, A., McFarland, K.A., McManus, H.R., Castang, S., Mogno, I., Dove, S.L. and Lory, S., 2009. The GacS/GacA signal transduction system of *Pseudomonas aeruginosa* acts exclusively through its control over the transcription of the RsmY and RsmZ regulatory small RNAs. *Molecular microbiology*, 73(3), pp.434-445.

Brint, J.M. and Ohman, D.E., 1995. Synthesis of multiple exoproducts in *Pseudomonas aeruginosa* is under the control of RhlR-RhlI, another set of regulators in strain PAO1 with homology to the autoinducer-responsive LuxR-LuxI family. *Journal of bacteriology*, 177(24), pp.7155-7163.

Britigan, B.E., Roeder, T.L., Rasmussen, G.T., Shasby, D.M., McCormick, M.L. and Cox, C.D., 1992. Interaction of the *Pseudomonas aeruginosa* secretory products pyocyanin and pyochelin generates hydroxyl radical and causes synergistic damage to endothelial cells. Implications for *Pseudomonas*-associated tissue injury. *The Journal of clinical investigation*, 90(6), pp.2187-2196.

Buckley, A.M., Webber, M.A., Cooles, S., Randall, L.P., La Ragione, R.M., Woodward, M.J. and Piddock, L.J., 2006. The AcrAB–TolC efflux system of *Salmonella enterica* serovar Typhimurium plays a role in pathogenesis. *Cellular microbiology*, 8(5), pp.847-856.

Burrows, L.L., 2012. *Pseudomonas aeruginosa* twitching motility: type IV pili in action. *Annual review of microbiology*, 66, pp.493-520.

Caballero, A.R., Moreau, J.M., Engel, L.S., Marquart, M.E., Hill, J.M. and O'Callaghan, R.J., 2001. *Pseudomonas aeruginosa* protease IV enzyme assays and comparison to other *Pseudomonas* proteases. *Analytical biochemistry*, 290(2), pp.330-337.

Cabot, G., Ocampo-Sosa, A.A., Tubau, F., Macia, M.D., Rodríguez, C., Moya, B., Zamorano, L., Suárez, C., Peña, C., Martínez-Martínez, L. and Oliver, A., 2011. Overexpression of AmpC and efflux pumps in *Pseudomonas aeruginosa* isolates from bloodstream infections: prevalence and impact on resistance in a Spanish multicenter study. *Antimicrobial agents and chemotherapy*, 55(5), pp.1906-1911.

Cadoret, F., Ball, G., Douzi, B. and Voulhoux, R., 2014. Txc, a new type II secretion system of *Pseudomonas aeruginosa* strain PA7, is regulated by the TtsS/TtsR two-component system and directs specific secretion of the CbpE chitin-binding protein. *Journal of bacteriology*, 196(13), pp.2376-2386.

Cahan, R., Axelrad, I., Safrin, M., Ohman, D.E. and Kessler, E., 2001. A secreted aminopeptidase of *Pseudomonas aeruginosa*: identification, primary structure, and relationship to other aminopeptidases. *Journal of Biological Chemistry*, 276(47), pp.43645-43652.

Cai, Q., Li, Z., Ouyang, Q., Luo, C. and Gordon, V.D., 2016. Singly flagellated *Pseudomonas aeruginosa* chemotaxes efficiently by unbiased motor regulation. *MBio*, 7(2), pp.e00013-16.

Caille, O., Rossier, C. and Perron, K., 2007. A copper-activated two-component system interacts with zinc and imipenem resistance in *Pseudomonas aeruginosa. Journal of bacteriology*, 189(13), pp.4561-4568.

Caiazza, N.C., Shanks, R.M. and O'Toole, G.A., 2005. Rhamnolipids modulate swarming motility patterns of *Pseudomonas aeruginosa. Journal of bacteriology*, 187(21), pp.7351-7361.

Campodónico, V.L., Llosa, N.J., Grout, M., Döring, G., Maira-Litrán, T. and Pier, G.B., 2010. Evaluation of flagella and flagellin of *Pseudomonas aeruginosa* as vaccines. *Infection and immunity*, 78(2), pp.746-755.

Cao, H., Krishnan, G., Goumnerov, B., Tsongalis, J., Tompkins, R. and Rahme, L.G., 2001. A quorum sensing-associated virulence gene of *Pseudomonas aeruginosa* encodes a LysR-like transcription regulator with a unique self-regulatory mechanism. *Proceedings of the National Academy of Sciences*, 98(25), pp.14613-14618.

Cao, L., Srikumar, R. and Poole, K., 2004. MexAB-OprM hyperexpression in NalC-type multidrug-resistant *Pseudomonas aeruginosa*: identification and characterization of the *nalC* gene encoding a repressor of PA3720-PA3719. *Molecular microbiology*, 53(5), pp.1423-1436.

Cao, Q., Wang, Y., Chen, F., Xia, Y., Lou, J., Zhang, X., Yang, N., Sun, X., Zhang, Q., Zhuo, C. and Huang, X., 2014. A novel signal transduction pathway that modulates *rhl* quorum sensing and bacterial virulence in *Pseudomonas aeruginosa. PLoS pathogens*, 10(8), p.e1004340.

Carter, M.Q., Chen, J. and Lory, S., 2010. The *Pseudomonas aeruginosa* pathogenicity island PAPI-1 is transferred via a novel type IV pilus. *Journal of bacteriology*, 192(13), pp.3249-3258.

Carver, T., Harris, S.R., Berriman, M., Parkhill, J. and McQuillan, J.A., 2012. Artemis: an integrated platform for visualization and analysis of high-throughput sequence-based experimental data. *Bioinformatics*, 28(4), pp.464-469.

Castellani, C., Cuppens, H., Macek Jr, M., Cassiman, J.J., Kerem, E., Durie, P., Tullis, E., Assael, B.M., Bombieri, C., Brown, A. and Casals, T., 2008. Consensus on the use and interpretation of cystic fibrosis mutation analysis in clinical practice. *Journal of cystic fibrosis*, 7(3), pp.179-196.

Castellani, C., Duff, A.J., Bell, S.C., Heijerman, H.G., Munck, A., Ratjen, F., Sermet-Gaudelus, I., Southern, K.W., Barben, J., Flume, P.A. and Hodková, P., 2018. ECFS best practice guidelines: the 2018 revision. *Journal of cystic fibrosis*, 17(2), pp.153-178.

Ceri, H., Olson, M.E., Stremick, C., Read, R.R., Morck, D. and Buret, A., 1999. The Calgary Biofilm Device: new technology for rapid determination of antibiotic susceptibilities of bacterial biofilms. *Journal of clinical microbiology*, 37(6), pp.1771-1776.

Chan, Y.Y., Bian, H.S., Tan, T.M.C., Mattmann, M.E., Geske, G.D., Igarashi, J., Hatano, T., Suga, H., Blackwell, H.E. and Chua, K.L., 2007. Control of quorum sensing by a *Burkholderia pseudomallei* multidrug efflux pump. *Journal of bacteriology*, 189(11), pp.4320-4324.

Chapon-Hervé, V., Akrim, M., Latifi, A., Williams, P., Lazdunski, A. and Bally, M., 1997. Regulation of the *xcp* secretion pathway by multiple quorum-sensing modulons in *Pseudomonas aeruginosa. Molecular microbiology*, 24(6), pp.1169-1178.

Charif, D. and Lobry, J.R., 2007. SeqinR 1.0-2: a contributed package to the R project for statistical computing devoted to biological sequences retrieval and analysis. In Structural approaches to sequence evolution (pp. 207-232). Springer, Berlin, Heidelberg.

Chen, H., Hu, J., Chen, P.R., Lan, L., Li, Z., Hicks, L.M., Dinner, A.R. and He, C., 2008. The *Pseudomonas aeruginosa* multidrug efflux regulator MexR uses an oxidation-sensing mechanism. *Proceedings of the National Academy of Sciences*, 105(36), pp.13586-13591.

Chen, W., Wang, D., Zhou, W., Sang, H., Liu, X., Ge, Z., Zhang, J., Lan, L., Yang, C.G. and Chen, H., 2016. Novobiocin binding to NalD induces the expression of the MexAB-OprM pump in *Pseudomonas aeruginosa. Molecular microbiology*, 100(5), pp.749-758.

Chen, W., Zhang, Y., Zhang, Y., Pi, Y., Gu, T., Song, L., Wang, Y. and Ji, Q., 2018. CRISPR/Cas9-based genome editing in *Pseudomonas aeruginosa* and cytidine deaminase-mediated base editing in *Pseudomonas* species. *IScience*, 6, pp.222-231.

Chen, L., Zou, Y., Kronfl, A.A. and Wu, Y., 2020. Type VI secretion system of *Pseudomonas aeruginosa* is associated with biofilm formation but not environmental adaptation. *MicrobiologyOpen*, 9(3), p.e991.

Chiang, P., Habash, M. and Burrows, L.L., 2005. Disparate subcellular localization patterns of *Pseudomonas aeruginosa* type IV pilus ATPases involved in twitching motility. *Journal of bacteriology*, 187(3), pp.829-839.

Choi, K.H., Kumar, A. and Schweizer, H.P., 2006. A 10-min method for preparation of highly electrocompetent *Pseudomonas aeruginosa* cells: application for DNA fragment transfer between chromosomes and plasmid transformation. *Journal of microbiological methods*, 64(3), pp.391-397.

Choi, Y. and Chan, A.P., 2015. PROVEAN web server: a tool to predict the functional effect of amino acid substitutions and indels. *Bioinformatics*, 31(16), pp.2745-2747.

Choi, Y., Park, H.Y., Park, S.J., Park, S.J., Kim, S.K., Ha, C., Im, S.J. and Lee, J.H., 2011. Growth phase-differential quorum sensing regulation of anthranilate metabolism in *Pseudomonas aeruginosa. Molecules and cells*, 32(1), pp.57-65.

Chu, W.H., 2007. Optimization of extracellular alkaline protease production from species of Bacillus. *Journal of industrial microbiology and biotechnology*, 34(3), pp.241-245.

Chuanchuen, R., Narasaki, C.T. and Schweizer, H.P., 2002. The MexJK efflux pump of *Pseudomonas aeruginosa* requires OprM for antibiotic efflux but not for efflux of triclosan. *Journal of bacteriology*, 184(18), pp.5036-5044.

Chuanchuen, R., Gaynor, J.B., Karkhoff-Schweizer, R. and Schweizer, H.P., 2005. Molecular characterization of MexL, the transcriptional repressor of the *mexJK* multidrug efflux operon in *Pseudomonas aeruginosa. Antimicrobial agents and chemotherapy*, 49(5), pp.1844-1851.

Chugani, S.A., Whiteley, M., Lee, K.M., D'Argenio, D., Manoil, C. and Greenberg, E.P., 2001. QscR, a modulator of quorum-sensing signal synthesis and virulence in *Pseudomonas aeruginosa. Proceedings of the national academy of sciences*, 98(5), pp.2752-2757.

Ciofu, O., Mandsberg, L.F., Bjarnsholt, T., Wassermann, T. and Høiby, N., 2010. Genetic adaptation of *Pseudomonas aeruginosa* during chronic lung infection of patients with cystic fibrosis: strong and weak mutators with heterogeneous genetic backgrounds emerge in *mucA* and/or *lasR* mutants. *Microbiology*, 156(4), pp.1108-1119.

Coleman, J.P., Hudson, L.L., McKnight, S.L., Farrow III, J.M., Calfee, M.W., Lindsey, C.A. and Pesci, E.C., 2008. *Pseudomonas aeruginosa* PqsA is an anthranilate-coenzyme A ligase. *Journal of bacteriology*, 190(4), pp.1247-1255.

Cornelis, P. and Dingemans, J., 2013. *Pseudomonas aeruginosa* adapts its iron uptake strategies in function of the type of infections. *Frontiers in cellular and infection microbiology*, 3, p.75.

Cornelis, P., 2020. Putting an end to the *Pseudomonas aeruginosa* IQS controversy. *Microbiologyopen*, 9(2), p.e962.

Costerton, J.W., Stewart, P.S. and Greenberg, E.P., 1999. Bacterial biofilms: a common cause of persistent infections. *Science*, 284(5418), pp.1318-1322.

Cox, G., Ejim, L., Stogios, P.J., Koteva, K., Bordeleau, E., Evdokimova, E., Sieron, A.O., Savchenko, A., Serio, A.W., Krause, K.M. and Wright, G.D., 2018. Plazomicin retains antibiotic activity against most aminoglycoside modifying enzymes. *ACS infectious diseases*, *4*(6), pp.980-987.

Cunliffe, H.E., Merriman, T.R. and Lamont, I.L., 1995. Cloning and characterization of *pvdS*, a gene required for pyoverdine synthesis in *Pseudomonas aeruginosa*: PvdS is probably an alternative sigma factor. *Journal of bacteriology*, 177(10), pp.2744-2750.

Cuthbertson, L. and Nodwell, J.R., 2013. The TetR family of regulators. *Microbiology and Molecular Biology Reviews*, 77(3), pp.440-475.

Daddaoua, A., Molina-Santiago, C., la Torre, J.D., Krell, T. and Ramos, J.L., 2014. GtrS and GltR form a two-component system: the central role of 2-ketogluconate in the expression of exotoxin A and glucose catabolic enzymes in *Pseudomonas aeruginosa. Nucleic acids research*, 42(12), pp.7654-7665.

Daigle, D.M., Cao, L., Fraud, S., Wilke, M.S., Pacey, A., Klinoski, R., Strynadka, N.C., Dean, C.R. and Poole, K., 2007. Protein modulator of multidrug efflux gene expression in *Pseudomonas aeruginosa. Journal of bacteriology*, 189(15), pp.5441-5451.

Darzins, A., 1993. The *pilG* gene product, required for *Pseudomonas aeruginosa* pilus production and twitching motility, is homologous to the enteric, single-domain response regulator CheY. *Journal of bacteriology*, 175(18), pp.5934-5944.

Darzins, A., 1994. Characterization of a *Pseudomonas aeruginosa* gene cluster involved in pilus biosynthesis and twitching motility: sequence similarity to the chemotaxis proteins of enterics and the gliding bacterium *Myxococcus xanthus. Molecular microbiology*, 11(1), pp.137-153.

Darzins, A., 1995. The *Pseudomonas aeruginosa pilK* gene encodes a chemotactic methyltransferase (CheR) homologue that is translationally regulated. *Molecular microbiology*, 15(4), pp.703-717.

Dasgupta, N., Wolfgang, M.C., Goodman, A.L., Arora, S.K., Jyot, J., Lory, S. and Ramphal, R., 2003. A four-tiered transcriptional regulatory circuit controls flagellar biogenesis in *Pseudomonas aeruginosa. Molecular microbiology*, 50(3), pp.809-824.

Datsenko, K.A. and Wanner, B.L., 2000. One-step inactivation of chromosomal genes in *Escherichia coli* K-12 using PCR products. *Proceedings of the National Academy of Sciences*, 97(12), pp.6640-6645.

Deininger, K.N., Horikawa, A., Kitko, R.D., Tatsumi, R., Rosner, J.L., Wachi, M. and Slonczewski, J.L., 2011. A requirement of TolC and MDR efflux pumps for acid adaptation and GadAB induction in *Escherichia coli. PLoS One*, 6(4), p.e18960.

De Kievit, T., Seed, P.C., Nezezon, J., Passador, L. and Iglewski, B.H., 1999. RsaL, a novel repressor of virulence gene expression in *Pseudomonas aeruginosa. Journal of bacteriology*, 181(7), pp.2175-2184.

De Kievit, T.R., Parkins, M.D., Gillis, R.J., Srikumar, R., Ceri, H., Poole, K., Iglewski, B.H. and Storey, D.G., 2001. Multidrug efflux pumps: expression patterns and contribution to antibiotic resistance in *Pseudomonas aeruginosa* biofilms. *Antimicrobial agents and chemotherapy*, 45(6), pp.1761-1770.

De Lorenzo, V., Cases, I., Herrero, M. and Timmis, K., 1993. Early and late responses of TOL promoters to pathway inducers: identification of postexponential promoters in *Pseudomonas putida* with lacZ-tet bicistronic reporters. *Journal of Bacteriology*, 175(21), pp.6902-6907.

Denning, G.M., Wollenweber, L.A., Railsback, M.A., Cox, C.D., Stoll, L.L. and Britigan, B.E., 1998. *Pseudomonas* pyocyanin increases interleukin-8 expression by human airway epithelial cells. *Infection and immunity*, 66(12), pp.5777-5784.

Desbois, A.P. and Coote, P.J., 2011. Wax moth larva (*Galleria mellonella*): an *in vivo* model for assessing the efficacy of antistaphylococcal agents. *Journal of Antimicrobial Chemotherapy*, 66(8), pp.1785-1790.

Devaraj, A., Buzzo, J.R., Mashburn-Warren, L., Gloag, E.S., Novotny, L.A., Stoodley, P., Bakaletz, L.O. and Goodman, S.D., 2019. The extracellular DNA lattice of bacterial biofilms is structurally related to Holliday junction recombination intermediates. *Proceedings of the National Academy of Sciences*, 116(50), pp.25068-25077.

Dieppois, G., Ducret, V., Caille, O. and Perron, K., 2012. The transcriptional regulator CzcR modulates antibiotic resistance and quorum sensing in *Pseudomonas aeruginosa. PloS one*, 7(5), p.e38148.

Dietrich, L.E., Price-Whelan, A., Petersen, A., Whiteley, M. and Newman, D.K., 2006. The phenazine pyocyanin is a terminal signalling factor in the quorum sensing network of *Pseudomonas aeruginosa. Molecular microbiology*, 61(5), pp.1308-1321.

Diggle, S.P., Winzer, K., Lazdunski, A., Williams, P. and Cámara, M., 2002. Advancing the quorum in *Pseudomonas aeruginosa*: MvaT and the regulation of N-acylhomoserine lactone production and virulence gene expression. *Journal of Bacteriology*, 184(10), pp.2576-2586.

Diggle, S.P., Stacey, R.E., Dodd, C., Cámara, M., Williams, P. and Winzer, K., 2006. The galactophilic lectin, LecA, contributes to biofilm development in *Pseudomonas aeruginosa. Environmental microbiology*, 8(6), pp.1095-1104.

Dong, Y., Zhang, X.F., An, S.W., Xu, J.L. and Zhang, L.H., 2008. A novel two-component system BqsS-BqsR modulates quorum sensing-dependent biofilm decay in *Pseudomonas aeruginosa. Communicative & Integrative Biology*, 1(1), pp.88-96.

Dubern, J., Romero, M., Mai-Prochnow, A., Messina, M., Trampari, E., Naghra-van Gijzel, H., Chan, K.G., Carabelli, A., Barraud, N., Lazenby, J., Chen, Y., Robertson, S., Malone, J., Williams, P., Heeb, S. and Cámara, M., 2022. ToxR is a c-di-GMP binding protein that modulates surface-associated behaviour in *Pseudomonas aeruginosa. NPJ biofilms and microbiomes*, 8(1), 64.

Ducret, V., Gonzalez, M.R., Leoni, S., Valentini, M. and Perron, K., 2020. The CzcCBA efflux system requires the CadA P-type ATPase for timely expression upon zinc excess in *Pseudomonas aeruginosa. Frontiers in microbiology*, 11, p.911.

Dueholm, M.S., Søndergaard, M.T., Nilsson, M., Christiansen, G., Stensballe, A., Overgaard, M.T., Givskov, M., Tolker-Nielsen, T., Otzen, D.E. and Nielsen, P.H., 2013. Expression of Fap amyloids in *Pseudomonas aeruginosa, P. fluorescens*, and *P. putida* results in aggregation and increased biofilm formation. *Microbiologyopen*, 2(3), pp.365-382.

Duong, F., Lazdunski, A., Carni, B. and Murgier, M., 1992. Sequence of a cluster of genes controlling synthesis and secretion of alkaline protease in *Pseudomonas aeruginosa*: relationships to other secretory pathways. *Gene*, 121(1), pp.47-54.

Duong, F., Bonnet, E., Géli, V., Lazdunski, A., Murgier, M. and Filloux, A., 2001. The AprX protein of *Pseudomonas aeruginosa*: a new substrate for the Apr type I secretion system. *Gene*, 262(1-2), pp.147-153.

Elborn, J.S., 2016. Cystic fibrosis. *The lancet*, 388(10059), pp.2519-2531.

Emerson, J., Rosenfeld, M., McNamara, S., Ramsey, B. and Gibson, R.L., 2002. *Pseudomonas aeruginosa* and other predictors of mortality and morbidity in young children with cystic fibrosis. *Pediatric pulmonology*, 34(2), pp.91-100.

Engel, L.S., Hill, J.M., Caballero, A.R., Green, L.C. and O'Callaghan, R.J., 1998. Protease IV, a unique extracellular protease and virulence factor from *Pseudomonas aeruginosa. Journal of Biological Chemistry*, 273(27), pp.16792-16797.

Engel, J. and Balachandran, P., 2009. Role of *Pseudomonas aeruginosa* type III effectors in disease. *Current opinion in microbiology*, 12(1), pp.61-66.

Essar, D.W., Eberly, L.E.E., Hadero, A. and Crawford, I.P., 1990. Identification and characterization of genes for a second anthranilate synthase in *Pseudomonas aeruginosa*: interchangeability of the two anthranilate synthases and evolutionary implications. *Journal of bacteriology*, 172(2), pp.884-900.

Evans, K., Passador, L., Srikumar, R., Tsang, E., Nezezon, J. and Poole, K., 1998. Influence of the MexAB-OprM multidrug efflux system on quorum sensing in *Pseudomonas aeruginosa*. *Journal of bacteriology*, 180(20), pp.5443-5447.

Evans, K. and Poole, K., 1999. The MexA-MexB-OprM multidrug efflux system of *Pseudomonas aeruginosa* is growth-phase regulated. *FEMS microbiology letters*, 173(1), pp.35-39.

Ewels, P., Magnusson, M., Lundin, S. and Käller, M., 2016. MultiQC: summarize analysis results for multiple tools and samples in a single report. *Bioinformatics*, 32(19), pp.3047-3048.

Farrow III, J.M., Hudson, L.L., Wells, G., Coleman, J.P. and Pesci, E.C., 2015. CysB negatively affects the transcription of *pqsR* and *Pseudomonas* quinolone signal production in *Pseudomonas aeruginosa. Journal of bacteriology*, 197(12), pp.1988-2002.

Feldman, M., Bryan, R., Rajan, S., Scheffler, L., Brunnert, S., Tang, H. and Prince, A., 1998. Role of flagella in pathogenesis of *Pseudomonas aeruginosa* pulmonary infection. *Infection and immunity*, 66(1), pp.43-51.

Fenn, S., Dubern, J.F., Cigana, C., De Simone, M., Lazenby, J., Juhas, M., Schwager, S., Bianconi, I., Döring, G., Elmsley, J. and Eberl, L., 2021. NirA is an alternative nitrite reductase from *Pseudomonas aeruginosa* with potential as an antivirulence target. *Mbio*, 12(2), pp.e00207-21.

Fernández, L., Gooderham, W.J., Bains, M., McPhee, J.B., Wiegand, I. and Hancock, R.E., 2010. Adaptive resistance to the “last hope” antibiotics polymyxin B and colistin in *Pseudomonas aeruginosa* is mediated by the novel two-component regulatory system ParR-ParS. *Antimicrobial agents and chemotherapy*, 54(8), pp.3372-3382.

Fetar, H., Gilmour, C., Klinoski, R., Daigle, D.M., Dean, C.R. and Poole, K., 2011. *mexEF-oprN* multidrug efflux operon of *Pseudomonas aeruginosa*: regulation by the MexT activator in response to nitrosative stress and chloramphenicol. *Antimicrobial agents and chemotherapy*, 55(2), pp.508-514.

Fewson, C.A. and Nicholas, D.J.D., 1961. Nitrate reductase from *Pseudomonas aeruginosa. Biochimica et biophysica acta*, 49(2), pp.335-349.

Fillgrove, K.L., Pakhomova, S., Schaab, M.R., Newcomer, M.E. and Armstrong, R.N., 2007. Structure and mechanism of the genomically encoded fosfomycin resistance protein, FosX, from *Listeria monocytogenes. Biochemistry*, 46(27), pp.8110-8120.

Filloux, A., Bally, M., Soscia, C., Murgier, M. and Lazdunski, A., 1988. Phosphate regulation in *Pseudomonas aeruginosa*: cloning of the alkaline phosphatase gene and identification of *phoB*-and *phoR*-like genes. *Molecular and General Genetics MGG*, 212(3), pp.510-513.

FitzSimmons, S.C., 1993. The changing epidemiology of cystic fibrosis. *The Journal of pediatrics*, 122(1), pp.1-9.

Folkesson, A., Jelsbak, L., Yang, L., Johansen, H.K., Ciofu, O., Høiby, N. and Molin, S., 2012. Adaptation of *Pseudomonas aeruginosa* to the cystic fibrosis airway: an evolutionary perspective. *Nature Reviews Microbiology*, 10(12), pp.841-851.

Frank, L.H. and DeMoss, R.D., 1959. On the biosynthesis of pyocyanine. *Journal of Bacteriology*, 77(6), pp.776-782.

Franke, S., Grass, G., Rensing, C. and Nies, D.H., 2003. Molecular analysis of the copper-transporting efflux system CusCFBA of *Escherichia coli. Journal of bacteriology*, 185(13), pp.3804-3812.

Fraud, S., Campigotto, A.J., Chen, Z. and Poole, K., 2008. MexCD-OprJ multidrug efflux system of *Pseudomonas aeruginosa*: involvement in chlorhexidine resistance and induction by membrane-damaging agents dependent upon the AlgU stress response sigma factor. *Antimicrobial agents and chemotherapy*, 52(12), pp.4478-4482.

Fraud, S. and Poole, K., 2011. Oxidative stress induction of the MexXY multidrug efflux genes and promotion of aminoglycoside resistance development in *Pseudomonas aeruginosa. Antimicrobial agents and chemotherapy*, 55(3), pp.1068-1074.

Freschi, L., Jeukens, J., Kukavica-Ibrulj, I., Boyle, B., Dupont, M.J., Laroche, J., Larose, S., Maaroufi, H., Fothergill, J.L., Moore, M. and Winsor, G.L., 2015. Clinical utilization of genomics data produced by the international *Pseudomonas aeruginosa* consortium. *Frontiers in microbiology*, 6, p.1036.

Freschi, L., Vincent, A.T., Jeukens, J., Emond-Rheault, J.G., Kukavica-Ibrulj, I., Dupont, M.J., Charette, S.J., Boyle, B. and Levesque, R.C., 2019. The *Pseudomonas aeruginosa* pan-genome provides new insights on its population structure, horizontal gene transfer, and pathogenicity. *Genome biology and evolution*, 11(1), pp.109-120.

Fruci, M. and Poole, K., 2018. Aminoglycoside-inducible expression of the *mexAB-oprM* multidrug efflux operon in *Pseudomonas aeruginosa*: Involvement of the envelope stress-responsive AmgRS two-component system. *PloS one*, 13(10), p.e0205036.

Furukawa, S., Kuchma, S.L. and O'toole, G.A., 2006. Keeping their options open: acute versus persistent infections. *Journal of bacteriology*, 188(4), pp.1211-1217.

Gallagher, L.A., McKnight, S.L., Kuznetsova, M.S., Pesci, E.C. and Manoil, C., 2002. Functions required for extracellular quinolone signaling by *Pseudomonas aeruginosa*. *Journal of bacteriology*, 184(23), pp.6472-6480.

Gambello, M.J. and Iglewski, B.H., 1991. Cloning and characterization of the *Pseudomonas aeruginosa lasR* gene, a transcriptional activator of elastase expression. *Journal of bacteriology*, 173(9), pp.3000-3009.

Gambello, M.J., Kaye, S. and Iglewski, B.H., 1993. LasR of *Pseudomonas aeruginosa* is a transcriptional activator of the alkaline protease gene (*apr*) and an enhancer of exotoxin A expression. *Infection and immunity*, 61(4), pp.1180-1184.

Garcia, M., Morello, E., Garnier, J., Barrault, C., Garnier, M., Burucoa, C., Lecron, J.C., Si-Tahar, M., Bernard, F.X. and Bodet, C., 2018. *Pseudomonas aeruginosa* flagellum is critical for invasion, cutaneous persistence and induction of inflammatory response of skin epidermis. *Virulence*, 9(1), pp.1163-1175.

Gibiansky, M.L., Conrad, J.C., Jin, F., Gordon, V.D., Motto, D.A., Mathewson, M.A., Stopka, W.G., Zelasko, D.C., Shrout, J.D. and Wong, G.C., 2010. Bacteria use type IV pili to walk upright and detach from surfaces. *Science*, 330(6001), pp.197-197.

Giltner, C.L., Van Schaik, E.J., Audette, G.F., Kao, D., Hodges, R.S., Hassett, D.J. and Irvin, R.T., 2006. The *Pseudomonas aeruginosa* type IV pilin receptor binding domain functions as an adhesin for both biotic and abiotic surfaces. *Molecular microbiology*, 59(4), pp.1083-1096.

Giraud, C., Bernard, C.S., Calderon, V., Yang, L., Filloux, A., Molin, S., Fichant, G., Bordi, C. and de Bentzmann, S., 2011. The PprA–PprB two-component system activates CupE, the first non-archetypal *Pseudomonas aeruginosa* chaperone–usher pathway system assembling fimbriae. *Environmental microbiology*, 13(3), pp.666-683.

Glessner, A., Smith, R.S., Iglewski, B.H. and Robinson, J.B., 1999. Roles of *Pseudomonas aeruginosa las* and *rhl* quorum-sensing systems in control of twitching motility. *Journal of bacteriology*, 181(5), pp.1623-1629.

Glick, R., Gilmour, C., Tremblay, J., Satanower, S., Avidan, O., Déziel, E., Greenberg, E.P., Poole, K. and Banin, E., 2010. Increase in rhamnolipid synthesis under iron-limiting conditions influences surface motility and biofilm formation in *Pseudomonas aeruginosa*. *Journal of bacteriology*, 192(12), pp.2973-2980.

Goetz, J.A., Kuehfuss, N.M., Botschner, A.J., Zhu, S., Thompson, L.K. and Cox, G., 2022. Exploring functional interplay amongst *Escherichia coli* efflux pumps. *Microbiology*, 168(11), p.001261.

Goodman, A.L., Merighi, M., Hyodo, M., Ventre, I., Filloux, A. and Lory, S., 2009. Direct interaction between sensor kinase proteins mediates acute and chronic disease phenotypes in a bacterial pathogen. *Genes & development*, 23(2), pp.249-259.

Green, A.E., Amezquita, A., Le Marc, Y., Bull, M.J., Connor, T.R. and Mahenthiralingam, E., 2018. The consistent differential expression of genetic pathways following exposure of an industrial *Pseudomonas aeruginosa* strain to preservatives and a laundry detergent formulation. *FEMS microbiology letters*, 365(9), p.fny062.

Guilbaud, M., Bruzaud, J., Bouffartigues, E., Orange, N., Guillot, A., Aubert-Frambourg, A., Monnet, V., Herry, J.M., Chevalier, S. and Bellon-Fontaine, M.N., 2017. Proteomic response of *Pseudomonas aeruginosa* PAO1 adhering to solid surfaces. *Frontiers in Microbiology*, 8, p.1465.

Guragain, M., King, M.M., Williamson, K.S., Pérez-Osorio, A.C., Akiyama, T., Khanam, S., Patrauchan, M.A. and Franklin, M.J., 2016. The *Pseudomonas aeruginosa* PAO1 two-component regulator CarSR regulates calcium homeostasis and calcium-induced virulence factor production through its regulatory targets CarO and CarP. *Journal of bacteriology*, 198(6), pp.951-963.

Guzzo, J., Pages, J.M., Duong, F., Lazdunski, A. and Murgier, M., 1991. *Pseudomonas aeruginosa* alkaline protease: evidence for secretion genes and study of secretion mechanism. *Journal of bacteriology*, 173(17), pp.5290-5297.

Hall, M.P., Unch, J., Binkowski, B.F., Valley, M.P., Butler, B.L., Wood, M.G., Otto, P., Zimmerman, K., Vidugiris, G., Machleidt, T. and Robers, M.B., 2012. Engineered luciferase reporter from a deep sea shrimp utilizing a novel imidazopyrazinone substrate. *ACS chemical biology*, 7(11), pp.1848-1857.

Hall, C.W., Zhang, L. and Mah, T.F., 2017. PA3225 is a transcriptional repressor of antibiotic resistance mechanisms in *Pseudomonas aeruginosa. Antimicrobial agents and chemotherapy*, 61(8), pp.e02114-16.

Hassan, M., van der Lelie, D., Springael, D., Römling, U., Ahmed, N. and Mergeay, M., 1999. Identification of a gene cluster, *czr*, involved in cadmium and zinc resistance in *Pseudomonas aeruginosa. Gene*, 238(2), pp.417-425.

He, G.X., Kuroda, T., Mima, T., Morita, Y., Mizushima, T. and Tsuchiya, T., 2004. An H+-coupled multidrug efflux pump, PmpM, a member of the MATE family of transporters, from *Pseudomonas aeruginosa. Journal of bacteriology*, 186(1), pp.262-265.

Heacock-Kang, Y., Sun, Z., Zarzycki-Siek, J., Poonsuk, K., McMillan, I.A., Chuanchuen, R. and Hoang, T.T., 2018. Two regulators, PA3898 and PA2100, modulate the *Pseudomonas aeruginosa* multidrug resistance MexAB-OprM and EmrAB efflux pumps and biofilm formation. *Antimicrobial agents and chemotherapy*, 62(12), pp.e01459-18.

Heck, L.W., Morihara, K. and Abrahamson, D.R., 1986. Degradation of soluble laminin and depletion of tissue-associated basement membrane laminin by *Pseudomonas aeruginosa* elastase and alkaline protease. *Infection and immunity*, 54(1), pp.149-153.

Hegde, S.S., Vetting, M.W., Mitchenall, L.A., Maxwell, A. and Blanchard, J.S., 2011. Structural and biochemical analysis of the pentapeptide repeat protein Efs Qnr, a potent DNA gyrase inhibitor. *Antimicrobial agents and chemotherapy*, 55(1), pp.110-117.

Henderson, P.J., Maher, C., Elbourne, L.D., Eijkelkamp, B.A., Paulsen, I.T. and Hassan, K.A., 2021. Physiological functions of bacterial “multidrug” efflux pumps. *Chemical reviews*, 121(9), pp.5417-5478.

Hentzer, M., Wu, H., Andersen, J.B., Riedel, K., Rasmussen, T.B., Bagge, N., Kumar, N., Schembri, M.A., Song, Z., Kristoffersen, P. and Manefield, M., 2003. Attenuation of *Pseudomonas aeruginosa* virulence by quorum sensing inhibitors. *The EMBO journal*, 22(15), pp.3803-3815.

Hernando-Amado, S., Blanco, P., Alcalde-Rico, M., Corona, F., Reales-Calderón, J.A., Sánchez, M.B. and Martínez, J.L., 2016. Multidrug efflux pumps as main players in intrinsic and acquired resistance to antimicrobials. *Drug Resistance Updates*, 28, pp.13-27.

Heytler, P.G., 1963. Uncoupling of oxidative phosphorylation by carbonyl cyanide phenylhydrazones. I. Some characteristics of m-CI-CCP action on mitochondria and chloroplasts. *Biochemistry*, 2(2), pp.357-361.

Hickman, J.W., Tifrea, D.F. and Harwood, C.S., 2005. A chemosensory system that regulates biofilm formation through modulation of cyclic diguanylate levels. *Proceedings of the National Academy of Sciences*, 102(40), pp.14422-14427.

Hickman, J.W. and Harwood, C.S., 2008. Identification of FleQ from *Pseudomonas aeruginosa* as ac-di-GMP-responsive transcription factor. *Molecular microbiology*, 69(2), pp.376-389.

Higgins, S., Heeb, S., Rampioni, G., Fletcher, M.P., Williams, P. and Cámara, M., 2018. Differential regulation of the phenazine biosynthetic operons by quorum sensing in *Pseudomonas aeruginosa* PAO1-N. *Frontiers in cellular and infection microbiology*, 8, p.252.

Hirakata, Y., Srikumar, R., Poole, K., Gotoh, N., Suematsu, T., Kohno, S., Kamihira, S., Hancock, R.E. and Speert, D.P., 2002. Multidrug efflux systems play an important role in the invasiveness of *Pseudomonas aeruginosa. The Journal of experimental medicine*, 196(1), pp.109-118.

Heurlier, K., Dénervaud, V., Pessi, G., Reimmann, C. and Haas, D., 2003. Negative control of quorum sensing by RpoN (σ54) in *Pseudomonas aeruginosa* PAO1. *Journal of bacteriology*, 185(7), pp.2227-2235.

Hmelo, L.R., Borlee, B.R., Almblad, H., Love, M.E., Randall, T.E., Tseng, B.S., Lin, C., Irie, Y., Storek, K.M., Yang, J.J. and Siehnel, R.J., 2015. Precision-engineering the *Pseudomonas aeruginosa* genome with two-step allelic exchange. *Nature protocols*, 10(11), pp.1820-1841.

Hoang, T.T., Karkhoff-Schweizer, R.R., Kutchma, A.J. and Schweizer, H.P., 1998. A broad-host-range Flp-FRT recombination system for site-specific excision of chromosomally-located DNA sequences: application for isolation of unmarked *Pseudomonas aeruginosa* mutants. *Gene*, 212(1), pp.77-86.

Hobbs, M., Collie, E.S.R., Free, P.D., Livingston, S.P. and Mattick, J.S., 1993. PilS and PilR, a two-component transcriptional regulatory system controlling expression of type 4 fimbriae in *Pseudomonas aeruginosa. Molecular microbiology*, 7(5), pp.669-682.

Hodgkinson, J.T., Gross, J., Baker, Y.R., Spring, D.R. and Welch, M., 2016. A new *Pseudomonas* quinolone signal (PQS) binding partner: MexG. *Chemical science*, 7(4), pp.2553-2562.

Holloway, B.W., 1955. Genetic recombination in *Pseudomonas aeruginosa. Microbiology*, 13(3), pp.572-581.

Hong, T.P., Carter, M.Q., Struffi, P., Casonato, S., Hao, Y., Lam, J.S., Lory, S. and Jousson, O., 2017. Conjugative type IVb pilus recognizes lipopolysaccharide of recipient cells to initiate PAPI-1 pathogenicity island transfer in *Pseudomonas aeruginosa. BMC microbiology*, 17(1), pp.1-11.

Hood, R.D., Singh, P., Hsu, F., Güvener, T., Carl, M.A., Trinidad, R.R., Silverman, J.M., Ohlson, B.B., Hicks, K.G., Plemel, R.L. and Li, M., 2010. A type VI secretion system of *Pseudomonas aeruginosa* targets a toxin to bacteria. *Cell host & microbe*, 7(1), pp.25-37.

Horsburgh, M.J., Aish, J.L., White, I.J., Shaw, L., Lithgow, J.K. and Foster, S.J., 2002. σB modulates virulence determinant expression and stress resistance: characterization of a functional *rsbU* strain derived from *Staphylococcus aureus* 8325-4. *Journal of bacteriology*, 184(19), pp.5457-5467.

Huang, W. and Wilks, A., 2017. A rapid seamless method for gene knockout in *Pseudomonas aeruginosa. BMC microbiology*, 17(1), pp.1-8.

Imperi, F., Tiburzi, F. and Visca, P., 2009. Molecular basis of pyoverdine siderophore recycling in *Pseudomonas aeruginosa. Proceedings of the National Academy of Sciences*, 106(48), pp.20440-20445.

Jennings, L.K., Storek, K.M., Ledvina, H.E., Coulon, C., Marmont, L.S., Sadovskaya, I., Secor, P.R., Tseng, B.S., Scian, M., Filloux, A. and Wozniak, D.J., 2015. Pel is a cationic exopolysaccharide that cross-links extracellular DNA in the *Pseudomonas aeruginosa* biofilm matrix. *Proceedings of the National Academy of Sciences*, 112(36), pp.11353-11358.

Jensen, P.Ø., Bjarnsholt, T., Phipps, R., Rasmussen, T.B., Calum, H., Christoffersen, L., Moser, C., Williams, P., Pressler, T., Givskov, M. and Høiby, N., 2007. Rapid necrotic killing of polymorphonuclear leukocytes is caused by quorum-sensing-controlled production of rhamnolipid by *Pseudomonas aeruginosa. Microbiology*, 153(5), pp.1329-1338.

Jerse, A.E., Sharma, N.D., Simms, A.N., Crow, E.T., Snyder, L.A. and Shafer, W.M., 2003. A gonococcal efflux pump system enhances bacterial survival in a female mouse model of genital tract infection. *Infection and immunity*, 71(10), pp.5576-5582.

Jia, B., Raphenya, A.R., Alcock, B., Waglechner, N., Guo, P., Tsang, K.K., Lago, B.A., Dave, B.M., Pereira, S., Sharma, A.N. and Doshi, S., 2016. CARD 2017: expansion and model-centric curation of the comprehensive antibiotic resistance database. *Nucleic acids research*, p.gkw1004.

Jin, F., Conrad, J.C., Gibiansky, M.L. and Wong, G.C., 2011. Bacteria use type-IV pili to slingshot on surfaces. *Proceedings of the National Academy of Sciences*, 108(31), pp.12617-12622.

Jinek, M., Chylinski, K., Fonfara, I., Hauer, M., Doudna, J.A. and Charpentier, E., 2012. A programmable dual-RNA–guided DNA endonuclease in adaptive bacterial immunity. science, 337(6096), pp.816-821.

Jones, S., Yu, B., Bainton, N.A., Birdsall, M., Bycroft, B.W., Chhabra, S.R., Cox, A.J., Golby, P., Reeves, P.J. and Stephens, S., 1993. The *lux* autoinducer regulates the production of exoenzyme virulence determinants in *Erwinia carotovora* and *Pseudomonas aeruginosa. The EMBO journal*, 12(6), pp.2477-2482.

Jude, F., Köhler, T., Branny, P., Perron, K., Mayer, M.P., Comte, R. and Van Delden, C., 2003. Posttranscriptional control of quorum-sensing-dependent virulence genes by DksA in *Pseudomonas aeruginosa. Journal of bacteriology*, 185(12), pp.3558-3566.

Juhas, M., Wiehlmann, L., Huber, B., Jordan, D., Lauber, J., Salunkhe, P., Limpert, A.S., von Götz, F., Steinmetz, I., Eberl, L. and Tümmler, B., 2004. Global regulation of quorum sensing and virulence by VqsR in *Pseudomonas aeruginosa. Microbiology*, 150(4), pp.831-841.

Kahl, L.J., Price-Whelan, A. and Dietrich, L.E., 2020. Light-mediated decreases in cyclic di-GMP levels inhibit structure formation in *Pseudomonas aeruginosa* biofilms. *Journal of bacteriology*, 202(14), pp.e00117-20.

Kato, J., Nakamura, T., Kuroda, A. and Ohtake, H., 1999. Cloning and characterization of chemotaxis genes in *Pseudomonas aeruginosa. Bioscience, biotechnology, and biochemistry*, 63(1), pp.155-161.

Kessler, E., Safrin, M., Olson, J.C. and Ohman, D.E., 1993. Secreted LasA of *Pseudomonas aeruginosa* is a staphylolytic protease. *Journal of Biological Chemistry*, 268(10), pp.7503-7508.

Kessler, E., Safrin, M., Gustin, J.K. and Ohman, D.E., 1998. Elastase and the LasA protease of *Pseudomonas aeruginosa* are secreted with their propeptides. *Journal of Biological Chemistry*, 273(46), pp.30225-30231.

Kida, Y., Higashimoto, Y., Inoue, H., Shimizu, T. and Kuwano, K., 2008. A novel secreted protease from *Pseudomonas aeruginosa* activates NF-κB through protease-activated receptors. *Cellular microbiology*, 10(7), pp.1491-1504.

Klockgether, J., Munder, A., Neugebauer, J., Davenport, C.F., Stanke, F., Larbig, K.D., Heeb, S., Schöck, U., Pohl, T.M., Wiehlmann, L. and Tümmler, B., 2010. Genome diversity of *Pseudomonas aeruginosa* PAO1 laboratory strains. *Journal of bacteriology*, 192(4), pp.1113-1121.

Köhler, T., Michéa-Hamzehpour, M., Henze, U., Gotoh, N., Kocjancic Curty, L. and Pechère, J.C., 1997. Characterization of MexE–MexF–OprN, a positively regulated multidrug efflux system of *Pseudomonas aeruginosa. Molecular microbiology*, 23(2), pp.345-354.

Köhler, T., Epp, S.F., Curty, L.K. and Pechère, J.C., 1999. Characterization of MexT, the regulator of the MexE-MexF-OprN multidrug efflux system of *Pseudomonas aeruginosa. Journal of bacteriology*, 181(20), pp.6300-6305.

Köhler, T., Curty, L.K., Barja, F., Van Delden, C. and Pechère, J.C., 2000. Swarming of *Pseudomonas aeruginosa* is dependent on cell-to-cell signaling and requires flagella and pili. *Journal of bacteriology*, 182(21), pp.5990-5996.

Köhler, T., Van Delden, C., Curty, L.K., Hamzehpour, M.M. and Pechere, J.C., 2001. Overexpression of the MexEF-OprN multidrug efflux system affects cell-to-cell signaling in *Pseudomonas aeruginosa. Journal of Bacteriology*, 183(18), pp.5213-5222.

Kong, K.F., Jayawardena, S.R., Indulkar, S.D., Del Puerto, A., Koh, C.L., Høiby, N. and Mathee, K., 2005. *Pseudomonas aeruginosa* AmpR is a global transcriptional factor that regulates expression of AmpC and PoxB β-lactamases, proteases, quorum sensing, and other virulence factors. *Antimicrobial Agents and Chemotherapy*, 49(11), pp.4567-4575.

Kuchma, S.L., Connolly, J.P. and O'toole, G.A., 2005. A three-component regulatory system regulates biofilm maturation and type III secretion in *Pseudomonas aeruginosa*. *Journal of bacteriology*, 187(4), pp.1441-1454.

Kulasekara, H.D., Ventre, I., Kulasekara, B.R., Lazdunski, A., Filloux, A. and Lory, S., 2005. A novel two-component system controls the expression of *Pseudomonas aeruginosa* fimbrial cup genes. *Molecular microbiology*, 55(2), pp.368-380.

Lamarche, M.G. and Déziel, E., 2011. MexEF-OprN efflux pump exports the *Pseudomonas* quinolone signal (PQS) precursor HHQ (4-hydroxy-2-heptylquinoline). *PloS one*, 6(9), p.e24310.

Lamers, R.P., Cavallari, J.F. and Burrows, L.L., 2013. The efflux inhibitor phenylalanine-arginine beta-naphthylamide (PAβN) permeabilizes the outer membrane of gram-negative bacteria. *PloS one*, 8(3), p.e60666.

Lamont, I.L., Beare, P.A., Ochsner, U., Vasil, A.I. and Vasil, M.L., 2002. Siderophore-mediated signaling regulates virulence factor production in *Pseudomonas aeruginosa. Proceedings of the National Academy of Sciences*, 99(10), pp.7072-7077.

Langmead, B. and Salzberg, S.L., 2012. Fast gapped-read alignment with Bowtie 2. *Nature methods*, 9(4), pp.357-359.

Langridge, G.C., Phan, M.D., Turner, D.J., Perkins, T.T., Parts, L., Haase, J., Charles, I., Maskell, D.J., Peters, S.E., Dougan, G. and Wain, J., 2009. Simultaneous assay of every *Salmonella* Typhi gene using one million transposon mutants. *Genome research*, 19(12), pp.2308-2316.

Latifi, A., Foglino, M., Tanaka, K., Williams, P. and Lazdunski, A., 1996. A hierarchical quorum-sensing cascade in *Pseudomonas aeruginosa* links the transcriptional activators LasR and RhIR (VsmR) to expression of the stationary-phase sigma factor RpoS. *Molecular microbiology*, 21(6), pp.1137-1146.

Lau, G.W., Ran, H., Kong, F., Hassett, D.J. and Mavrodi, D., 2004. *Pseudomonas aeruginosa* pyocyanin is critical for lung infection in mice. *Infection and immunity*, 72(7), pp.4275-4278.

Lau, C.H.F., Krahn, T., Gilmour, C., Mullen, E. and Poole, K., 2015. AmgRS-mediated envelope stress-inducible expression of the *mexXY* multidrug efflux operon of *Pseudomonas aeruginosa. Microbiologyopen*, 4(1), pp.121-135.

Ledgham, F., Soscia, C., Chakrabarty, A., Lazdunski, A. and Foglino, M., 2003a. Global regulation in *Pseudomonas aeruginosa*: the regulatory protein AlgR2 (AlgQ) acts as a modulator of quorum sensing. *Research in microbiology*, 154(3), pp.207-213.

Ledgham, F., Ventre, I., Soscia, C., Foglino, M., Sturgis, J.N. and Lazdunski, A., 2003b. Interactions of the quorum sensing regulator QscR: interaction with itself and the other regulators of *Pseudomonas aeruginosa* LasR and RhlR. *Molecular microbiology*, 48(1), pp.199-210.

Lee, V.T., Matewish, J.M., Kessler, J.L., Hyodo, M., Hayakawa, Y. and Lory, S., 2007. A cyclic-di-GMP receptor required for bacterial exopolysaccharide production. *Molecular microbiology*, 65(6), pp.1474-1484.

Lee, J., Wu, J., Deng, Y., Wang, J., Wang, C., Wang, J., Chang, C., Dong, Y., Williams, P. and Zhang, L.H., 2013. A cell-cell communication signal integrates quorum sensing and stress response. *Nature chemical biology*, 9(5), pp.339-343.

Lennox, E.S., 1955. Transduction of linked genetic characters of the host by bacteriophage P1. *Virology*, 1(2), pp.190-206.

Lépine, F., Milot, S., Déziel, E., He, J. and Rahme, L.G., 2004. Electrospray/mass spectrometric identification and analysis of 4-hydroxy-2-alkylquinolines (HAQs) produced by *Pseudomonas aeruginosa. Journal of the American Society for Mass Spectrometry*, 15(6), pp.862-869.

Lesic, B. and Rahme, L.G., 2008. Use of the lambda Red recombinase system to rapidly generate mutants in *Pseudomonas aeruginosa. BMC molecular biology*, 9(1), pp.1-9.

Létoffé, S., Redeker, V. and Wandersman, C., 1998. Isolation and characterization of an extracellular haem-binding protein from *Pseudomonas aeruginosa* that shares function and sequence similarities with the *Serratia marcescens* HasA haemophore. *Molecular microbiology*, 28(6), pp.1223-1234.

Lewis, K., 2010. Persister cells. *Annual review of microbiology*, 64, pp.357-372.

Li, X.Z., Nikaido, H. and Poole, K., 1995. Role of *mexA-mexB-oprM* in antibiotic efflux in *Pseudomonas aeruginosa. Antimicrobial agents and chemotherapy*, 39(9), pp.1948-1953.

Li, X.Z., Zhang, L. and Poole, K., 1998. Role of the multidrug efflux systems of *Pseudomonas aeruginosa* in organic solvent tolerance. *Journal of bacteriology*, 180(11), pp.2987-2991.

Li, Y., Mima, T., Komori, Y., Morita, Y., Kuroda, T., Mizushima, T. and Tsuchiya, T., 2003. A new member of the tripartite multidrug efflux pumps, MexVW–OprM, in *Pseudomonas aeruginosa. Journal of Antimicrobial Chemotherapy*, 52(4), pp.572-575.

Li, H., Handsaker, B., Wysoker, A., Fennell, T., Ruan, J., Homer, N., Marth, G., Abecasis, G. and Durbin, R., 2009. The sequence alignment/map format and SAMtools. *Bioinformatics*, 25(16), pp.2078-2079.

Li, Y., Heine, S., Entian, M., Sauer, K. and Frankenberg-Dinkel, N., 2013. NO-induced biofilm dispersion in *Pseudomonas aeruginosa* is mediated by an MHYT domain-coupled phosphodiesterase. *Journal of bacteriology*, 195(16), pp.3531-3542.

Li, Y., Petrova, O.E., Su, S., Lau, G.W., Panmanee, W., Na, R., Hassett, D.J., Davies, D.G. and Sauer, K., 2014. BdlA, DipA and induced dispersion contribute to acute virulence and chronic persistence of *Pseudomonas aeruginosa. PLoS pathogens*, 10(6), p.e1004168.

Li, Y., Bai, F., Xia, H., Zhuang, L., Xu, H., Jin, Y., Zhang, X., Bai, Y. and Qiao, M., 2015. A novel regulator PA5022 (aefA) is involved in swimming motility, biofilm formation and elastase activity of *Pseudomonas aeruginosa. Microbiological research*, 176, pp.14-20.

Liang, H., Li, L., Dong, Z., Surette, M.G. and Duan, K., 2008. The YebC family protein PA0964 negatively regulates the *Pseudomonas aeruginosa* quinolone signal system and pyocyanin production. *Journal of bacteriology*, 190(18), pp.6217-6227.

Liang, H., Li, L., Kong, W., Shen, L. and Duan, K., 2009. Identification of a novel regulator of the quorum-sensing systems in *Pseudomonas aeruginosa. FEMS microbiology letters*, 293(2), pp.196-204.

Liao, J., Schurr, M.J. and Sauer, K., 2013. The MerR-like regulator BrlR confers biofilm tolerance by activating multidrug efflux pumps in *Pseudomonas aeruginosa* biofilms. *Journal of bacteriology*, 195(15), pp.3352-3363.

Liao, Y., Smyth, G.K. and Shi, W., 2019. The R package Rsubread is easier, faster, cheaper and better for alignment and quantification of RNA sequencing reads. *Nucleic acids research*, 47(8), pp.e47-e47.

Linares, J.F., López, J.A., Camafeita, E., Albar, J.P., Rojo, F. and Martínez, J.L., 2005. Overexpression of the multidrug efflux pumps MexCD-OprJ and MexEF-OprN is associated with a reduction of type III secretion in *Pseudomonas aeruginosa. Journal of bacteriology*, 187(4), pp.1384-1391.

Lin Pedersen, T., (2020). patchwork: The Composer of Plots. R package version 1.1.1. https://CRAN.R-project.org/package=patchwork

Little, A.S., Okkotsu, Y., Reinhart, A.A., Damron, F.H., Barbier, M., Barrett, B., Oglesby-Sherrouse, A.G., Goldberg, J.B., Cody, W.L., Schurr, M.J. and Vasil, M.L., 2018. *Pseudomonas aeruginosa* AlgR phosphorylation status differentially regulates pyocyanin and pyoverdine production. *MBio*, 9(1), pp.e02318-17.

Liu, Y.Y., Wang, Y., Walsh, T.R., Yi, L.X., Zhang, R., Spencer, J., Doi, Y., Tian, G., Dong, B., Huang, X. and Yu, L.F., 2016. Emergence of plasmid-mediated colistin resistance mechanism MCR-1 in animals and human beings in China: a microbiological and molecular biological study. *The Lancet infectious diseases*, 16(2), pp.161-168.

Llanes, C., Köhler, T., Patry, I., Dehecq, B., Van Delden, C. and Plésiat, P., 2011. Role of the MexEF-OprN efflux system in low-level resistance of *Pseudomonas aeruginosa* to ciprofloxacin. *Antimicrobial agents and chemotherapy*, 55(12), pp.5676-5684.

Lomovskaya, O., Warren, M.S., Lee, A., Galazzo, J., Fronko, R., Lee, M.A.Y., Blais, J., Cho, D., Chamberland, S., Renau, T. and Leger, R., 2001. Identification and characterization of inhibitors of multidrug resistance efflux pumps in *Pseudomonas aeruginosa*: novel agents for combination therapy. *Antimicrobial agents and chemotherapy*, 45(1), pp.105-116.

Love, M.I., Huber, W. and Anders, S., 2014. Moderated estimation of fold change and dispersion for RNA-seq data with DESeq2. *Genome biology*, 15(12), pp.1-21.

LoVullo, E.D. and Schweizer, H.P., 2020. *Pseudomonas aeruginosa mexT* is an indicator of PAO1 strain integrity. *Journal of medical microbiology*, 69(1), p.139.

Lu, H.M., Mizushima, S. and Lory, S., 1993. A periplasmic intermediate in the extracellular secretion pathway of *Pseudomonas aeruginosa* exotoxin A. *Journal of bacteriology*, 175(22), pp.7463-7467.

Lu, J., Huang, X., Li, K., Li, S., Zhang, M., Wang, Y., Jiang, H. and Xu, Y., 2009. LysR family transcriptional regulator PqsR as repressor of pyoluteorin biosynthesis and activator of phenazine-1-carboxylic acid biosynthesis in *Pseudomonas sp*. M18. *Journal of biotechnology*, 143(1), pp.1-9.

Lundgren, B.R., Thornton, W., Dornan, M.H., Villegas-Peñaranda, L.R., Boddy, C.N. and Nomura, C.T., 2013. Gene PA2449 is essential for glycine metabolism and pyocyanin biosynthesis in *Pseudomonas aeruginosa* PAO1. *Journal of bacteriology*, 195(9), pp.2087-2100.

Luo, Y., Zhao, K., Baker, A.E., Kuchma, S.L., Coggan, K.A., Wolfgang, M.C., Wong, G.C. and O'Toole, G.A., 2015. A hierarchical cascade of second messengers regulates *Pseudomonas aeruginosa* surface behaviors. *MBio*, 6(1), pp.e02456-14.

Ma, S., Wozniak, D.J. and Ohman, D.E., 1997. Identification of the Histidine Protein Kinase KinB in *Pseudomonas aeruginosa* and Its Phosphorylation of the Alginate Regulator AlgB. *Journal of Biological Chemistry*, 272(29), pp.17952-17960.

Ma, L., Lu, H., Sprinkle, A., Parsek, M.R. and Wozniak, D.J., 2007. *Pseudomonas aeruginosa* Psl is a galactose-and mannose-rich exopolysaccharide. *Journal of bacteriology*, 189(22), pp.8353-8356.

Macfarlane, E.L., Kwasnicka, A., Ochs, M.M. and Hancock, R.E., 1999. PhoP–PhoQ homologues in *Pseudomonas aeruginosa* regulate expression of the outer-membrane protein OprH and polymyxin B resistance. *Molecular microbiology*, 34(2), pp.305-316.

Magiorakos, A.P., Srinivasan, A., Carey, R.B., Carmeli, Y., Falagas, M.E., Giske, C.G., Harbarth, S., Hindler, J.F., Kahlmeter, G., Olsson-Liljequist, B. and Paterson, D.L., 2012. Multidrug-resistant, extensively drug-resistant and pandrug-resistant bacteria: an international expert proposal for interim standard definitions for acquired resistance. *Clinical microbiology and infection*, 18(3), pp.268-281.

Malgaonkar, A. and Nair, M., 2019. Quorum sensing in *Pseudomonas aeruginosa* mediated by RhlR is regulated by a small RNA PhrD. *Scientific reports*, 9(1), pp.1-11.

Marquart, M.E., Caballero, A.R., Chomnawang, M., Thibodeaux, B.A., Twining, S.S. and O'Callaghan, R.J., 2005. Identification of a novel secreted protease from *Pseudomonas aeruginosa* that causes corneal erosions. *Investigative ophthalmology & visual science*, 46(10), pp.3761-3768.

Marquart, M.E. and O'Callaghan, R.J., 2013. Infectious keratitis: secreted bacterial proteins that mediate corneal damage. *Journal of ophthalmology*, 2013.

Marshall, R.L., Lloyd, G.S., Lawler, A.J., Element, S.J., Kaur, J., Ciusa, M.L., Ricci, V., Tschumi, A., Kühne, H., Alderwick, L.J. and Piddock, L.J., 2020. New multidrug efflux inhibitors for Gram-negative bacteria. *Mbio*, 11(4), pp.e01340-20.

Masuda, N., Sakagawa, E., Ohya, S., Gotoh, N., Tsujimoto, H. and Nishino, T., 2000. Substrate specificities of MexAB-OprM, MexCD-OprJ, and MexXY-oprM efflux pumps in *Pseudomonas aeruginosa. Antimicrobial agents and chemotherapy*, 44(12), pp.3322-3327.

Maseda, H., Saito, K., Nakajima, A. and Nakae, T., 2000. Variation of the *mexT* gene, a regulator of the MexEF-oprN efflux pump expression in wild-type strains of *Pseudomonas aeruginosa. FEMS microbiology letters*, 192(1), pp.107-112.

Maseda, H., Sawada, I., Saito, K., Uchiyama, H., Nakae, T. and Nomura, N., 2004. Enhancement of the *mexAB-oprM* efflux pump expression by a quorum-sensing autoinducer and its cancellation by a regulator, MexT, of the *mexEF-oprN* efflux pump operon in *Pseudomonas aeruginosa. Antimicrobial agents and chemotherapy*, 48(4), pp.1320-1328.

Mashburn, L.M. and Whiteley, M., 2005. Membrane vesicles traffic signals and facilitate group activities in a prokaryote. *Nature*, 437(7057), pp.422-425.

Matsuo, Y., Eda, S., Gotoh, N., Yoshihara, E. and Nakae, T., 2004. MexZ-mediated regulation of *mexXY* multidrug efflux pump expression in *Pseudomonas aeruginosa* by binding on the *mexZ-mexX* intergenic DNA. *FEMS microbiology letters*, 238(1), pp.23-28.

Maura, D., Hazan, R., Kitao, T., Ballok, A.E. and Rahme, L.G., 2016. Evidence for direct control of virulence and defense gene circuits by the *Pseudomonas aeruginosa* quorum sensing regulator, MvfR. *Scientific reports*, 6(1), pp.1-14.

Mavrodi, D.V., Bonsall, R.F., Delaney, S.M., Soule, M.J., Phillips, G. and Thomashow, L.S., 2001. Functional analysis of genes for biosynthesis of pyocyanin and phenazine-1-carboxamide from *Pseudomonas aeruginosa* PAO1. *Journal of bacteriology*, 183(21), pp.6454-6465.

McIver, K., Kessler, E. and Ohman, D.E., 1991. Substitution of active-site His-223 in *Pseudomonas aeruginosa* elastase and expression of the mutated *lasB* alleles in *Escherichia coli* show evidence for autoproteolytic processing of proelastase. *Journal of bacteriology*, 173(24), pp.7781-7789.

McKinnell, J.A., Dwyer, J.P., Talbot, G.H., Connolly, L.E., Friedland, I., Smith, A., Jubb, A.M., Serio, A.W., Krause, K.M. and Daikos, G.L., 2019. Plazomicin for infections caused by carbapenem-resistant Enterobacteriaceae. *New England Journal of Medicine*, 380(8), pp.791-793.

McNeil, H.E., Alav, I., Torres, R.C., Rossiter, A.E., Laycock, E., Legood, S., Kaur, I., Davies, M., Wand, M., Webber, M.A. and Bavro, V.N., 2019. Identification of binding residues between periplasmic adapter protein (PAP) and RND efflux pumps explains PAP-pump promiscuity and roles in antimicrobial resistance. *PLoS pathogens*, 15(12), p.e1008101.

Medina, G., Juárez, K., Valderrama, B. and Soberón-Chávez, G., 2003. Mechanism of *Pseudomonas aeruginosa* RhlR transcriptional regulation of the *rhlAB* promoter. *Journal of Bacteriology*, 185(20), pp.5976-5983.

Mehla, J., Malloci, G., Mansbach, R., López, C.A., Tsivkovski, R., Haynes, K., Leus, I.V., Grindstaff, S.B., Cascella, R.H., D'Cunha, N. and Herndon, L., 2021. Predictive Rules of Efflux Inhibition and Avoidance in *Pseudomonas aeruginosa. Mbio*, 12(1), pp.e02785-20.

Meng, X., Ahator, S.D. and Zhang, L.H., 2020. Molecular mechanisms of phosphate stress activation of *Pseudomonas aeruginosa* quorum sensing systems. *MSphere*, 5(2), pp.e00119-20.

Merighi, M., Lee, V.T., Hyodo, M., Hayakawa, Y. and Lory, S., 2007. The second messenger bis-(3'-5')-cyclic-GMP and its PilZ domain-containing receptor Alg44 are required for alginate biosynthesis in *Pseudomonas aeruginosa. Molecular microbiology*, 65(4), pp.876-895.

Mesquita, C.S., Ribeiro, A., Gomes, A.C. and Santos, P.M., 2021. Absence of light exposure increases pathogenicity of *Pseudomonas aeruginosa* pneumonia-associated clinical isolates. *Biology*, 10(9), p.837.

Mikheenko, A., Prjibelski, A., Saveliev, V., Antipov, D. and Gurevich, A., 2018. Versatile genome assembly evaluation with QUAST-LG. *Bioinformatics*, 34(13), pp.i142-i150.

Mikkelsen, H., Ball, G., Giraud, C. and Filloux, A., 2009. Expression of *Pseudomonas aeruginosa* CupD fimbrial genes is antagonistically controlled by RcsB and the EAL-containing PvrR response regulators. *PloS one*, 4(6), p.e6018.

Mima, T., Sekiya, H., Mizushima, T., Kuroda, T. and Tsuchiya, T., 2005. Gene cloning and properties of the RND-type multidrug efflux pumps MexPQ-OpmE and MexMN-OprM from *Pseudomonas aeruginosa. Microbiology and immunology*, 49(11), pp.999-1002.

Mima, T., Joshi, S., Gomez-Escalada, M. and Schweizer, H.P., 2007. Identification and characterization of TriABC-OpmH, a triclosan efflux pump of *Pseudomonas aeruginosa* requiring two membrane fusion proteins. *Journal of bacteriology*, 189(21), pp.7600-7609.

Mima, T., Kohira, N., Li, Y., Sekiya, H., Ogawa, W., Kuroda, T. and Tsuchiya, T., 2009. Gene cloning and characteristics of the RND-type multidrug efflux pump MuxABC-OpmB possessing two RND components in *Pseudomonas aeruginosa. Microbiology*, 155(11), pp.3509-3517.

Minagawa, S., Inami, H., Kato, T., Sawada, S., Yasuki, T., Miyairi, S., Horikawa, M., Okuda, J. and Gotoh, N., 2012. RND type efflux pump system MexAB-OprM of *Pseudomonas aeruginosa* selects bacterial languages, 3-oxo-acyl-homoserine lactones, for cell-to-cell communication. *BMC microbiology*, 12(1), pp.1-10.

Mine, T., Morita, Y., Kataoka, A., Mizushima, T. and Tsuchiya, T., 1999. Expression in *Escherichia coli* of a new multidrug efflux pump, MexXY, from *Pseudomonas aeruginosa. Antimicrobial agents and chemotherapy*, 43(2), pp.415-417.

Moradali, M.F., Ghods, S. and Rehm, B.H., 2017. *Pseudomonas aeruginosa* lifestyle: a paradigm for adaptation, survival, and persistence. *Frontiers in cellular and infection microbiology*, 7, p.39.

Morihara, K., 1964. Production of elastase and proteinase by *Pseudomonas aeruginosa. Journal of Bacteriology*, 88(3), pp.745-757.

Morita, Y., Komori, Y., Mima, T., Kuroda, T., Mizushima, T. and Tsuchiya, T., 2001. Construction of a series of mutants lacking all of the four major *mex* operons for multidrug efflux pumps or possessing each one of the operons from *Pseudomonas aeruginosa* PAO1: MexCD-OprJ is an inducible pump. *FEMS microbiology letters*, 202(1), pp.139-143.

Morita, Y., Murata, T., Mima, T., Shiota, S., Kuroda, T., Mizushima, T., Gotoh, N., Nishino, T. and Tsuchiya, T., 2003. Induction of *mexCD-oprJ* operon for a multidrug efflux pump by disinfectants in wild-type *Pseudomonas aeruginosa* PAO1. *Journal of antimicrobial chemotherapy*, 51(4), pp.991-994.

Morita, Y., Sobel, M.L. and Poole, K., 2006. Antibiotic inducibility of the MexXY multidrug efflux system of *Pseudomonas aeruginosa*: involvement of the antibiotic-inducible PA5471 gene product. *Journal of bacteriology*, 188(5), pp.1847-1855.

Morita, Y., Gilmour, C., Metcalf, D. and Poole, K., 2009. Translational control of the antibiotic inducibility of the PA5471 gene required for *mexXY* multidrug efflux gene expression in *Pseudomonas aeruginosa. Journal of bacteriology*, 191(15), pp.4966-4975.

Morita, Y., Tomida, J. and Kawamura, Y., 2012. Primary mechanisms mediating aminoglycoside resistance in the multidrug-resistant *Pseudomonas aeruginosa* clinical isolate PA7. *Microbiology*, 158(4), pp.1071-1083.

Morris, E.R., Hall, G., Li, C., Heeb, S., Kulkarni, R.V., Lovelock, L., Silistre, H., Messina, M., Cámara, M., Emsley, J. and Williams, P., 2013. Structural rearrangement in an RsmA/CsrA ortholog of *Pseudomonas aeruginosa* creates a dimeric RNA-binding protein, RsmN. *Structure*, 21(9), pp.1659-1671.

Mukherjee, S., Jemielita, M., Stergioula, V., Tikhonov, M. and Bassler, B.L., 2019. Photosensing and quorum sensing are integrated to control *Pseudomonas aeruginosa* collective behaviors. *PLoS biology*, 17(12), p.e3000579.

Muller, C., Plésiat, P. and Jeannot, K., 2011. A two-component regulatory system interconnects resistance to polymyxins, aminoglycosides, fluoroquinolones, and β-lactams in *Pseudomonas aeruginosa. Antimicrobial agents and chemotherapy*, 55(3), pp.1211-1221.

Murakami, S., Nakashima, R., Yamashita, E., Matsumoto, T. and Yamaguchi, A., 2006. Crystal structures of a multidrug transporter reveal a functionally rotating mechanism. *Nature*, 443(7108), pp.173-179.

Nakashima, R., Sakurai, K., Yamasaki, S., Hayashi, K., Nagata, C., Hoshino, K., Onodera, Y., Nishino, K. and Yamaguchi, A., 2013. Structural basis for the inhibition of bacterial multidrug exporters. *Nature*, 500(7460), pp.102-106.

Nehme, D., Li, X.Z., Elliot, R. and Poole, K., 2004. Assembly of the MexAB-OprM multidrug efflux system of *Pseudomonas aeruginosa*: identification and characterization of mutations in *mexA* compromising MexA multimerization and interaction with MexB. *Journal of bacteriology*, 186(10), pp.2973-2983.

Ochsner, U.A., Koch, A.K., Fiechter, A. and Reiser, J., 1994. Isolation and characterization of a regulatory gene affecting rhamnolipid biosurfactant synthesis in *Pseudomonas aeruginosa. Journal of bacteriology*, 176(7), pp.2044-2054.

Olivares, J., Alvarez-Ortega, C., Linares, J.F., Rojo, F., Köhler, T. and Martínez, J.L., 2012. Overproduction of the multidrug efflux pump MexEF-OprN does not impair *Pseudomonas aeruginosa* fitness in competition tests, but produces specific changes in bacterial regulatory networks. *Environmental microbiology*, 14(8), pp.1968-1981.

Olivares, J., Álvarez-Ortega, C. and Martinez, J.L., 2014. Metabolic compensation of fitness costs associated with overexpression of the multidrug efflux pump MexEF-OprN in *Pseudomonas aeruginosa. Antimicrobial agents and chemotherapy*, 58(7), pp.3904-3913.

Olivares Pacheco, J., Alvarez-Ortega, C., Alcalde Rico, M. and Martínez, J.L., 2017. Metabolic compensation of fitness costs is a general outcome for antibiotic-resistant *Pseudomonas aeruginosa* mutants overexpressing efflux pumps. *MBio*, 8(4), pp.e00500-17.

Ortori, C.A., Dubern, J.F., Chhabra, S.R., Cámara, M., Hardie, K., Williams, P. and Barrett, D.A., 2011. Simultaneous quantitative profiling of N-acyl-L-homoserine lactone and 2-alkyl-4 (1 H)-quinolone families of quorum-sensing signaling molecules using LC-MS/MS. *Analytical and bioanalytical chemistry*, 399(2), pp.839-850.

O'Toole, G.A., Gibbs, K.A., Hager, P.W., Phibbs Jr, P.V. and Kolter, R., 2000. The global carbon metabolism regulator Crc is a component of a signal transduction pathway required for biofilm development by *Pseudomonas aeruginosa. Journal of bacteriology*, 182(2), pp.425-431.

Padilla, E., Llobet, E., Doménech-Sánchez, A., Martínez-Martínez, L., Bengoechea, J.A. and Albertí, S., 2010. *Klebsiella pneumoniae* AcrAB efflux pump contributes to antimicrobial resistance and virulence. *Antimicrobial agents and chemotherapy*, 54(1), pp.177-183.

Palma, M., Zurita, J., Ferreras, J.A., Worgall, S., Larone, D.H., Shi, L., Campagne, F. and Quadri, L.E., 2005. *Pseudomonas aeruginosa* SoxR does not conform to the archetypal paradigm for SoxR-

dependent regulation of the bacterial oxidative stress adaptive response. *Infection and immunity*, 73(5), pp.2958-2966.

Palmer, G.C., Jorth, P.A. and Whiteley, M., 2013. The role of two *Pseudomonas aeruginosa* anthranilate synthases in tryptophan and quorum signal production. *Microbiology*, 159(Pt 5), p.959.

Pamp, S.J. and Tolker-Nielsen, T., 2007. Multiple roles of biosurfactants in structural biofilm development by *Pseudomonas aeruginosa*. *Journal of bacteriology*, 189(6), pp.2531-2539.

Paradis, E. and Schliep, K., 2019. ape 5.0: an environment for modern phylogenetics and evolutionary analyses in R. *Bioinformatics*, 35(3), pp.526-528.

Park, P.W., Pier, G.B., Preston, M.J., Goldberger, O., Fitzgerald, M.L. and Bernfield, M., 2000. Syndecan-1 shedding is enhanced by LasA, a secreted virulence factor of *Pseudomonas aeruginosa*. *Journal of Biological Chemistry*, 275(5), pp.3057-3064.

Parmely, M., Gale, A., Clabaugh, M., Horvat, R.. and Zhou, W.W., 1990. Proteolytic inactivation of cytokines by *Pseudomonas aeruginosa. Infection and immunity*, 58(9), pp.3009-3014.

Passador, L., Cook, J.M., Gambello, M.J., Rust, L. and Iglewski, B.H., 1993. Expression of *Pseudomonas aeruginosa* virulence genes requires cell-to-cell communication. *Science*, 260(5111), pp.1127-1130.

Pearson, J.P., Pesci, E.C. and Iglewski, B.H., 1997. Roles of *Pseudomonas aeruginosa las* and *rhl* quorum-sensing systems in control of elastase and rhamnolipid biosynthesis genes. *Journal of bacteriology*, 179(18), pp.5756-5767.

Pearson, J.P., Van Delden, C. and Iglewski, B.H., 1999. Active efflux and diffusion are involved in transport of *Pseudomonas aeruginosa* cell-to-cell signals. *Journal of bacteriology*, 181(4), pp.1203-1210.

Pena, R.T., Blasco, L., Ambroa, A., González-Pedrajo, B., Fernández-García, L., López, M., Bleriot, I., Bou, G., García-Contreras, R., Wood, T.K. and Tomás, M., 2019. Relationship between quorum sensing and secretion systems. *Frontiers in microbiology*, 10, p.1100.

Peng, J., Chen, G., Xu, X., Wang, T. and Liang, H., 2020. Iron facilitates the RetS-Gac-Rsm cascade to inversely regulate protease IV (*piv*) expression via the sigma factor PvdS in *Pseudomonas aeruginosa. Environmental Microbiology*, 22(12), pp.5402-5413.

Pérez, A., Poza, M., Fernández, A., del Carmen Fernández, M., Mallo, S., Merino, M., Rumbo-Feal, S., Cabral, M.P. and Bou, G., 2012. Involvement of the AcrAB-TolC efflux pump in the resistance,

fitness, and virulence of *Enterobacter cloacae. Antimicrobial agents and chemotherapy*, 56(4), pp.2084-2090.

Perron, K., Caille, O., Rossier, C., Van Delden, C., Dumas, J.L. and Köhler, T., 2004. CzcR-CzcS, a two-component system involved in heavy metal and carbapenem resistance in *Pseudomonas aeruginosa. Journal of Biological Chemistry*, 279(10), pp.8761-8768.

Pesci, E.C., Milbank, J.B., Pearson, J.P., McKnight, S., Kende, A.S., Greenberg, E.P. and Iglewski, B.H., 1999. Quinolone signaling in the cell-to-cell communication system of *Pseudomonas aeruginosa. Proceedings of the National Academy of Sciences*, 96(20), pp.11229-11234.

Pessi, G., Williams, F., Hindle, Z., Heurlier, K., Holden, M.T., Cámara, M., Haas, D. and Williams, P., 2001. The global posttranscriptional regulator RsmA modulates production of virulence determinants and N-acylhomoserine lactones in *Pseudomonas aeruginosa. Journal of bacteriology*, 183(22), pp.6676-6683.

Petrova, O.E. and Sauer, K., 2009. A novel signaling network essential for regulating *Pseudomonas aeruginosa* biofilm development. *PLoS pathogens*, 5(11), p.e1000668.

Phan, G., Benabdelhak, H., Lascombe, M.B., Benas, P., Rety, S., Picard, M., Ducruix, A., Etchebest, C. and Broutin, I., 2010. Structural and dynamical insights into the opening mechanism of *P. aeruginosa* OprM channel. *Structure*, 18(4), pp.507-517.

Piddock, L.J., 2006. Multidrug-resistance efflux pumps? not just for resistance. *Nature Reviews Microbiology*, 4(8), pp.629-636.

Pletzer, D., Mansour, S.C., Wuerth, K., Rahanjam, N. and Hancock, R.E., 2017. New mouse model for chronic infections by Gram-negative bacteria enabling the study of anti-infective efficacy and host-microbe interactions. *MBio*, 8(1), pp.e00140-17.

Pontel, L.B., Audero, M.E.P., Espariz, M., Checa, S.K. and Soncini, F.C., 2007. GolS controls the response to gold by the hierarchical induction of *Salmonella*-specific genes that include a CBA efflux-coding operon. *Molecular microbiology*, 66(3), pp.814-825.

Poole, K., Krebes, K., McNally, C. and Neshat, S.H.A.D.I., 1993. Multiple antibiotic resistance in *Pseudomonas aeruginosa*: evidence for involvement of an efflux operon. *Journal of bacteriology*, 175(22), pp.7363-7372.

Poole, K., Tetro, K., Zhao, Q., Neshat, S., Heinrichs, D.E. and Bianco, N., 1996a. Expression of the multidrug resistance operon *mexA-mexB-oprM* in *Pseudomonas aeruginosa: mexR* encodes a regulator of operon expression. *Antimicrobial agents and chemotherapy*, 40(9), pp.2021-2028.

Poole, K., Gotoh, N., Tsujimoto, H., Zhao, Q., Wada, A., Yamasaki, T., Neshat, S., Yamagishi, J.I., Li, X.Z. and Nishino, T., 1996b. Overexpression of the *mexC–mexD–oprJ* efflux operon in *nfxB*-type multidrug-resistant strains of *Pseudomonas aeruginosa. Molecular microbiology*, 21(4), pp.713-725.

Poole, K., 2007. Efflux pumps as antimicrobial resistance mechanisms. *Annals of medicine*, 39(3), pp.162-176.

Poudyal, B. and Sauer, K., 2018. The ABC of biofilm drug tolerance: the MerR-like regulator BrlR is an activator of ABC transport systems, with PA1874-77 contributing to the tolerance of *Pseudomonas aeruginosa* biofilms to tobramycin. *Antimicrobial Agents and Chemotherapy*, 62(2), pp.e01981-17.

Popat, R., Crusz, S.A., Messina, M., Williams, P., West, S.A. and Diggle, S.P., 2012. Quorum-sensing and cheating in bacterial biofilms. *Proceedings of the Royal Society B: Biological Sciences*, 279(1748), pp.4765-4771.

Prjibelski, A., Antipov, D., Meleshko, D., Lapidus, A. and Korobeynikov, A., 2020. Using SPAdes *de novo* assembler. *Current protocols in bioinformatics*, 70(1), p.e102.

Public Health England., 2015. Identification of *Pseudomonas* species and other Non-Glucose Fermenters. UK Standards for Microbiology Investigations.

Purssell, A., Fruci, M., Mikalauskas, A., Gilmour, C. and Poole, K., 2015. EsrC, an envelope stress-regulated repressor of the *mexCD-oprJ* multidrug efflux operon in *Pseudomonas aeruginosa. Environmental microbiology*, 17(1), pp.186-198.

Quale, J., Bratu, S., Gupta, J. and Landman, D., 2006. Interplay of efflux system, *ampC*, and *oprD* expression in carbapenem resistance of *Pseudomonas aeruginosa* clinical isolates. *Antimicrobial agents and chemotherapy*, 50(5), pp.1633-1641.

R Core Team. "R: A language and environment for statistical computing." (2021): 201. URL https://www.R-project.org/

Rahbar, M., Hamidi-Farahani, R., Asgari, A., Esmailkhani, A. and Soleiman-Meigooni, S., 2021. Expression of RND efflux pumps mediated antibiotic resistance in *Pseudomonas aeruginosa* clinical strains. *Microbial Pathogenesis*, 153, p.104789.

Rahim, R., Ochsner, U.A., Olvera, C., Graninger, M., Messner, P., Lam, J.S. and Soberón-Chávez, G., 2001. Cloning and functional characterization of the *Pseudomonas aeruginosa rhlC* gene that encodes rhamnosyltransferase 2, an enzyme responsible for di-rhamnolipid biosynthesis. *Molecular microbiology*, 40(3), pp.708-718.

Rahmati, S., Yang, S., Davidson, A.L. and Zechiedrich, E.L., 2002. Control of the AcrAB multidrug efflux pump by quorum-sensing regulator SdiA. *Molecular microbiology*, 43(3), pp.677-685.

Rampioni, G., Bertani, I., Zennaro, E., Polticelli, F., Venturi, V. and Leoni, L., 2006. The quorum-sensing negative regulator RsaL of *Pseudomonas aeruginosa* binds to the *lasI* promoter. *Journal of bacteriology*, 188(2), pp.815-819.

Rampioni, G., Schuster, M., Greenberg, E.P., Zennaro, E. and Leoni, L., 2009. Contribution of the RsaL global regulator to *Pseudomonas aeruginosa* virulence and biofilm formation. *FEMS microbiology letters*, 301(2), pp.210-217.

Rampioni, G., Pustelny, C., Fletcher, M.P., Wright, V.J., Bruce, M., Rumbaugh, K.P., Heeb, S., Cámara, M. and Williams, P., 2010. Transcriptomic analysis reveals a global alkyl-quinolone-independent regulatory role for PqsE in facilitating the environmental adaptation of *Pseudomonas aeruginosa* to plant and animal hosts. *Environmental microbiology*, 12(6), pp.1659-1673.

Rampioni, G., Pillai, C.R., Longo, F., Bondì, R., Baldelli, V., Messina, M., Imperi, F., Visca, P. and Leoni, L., 2017. Effect of efflux pump inhibition on *Pseudomonas aeruginosa* transcriptome and virulence. *Scientific reports*, 7(1), pp.1-14.

Ramsey, M.M. and Whiteley, M., 2004. *Pseudomonas aeruginosa* attachment and biofilm development in dynamic environments. *Molecular microbiology*, 53(4), pp.1075-1087.

Ranjitkar, S., Jones, A.K., Mostafavi, M., Zwirko, Z., Iartchouk, O., Barnes, S.W., Walker, J.R., Willis, T.W., Lee, P.S. and Dean, C.R., 2019. Target (MexB)-and efflux-based mechanisms decreasing the effectiveness of the efflux pump inhibitor D13-9001 in *Pseudomonas aeruginosa* PAO1: uncovering a new role for MexMN-OprM in efflux of β-lactams and a novel regulatory circuit (MmnRS) controlling MexMN expression. *Antimicrobial agents and chemotherapy*, 63(2), pp.e01718-18.

Rashid, M.H. and Kornberg, A., 2000. Inorganic polyphosphate is needed for swimming, swarming, and twitching motilities of *Pseudomonas aeruginosa. Proceedings of the National Academy of Sciences,* 97(9), pp.4885-4890.

Recinos, D.A., Sekedat, M.D., Hernandez, A., Cohen, T.S., Sakhtah, H., Prince, A.S., Price-Whelan, A. and Dietrich, L.E., 2012. Redundant phenazine operons in *Pseudomonas aeruginosa* exhibit environment-dependent expression and differential roles in pathogenicity. *Proceedings of the National Academy of Sciences*, 109(47), pp.19420-19425.

Reimmann, C., Beyeler, M., Latifi, A., Winteler, H., Foglino, M., Lazdunski, A. and Haas, D., 1997. The global activator GacA of *Pseudomonas aeruginosa* PAO positively controls the production of the

autoinducer N-butyryl-homoserine lactone and the formation of the virulence factors pyocyanin, cyanide, and lipase. *Molecular microbiology*, 24(2), pp.309-319.

Reimmann, C., Serino, L., Beyeler, M. and Haas, D., 1998. Dihydroaeruginoic acid synthetase and pyochelin synthetase, products of the *pchEF*, are induced by extracellular pyochelin in *Pseudornonas aeruginosa. Microbiology*, 144(11), pp.3135-3148.

Reimmann, C., Patel, H.M., Serino, L., Barone, M., Walsh, C.T. and Haas, D., 2001. Essential PchG-dependent reduction in pyochelin biosynthesis of *Pseudomonas aeruginosa. Journal of bacteriology*, 183(3), pp.813-820.

Renau, T.E., 1999. Inhibitors of efflux pumps in *Pseudomonas aeruginosa* potentiate the activity of the fluoroquinolone antibacterial levofloxacin. *J Med Chem*, 42, pp.4928-4931.

Robicsek, A., Strahilevitz, J., Jacoby, G.A., Macielag, M., Abbanat, D., Hye Park, C., Bush, K. and Hooper, D.C., 2006. Fluoroquinolone-modifying enzyme: a new adaptation of a common aminoglycoside acetyltransferase. *Nature medicine*, 12(1), pp.83-88.

Rodesney, C.A., Roman, B., Dhamani, N., Cooley, B.J., Katira, P., Touhami, A. and Gordon, V.D., 2017. Mechanosensing of shear by *Pseudomonas aeruginosa* leads to increased levels of the cyclic-di-GMP signal initiating biofilm development. *Proceedings of the National Academy of Sciences*, 114(23), pp.5906-5911.

Rodrigue, A., Quentin, Y., Lazdunski, A., Méjean, V. and Foglino, M., 2000. Cell signalling by oligosaccharides. Two-component systems in *Pseudomonas aeruginosa*: why so many?. *Trends in microbiology*, 8(11), pp.498-504.

Roeters, S.J., Golbek, T.W., Bregnhøj, M., Drace, T., Alamdari, S., Roseboom, W., Kramer, G., Šantl-Temkiv, T., Finster, K., Pfaendtner, J. and Woutersen, S., 2021. Ice-nucleating proteins are activated by low temperatures to control the structure of interfacial water. *Nature communications*, 12(1), pp.1-9.

Rumbo-Feal, S., Gomez, M.J., Gayoso, C., Álvarez-Fraga, L., Cabral, M.P., Aransay, A.M., Rodríguez-Ezpeleta, N., Fullaondo, A., Valle, J., Tomás, M. and Bou, G., 2013. Whole transcriptome analysis of *Acinetobacter baumannii* assessed by RNA-sequencing reveals different mRNA expression profiles in biofilm compared to planktonic cells. *PloS one*, 8(8), p.e72968.

Rybtke, M., Berthelsen, J., Yang, L., Høiby, N., Givskov, M. and Tolker-Nielsen, T., 2015. The LapG protein plays a role in *Pseudomonas aeruginosa* biofilm formation by controlling the presence of the CdrA adhesin on the cell surface. *Microbiologyopen*, 4(6), pp.917-930.

Saha, S., Takeshita, F., Matsuda, T., Jounai, N., Kobiyama, K., Matsumoto, T., Sasaki, S., Yoshida, A., Xin, K.Q., Klinman, D.M. and Uematsu, S., 2007. Blocking of the TLR5 activation domain hampers protective potential of flagellin DNA vaccine. *The Journal of Immunology*, 179(2), pp.1147-1154.

Saier Jr, M.H., Paulsen, I.T., Marek, K.S., Pao, S.S., Ronald, A.S. and Nikaido, H., 1998. Evolutionary origins of multidrug and drug-specific efflux pumps in bacteria. *The FASEB Journal*, 12(3), pp.265-274.

Sakhtah, H., Koyama, L., Zhang, Y., Morales, D.K., Fields, B.L., Price-Whelan, A., Hogan, D.A., Shepard, K. and Dietrich, L.E., 2016. The *Pseudomonas aeruginosa* efflux pump MexGHI-OpmD transports a natural phenazine that controls gene expression and biofilm development. *Proceedings of the National Academy of Sciences*, 113(25), pp.E3538-E3547.

Salacha, R., Kovačić, F., Brochier-Armanet, C., Wilhelm, S., Tommassen, J., Filloux, A., Voulhoux, R. and Bleves, S., 2010. The *Pseudomonas aeruginosa* patatin-like protein PlpD is the archetype of a novel Type V secretion system. *Environmental microbiology*, 12(6), pp.1498-1512.

Salamov, V.S.A. and Solovyevand, A., 2011. Automatic annotation of microbial genomes and metagenomic sequences. *Metagenomics and Its Applications in Agriculture, Biomedicine and Environmental Studies*; Li, RW, Ed, pp.61-78.

Sánchez, P., Linares, J.F., Ruiz-Díez, B., Campanario, E., Navas, A., Baquero, F. and Martínez, J.L., 2002. Fitness of in vitro selected *Pseudomonas aeruginosa nalB* and *nfxB* multidrug resistant mutants. *Journal of Antimicrobial Chemotherapy*, 50(5), pp.657-664.

Sawada, I., Maseda, H., Nakae, T., Uchiyama, H. and Nomura, N., 2004. A quorum-sensing autoinducer enhances the *mexAB-oprM* efflux-pump expression without the MexR-mediated regulation in *Pseudomonas aeruginosa. Microbiology and immunology*, 48(5), pp.435-439.

Schembri, M.A., Kjærgaard, K. and Klemm, P., 2003. Global gene expression in *Escherichia coli* biofilms. *Molecular microbiology*, 48(1), pp.253-267.

Schertzer, J.W., Brown, S.A. and Whiteley, M., 2010. Oxygen levels rapidly modulate *Pseudomonas aeruginosa* social behaviours via substrate limitation of PqsH. *Molecular microbiology*, 77(6), pp.1527-1538.

Schuster, M., Lostroh, C.P., Ogi, T. and Greenberg, E.P., 2003. Identification, timing, and signal specificity of *Pseudomonas aeruginosa* quorum-controlled genes: a transcriptome analysis. *Journal of bacteriology*, 185(7), pp.2066-2079.

Seed, P.C., Passador, L. and Iglewski, B.H., 1995. Activation of the *Pseudomonas aeruginosa lasI* gene by LasR and the *Pseudomonas autoinducer* PAI: an autoinduction regulatory hierarchy. *Journal of bacteriology*, 177(3), pp.654-659.

Seemann, T., 2014. Prokka: rapid prokaryotic genome annotation. *Bioinformatics*, 30(14), pp.2068-2069.

Seet, Q. and Zhang, L.H., 2011. Anti-activator QslA defines the quorum sensing threshold and response in *Pseudomonas aeruginosa. Molecular microbiology*, 80(4), pp.951-965.

Sekiya, H., Mima, T., Morita, Y., Kuroda, T., Mizushima, T. and Tsuchiya, T., 2003. Functional cloning and characterization of a multidrug efflux pump, *mexHI-opmD*, from a *Pseudomonas aeruginosa* mutant. *Antimicrobial agents and chemotherapy*, 47(9), pp.2990-2992.

Sennhauser, G., Bukowska, M.A., Briand, C. and Grütter, M.G., 2009. Crystal structure of the multidrug exporter MexB from *Pseudomonas aeruginosa. Journal of molecular biology*, 389(1), pp.134-145.

Serino, L., Reimmann, C., Visca, P., Beyeler, M., Chiesa, V.D. and Haas, D., 1997. Biosynthesis of pyochelin and dihydroaeruginoic acid requires the iron-regulated *pchDCBA* operon in *Pseudomonas aeruginosa. Journal of bacteriology*, 179(1), pp.248-257.

Shiba, T., Ishiguro, K., Takemoto, N., Koibuchi, H. and Sugimoto, K., 1995. Purification and characterization of the *Pseudomonas aeruginosa* NfxB protein, the negative regulator of the *nfxB* gene. *Journal of bacteriology*, 177(20), pp.5872-5877.

Shigemura, K., Osawa, K., Kato, A., Tokimatsu, I., Arakawa, S., Shirakawa, T. and Fujisawa, M., 2015. Association of overexpression of efflux pump genes with antibiotic resistance in *Pseudomonas aeruginosa* strains clinically isolated from urinary tract infection patients. *The Journal of antibiotics*, 68(9), pp.568-572.

Siehnel, R., Traxler, B., An, D.D., Parsek, M.R., Schaefer, A.L. and Singh, P.K., 2010. A unique regulator controls the activation threshold of quorum-regulated genes in *Pseudomonas aeruginosa. Proceedings of the National Academy of Sciences*, 107(17), pp.7916-7921.

Silvestrini, M.C., Galeotti, C.L., Gervais, M., Schininà, E., Barra, D., Bossa, F. and Brunori, M., 1989. Nitrite reductase from *Pseudomonas aeruginosa*: sequence of the gene and the protein. *FEBS letters*, 254(1-2), pp.33-38.

Simanek, K.A., Taylor, I.R., Richael, E.K., Lasek-Nesselquist, E., Bassler, B.L. and Paczkowski, J.E., 2022. The PqsE-RhlR Interaction Regulates RhlR DNA Binding to Control Virulence Factor Production in *Pseudomonas aeruginosa. Microbiology spectrum*, 10(1), pp.e02108-21.

Sivaneson, M., Mikkelsen, H., Ventre, I., Bordi, C. and Filloux, A., 2011. Two-component regulatory systems in *Pseudomonas aeruginosa*: an intricate network mediating fimbrial and efflux pump gene expression. *Molecular microbiology*, 79(5), pp.1353-1366.

Skerker, J.M. and Berg, H.C., 2001. Direct observation of extension and retraction of type IV pili. *Proceedings of the National Academy of Sciences*, 98(12), pp.6901-6904.

Sobel, M.L., Hocquet, D., Cao, L., Plesiat, P. and Poole, K., 2005a. Mutations in PA3574 (*nalD*) lead to increased MexAB-OprM expression and multidrug resistance in laboratory and clinical isolates of *Pseudomonas aeruginosa. Antimicrobial agents and chemotherapy*, 49(5), pp.1782-1786.

Sobel, M.L., Neshat, S. and Poole, K., 2005b. Mutations in PA2491 (*mexS*) promote MexT-dependent *mexEF-oprN* expression and multidrug resistance in a clinical strain of *Pseudomonas aeruginosa. Journal of bacteriology*, 187(4), pp.1246-1253.

Stover, C.K., Pham, X.Q., Erwin, A.L., Mizoguchi, S.D., Warrener, P., Hickey, M.J., Brinkman, F.S.L., Hufnagle, W.O., Kowalik, D.J., Lagrou, M. and Garber, R.L., 2000. Complete genome sequence of *Pseudomonas aeruginosa* PAO1, an opportunistic pathogen. *Nature*, *406*(6799), pp.959-964.

Taylor, I.R., Paczkowski, J.E., Jeffrey, P.D., Henke, B.R., Smith, C.D. and Bassler, B.L., 2021. Inhibitor mimetic mutations in the *Pseudomonas aeruginosa* PqsE enzyme reveal a protein–protein interaction with the quorum-sensing receptor RhlR that is vital for virulence factor production. *ACS chemical biology*, 16(4), pp.740-752.

Teelucksingh, T., Thompson, L.K., Zhu, S., Kuehfuss, N.M., Goetz, J.A., Gilbert, S.E., MacNair, C.R., Geddes-McAlister, J., Brown, E.D. and Cox, G., 2022. A genetic platform to investigate the functions of bacterial drug efflux pumps. *Nature Chemical Biology*, 18(12), pp.1399-1409.

Teitzel, G.M., Geddie, A., De Long, S.K., Kirisits, M.J., Whiteley, M. and Parsek, M.R., 2006. Survival and growth in the presence of elevated copper: transcriptional profiling of copper-stressed *Pseudomonas aeruginosa. Journal of bacteriology*, 188(20), pp.7242-7256.

Thaden, J.T., Lory, S. and Gardner, T.S., 2010. Quorum-sensing regulation of a copper toxicity system in *Pseudomonas aeruginosa. Journal of bacteriology*, 192(10), pp.2557-2568.

Thomas, C.M. and Nielsen, K.M., 2005. Mechanisms of, and barriers to, horizontal gene transfer between bacteria. *Nature reviews microbiology*, 3(9), pp.711-721.

Tian, Z.X., Fargier, E., Mac Aogain, M., Adams, C., Wang, Y.P. and O'Gara, F., 2009a. Transcriptome profiling defines a novel regulon modulated by the LysR-type transcriptional regulator MexT in *Pseudomonas aeruginosa. Nucleic acids research*, 37(22), pp.7546-7559.

Tian, Z.X., Mac Aogain, M., O'Connor, H.F., Fargier, E., Mooij, M.J., Adams, C., Wang, Y.P. and O'Gara, F., 2009b. MexT modulates virulence determinants in *Pseudomonas aeruginosa* independent of the MexEF-OprN efflux pump. *Microbial pathogenesis*, 47(4), pp.237-241.

Tian, Z.X., Yi, X.X., Cho, A., O'Gara, F. and Wang, Y.P., 2016. CpxR activates MexAB-OprM efflux pump expression and enhances antibiotic resistance in both laboratory and clinical *nalB*-type isolates of *Pseudomonas aeruginosa. PLoS pathogens*, 12(10), p.e1005932.

Tielker, D., Hacker, S., Loris, R., Strathmann, M., Wingender, J., Wilhelm, S., Rosenau, F. and Jaeger, K.E., 2005. *Pseudomonas aeruginosa* lectin LecB is located in the outer membrane and is involved in biofilm formation. *Microbiology*, 151(5), pp.1313-1323.

Toder, D.S., Gambello, M.J. and Iglewski, B.H., 1991. *Pseudomonas aeruginosa* LasA: a second elastase under the transcriptional control of *lasR. Molecular microbiology*, 5(8), pp.2003-2010.

Traidej, M., Caballero, A.R., Marquart, M.E., Thibodeaux, B.A. and O'Callaghan, R.J., 2003. Molecular analysis of *Pseudomonas aeruginosa* protease IV expressed in *Pseudomonas putida*. *Investigative ophthalmology & visual science*, 44(1), pp.190-196.

Tseng, B.S., Zhang, W., Harrison, J.J., Quach, T.P., Song, J.L., Penterman, J., Singh, P.K., Chopp, D.L., Packman, A.I. and Parsek, M.R., 2013. The extracellular matrix protects *Pseudomonas aeruginosa* biofilms by limiting the penetration of tobramycin. *Environmental microbiology*, 15(10), pp.2865-2878.

Tsutsumi, K., Yonehara, R., Ishizaka-Ikeda, E., Miyazaki, N., Maeda, S., Iwasaki, K., Nakagawa, A. and Yamashita, E., 2019. Structures of the wild-type MexAB–OprM tripartite pump reveal its complex formation and drug efflux mechanism. *Nature communications*, 10(1), pp.1-10.

Tzeng, Y.L., Ambrose, K.D., Zughaier, S., Zhou, X., Miller, Y.K., Shafer, W.M. and Stephens, D.S., 2005. Cationic antimicrobial peptide resistance in *Neisseria meningitidis. Journal of bacteriology*, 187(15), pp.5387-5396.

Vaillancourt, M., Limsuwannarot, S.P., Bresee, C., Poopalarajah, R. and Jorth, P., 2021. *Pseudomonas aeruginosa mexR* and *mexEF* Antibiotic Efflux Pump Variants Exhibit Increased Virulence. *Antibiotics*, 10(10), p.1164.

Vallet, I., Olson, J.W., Lory, S., Lazdunski, A. and Filloux, A., 2001. The chaperone/usher pathways of *Pseudomonas aeruginosa*: identification of fimbrial gene clusters (*cup*) and their involvement in biofilm formation. *Proceedings of the National Academy of Sciences*, 98(12), pp.6911-6916.

Van Delden, C., Comte, R. and Bally, A.M., 2001. Stringent response activates quorum sensing and modulates cell density-dependent gene expression in *Pseudomonas aeruginosa. Journal of bacteriology*, 183(18), pp.5376-5384.

Van Gennip, M., Christensen, L.D., Alhede, M., Phipps, R., Jensen, P.Ø., Christophersen, L., Pamp, S.J., Moser, C., Mikkelsen, P.J., Koh, A.Y. and TOLKER-NIELSEN, T.I.M., 2009. Inactivation of the *rhlA* gene in *Pseudomonas aeruginosa* prevents rhamnolipid production, disabling the protection against polymorphonuclear leukocytes. *Apmis*, 117(7), pp.537-546.

Van Opijnen, T., Bodi, K.L. and Camilli, A., 2009. Tn-seq: high-throughput parallel sequencing for fitness and genetic interaction studies in microorganisms. *Nature methods*, 6(10), pp.767-772.

Van Schaik, E.J., Giltner, C.L., Audette, G.F., Keizer, D.W., Bautista, D.L., Slupsky, C.M., Sykes, B.D. and Irvin, R.T., 2005. DNA binding: a novel function of *Pseudomonas aeruginosa* type IV pili. *Journal of bacteriology*, 187(4), pp.1455-1464.

Vater, S.M., Weiße, S., Maleschlijski, S., Lotz, C., Koschitzki, F., Schwartz, T., Obst, U. and Rosenhahn, A., 2014. Swimming behavior of *Pseudomonas aeruginosa* studied by holographic 3D tracking. *PloS one*, 9(1), p.e87765.

Vercammen, K., Wei, Q., Charlier, D., Dötsch, A., Haüssler, S., Schulz, S., Salvi, F., Gadda, G., Spain, J., Rybtke, M.L. and Tolker-Nielsen, T., 2015. *Pseudomonas aeruginosa* LysR PA4203 regulator NmoR acts as a repressor of the PA4202 *nmoA* gene, encoding a nitronate monooxygenase. *Journal of bacteriology*, 197(6), pp.1026-1039.

Vogne, C., Aires, J.R., Bailly, C., Hocquet, D. and Plésiat, P., 2004. Role of the multidrug efflux system MexXY in the emergence of moderate resistance to aminoglycosides among *Pseudomonas aeruginosa* isolates from patients with cystic fibrosis. *Antimicrobial agents and chemotherapy*, 48(5), pp.1676-1680.

Wade, D.S., Calfee, M.W., Rocha, E.R., Ling, E.A., Engstrom, E., Coleman, J.P. and Pesci, E.C., 2005. Regulation of *Pseudomonas* quinolone signal synthesis in *Pseudomonas aeruginosa. Journal of bacteriology*, 187(13), pp.4372-4380.

Wagner, V.E., Bushnell, D., Passador, L., Brooks, A.I. and Iglewski, B.H., 2003. Microarray analysis of *Pseudomonas aeruginosa* quorum-sensing regulons: effects of growth phase and environment. *Journal of bacteriology*, 185(7), pp.2080-2095.

Waite, R.D., Papakonstantinopoulou, A., Littler, E. and Curtis, M.A., 2005. Transcriptome analysis of *Pseudomonas aeruginosa* growth: comparison of gene expression in planktonic cultures and developing and mature biofilms. *Journal of bacteriology*, 187(18), pp.6571-6576.

Wang, D., Seeve, C., Pierson, L.S. and Pierson, E.A., 2013. Transcriptome profiling reveals links between ParS/ParR, MexEF-OprN, and quorum sensing in the regulation of adaptation and virulence in *Pseudomonas aeruginosa. BMC genomics*, 14(1), pp.1-14.

Wang, Y.T., Lee, M.F. and Peng, C.F., 2014. Mutations in the quinolone resistance-determining regions associated with ciprofloxacin resistance in *Pseudomonas aeruginosa* isolates from Southern Taiwan. *Biomarkers and Genomic Medicine*, 6(2), pp.79-83.

Wang-Kan, X., Blair, J.M., Chirullo, B., Betts, J., La Ragione, R.M., Ivens, A., Ricci, V., Opperman, T.J. and Piddock, L.J., 2017. Lack of AcrB efflux function confers loss of virulence on *Salmonella enterica* serovar Typhimurium. *MBio*, *8*(4), pp.e00968-17.

Wang-Kan, X., Rodríguez-Blanco, G., Southam, A.D., Winder, C.L., Dunn, W.B., Ivens, A. and Piddock, L.J., 2021. Metabolomics reveal potential natural substrates of AcrB in *Escherichia coli* and *Salmonella enterica* Serovar Typhimurium. *MBio*, 12(2), pp.e00109-21

Watkins, W.J., Landaverry, Y., Léger, R., Litman, R., Renau, T.E., Williams, N., Yen, R., Zhang, J.Z., Chamberland, S., Madsen, D. and Griffith, D., 2003. The relationship between physicochemical properties, *in vitro* activity and pharmacokinetic profiles of analogues of diamine-containing efflux pump inhibitors. *Bioorganic & Medicinal Chemistry Letters*, 13(23), pp.4241-4244.

Weeks, J.W., Nickels, L.M., Ntreh, A.T. and Zgurskaya, H.I., 2015. Non-equivalent roles of two periplasmic subunits in the function and assembly of triclosan pump TriABC from *Pseudomonas aeruginosa. Molecular microbiology*, 98(2), pp.343-356.

Westfall, L.W., Carty, N.L., Layland, N., Kuan, P., Colmer-Hamood, J.A. and Hamood, A.N., 2006. *mvaT* mutation modifies the expression of the *Pseudomonas aeruginosa* multidrug efflux operon *mexEF-oprN. FEMS microbiology letters*, 255(2), pp.247-254.

Whitchurch, C.B., Alm, R.A. and Mattick, J.S., 1996. The alginate regulator AlgR and an associated sensor FimS are required for twitching motility in *Pseudomonas aeruginosa. Proceedings of the National Academy of Sciences*, 93(18), pp.9839-9843.

Whitchurch, C.B., Tolker-Nielsen, T., Ragas, P.C. and Mattick, J.S., 2002. Extracellular DNA required for bacterial biofilm formation. *Science*, 295(5559), pp.1487-1487.

Whitchurch, C.B., Leech, A.J., Young, M.D., Kennedy, D., Sargent, J.L., Bertrand, J.J., Semmler, A.B., Mellick, A.S., Martin, P.R., Alm, R.A. and Hobbs, M., 2004. Characterization of a complex chemosensory signal transduction system which controls twitching motility in *Pseudomonas aeruginosa. Molecular microbiology*, 52(3), pp.873-893.

Whittle, E.E., Legood, S.W., Alav, I., Dulyayangkul, P., Overton, T.W. and Blair, J.M., 2019. Flow cytometric analysis of efflux by dye accumulation. *Frontiers in microbiology*, 10, p.2319.

WHO. (2017) Global Priority List of Antibiotic-Resistant Bacteria to Guide Research, Discovery, and Development of New Antibiotics. World Health Organization: Essential medicines and health products, p. 7). Geneva, Switzerland: World Health Organization.

Wick, R.R., Schultz, M.B., Zobel, J. and Holt, K.E., 2015. Bandage: interactive visualization of de novo genome assemblies. *Bioinformatics*, 31(20), pp.3350-3352.

Wickham, H., 2016. ggplot2: elegant graphics for data analysis. springer.

Wickham, H., François, R., Henry, L., and Müller, K., (2022). dplyr: A Grammar of Data Manipulation.

Wickham, H., and Seidel, D., (2022). scales: Scale Functions for Visualization. R package version 1.2.0. https://CRAN.R-project.org/package=scales

Wilderman, P.J., Vasil, A.I., Johnson, Z., Wilson, M.J., Cunliffe, H.E., Lamont, I.L. and Vasil, M.L., 2001. Characterization of an endoprotease (PrpL) encoded by a PvdS-regulated gene in *Pseudomonas aeruginosa. Infection and immunity*, 69(9), pp.5385-5394.

Wilhelm, S., Tommassen, J. and Jaeger, K.E., 1999. A novel lipolytic enzyme located in the outer membrane of *Pseudomonas aeruginosa. Journal of bacteriology*, 181(22), pp.6977-6986.

Wilhelm, S., Gdynia, A., Tielen, P., Rosenau, F. and Jaeger, K.E., 2007. The autotransporter esterase EstA of *Pseudomonas aeruginosa* is required for rhamnolipid production, cell motility, and biofilm formation. *Journal of bacteriology*, 189(18), pp.6695-6703.

Williams, P. and Cámara, M., 2009. Quorum sensing and environmental adaptation in *Pseudomonas aeruginosa*: a tale of regulatory networks and multifunctional signal molecules. *Current opinion in microbiology*, 12(2), pp.182-191.

Wilton, M., Charron-Mazenod, L., Moore, R. and Lewenza, S., 2016. Extracellular DNA acidifies biofilms and induces aminoglycoside resistance in *Pseudomonas aeruginosa. Antimicrobial agents and chemotherapy*, 60(1), pp.544-553.

Wilton, R., Ahrendt, A.J., Shinde, S., Sholto-Douglas, D.J., Johnson, J.L., Brennan, M.B. and Kemner, K.M., 2018. A new suite of plasmid vectors for fluorescence-based imaging of root colonizing *Pseudomonads. Frontiers in plant science*, 8, p.2242.

Winson, M.K., Cámara, M., Latifi, A., Foglino, M., Chhabra, S.R., Daykin, M., Bally, M., Chapon, V., Salmond, G.P. and Bycroft, B.W., 1995. Multiple N-acyl-L-homoserine lactone signal molecules

regulate production of virulence determinants and secondary metabolites in *Pseudomonas aeruginosa. Proceedings of the National Academy of Sciences*, 92(20), pp.9427-9431.

Winter, D.J., 2017. rentrez: An R package for the NCBI eUtils API (No. e3179v2). *PeerJ Preprints*.

Winzer, K., Falconer, C., Garber, N.C., Diggle, S.P., Cámara, M. and Williams, P., 2000. The *Pseudomonas aeruginosa* lectins PA-IL and PA-IIL are controlled by quorum sensing and by RpoS. *Journal of bacteriology*, 182(22), pp.6401-6411.

Wiriyathanawudhiwong, N., Ohtsu, I., Li, Z.D., Mori, H. and Takagi, H., 2009. The outer membrane TolC is involved in cysteine tolerance and overproduction in *Escherichia coli. Applied microbiology and biotechnology*, 81, pp.903-913.

Wolloscheck, D., Krishnamoorthy, G., Nguyen, J. and Zgurskaya, H.I., 2018. Kinetic control of quorum sensing in *Pseudomonas aeruginosa* by multidrug efflux pumps. *ACS infectious diseases*, 4(2), pp.185-195.

Xavier, D.E., Picão, R.C., Girardello, R., Fehlberg, L.C. and Gales, A.C., 2010. Efflux pumps expression and its association with porin down-regulation and β-lactamase production among *Pseudomonas aeruginosa* causing bloodstream infections in Brazil. *BMC microbiology*, 10(1), pp.1-7.

Xiao, G., Déziel, E., He, J., Lépine, F., Lesic, B., Castonguay, M.H., Milot, S., Tampakaki, A.P., Stachel, S.E. and Rahme, L.G., 2006. MvfR, a key *Pseudomonas aeruginosa* pathogenicity LTTR-class regulatory protein, has dual ligands. *Molecular microbiology*, 62(6), pp.1689-1699.

Xu, Y., Moeller, A., Jun, S.Y., Le, M., Yoon, B.Y., Kim, J.S., Lee, K. and Ha, N.C., 2012. Assembly and channel opening of outer membrane protein in tripartite drug efflux pumps of Gram-negative bacteria. *Journal of Biological Chemistry*, 287(15), pp.11740-11750.

Yang, S., Lopez, C.R. and Zechiedrich, E.L., 2006. Quorum sensing and multidrug transporters in *Escherichia coli. Proceedings of the National Academy of Sciences*, 103(7), pp.2386-2391.

Yang, L., Chen, L., Shen, L., Surette, M. and Duan, K., 2011. Inactivation of MuxABC-OpmB transporter system in *Pseudomonas aeruginosa* leads to increased ampicillin and carbenicillin resistance and decreased virulence. *The Journal of Microbiology*, 49(1), pp.107-114.

Yao, X., Tao, F., Zhang, K., Tang, H. and Xu, P., 2017. Multiple roles for two efflux pumps in the polycyclic aromatic hydrocarbon-degrading *Pseudomonas putida* strain B6-2 (DSM 28064). *Applied and environmental microbiology*, 83(24), pp.e01882-17.

Yeung, A.T., Bains, M. and Hancock, R.E., 2011. The sensor kinase CbrA is a global regulator that modulates metabolism, virulence, and antibiotic resistance in *Pseudomonas aeruginosa. Journal of bacteriology*, 193(4), pp.918-931.

Yohannes, E., Barnhart, D.M. and Slonczewski, J.L., 2004. pH-dependent catabolic protein expression during anaerobic growth of *Escherichia coli* K-12. *Journal of Bacteriology*, 186(1), pp.192-199.

Yoneda, K., Chikumi, H., Murata, T., Gotoh, N., Yamamoto, H., Fujiwara, H., Nishino, T. and Shimizu, E., 2005. Measurement of *Pseudomonas aeruginosa* multidrug efflux pumps by quantitative real-time polymerase chain reaction. *FEMS microbiology letters*, 243(1), pp.125-131.

Yu, G., Smith, D.K., Zhu, H., Guan, Y. and Lam, T.T.Y., 2017. ggtree: an R package for visualization and annotation of phylogenetic trees with their covariates and other associated data. *Methods in Ecology and Evolution*, 8(1), pp.28-36.

Yuan, Y., Rosado-Lugo, J.D., Zhang, Y., Datta, P., Sun, Y., Cao, Y., Banerjee, A. and Parhi, A.K., 2021. Evaluation of Heterocyclic Carboxamides as Potential Efflux Pump Inhibitors in *Pseudomonas aeruginosa. Antibiotics*, 11(1), p.30.

Yum, S., Xu, Y., Piao, S., Sim, S.H., Kim, H.M., Jo, W.S., Kim, K.J., Kweon, H.S., Jeong, M.H., Jeon, H. and Lee, K., 2009. Crystal structure of the periplasmic component of a tripartite macrolide-specific efflux pump. *Journal of molecular biology*, 387(5), pp.1286-1297.

Zaoui, C., Overhage, J., Löns, D., Zimmermann, A., Müsken, M., Bielecki, P., Pustelny, C., Becker, T., Nimtz, M. and Häussler, S., 2012. An orphan sensor kinase controls quinolone signal production via MexT in *Pseudomonas aeruginosa. Molecular microbiology*, 83(3), pp.536-547.

Zhang, L., Murphy, P.J., Kerr, A. and Tate, M.E., 1993. *Agrobacterium* conjugation and gene regulation by N-acyl-L-homoserine lactones. *Nature*, 362(6419), pp.446-448.

Zhang, Y.M., Frank, M.W., Zhu, K., Mayasundari, A. and Rock, C.O., 2008. PqsD Is Responsible for the Synthesis of 2, 4-Dihydroxyquinoline, an Extracellular Metabolite Produced by *Pseudomonas aeruginosa. Journal of Biological Chemistry*, 283(43), pp.28788-28794.

Zhang, Y., Rosado-Lugo, J.D., Datta, P., Sun, Y., Cao, Y., Banerjee, A., Yuan, Y. and Parhi, A.K., 2022. Evaluation of a Conformationally Constrained Indole Carboxamide as a Potential Efflux Pump Inhibitor in *Pseudomonas aeruginosa. Antibiotics*, 11(6), p.716.

Zhao, J., Hellwig, N., Djahanschiri, B., Khera, R., Morgner, N., Ebersberger, I., Wang, J. and Michel, H., 2022. Assembly and Functional Role of PACE Transporter PA2880 from *Pseudomonas aeruginosa. Microbiology Spectrum*, 10(2), pp.e01453-21.

Zhou, T., Huang, J.H., Feng, Q.S., Liu, Z.Q., Lin, Q.Q., Xu, Z. and Zhang, L.H., 2021. A two-component system FleS/FleR regulates multiple virulence-related traits in *Pseudomonas aeruginosa. BioRxiv*.

Zulianello, L., Canard, C., Köhler, T., Caille, D., Lacroix, J.S. and Meda, P., 2006. Rhamnolipids are virulence factors that promote early infiltration of primary human airway epithelia by *Pseudomonas aeruginosa. Infection and immunity*, 74(6), pp.3134-3147.

Zumft, W.G., Dreusch, A., LÖCHELT, S., Cuypers, H., Friedrich, B. and Schneider, B., 1992. Derived amino acid sequences of the *nosZ* gene (respiratory N_2O reductase) from *Alcaligenes eutrophus, Pseudomonas aeruginosa* and *Pseudomonas stutzeri* reveal potential copper-binding residues: Implications for the CuA site of N_2O reductase and cytochrome-c oxidase. *European journal of biochemistry*, 208(1), pp.31-40.

Appendix

Appendix A: GenBank protein accession numbers of RND transporters used to construct phylogenetic tree.

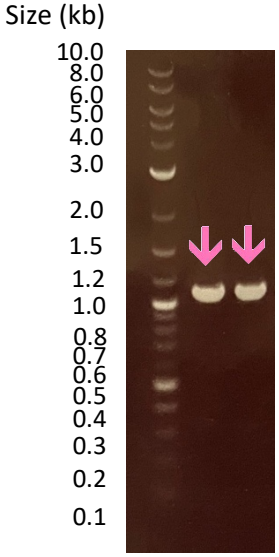
RND transporter	Protein ID	Organism
AdeJ	AXV53427.1	*Acinetobacter baumannii*
AdeG	WP_246891508.1	*Acinetobacter baumannii*
AdeB	AXV52326.1	*Acinetobacter baumannii*
CeoB	AZQ55395.1	*Burkholderia cenocepacia*
BpeB	WP_122837265.1	*Burkholderia pseudomallei*
BpeF	EDO92743.1	*Burkholderia pseudomallei*
CmeB	QZI67418.1	*Campylobacter jejuni*
CmeF	WP_002859176.1	*Campylobacter jejuni*
AcrB	WP_046201532.1	*Escherichia coli*
AcrD	CAD6000925.1	*Escherichia coli*
AcrF	UJY26197.1	*Escherichia coli*
CusA	AFX60847.1	*Escherichia coli*
MdtB	UKM84052.1	*Escherichia coli*
MdtC	UKM84053.1	*Escherichia coli*
MdtF	CAD5999802.1	*Escherichia coli*
AcrB	BBA21741.1	*Haemophilus influenzae*
HefB	TLR92093.1	*Helicobacter pylori*
AcrB	CDO13174.1	*Klebsiella pneumoniae*
AcrD	UKM00377.1	*Klebsiella pneumoniae*
AcrF	QTZ88054.1	*Klebsiella pneumoniae*
EefB	UKM01556.1	*Klebsiella pneumoniae*

MexF	AEW52749.1	*Legionella pneumophila*
LpeB	WP_106225839.1	*Legionella pneumophila*
AcrB	EKF84012.1	*Moraxella catarrhalis*
MtrD	WP_162503037.1	*Neisseria gonorrhoeae*
MexB	WP_003107312.1	*Pseudomonas aeruginosa*
MexD	WP_016852128.1	*Pseudomonas aeruginosa*
MexF	WP_022580472.1	*Pseudomonas aeruginosa*
MexI	WP_247073136.1	*Pseudomonas aeruginosa*
MexK	QPV53476.1	*Pseudomonas aeruginosa*
MexN	QPV56980.1	*Pseudomonas aeruginosa*
MexQ	QPV53262.1	*Pseudomonas aeruginosa*
MexW	QPV56214.1	*Pseudomonas aeruginosa*
MexY	QPV51482.1	*Pseudomonas aeruginosa*
CzcA	ARU39038.1	*Pseudomonas aeruginosa*
MuxB	QPV51993.1	*Pseudomonas aeruginosa*
MuxC	QPV51992.1	*Pseudomonas aeruginosa*
TriC	QPV54373.1	*Pseudomonas aeruginosa*
MexB	KWV78995.1	*Pseudomonas fluorescens*
MexD	WP_126450740.1	*Pseudomonas fluorescens*
MexF	WP_126450527.1	*Pseudomonas fluorescens*
EmhB	WP_169429189.1	*Pseudomonas fluorescens*
ArpB	ADR61754.1	*Pseudomonas putida*
MexB	ANY86932.1	*Pseudomonas putida*
MexD	AAN68426.1	*Pseudomonas putida*
MexF	AAN69028.1	*Pseudomonas putida*
MepB	EST15727.1	*Pseudomonas putida*
SrpB	WP_180689719.1	*Pseudomonas putida*

TtgB	WP_191086932.1	*Pseudomonas putida*
TtgE	WP_087535065.1	*Pseudomonas putida*
TtgH	ANY90612.1	*Pseudomonas putida*
PseC	ABN45754.1	*Pseudomonas syringae*
AcrB	WP_033572398.1	*Salmonella enterica*
AcrD	WP_224465528.1	*Salmonella enterica*
AcrF	GAR76895.1	*Salmonella enterica*
MdtB	QPE02574.1	*Salmonella enterica*
MdsB	WP_247258623.1	*Salmonella enterica*
SilA	QNI18372.1	*Salmonella enterica*
SdeB	TEW94312.1	*Serratia marcescens*
SdeY	TEW93145.1	*Serratia marcescens*
VexB	WP_053026105.1	*Vibrio cholerae*
VexD	UIP05065.1	*Vibrio cholerae*
VexF	UIP03601.1	*Vibrio cholerae*
VexH	WP_188963110.1	*Vibrio cholerae*
VexK	UIP05136.1	*Vibrio cholerae*
VmeB	UJX30477.1	*Vibrio parahaemolyticus*
VmeD	UJX29496.1	*Vibrio parahaemolyticus*
VmeF	UJX30373.1	*Vibrio parahaemolyticus*
VmeI	UJX28409.1	*Vibrio parahaemolyticus*
VmeK	WP_193249969.1	*Vibrio parahaemolyticus*
VmeQ	WP_193253204.1	*Vibrio parahaemolyticus*
VmeZ	UJX32405.1	*Vibrio parahaemolyticus*

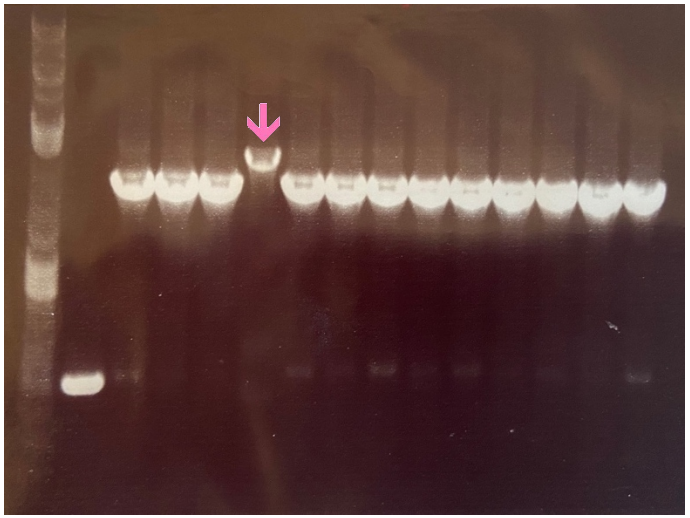
Appendix B: Chromosomal deletion of MexAB-OprM efflux pump A) Amplification of the 1047 bp region upstream of *mexA* using primers mexAB-oprM_+1000_fwd and mexAB-oprM_+1000_rev, and amplification of the 1051 bp region downstream of *oprM* using primers mexAB-oprM_-1000_fwd and mexAB-oprM_-1000_rev from PAO1-L-DS genomic DNA B) Screening for correct assembly of pEX18Gm::*ΔmexAB-oprM* using the pEX universal forward primer and the mexAB-oprM_-1000_rev primer. Correctly assembled suicide plasmids were 2456 bp C) Screening for the 2098 bp Δ*mexAB-oprM* mutant fragment using mexAB-oprM_+1000_fwd and mexAB-oprM_-1000_rev primers. All PCR products were electrophoresed on a 1% agarose gel. Fragments of the expected size are indicated with pink arrows.

A



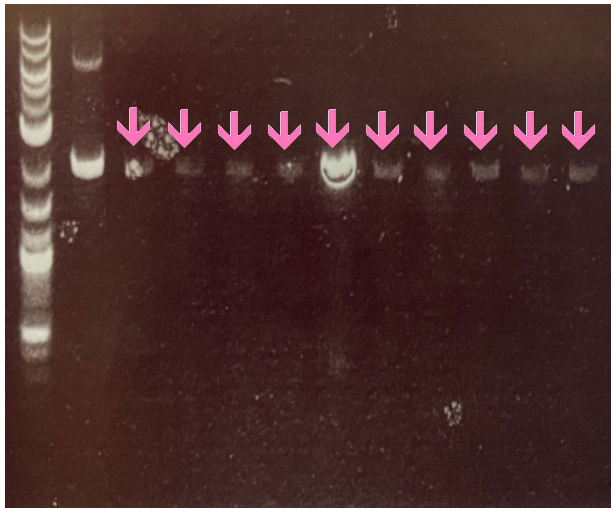
Lane	Sample
1	NEB 2-log ladder
2	+1000 bp fragment
3	-1000 bp fragment

B



Lane	Sample
1	NEB 2-log ladder
2	*E. coli* S17-1λ*pir* pEX18Gm
3 - 12	*E. coli* S17-1λ*pir* pEX18Gm::*ΔmexAB-oprM* candidates

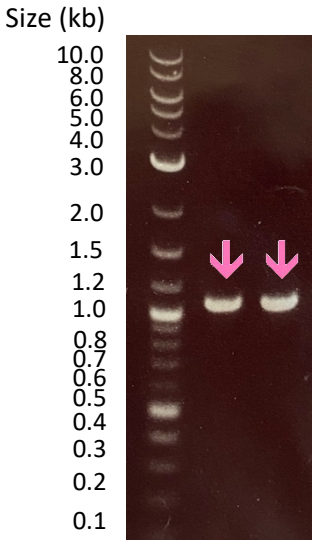
C



Lane	Sample
1	NEB 2-log ladder
2	PAO1-L-DS
3 - 12	PAO1-L-DS *ΔmexAB-oprM* candidates

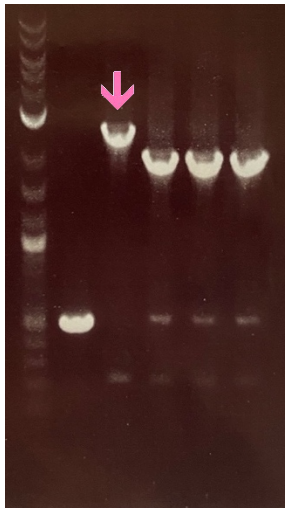
Appendix C: Chromosomal deletion of MexCD-OprJ efflux pump A) Amplification of the 1026 bp region upstream of *mexC* using primers mexCD-oprJ_+1000_fwd and mexCD-oprJ_+1000_rev, and amplification of the 1073 bp region downstream of *oprJ* using primers mexCD-oprJ_-1000_fwd and mexCD-oprJ_-1000_rev from PAO1-L-DS genomic DNA B) Screening for correct assembly of pEX18Gm::*ΔmexCD-oprJ* using the pEX universal forward primer and the mexCD-oprJ_-1000_rev primer. Correctly assembled suicide plasmids were 2457 bp C) Screening for the 148 bp Δ*mexCD-oprJ* mutant fragment using mexCD-oprJ_+100_fwd and mexCD-oprJ_-100_rev primers. All PCR products were electrophoresed on a 1% agarose gel. Fragments of the expected size are indicated with pink arrows.

A



Lane	Sample
1	NEB 2-log ladder
2	+1000 bp fragment
3	-1000 bp fragment

B



Lane	Sample
1	NEB 2-log ladder
2	*E. coli* S17-1λ*pir* pEX18Gm
3 - 6	*E. coli* S17-1λ*pir* pEX18Gm::*ΔmexCD-oprJ* candidates

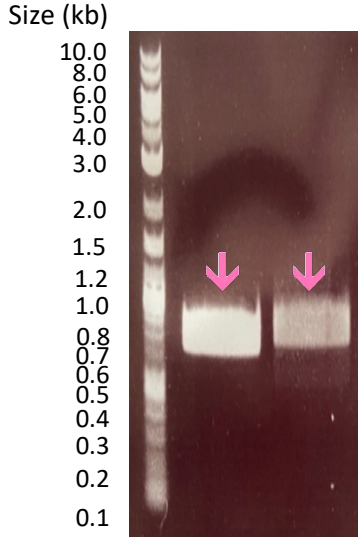
C



Lane	Sample
1	NEB 2-log ladder
2	PAO1-L-DS
3 - 12	PAO1-L-DS *ΔmexCD-oprJ* candidates

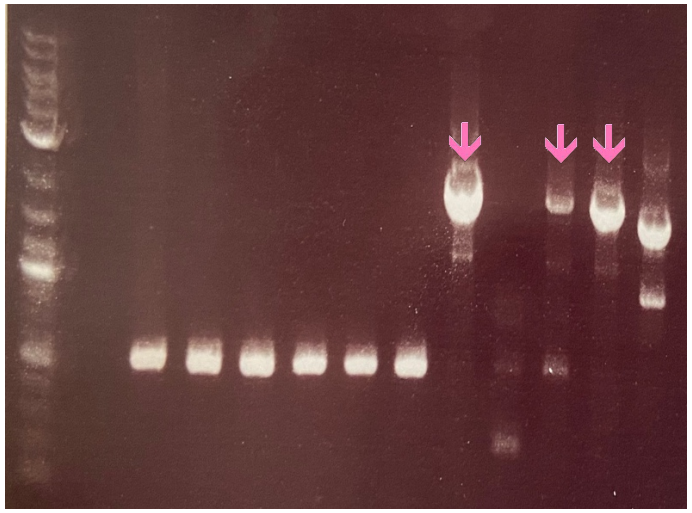
Appendix D: Chromosomal deletion of MexEF-OprN efflux pump A) Amplification of the 775 bp region upstream of *mexE* using primers mexEF-oprN_+500_fwd and mexEF-oprN_+500_rev, and amplification of the 815 bp region downstream of *oprN* using primers mexEF-oprN_-1000_fwd and mexEF-oprN_-500_rev from PAO1-L-DS genomic DNA B) Screening for correct assembly of pEX18Gm::*ΔmexEF-oprN* using the pEX universal forward primer and the mexEF-oprN_-500_rev primer. Correctly assembled suicide plasmids were 1590 bp C) Screening for the 195 bp Δ*mexEF-oprN* mutant fragment using mexEF-oprN_+1000_fwd and mexEF-oprN_-1000_rev primers. All PCR products were electrophoresed on a 1% agarose gel. Fragments of the expected size are indicated with pink arrows.

A



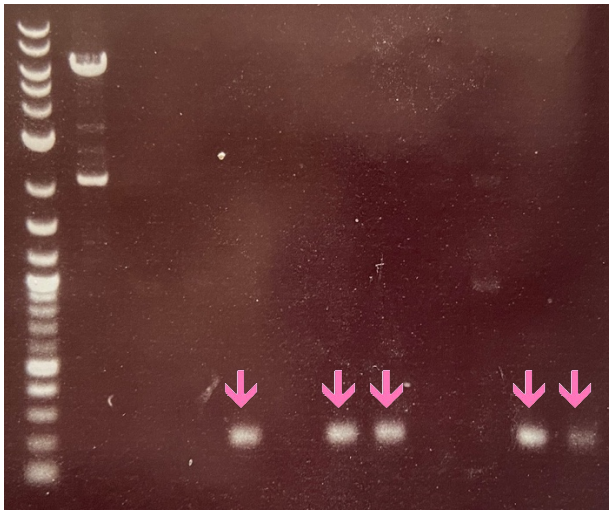
Lane	Sample
1	NEB 2-log ladder
2	+1000 bp fragment
3	-1000 bp fragment

B



Lane	Sample
1	NEB 2-log ladder
2	*E. coli* S17-1λ*pir* pEX18Gm
3 - 12	*E. coli* S17-1λ*pir* pEX18Gm::*ΔmexEF-oprN* candidates

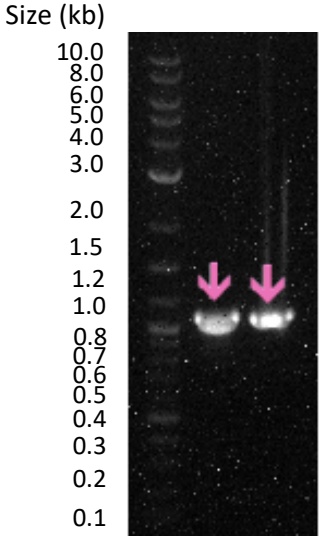
C



Lane	Sample
1	NEB 2-log ladder
2	PAO1-L-DS
3 - 12	PAO1-L-DS *ΔmexE-oprN* candidates

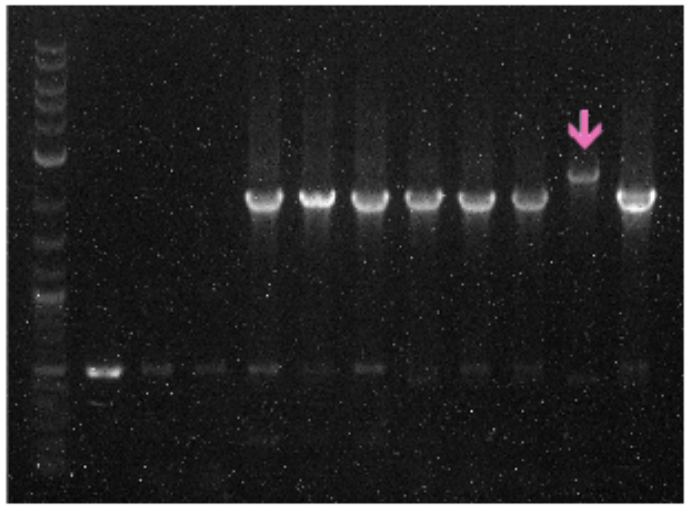
Appendix E: Chromosomal deletion of MexGHI-OpmD efflux pump A) Amplification of the 1050 bp region upstream of *mexG* using primers mexGHI-opmD_+1000_fwd and mexGHI-opmD_+1000_rev, and amplification of the 1046 bp region downstream of *opmD* using primers mexGHI-opmD_-1000_fwd and mexGHI-opmD_-1000_rev from PAO1-L-DS genomic DNA B) Screening for correct assembly of pEX18Gm::*ΔmexGHI-opmD* using the pEX universal forward primer and the mexGHI-opmD_-1000_rev primer. Correctly assembled suicide plasmids were 2454 bp C) Screening for the 2096 bp Δ*mexGHI-opmD* mutant fragment using mexGHI-opmD_+1000_fwd and mexGHI-opmD_-1000_rev primers. All PCR products were electrophoresed on a 1% agarose gel. Fragments of the expected size are indicated with pink arrows.

A



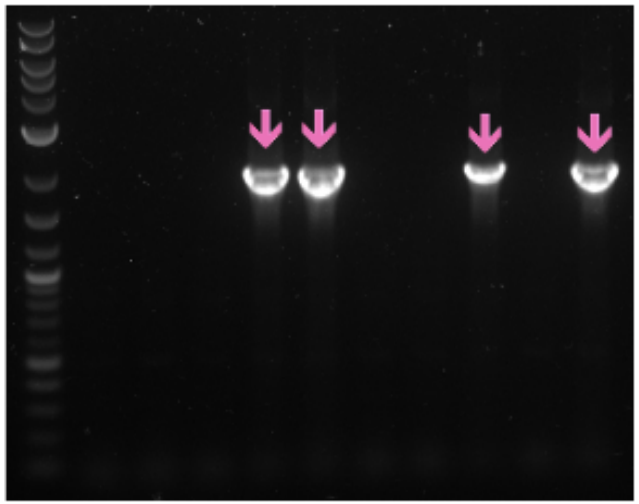
Lane	Sample
1	NEB 2-log ladder
2	+1000 bp fragment
3	-1000 bp fragment

B



Lane	Sample
1	NEB 2-log ladder
2	*E. coli* S17-1λ*pir* pEX18Gm
3 - 12	*E. coli* S17-1λ*pir* pEX18Gm::*ΔmexGHI-opmD* candidates

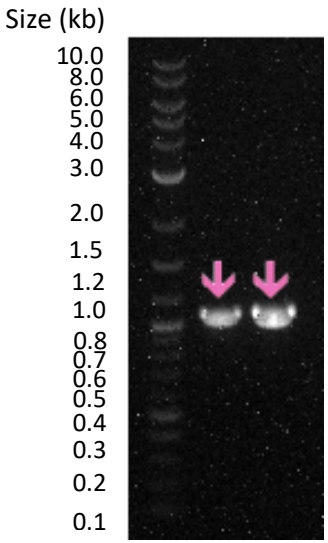
C



Lane	Sample
1	NEB 2-log ladder
2	PAO1-L-DS
3 - 12	PAO1-L-DS *ΔmexGHI-opmD* candidates

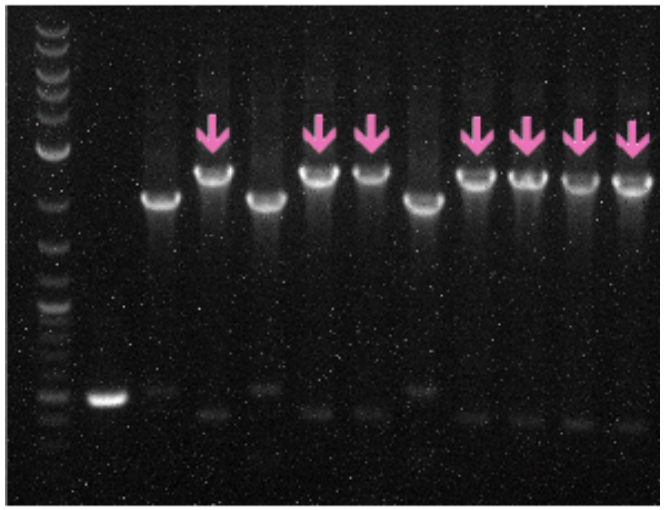
Appendix F: Chromosomal deletion of MexJK efflux pump A) Amplification of the 1047 bp region upstream of *mexJ* using primers mexJK_+1000_fwd and mexJK_+1000_rev, and amplification of the 1048 bp region downstream of *mexK* using primers mexJK_-1000_fwd and mexJK_-1000_rev from PAO1-L-DS genomic DNA B) Screening for correct assembly of pEX18Gm::*ΔmexJK* using the pEX universal forward primer and the mexJK_-1000_rev primer. Correctly assembled suicide plasmids were 2453 bp C) Screening for the 2095 bp Δ*mexJK* mutant fragment using mexJK_+1000_fwd and mexJK_-1000_rev primers. All PCR products were electrophoresed on a 1% agarose gel. Fragments of the expected size are indicated with pink arrows.

A



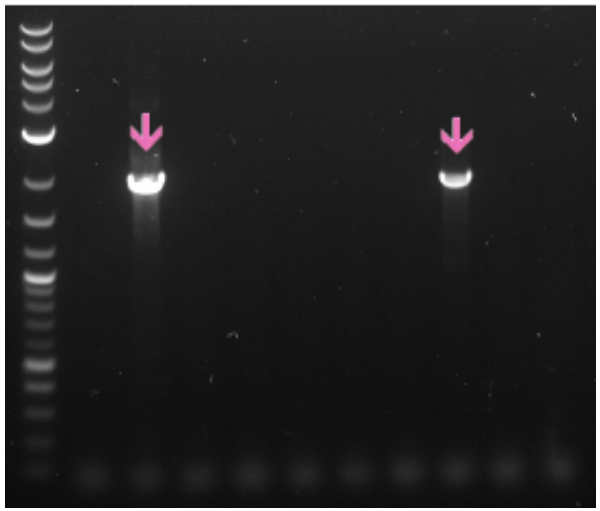
Lane	Sample
1	NEB 2-log ladder
2	+1000 bp fragment
3	-1000 bp fragment

B



Lane	Sample
1	NEB 2-log ladder
2	*E. coli* S17-1λ*pir* pEX18Gm
3 - 12	*E. coli* S17-1λ*pir* pEX18Gm::*ΔmexJK* candidates

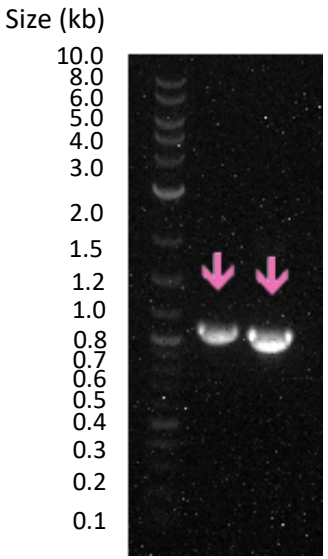
C



Lane	Sample
1	NEB 2-log ladder
2	PAO1-L-DS
3 - 12	PAO1-L-DS *ΔmexJK* candidates

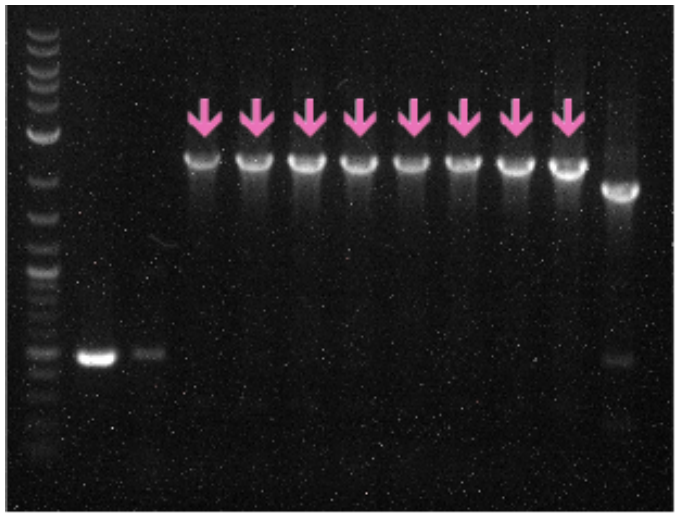
Appendix G: Chromosomal deletion of MexMN efflux pump A) Amplification of the 1049 bp region upstream of *mexM* using primers mexMN_+1000_fwd and mexMN_+1000_rev, and amplification of the 1046 bp region downstream of *mexN* using primers mexMN_-1000_fwd and mexMN_-1000_rev from PAO1-L-DS genomic DNA B) Screening for correct assembly of pEX18Gm::*ΔmexMN* using the pEX universal forward primer and the mexMN_-1000_rev primer. Correctly assembled suicide plasmids were 2453 bp C) Screening for the 2095 bp Δ*mexMN* mutant fragment using mexMN_+1000_fwd and mexMN_-1000_rev primers. All PCR products were electrophoresed on a 1% agarose gel. Fragments of the expected size are indicated with pink arrows.

A



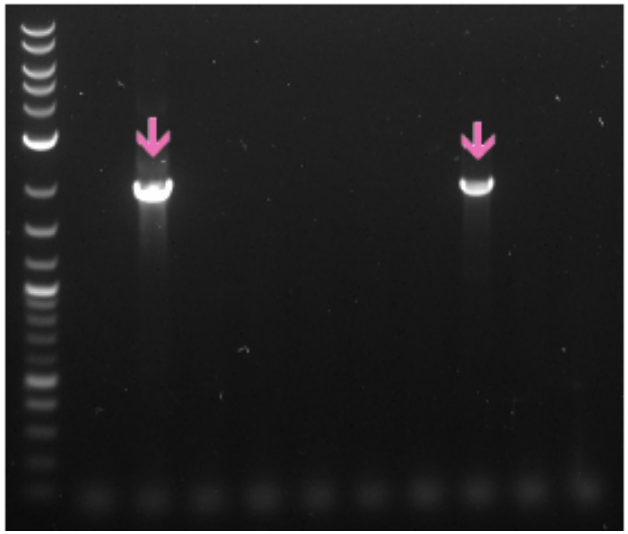
Lane	Sample
1	NEB 2-log ladder
2	+1000 bp fragment
3	-1000 bp fragment

B



Lane	Sample
1	NEB 2-log ladder
2	*E. coli* S17-1λ*pir* pEX18Gm
3 - 12	*E. coli* S17-1λ*pir* pEX18Gm::*ΔmexMN* candidates

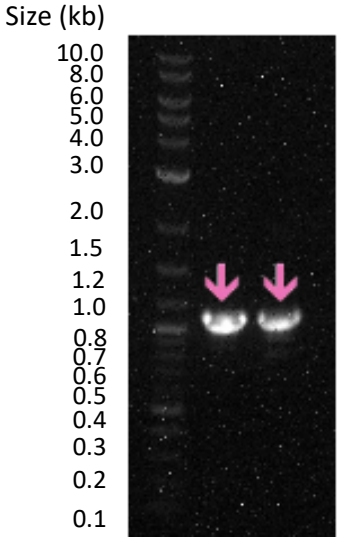
C



Lane	Sample
1	NEB 2-log ladder
2	PAO1-L-DS
3 - 12	PAO1-L-DS *ΔmexMN* candidates

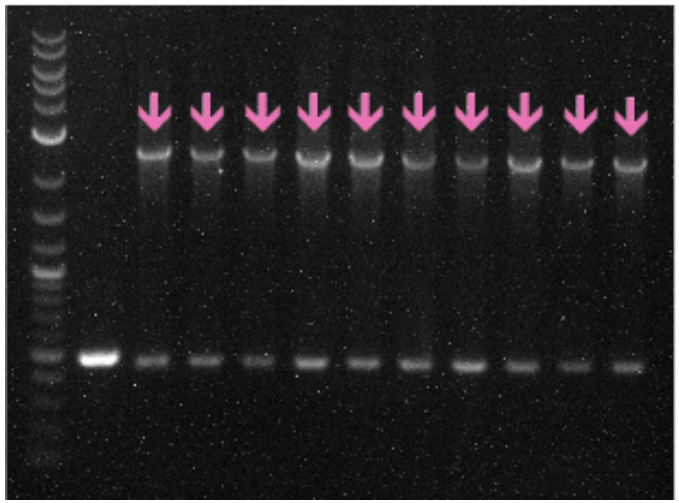
Appendix H: Chromosomal deletion of MexPQ-OpmE efflux pump A) Amplification of the 1050 bp region upstream of *mexP* using primers mexPQ-opmE_+1000_fwd and mexPQ-opmE_+1000_rev, and amplification of the 1055 bp region downstream of *opmE* using primers mexPQ-opmE_-1000_fwd and mexPQ-opmE_-1000_rev from PAO1-L-DS genomic DNA B) Screening for correct assembly of pEX18Gm::*ΔmexPQ-opmE* using the pEX universal forward primer and the mexPQ-opmE_-1000_rev primer. Correctly assembled suicide plasmids were 2463 bp C) Screening for the 2105 bp Δ*mexPQ-opmE* mutant fragment using mexPQ-opmE_+1000_fwd and mexPQ-opmE_-1000_rev primers. All PCR products were electrophoresed on a 1% agarose gel. Fragments of the expected size are indicated with pink arrows.

A



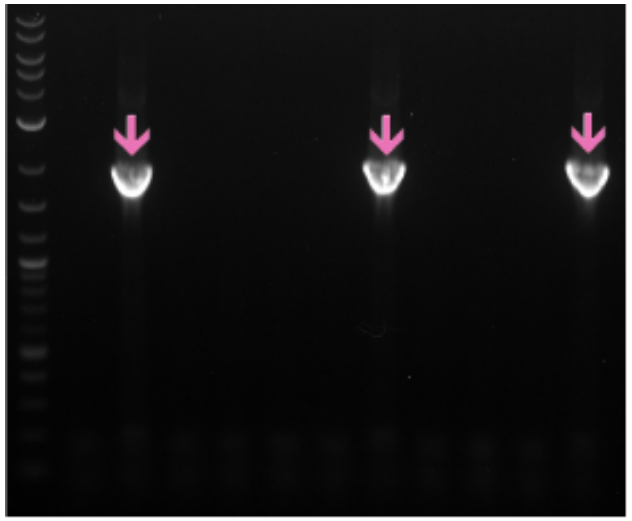
Lane	Sample
1	NEB 2-log ladder
2	+1000 bp fragment
3	-1000 bp fragment

B



Lane	Sample
1	NEB 2-log ladder
2	*E. coli* S17-1λ*pir* pEX18Gm
3 - 12	*E. coli* S17-1λ*pir* pEX18Gm::*ΔmexPQ-opmE* candidates

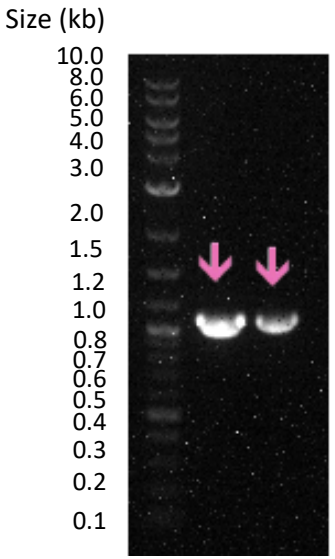
C



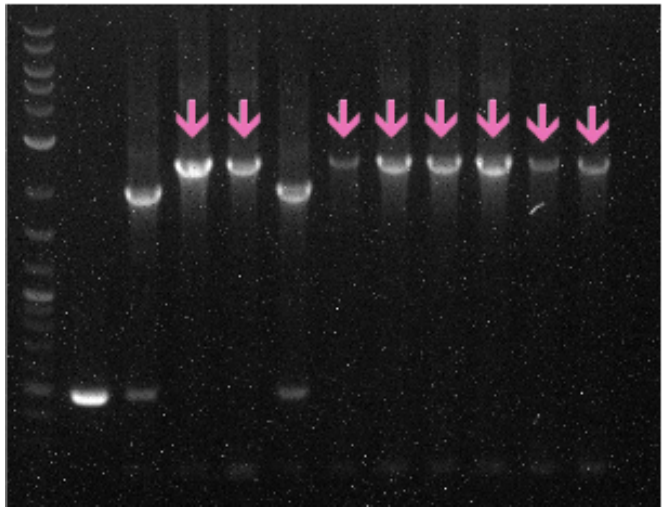
Lane	Sample
1	NEB 2-log ladder
2	PAO1-L-DS
3 - 12	PAO1-L-DS *ΔmexPQ-opmE* candidates

Appendix I: Chromosomal deletion of MexVW efflux pump A) Amplification of the 1050 bp region upstream of *mexV* using primers mexVW_+1000_fwd and mexVW_+1000_rev, and amplification of the 1056 bp region downstream of *mexW* using primers mexVW_-1000_fwd and mexVW_-1000_rev from PAO1-L-DS genomic DNA B) Screening for correct assembly of pEX18Gm::*ΔmexVW* using the pEX universal forward primer and the mexVW_-1000_rev primer. Correctly assembled suicide plasmids were 2456 bp C) Screening for the 2106 bp Δ*mexVW* mutant fragment using mexVW_+1000_fwd and mexVW_-1000_rev primers. All PCR products were electrophoresed on a 1% agarose gel. Fragments of the expected size are indicated with pink arrows.

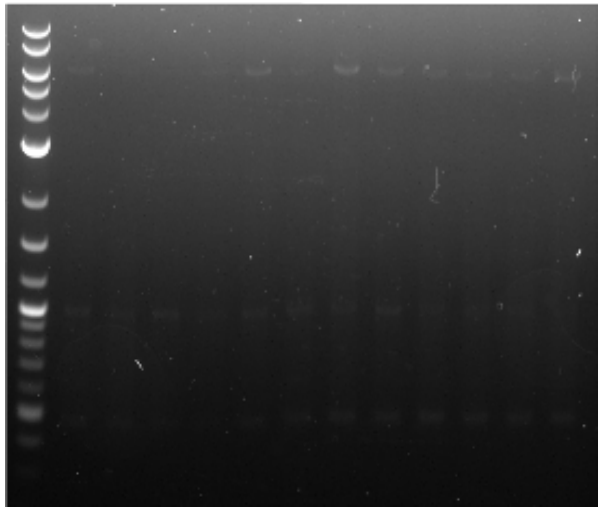
A



B



C



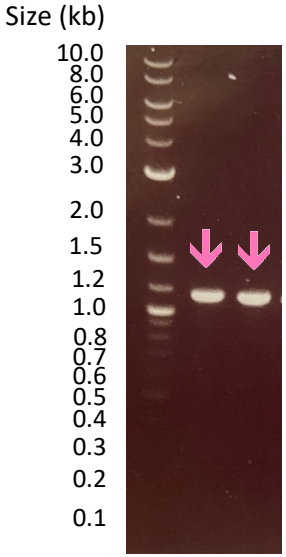
Lane	Sample
1	NEB 2-log ladder
2	+1000 bp fragment
3	-1000 bp fragment

Lane	Sample
1	NEB 2-log ladder
2	*E. coli* S17-1λ*pir* pEX18Gm
3 - 12	*E. coli* S17-1λ*pir* pEX18Gm::*ΔmexVW* candidates

Lane	Sample
1	NEB 2-log ladder
2	PAO1-L-DS
3 - 12	PAO1-L-DS *ΔmexVW* candidates

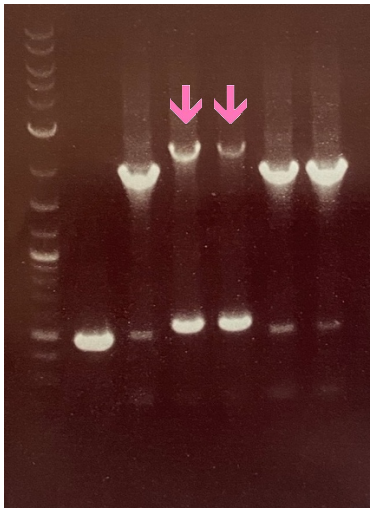
Appendix J: Chromosomal deletion of MexXY efflux pump A) Amplification of the 1093 bp region upstream of *mexX* using primers mexXY_+1000_fwd and mexXY_+1000_rev, and amplification of the 1006 bp region downstream of *mexY* using primers mexXY_-1000_fwd and mexXY_-1000_rev from PAO1-L-DS genomic DNA B) Screening for correct assembly of pEX18Gm::*ΔmexXY* using the pEX universal forward primer and the mexXY_-1000_rev primer. Correctly assembled suicide plasmids were 2457 bp C) Screening for the 244 bp *ΔmexXY* mutant fragment using mexXY_+100_fwd and mexXY_-100_rev primers. All PCR products were electrophoresed on a 1% agarose gel. Fragments of the expected size are indicated with pink arrows.

A



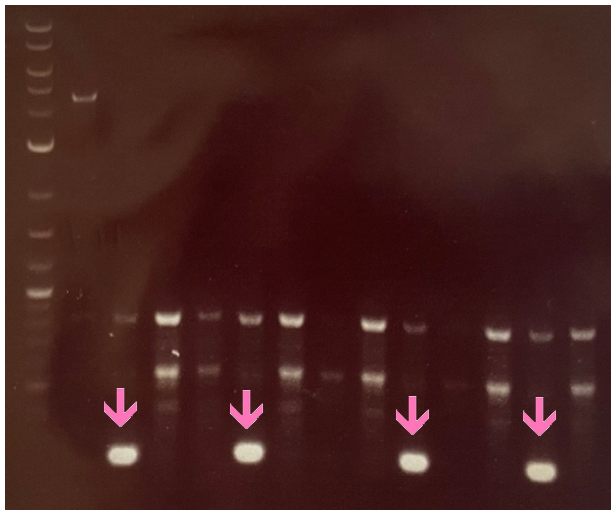
Lane	Sample
1	NEB 2-log ladder
2	+1000 bp fragment
3	-1000 bp fragment

B



Lane	Sample
1	NEB 2-log ladder
2	*E. coli* S17-1λ*pir* pEX18Gm
3 - 7	*E. coli* S17-1λ*pir* pEX18Gm::*ΔmexXY* candidates

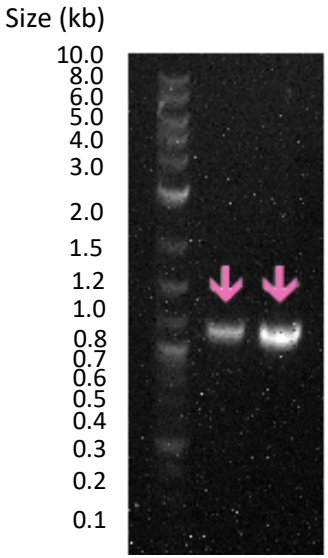
C



Lane	Sample
1	NEB 2-log ladder
2	PAO1-L-DS
3 - 12	PAO1-L-DS *ΔmexXY* candidates

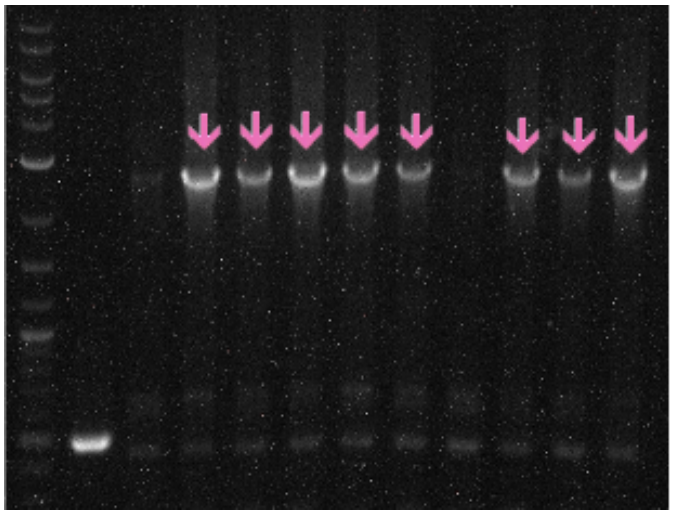
Appendix K: Chromosomal deletion of CzcCBA efflux pump A) Amplification of the 1132 bp region upstream of *czcC* using primers czcCBA_+1000_fwd and czcCBA_+1000_rev, and amplification of the 1120 bp region downstream of *czcA* using primers czcCBA_-1000_fwd2 and czcCBA_-1000_rev2 from PAO1-L-DS genomic DNA B) Screening for correct assembly of pEX18Gm::*ΔczcCBA* using the pEX universal forward primer and the czcCBA_-1000_rev2 primer. Correctly assembled suicide plasmids were 2610 bp C) Screening for the 2252 bp Δ*czcCBA* mutant fragment using czcCBA_+1000_fwd2 and czcCBA_-1000_rev2 primers. All PCR products were electrophoresed on a 1% agarose gel. Fragments of the expected size are indicated with pink arrows.

A



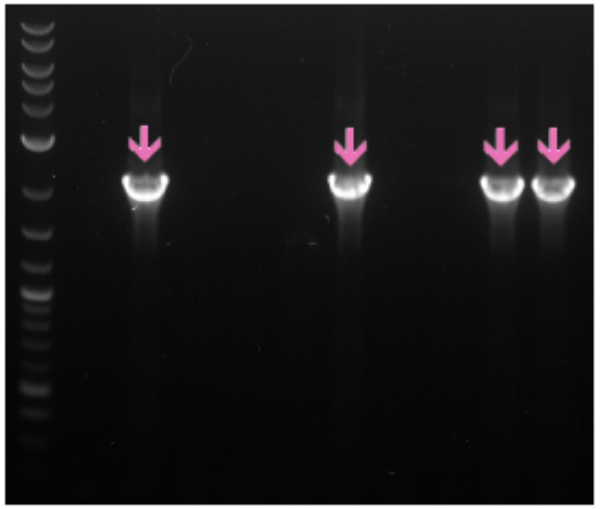
Lane	Sample
1	NEB 2-log ladder
2	+1000 bp fragment
3	-1000 bp fragment

B



Lane	Sample
1	NEB 2-log ladder
2	*E. coli* S17-1λ*pir* pEX18Gm
3 - 12	*E. coli* S17-1λ*pir* pEX18Gm::*ΔczcCBA* candidates

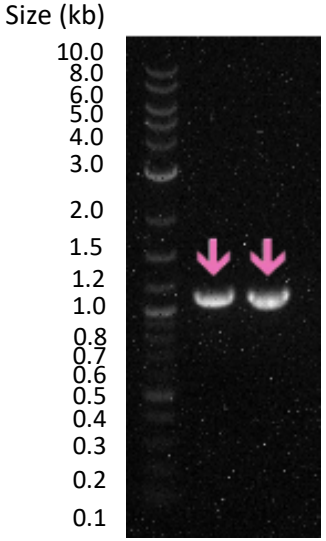
C



Lane	Sample
1	NEB 2-log ladder
2	PAO1-L-DS
3 - 12	PAO1-L-DS *ΔczcCBA* candidates

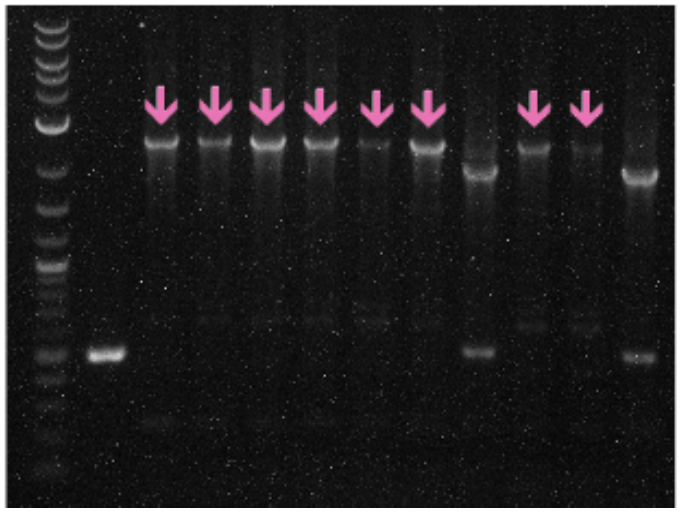
Appendix L: Chromosomal deletion of MuxABC-OpmB efflux pump A) Amplification of the 1049 bp region upstream of *muxA* using primers muxABC-opmB_+1000_fwd and muxABC-opmB_+1000_rev, and amplification of the 1046 bp region downstream of *opmB* using primers muxABC-opmB_-1000_fwd and muxABC-opmB_-1000_rev from PAO1-L-DS genomic DNA B) Screening for correct assembly of pEX18Gm::*ΔmuxABC-opmB* using the pEX universal forward primer and the muxABC-opmB_-1000_rev primer. Correctly assembled suicide plasmids were 2453 bp C) Screening for the 2095 bp Δ*muxABC-opmB* mutant fragment using muxABC-opmB_+1000_fwd and muxABC-opmB_-1000_rev primers. All PCR products were electrophoresed on a 1% agarose gel. Fragments of the expected size are indicated with pink arrows.

A



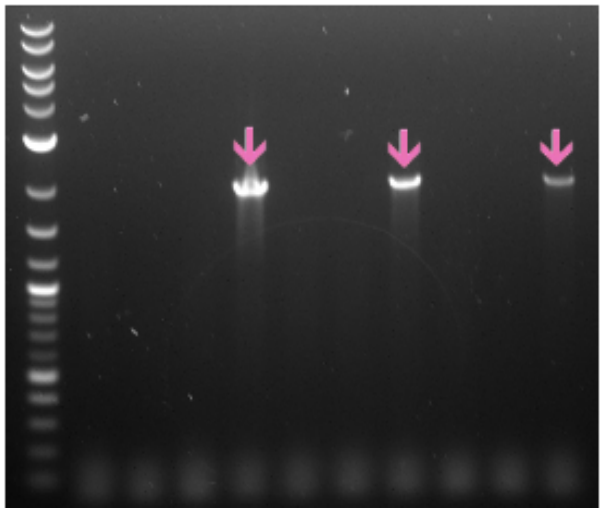
Lane	Sample
1	NEB 2-log ladder
2	+1000 bp fragment
3	-1000 bp fragment

B



Lane	Sample
1	NEB 2-log ladder
2	*E. coli* S17-1λ*pir* pEX18Gm
3 - 12	*E. coli* S17-1λ*pir* pEX18Gm::*ΔmuxABC-opmB* candidates

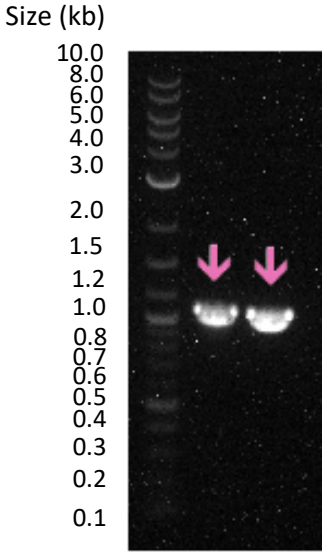
C



Lane	Sample
1	NEB 2-log ladder
2	PAO1-L-DS
3 - 12	PAO1-L-DS *ΔmuxABC-opmB* candidates

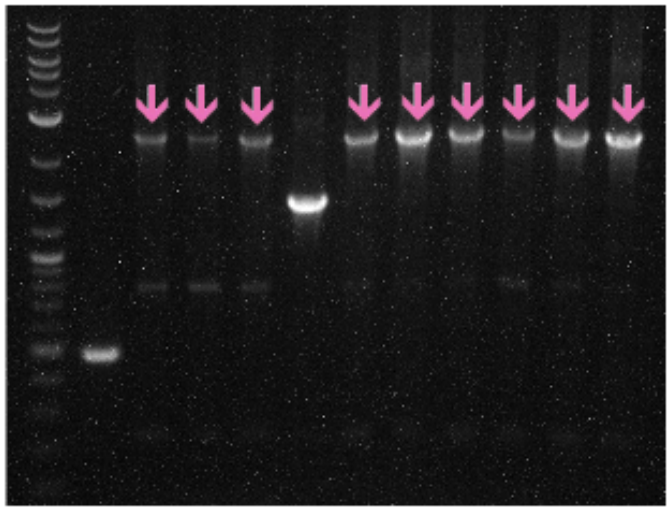
Appendix M: Chromosomal deletion of TriABC efflux pump A) Amplification of the 1049 bp region upstream of *triA* using primers triABC_+1000_fwd and triABC_+1000_rev, and amplification of the 1046 bp region downstream of *triC* using primers triABC_-1000_fwd and triABC_-1000_rev from PAO1-L-DS genomic DNA B) Screening for correct assembly of pEX18Gm::*ΔtriABC* using the pEX universal forward primer and the triABC_-1000_rev primer. Correctly assembled suicide plasmids were 2453 bp C) Screening for the 2095 bp Δ*triABC* mutant fragment using triABC_+1000_fwd and triABC_-1000_rev primers. All PCR products were electrophoresed on a 1% agarose gel. Fragments of the expected size are indicated with pink arrows.

A



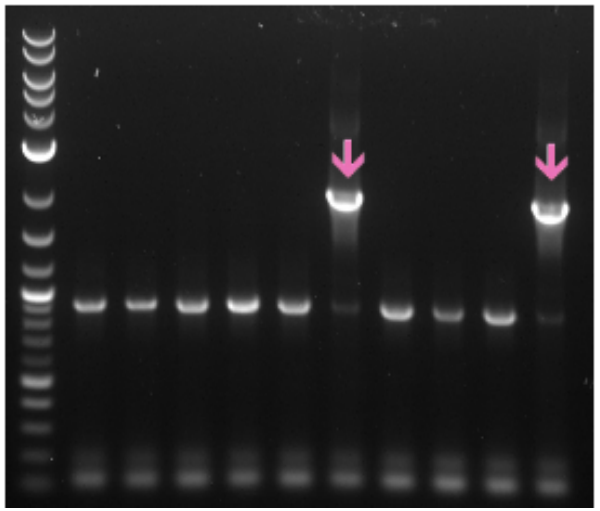
Lane	Sample
1	NEB 2-log ladder
2	+1000 bp fragment
3	-1000 bp fragment

B



Lane	Sample
1	NEB 2-log ladder
2	*E. coli* S17-1λ*pir* pEX18Gm
3 - 12	*E. coli* S17-1λ*pir* pEX18Gm::*ΔtriABC* candidates

C



Lane	Sample
1	NEB 2-log ladder
2	PAO1-L-DS
3 - 12	PAO1-L-DS *ΔtriABC* candidates

Appendix N: Scripts used for whole genome sequencing (WGS) analysis

```
---------------------------------------------

SCRIPT FOR WGS ANALYSIS

Danielle Scales

University of Nottingham

---------------------------------------------

### SCRIPT 1: ASSESS QUALITY OF RAW SEQUENCING DATA USING FASTQC AND
MULTIQC:


# Go to directory where paired reads are stored and run:

> fastqc -t 52 _*_trimmed.fastq.gz


# Compile FastQC results into a single report using MultiQC. Go to
directory where FastQC output files are stored and run:

> multiqc .


---------------------------------------------

### SCRIPT 2: DATA PRE-PROCESSING USING TRIMMOMATIC


> java -jar trimmomatic-0.35.jar PE -phred33 R1_1.fq.gz R1_2.fq.gz
  R1_1_paired.fq.gz R1_1_unpaired.fq.gz R1_2_paired.fq.gz
  R1_2_unpaired.fq.gz ILLUMINACLIP:TruSeq3-PE.fa:2:30:10 LEADING:3
  TRAILING:3 SLIDINGWINDOW:4:15 MINLEN:36


---------------------------------------------

### SCRIPT 3: RE-ASSESS READ QUALITY USING FASTQC AND MULTIQC


# Go to directory where paired reads are stored and run:

> fastqc -t 52 *.fq
```

```
# Compile FastQC results into a single report using MultiQC. Go to
directory where FastQC output files are stored and run:
> multiqc .

-----------------------------------------------
### SCRIPT 4: DE NOVO ASSEMBLIES USING SPADES

> spades.py --pe1-1 R1_1_trimmed.fastq.gz --pe1-2 R1_2_trimmed.fastq.gz –
  careful -o SPADES

-----------------------------------------------
### SCRIPT 5: ASSESS ASSEMBLY QUALITY USING QUAST

# Go to directory where SPAdes output files are stored and run:
> quast.py *.fasta -o QUAST

-----------------------------------------------
### SCRIPT 6: ANNOTATE CONTIGS USING PROKKA

> prokka --locustag R1.contigs.fasta --compliant --proteins NC_002516-2.faa
  --outdir PROKKA –prefix PROKKA_

-----------------------------------------------
### SCRIPT 7: ALIGN CONTIGS TO REFERENCE GENOME USING ABACAS

> perl abacas.1.3.1.pl -r NC_002516-2.fna -q R1.contigs.fasta -p nucmer -b
  -d -a -o R1_contigs_ordered
```

```
-----------------------------------------------

### SCRIPT 8: VARIANT CALLING USING SNIPPY

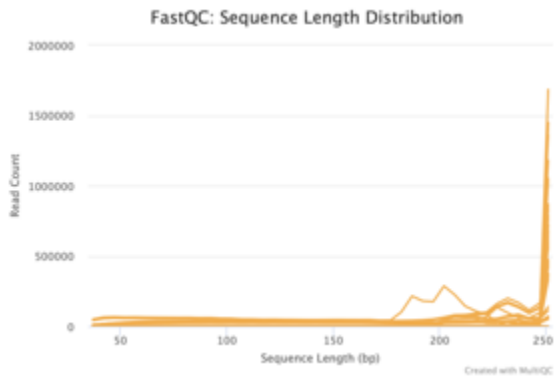

> snippy --report --outdir SNIPPY_R1 --prefix SNIPPY_ --ref NC_002516-
  2.gbff --unmapped --R1 R1_1_trimmed.fastq.gz --R2 R1_2_trimmed.fastq.gz
```

Appendix O: Raw read sequencing quality

Strain	Median insert size	Mean coverage	Mean coverage excluding 0s	Number of reads	Number of reads w/ insert size > 300
PAO1-L-DS	635	43.6101	43.6124	627929	523761
ΔAB	389	177.181	177.182	2722930	1618197
ΔCD	580	61.3676	61.3691	864947	749150
ΔEF	323	155.067	155.068	2502671	1289420
ΔGHI	771	37.2087	37.2116	513070	408729
ΔJK	704	69.9999	70.0037	956827	828489
ΔMN	704	73.2347	73.2386	989987	852110
ΔPQ	667	32.1468	32.1487	437166	389882
ΔXY	666	34.5145	34.5162	491967	424811
Δczc	636	98.1756	98.177	1303500	1195434
Δmux	648	37.0032	37.0091	498815	464734
Δtri	672	55.4446	55.4549	745749	681254
ΔABCD	332	165.435	165.435	2673919	1390148
ΔABEF	673	34.1464	34.1472	487591	417420
ΔABXY	536	70.8842	70.8869	992933	873132
ΔCDEF	606	42.0612	42.0622	592078	519480
ΔCDXY	608	34.2429	34.2429	496412	394870
ΔABCDEF	647	39.6493	39.6504	560797	487792
ΔABCDXY	290	171.19	171.19	2809030	1340438
ΔABCDEFXY	223	165.823	165.824	3168204	1267715
ΔABCDEFPQXY	699	58.6889	58.696	786489	672457

Appendix P: Quality control of WGS reads A) Sequence length distribution B) Mean quality score C) Per sequence quality scores D) Per base N content E) Sequence duplication levels F) Adapter content

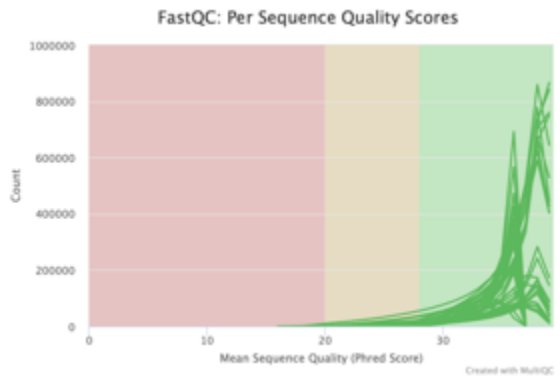
A



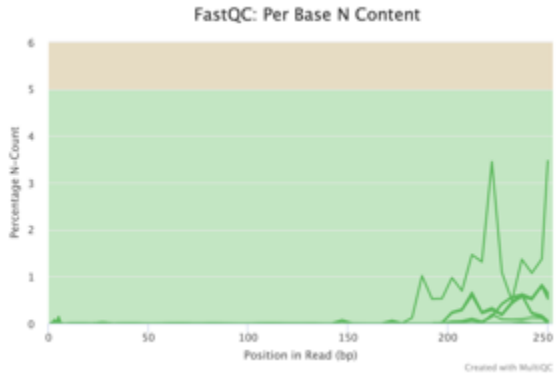
B



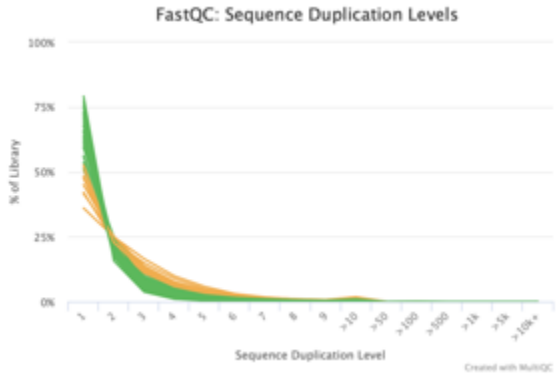
C



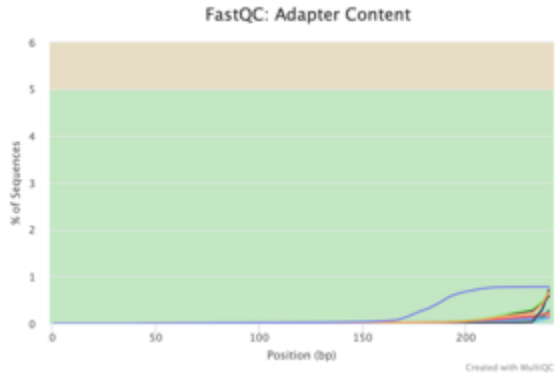
D



E



F



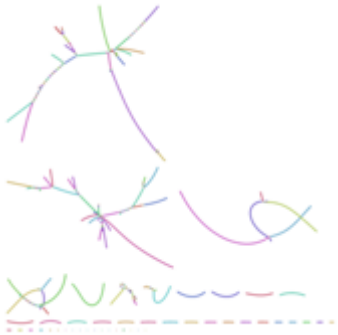
Appendix Q: Contig assembly metrics

Strain	# contigs (>= 0 bp)	# contigs (>= 1000 bp)	Total length (>= 0 bp)	Total length (>= 1000 bp)	# contigs	Largest contig	Total length	GC (%)	N50	N75	# N's per 100 kbp
PAO1-L-DS	126	100	6300086	6287336	109	396509	6294162	66.49	110064	59581	0
ΔAB	103	66	6300699	6283314	74	614915	6289390	66.49	211309	109982	0
ΔCD	115	100	6290966	6283752	105	470812	6287210	66.48	122639	65765	0
ΔEF	112	60	6304289	6281792	70	615987	6288924	66.49	215448	113248	0
ΔGHI	91	37	6243519	6225756	44	915236	6230672	66.57	316574	210235	0
ΔJK	47	24	6308428	6301418	26	1220554	6303166	66.49	642864	480098	0
ΔMN	53	19	6313591	6301417	21	1400955	6302934	66.49	642864	480098	0
ΔPQ	87	37	6310992	6290455	44	767477	6295023	66.49	348454	215159	0
ΔXY	126	107	6292906	6283139	115	396469	6289298	66.48	105513	51449	0
Δczc	97	24	6264064	6235743	30	1278040	6239709	66.56	571752	274398	0
Δmux	83	42	6232157	6216321	51	698764	6222427	66.56	261846	194856	0
Δtri	68	28	6303949	6290954	34	848374	6295350	66.49	485469	302866	0
ΔABCD	104	65	6298570	6280408	74	655914	6286832	66.48	220789	107403	0

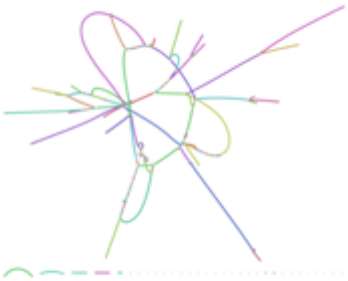
ΔABEF	148	121	6287115	6273832	129	348439	6280013	66.48	91912	53456	0.02
ΔABXY	139	91	6301607	6280328	97	346112	6284692	66.48	150406	68671	0
ΔCDEF	128	111	6284733	6275389	120	343234	6282114	66.48	95802	59581	0
ΔCDXY	130	113	6286030	6276965	120	349783	6282421	66.48	100401	53148	0
ΔABCDEF	126	98	6284666	6271353	105	410212	6276689	66.48	142464	62385	0
ΔABCDXY	109	67	6292053	6274920	75	610966	6280474	66.49	211309	110064	0
ΔABCDEFXY	92	46	6292785	6276063	51	625372	6279595	66.49	241813	155521	0
ΔABCDEFPQXY	71	30	6284536	6271269	35	851723	6274892	66.49	514149	240237	0

Appendix R: Visualisation of assemblies. Assembly graphs from SPAdes were visualised using the Bioinformatics Application for Navigating De novo Assembly Graphs Easily (Bandage) (Wick *et al.*, 2015).

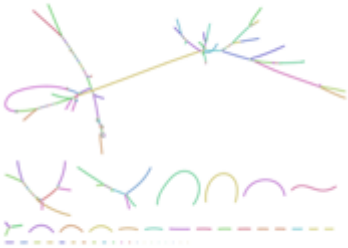
PAO1-L-DS



ΔAB



ΔCD



ΔEF



ΔGHI



ΔJK



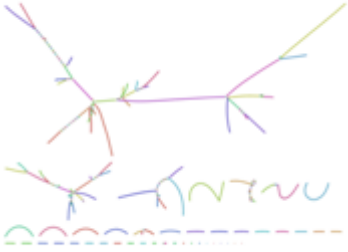
ΔMN



ΔPQ



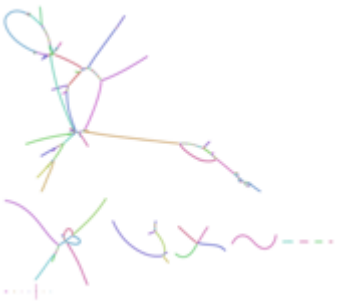
ΔXY



Δczc



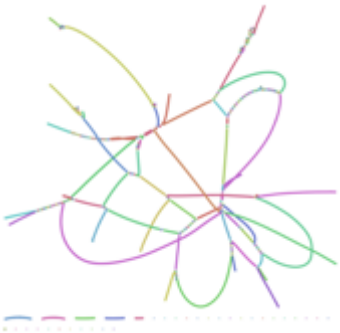
Δmux



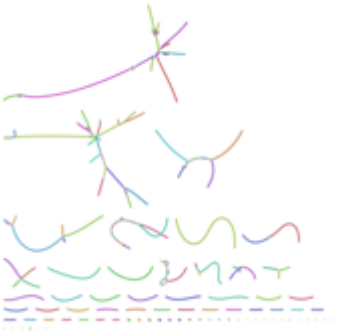
Δtri



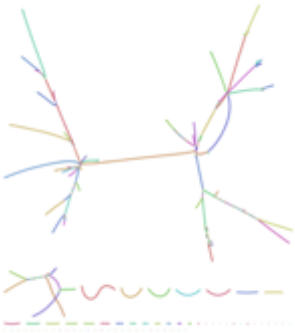
ΔABCD



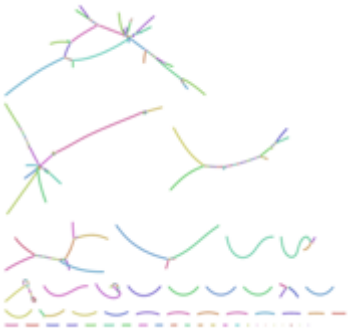
ΔABEF



ΔABXY



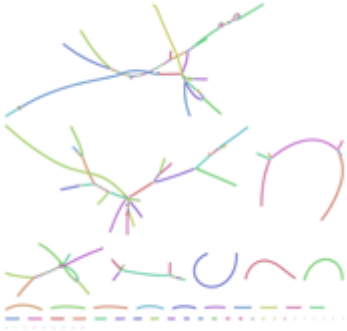
ΔCDEF



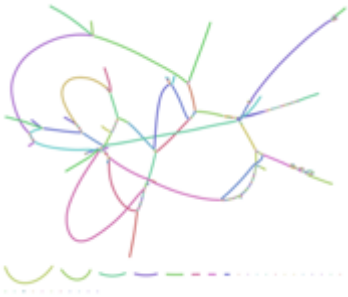
ΔCDXY



ΔABCDEF



ΔABCDXY



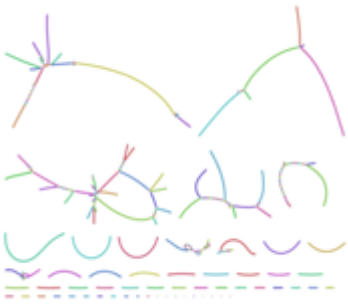
ΔABCDEFXY



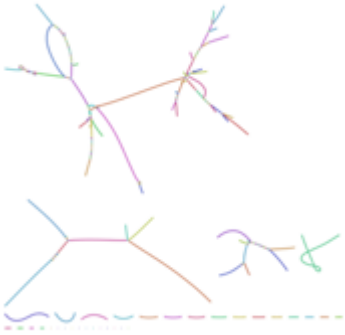
ΔABCDEFPQXY



K2732



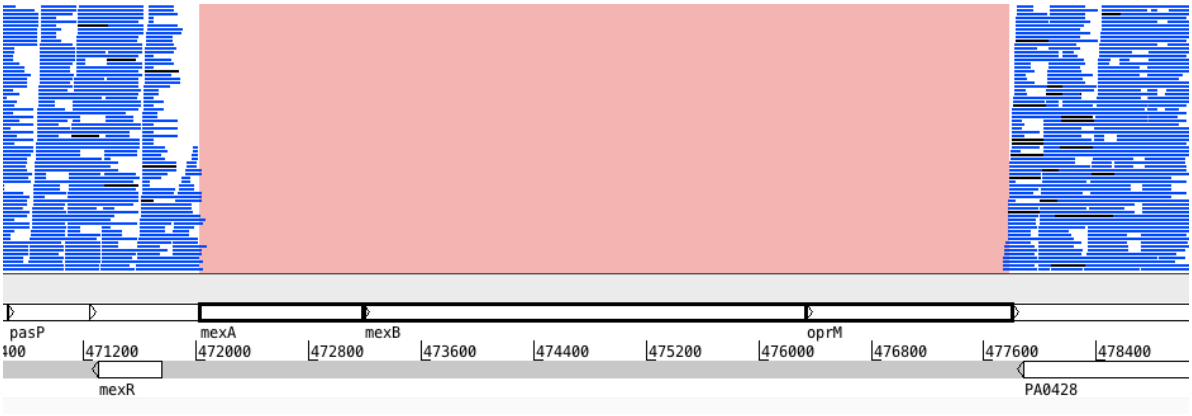
K2733



Appendix S: Visualisation of WGS results. Artemis (Carver *et al*., 2011) plot displays reads (blue lines) mapped to the PAO1-UW reference genome. Efflux pump genes are highlighted in red.

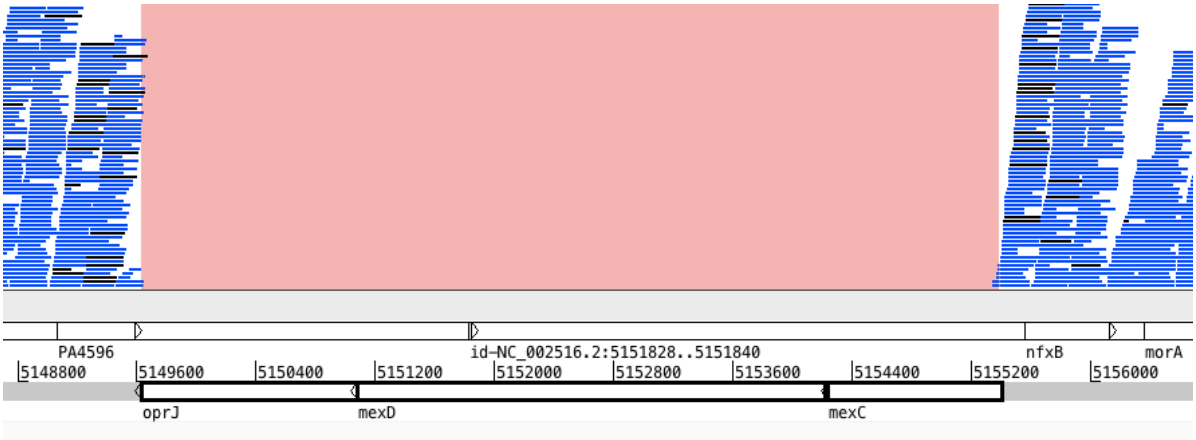
ΔAB

No reads mapped to MexAB-OprM



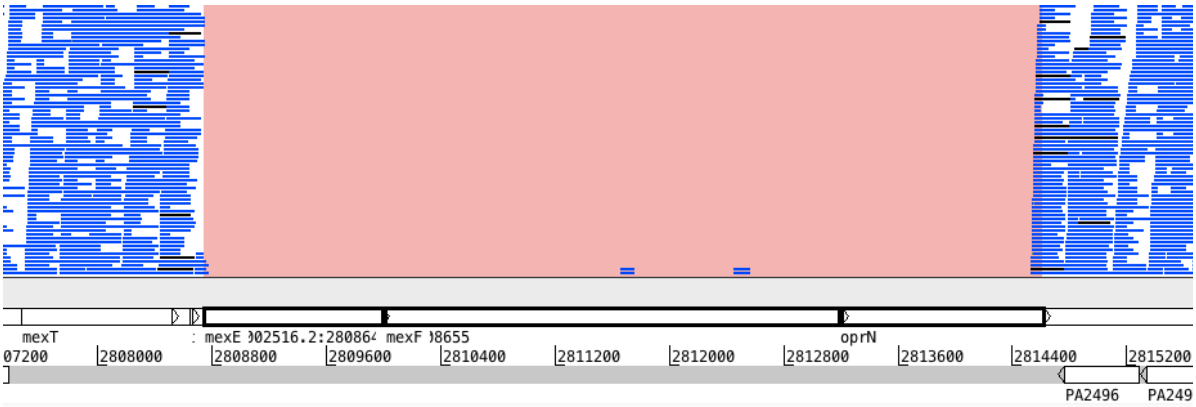
ΔCD

No reads mapped to MexCD-OprJ



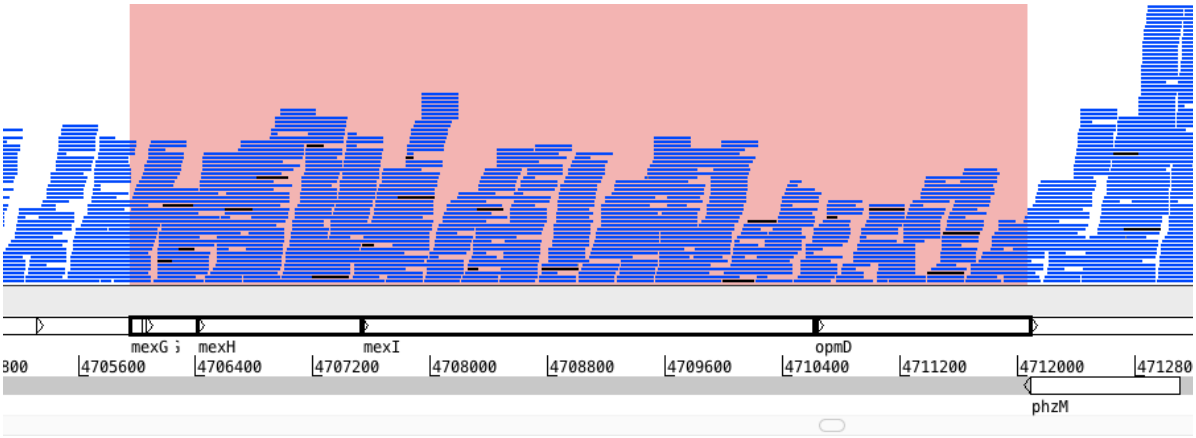
ΔEF

No reads mapped to MexEF-OprN



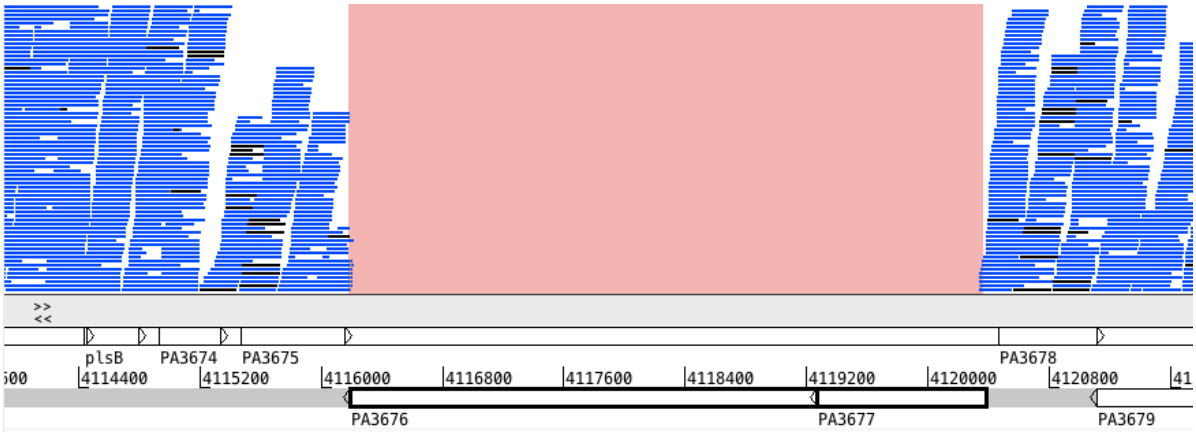
ΔGHI

Reads mapped to MexGHI-OpmD



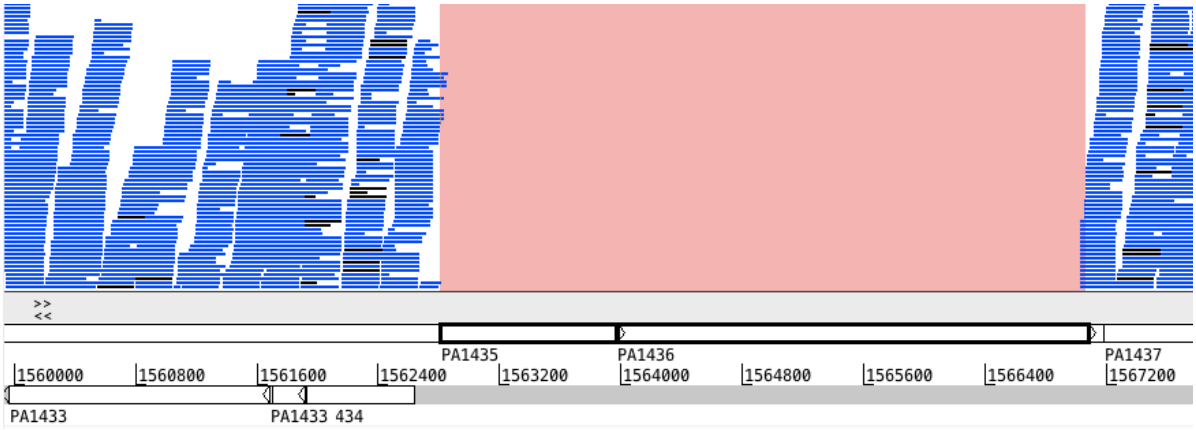
ΔJK

No reads mapped to MexJK



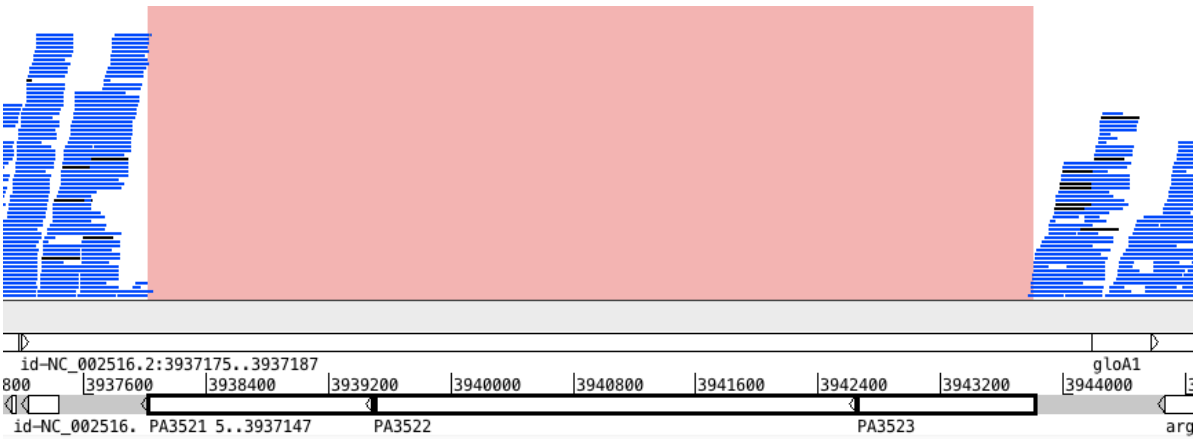
ΔMN

No reads mapped to MexMN



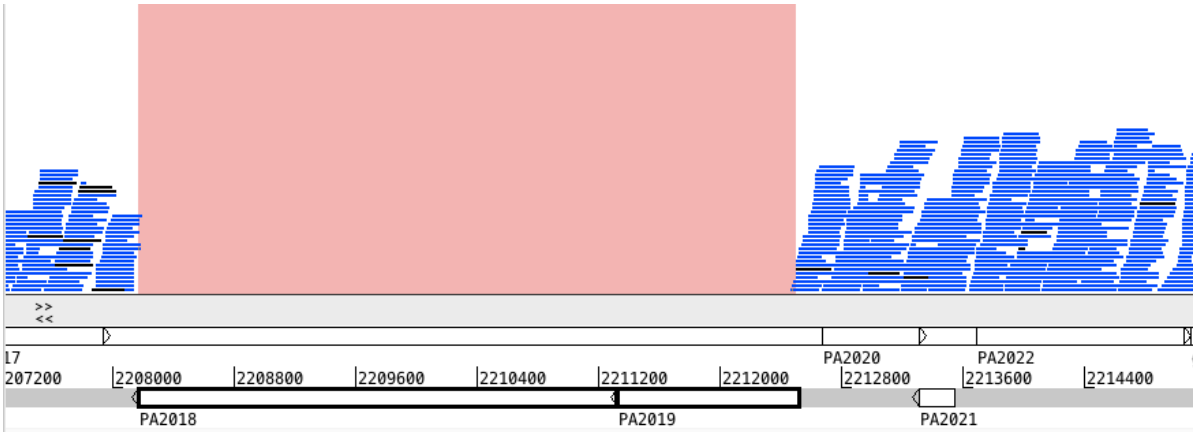
ΔPQ

No reads mapped to MexPQ-OpmE



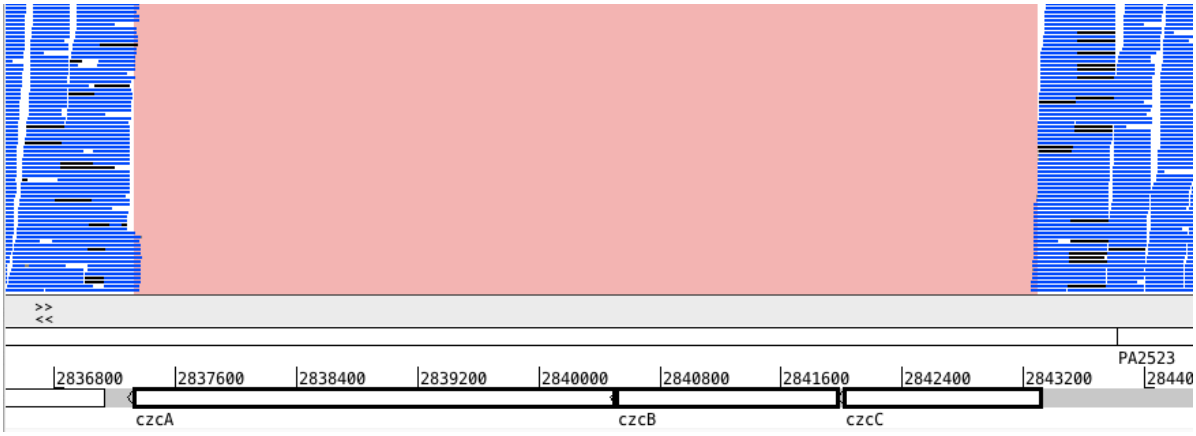
ΔXY

No reads mapped to MexXY



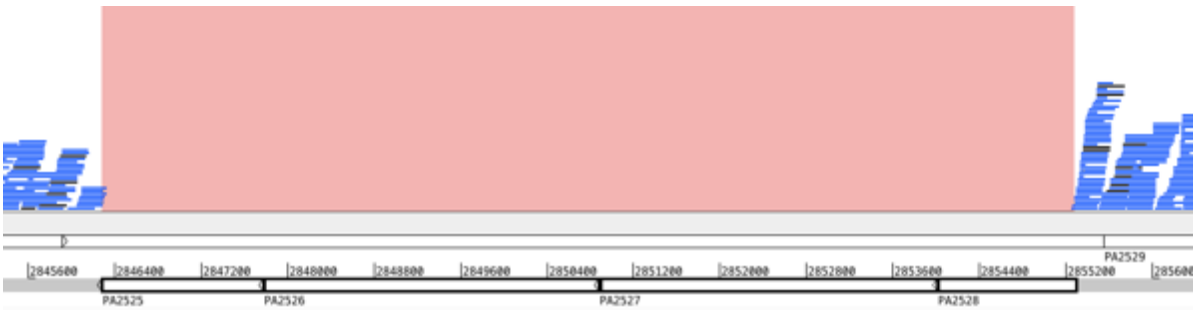
Δczc

No reads mapped to CzcCBA



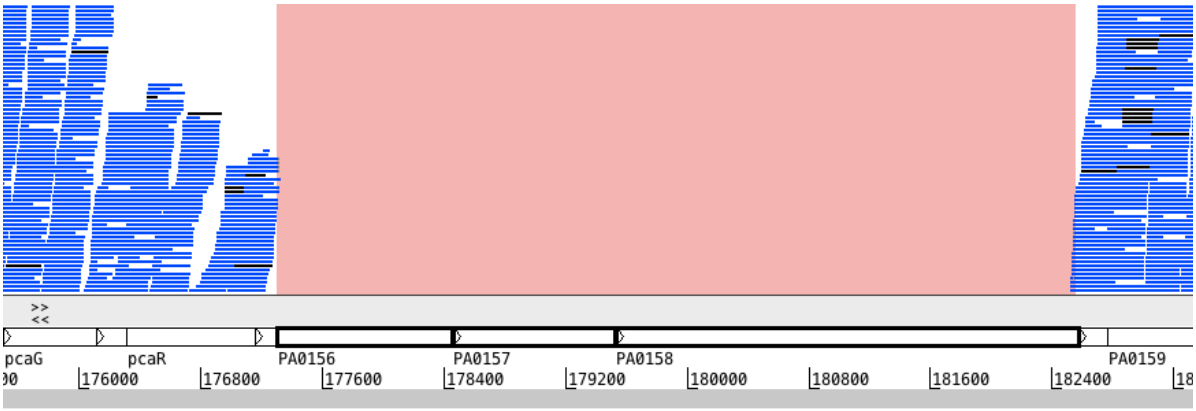
Δmux

No reads mapped to MuxABC-OpmB



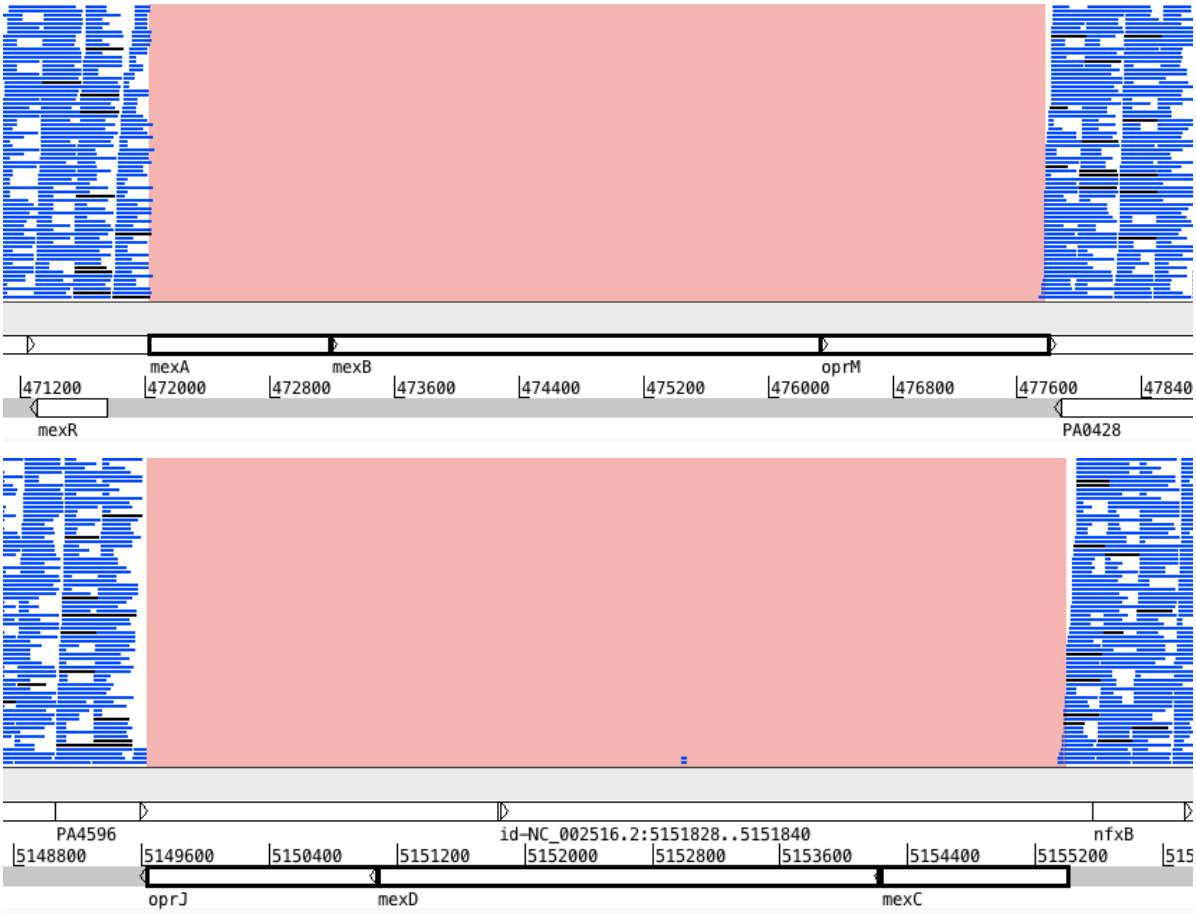
Δtri

No reads mapped to TriABC



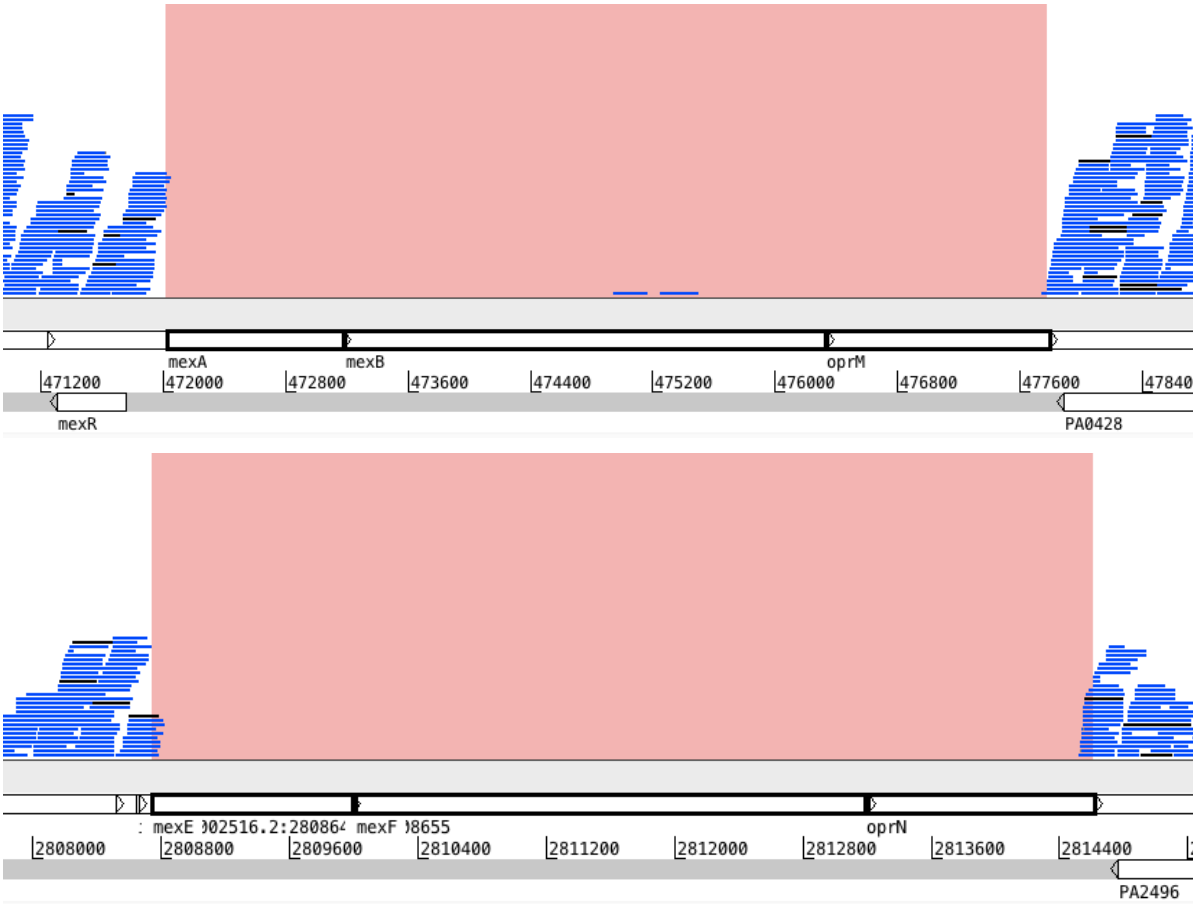
ΔABCD

No reads mapped to MexAB-OprM or MexCD-OprJ



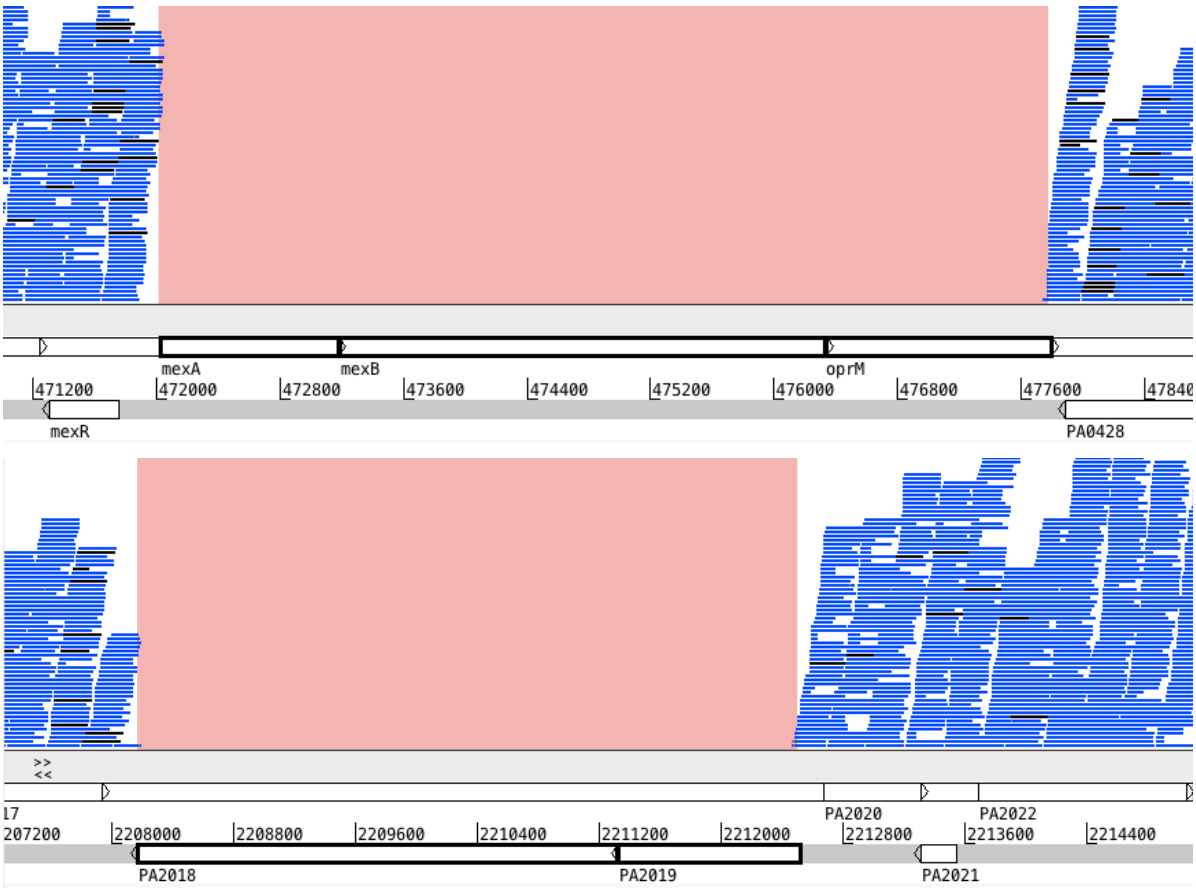
ΔABEF

No reads mapped to MexAB-OprM or MexEF-OprN



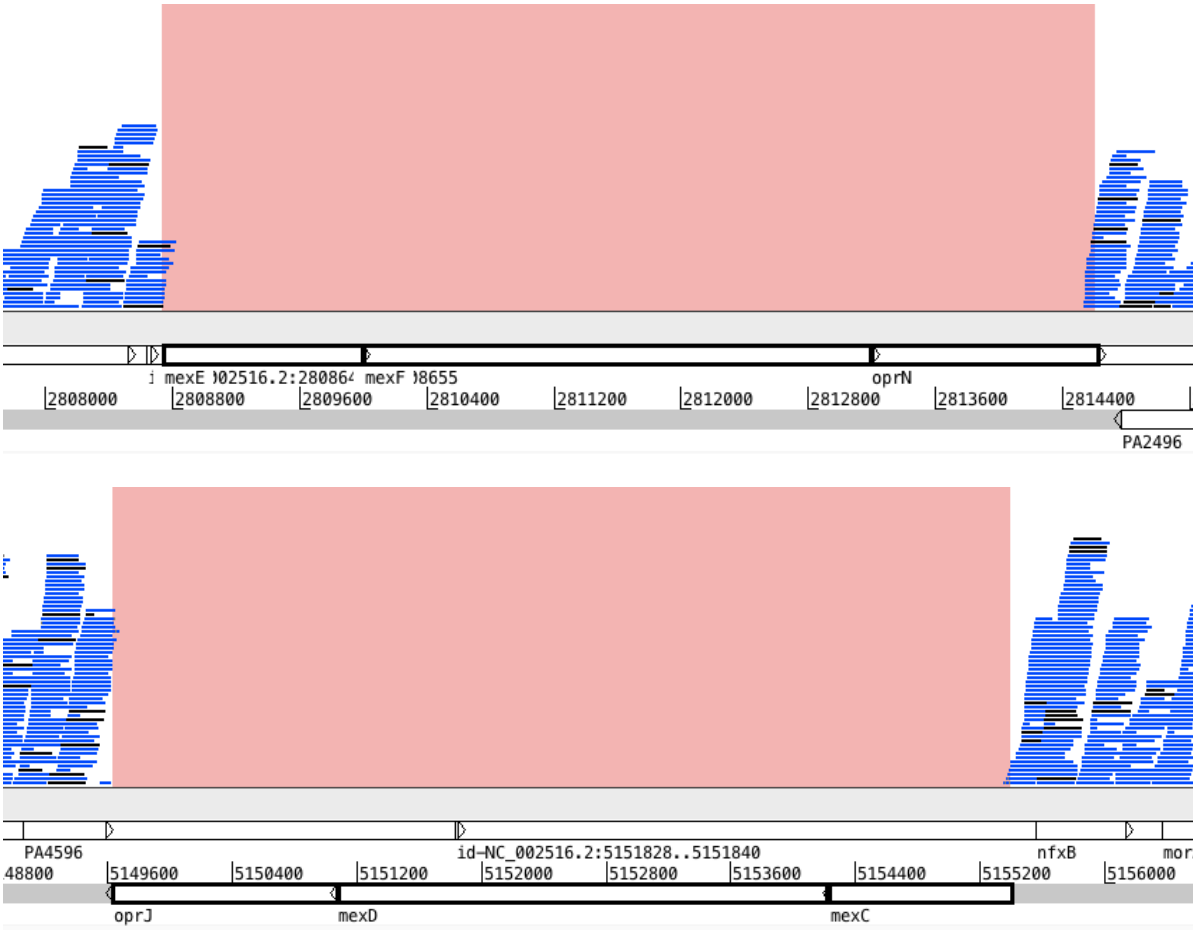
ΔABXY

No reads mapped to MexAB-OprM or MexXY



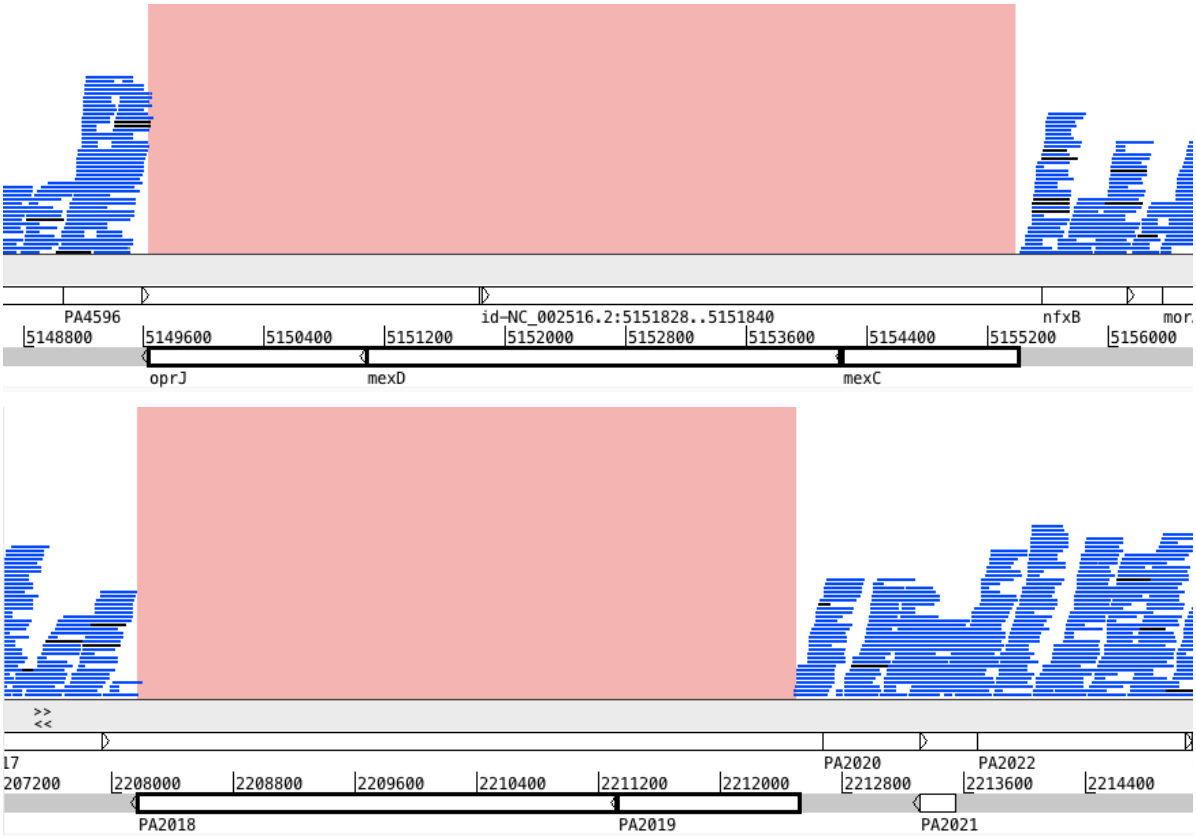
ΔCDEF

No reads mapped to MexCD-OprJ or MexEF-OprN



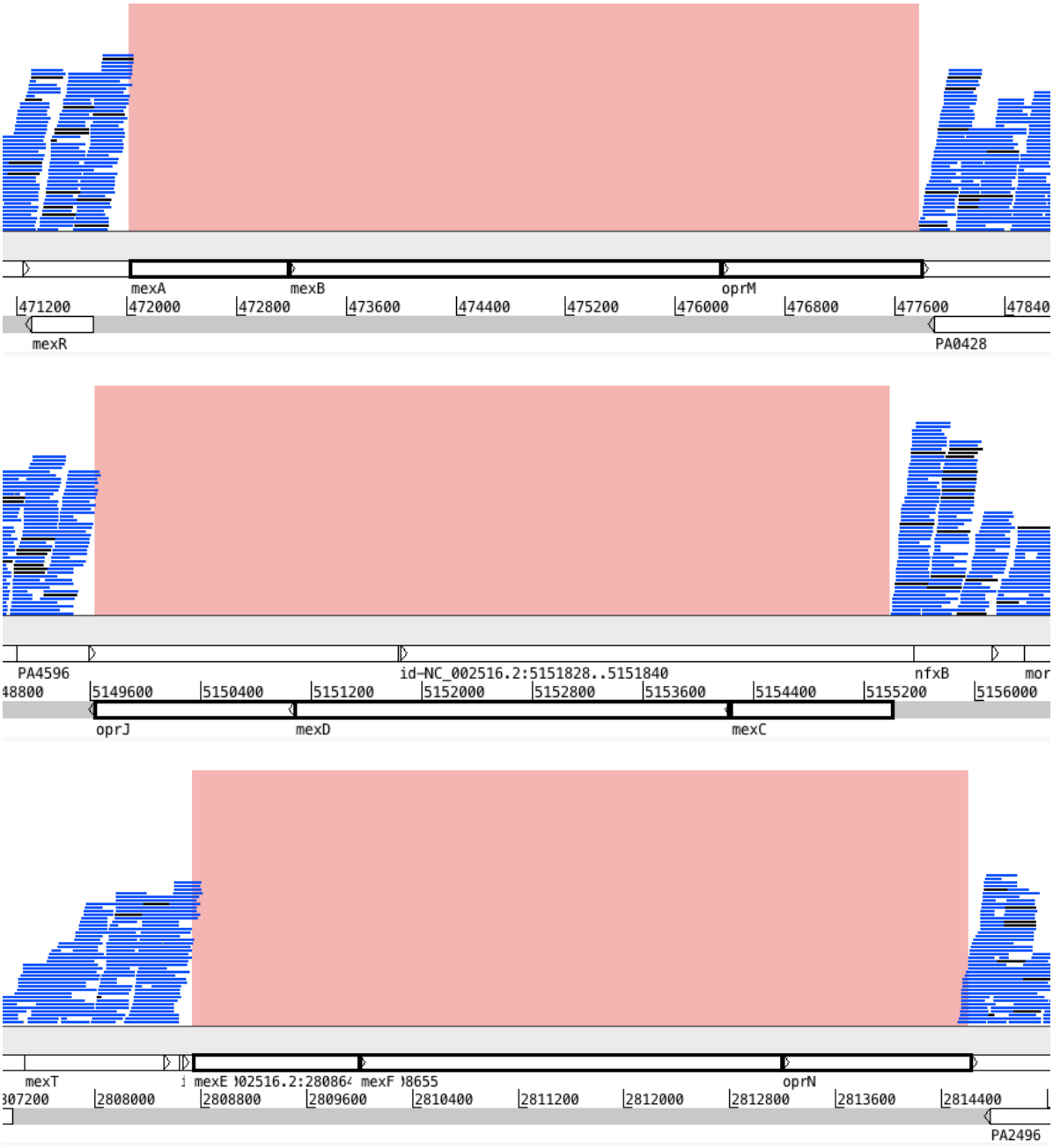
ΔCDXY

No reads mapped to MexCD-OprJ or MexXY



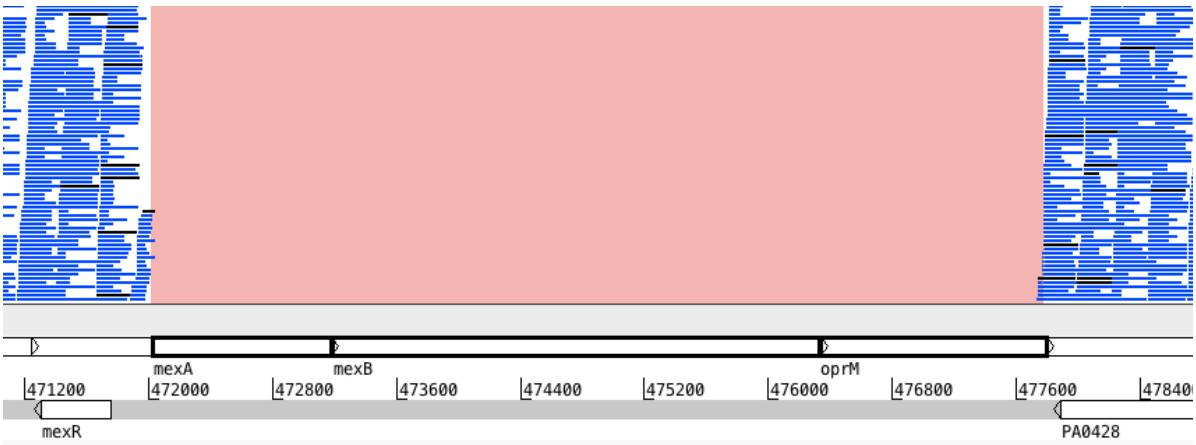
ΔABCDEF

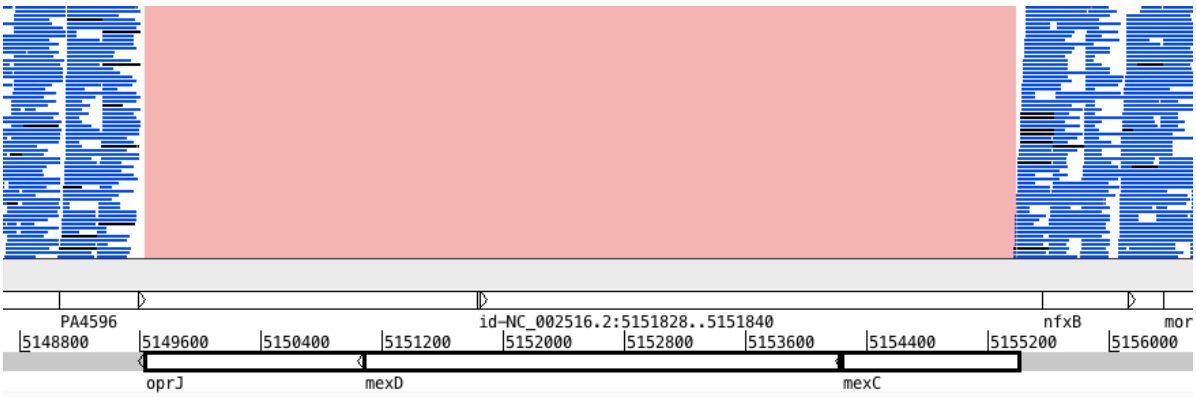
No reads mapped to MexAB-OprM, MexCD-OprJ or MexEF-OprN

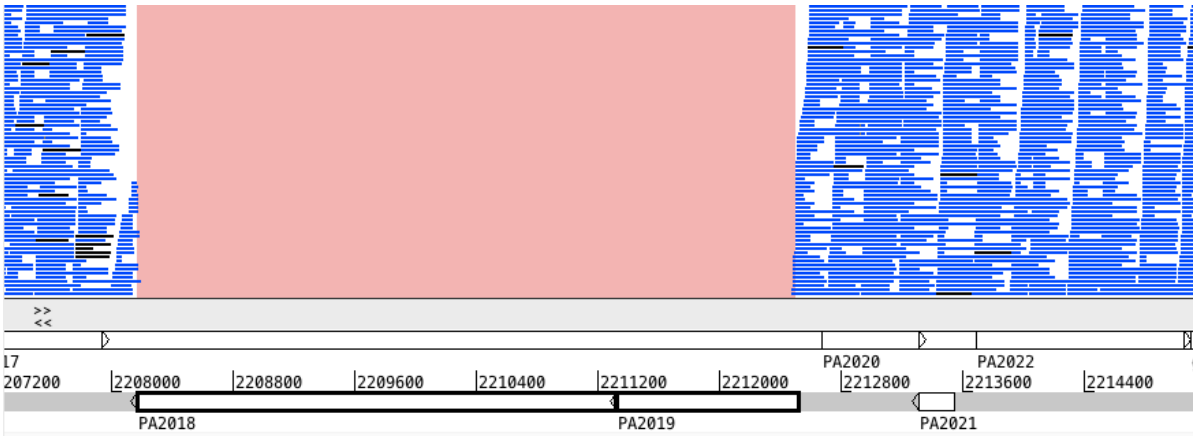


ΔABCDXY

No reads mapped to MexAB-OprM, MexCD-OprJ or MexXY

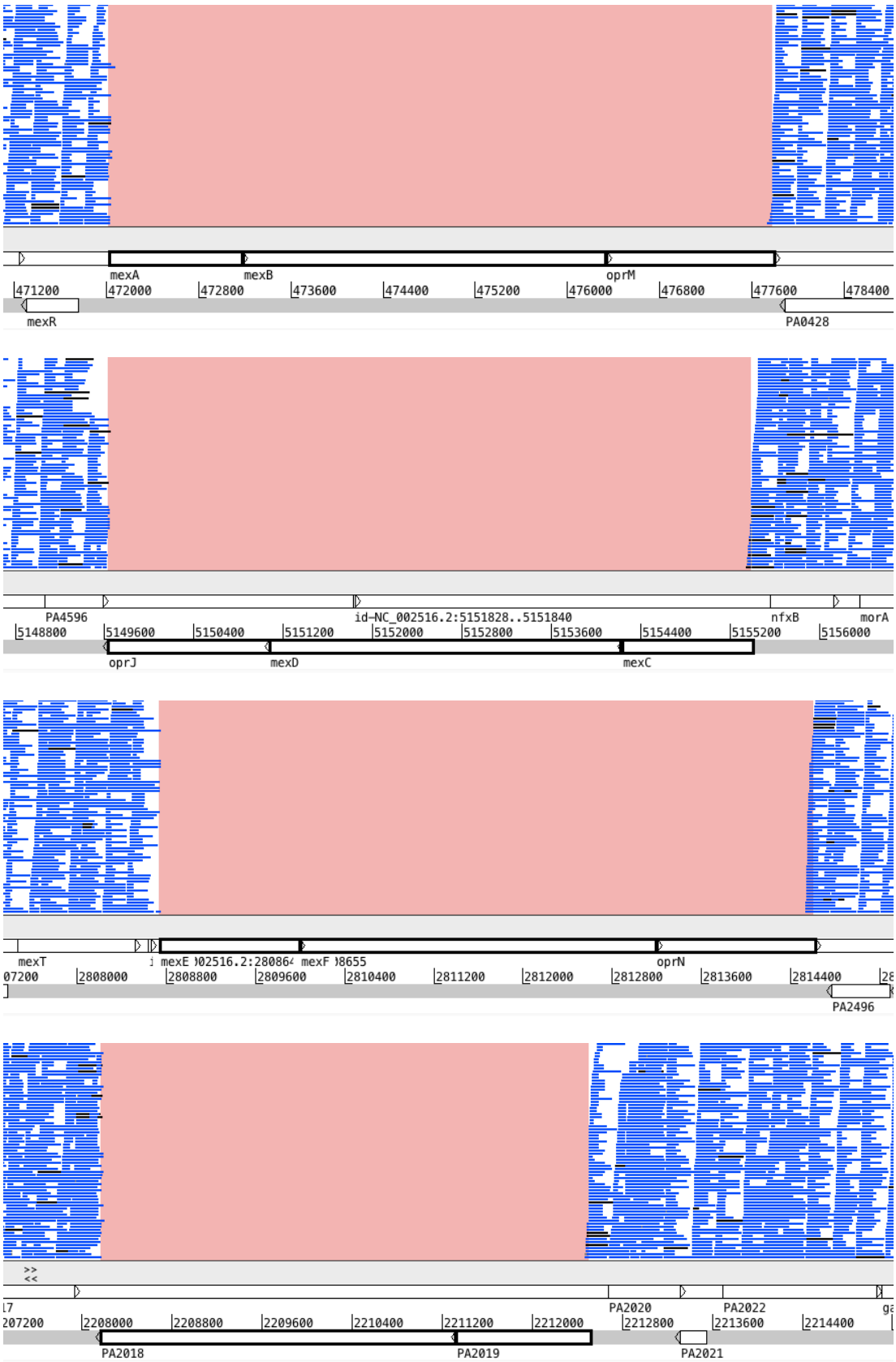






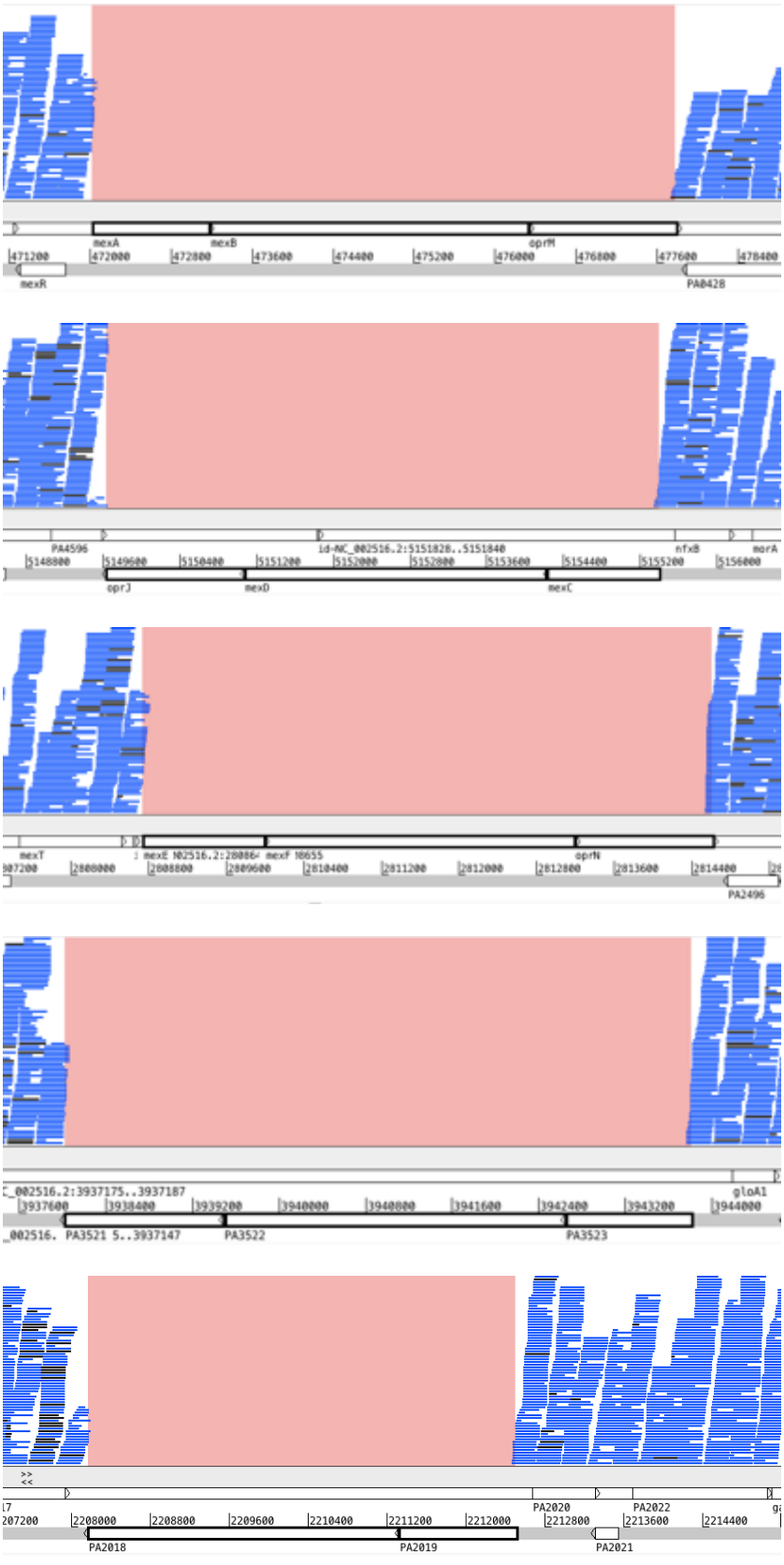
ΔABCDEFXY

No reads mapped to MexAB-OprM, MexCD-OprJ, MexEF-OprN or MexXY



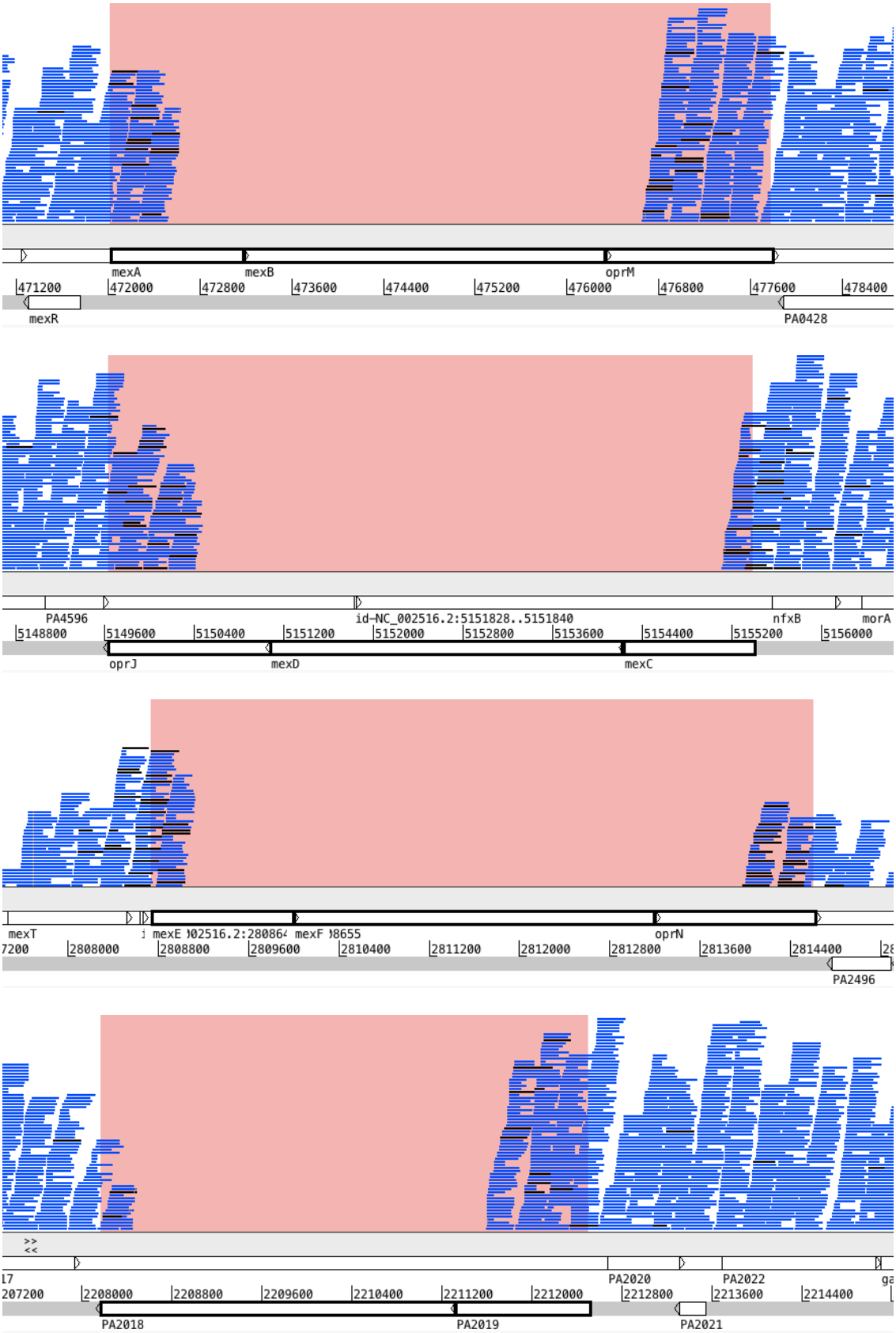
ΔABCDEFPQXY

No reads mapped to MexAB-OprM, MexCD-OprJ, MexEF-OprN, MexPQ-OpmE or MexXY



K2733

No reads mapped to MexAB-OprM, MexCD-OprJ, MexEF-OprN or MexXY



Appendix T: Antimicrobial resistance genes found in *P. aeruginosa* PAO1-L-DS. The resistome of PAO1-L-DS was predicted using the Resistance Gene Identifier (RGI) based on homology and SNP models from the Comprehensive Antibiotic Resistance Database (CARD) (Jia *et al*., 2016). Only perfect and strict gene hits are shown.

Family	AMR gene	Drug Class
APH(3')	APH(3')-IIb	aminoglycosides
Chloramphenicols acetyltransferase (CAT)	CatB7	phenicols
Fosfomycin thiol transferase	FosA	fosfomycin
Major facilitator superfamily (MFS) efflux pump	Bcr-1	bicyclomycin
Multidrug and toxic compound extrusion (MATE) transporter	PmpM	fluoroquinolones; aminoglycosides; disinfecting agents and antiseptics
Outer Membrane Porin (Opr)	ParR	macrolides; fluoroquinolones; monobactams; aminoglycosides; carbapenems; cephalosporins; cephamycins; penams; tetracyclines; phenicols; penems; disinfecting agents and antiseptics
	ParS	macrolides; fluoroquinolones; monobactams; aminoglycosides; carbapenems; cephalosporins; cephamycins; penams; tetracyclines; phenicols; penems; disinfecting agents and antiseptics
OXA beta-lactamase	OXA-50	carbapenems; cephalosporins; penams
PDC beta-lactamase	PDC-1	monobactams; carbapenems; cephalosporins
pmr phosphoethanolamine transferase	ArnA	peptides
	BasS	peptides

	CprR	peptides
	CprS	peptides
Resistance-Nodulation-Division (RND) efflux pump	CpxR	macrolides; fluoroquinolones; monobactams; aminoglycosides; carbapenems; cephalosporins; cephamycins; penams; tetracyclines; peptides; aminocoumarins; diaminopyrimidines; sulfonamides; phenicols; penems
	MexA	macrolides; fluoroquinolones; monobactams; carbapenems; cephalosporins; cephamycins; penams; tetracyclines; peptides; aminocoumarins; diaminopyrimidines; sulfonamides; phenicols
	MexB	macrolides; fluoroquinolones; monobactams; carbapenems; cephalosporins; cephamycins; penams; tetracyclines; peptides; aminocoumarins; diaminopyrimidines; sulfonamides; phenicols
	MexC	macrolides; fluoroquinolones; aminoglycosides; cephalosporins; penams; tetracyclines; aminocoumarins; diaminopyrimidines; phenicols
	MexD	macrolides; fluoroquinolones; aminoglycosides; cephalosporins; penams; tetracyclines; aminocoumarins; diaminopyrimidines; phenicols
	MexE	fluoroquinolones; diaminopyrimidines; phenicols
	MexF	fluoroquinolones; diaminopyrimidines; phenicols
	MexG	fluoroquinolones; tetracyclines; disinfecting agents and antiseptics
	MexH	fluoroquinolones; tetracyclines; disinfecting agents and antiseptics
	MexI	fluoroquinolones; tetracyclines; disinfecting agents and antiseptics
	MexJ	macrolides; tetracyclines; disinfecting agents and antiseptics

MexK	macrolides; tetracyclines; disinfecting agents and antiseptics
MexL	macrolides; tetracyclines; disinfecting agents and antiseptics
MexM	phenicols
MexN	phenicols
MexP	macrolides; carbapenems; tetracyclines; diaminopyrimidines; phenicols; disinfecting agents and antiseptics
MexQ	macrolides; carbapenems; tetracyclines; diaminopyrimidines; phenicols; disinfecting agents and antiseptics
MexR	macrolides; fluoroquinolones; monobactams; carbapenems; cephalosporins; cephamycins; penams; tetracyclines; peptides; aminocoumarins; diaminopyrimidines; sulfonamides; phenicols
MexS	fluoroquinolones; diaminopyrimidines; phenicols
MexT	fluoroquinolones; diaminopyrimidines; phenicols
MexV	macrolides; fluoroquinolones; tetracyclines; phenicols; disinfecting agents and antiseptics
MexW	macrolides; fluoroquinolones; tetracyclines; phenicols; disinfecting agents and antiseptics
mexY	macrolides; fluoroquinolones; aminoglycosides; carbapenems; cephalosporins; cephamycins; penams; tetracyclines; phenicols; disinfecting agents and antiseptics
MexZ	macrolides; fluoroquinolones; aminoglycosides; carbapenems; cephalosporins; cephamycins; penams; tetracyclines; phenicols; disinfecting agents and antiseptics
MuxA	macrolides; monobactams; tetracyclines; aminocoumarins

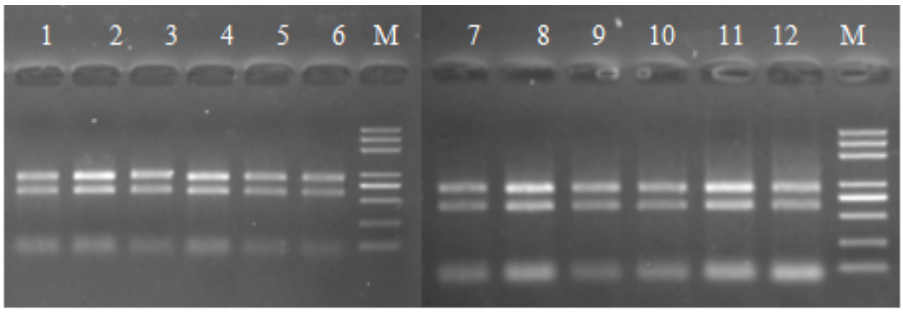
MuxB	macrolides; monobactams; tetracyclines; aminocoumarins
MuxC	macrolides; monobactams; tetracyclines; aminocoumarins
NalC	macrolides; fluoroquinolones; monobactams; carbapenems; cephalosporins; cephamycins; penams; tetracyclines; peptides; aminocoumarins; diaminopyrimidines; sulfonamides; phenicols
NalD	macrolides; fluoroquinolones; monobactams; carbapenems; cephalosporins; cephamycins; penams; tetracyclines; peptides; aminocoumarins; diaminopyrimidines; sulfonamides; phenicols
NfxB	macrolides; fluoroquinolones; cephalosporins; penams; tetracyclines; aminocoumarins; diaminopyrimidines; phenicols
OpmB	macrolides; monobactams; tetracyclines; aminocoumarins
OpmD	fluoroquinolones; tetracyclines; disinfecting agents and antiseptics
OpmE	macrolides; carbapenems; tetracyclines; diaminopyrimidines; phenicols; disinfecting agents and antiseptics
OpmH	disinfecting agents and antiseptics
OprJ	macrolides; fluoroquinolones; aminoglycosides; cephalosporins; penams; tetracyclines; aminocoumarins; diaminopyrimidines; phenicols
OprM	macrolides; fluoroquinolones; monobactams; aminoglycosides; carbapenems; cephalosporins; cephamycins; penams; tetracyclines; peptides; aminocoumarins; diaminopyrimidines; sulfonamides; phenicols; penems; disinfecting agents and antiseptics
OprN	fluoroquinolones; diaminopyrimidines; phenicols

	RsmA	fluoroquinolones; diaminopyrimidines; phenicols
	TriA	disinfecting agents and antiseptics
	TriB	disinfecting agents and antiseptics
	TriC	disinfecting agents and antiseptics
	YajC	fluoroquinolones; cephalosporins; glycylcycline; penams; tetracyclines; rifamycin; phenicols; disinfecting agents and antiseptics
Small multidrug resistance (SMR) efflux pump	EmrE	aminoglycosides

Appendix U: Novogene quality control results summary of RNA-Seq samples

Sample Name	Nucleic Acid ID	Concentration(ng/μl)	Volume(μl)	Total amount(μg)	Integrity value	Sample QC Results
PAO1-L-DS_exponential_1	FKRN210040938-1A	585	8.00	4.68000	6.60	Pass
PAO1-L-DS_exponential_2	FKRN210040939-1A	846	10.00	8.46000	10.00	Pass
PAO1-L-DS_exponential_3	FKRN210040940-1A	870	9.00	7.83000	10.00	Pass
ΔABCDEFXY_exponential_1	FKRN210040941-1A	850	9.00	7.65000	6.70	Pass
ΔABCDEFXY_exponential_2	FKRN210040942-1A	564	10.00	5.64000	10.00	Pass
ΔABCDEFXY_exponential_3	FKRN210040943-1A	538	9.00	4.84200	10.00	Pass
PAO1-L-DS_stationary_1	FKRN210040944-1A	1066	11.00	11.72600	10.00	Pass
PAO1-L-DS_stationary_2	FKRN210040945-1A	1350	11.00	14.85000	10.00	Pass
PAO1-L-DS_stationary_3	FKRN210040946-1A	1006	12.00	12.07200	10.00	Pass
ΔABCDEFXY_stationary_1	FKRN210040947-1A	1160	10.00	11.60000	10.00	Pass
ΔABCDEFXY_stationary_2	FKRN210040948-1A	821	11.00	9.03100	9.90	Pass
ΔABCDEFXY_stationary_3	FKRN210040949-1A	871	9.00	7.83900	9.50	Pass

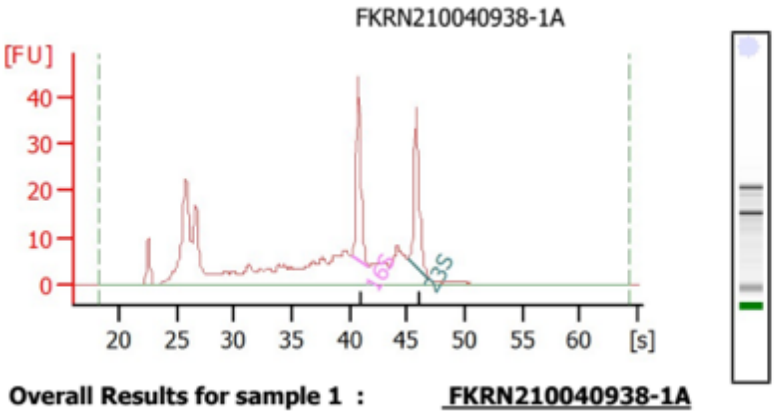
Appendix V: **Novogene agarose gel electrophoresis results**



Remark: M: Trans 2K Plus DNA ladder; 1-12: samples ranged in the order of upper table (1-6、11-12 loaded 1ul after 5 times diluted, 7-10 loaded 1ul after 10 times diluted).

Appendix W: Novogene Agilent 2100 integrity test results

PAO1-L-DS_exponential_1



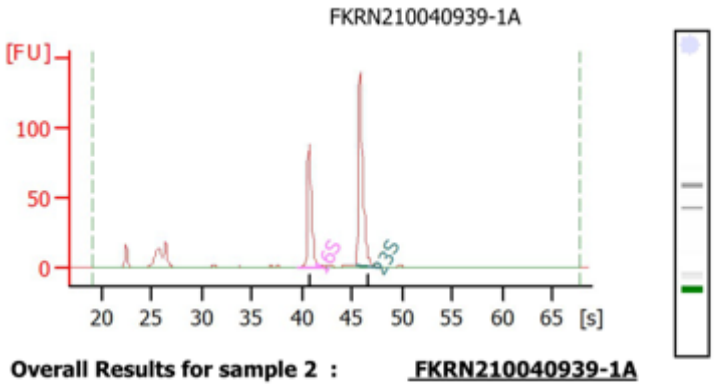
Overall Results for sample 1 : FKRN210040938-1A

RNA Area:	410.1
RNA Concentration:	117 ng/µl
rRNA Ratio [23s / 16s]:	0.8
RNA Integrity Number (RIN):	6.6 (B.02.10)
Result Flagging Color:	
Result Flagging Label:	RIN: 6.60

Fragment table for sample 1 : FKRN210040938-1A

Name	Start Time [s]	End Time [s]	Area	% of total Area
16S	40.19	41.59	45.0	11.0
23S	45.09	47.01	37.5	9.2

PAO1-L-DS_exponential_2



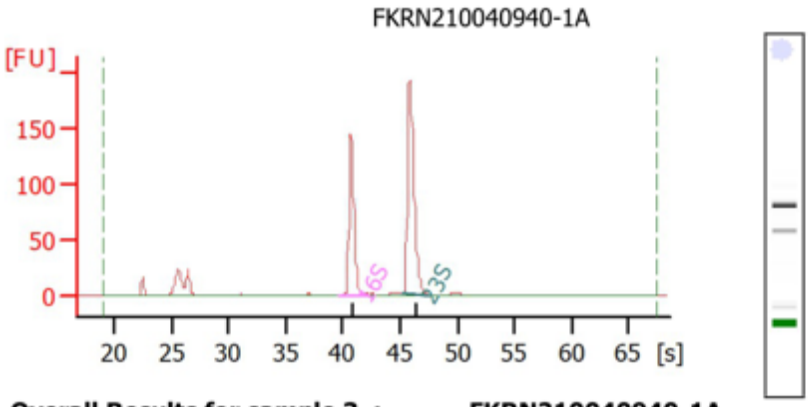
Overall Results for sample 2 : FKRN210040939-1A

RNA Area:	367.1
RNA Concentration:	175 ng/µl
rRNA Ratio [23s / 16s]:	1.5
RNA Integrity Number (RIN):	10 (B.02.10, Anomaly Threshold(s) manually adapted)
Result Flagging Color:	
Result Flagging Label:	RIN:10

Fragment table for sample 2 : FKRN210040939-1A

Name	Start Time [s]	End Time [s]	Area	% of total Area
16S	39.55	42.25	99.5	27.1
23S	45.39	47.85	153.2	41.7

PAO1-L-DS_exponential_3



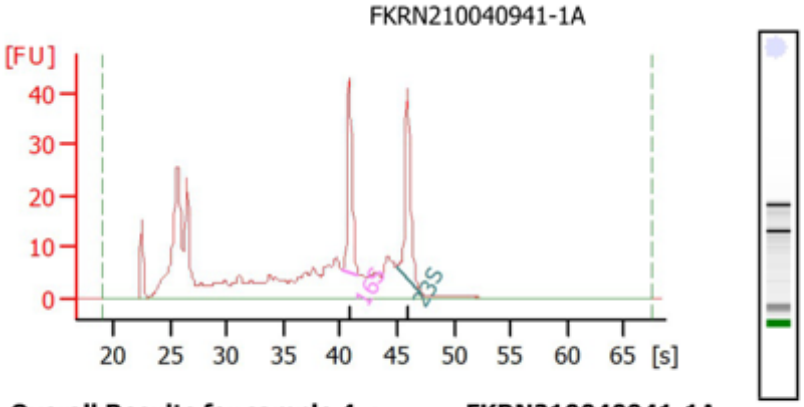
Overall Results for sample 3 : FKRN210040940-1A

RNA Area:	620.3
RNA Concentration:	296 ng/µl
rRNA Ratio [23s / 16s]:	1.6
RNA Integrity Number (RIN):	10 (B.02.10, Anomaly Threshold(s) manually adapted)
Result Flagging Color:	
Result Flagging Label:	RIN:10

Fragment table for sample 3 : FKRN210040940-1A

Name	Start Time [s]	End Time [s]	Area	% of total Area
16S	39.62	42.31	171.2	27.6
23S	45.29	47.59	265.9	42.9

ΔABCDEFXY_exponential_1



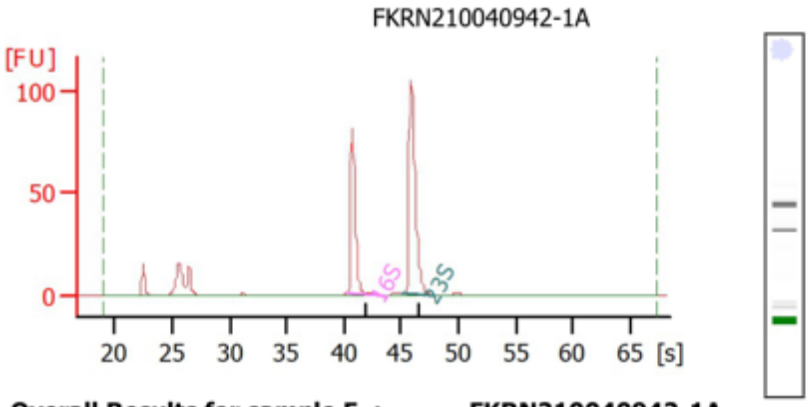
Overall Results for sample 4 : FKRN210040941-1A

RNA Area:	456.2
RNA Concentration:	218 ng/µl
rRNA Ratio [23s / 16s]:	1.0
RNA Integrity Number (RIN):	6.7 (B.02.10, Anomaly Threshold(s) manually adapted)
Result Flagging Color:	
Result Flagging Label:	RIN: 6.70

Fragment table for sample 4 : FKRN210040941-1A

Name	Start Time [s]	End Time [s]	Area	% of total Area
16S	40.11	41.63	44.4	9.7
23S	44.90	47.15	44.3	9.7

ΔABCDEFXY_exponential_2



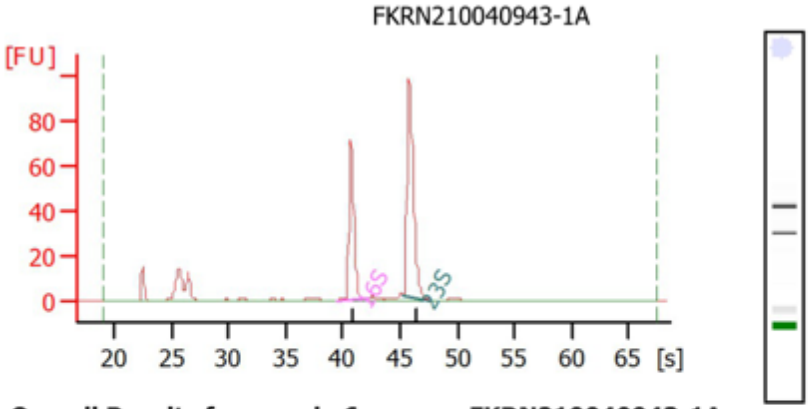
Overall Results for sample 5 : FKRN210040942-1A

RNA Area:	342.6
RNA Concentration:	164 ng/µl
rRNA Ratio [23s / 16s]:	1.5
RNA Integrity Number (RIN):	10 (B.02.10, Anomaly Threshold(s) manually adapted)
Result Flagging Color:	
Result Flagging Label:	RIN:10

Fragment table for sample 5 : FKRN210040942-1A

Name	Start Time [s]	End Time [s]	Area	% of total Area
16S	40.31	43.49	92.9	27.1
23S	45.10	47.93	143.6	41.9

ΔABCDEFXY_exponential_3



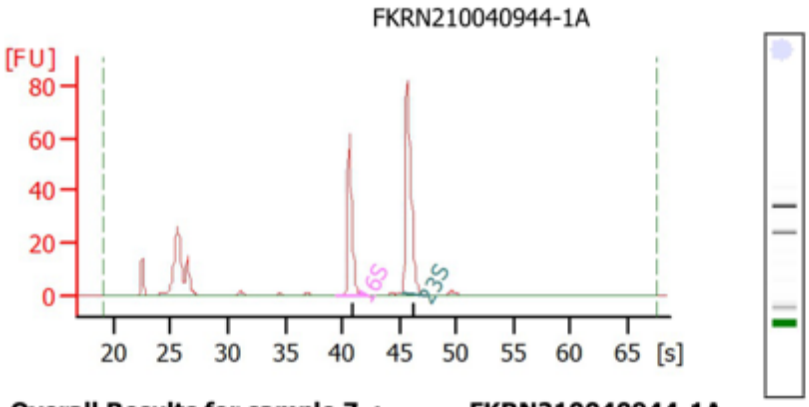
Overall Results for sample 6 : FKRN210040943-1A

RNA Area:	322.3
RNA Concentration:	154 ng/µl
rRNA Ratio [23s / 16s]:	1.6
RNA Integrity Number (RIN):	10 (B.02.10, Anomaly Threshold(s) manually adapted)
Result Flagging Color:	
Result Flagging Label:	RIN:10

Fragment table for sample 6 : FKRN210040943-1A

Name	Start Time [s]	End Time [s]	Area	% of total Area
16S	39.42	42.16	83.8	26.0
23S	45.29	47.64	131.4	40.8

PAO1-L-DS_stationary_1



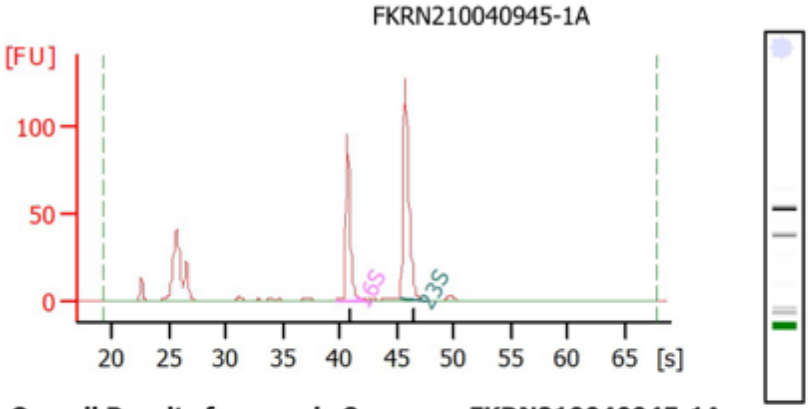
Overall Results for sample 7 : FKRN210040944-1A

RNA Area:	300.5
RNA Concentration:	144 ng/µl
rRNA Ratio [23s / 16s]:	1.6
RNA Integrity Number (RIN):	10 (B.02.10, Anomaly Threshold(s) manually adapted)
Result Flagging Color:	
Result Flagging Label:	RIN:10

Fragment table for sample 7 : FKRN210040944-1A

Name	Start Time [s]	End Time [s]	Area	% of total Area
16S	39.56	42.30	63.3	21.1
23S	45.25	47.30	99.3	33.0

PAO1-L-DS_stationary_2



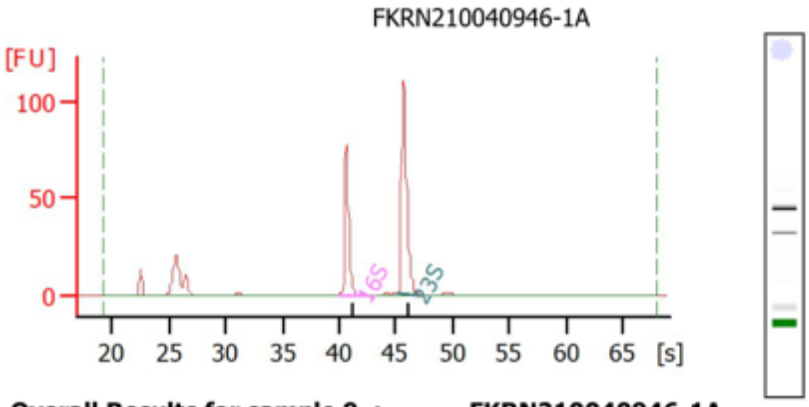
Overall Results for sample 8 : FKRN210040945-1A

RNA Area:	461.5
RNA Concentration:	220 ng/µl
rRNA Ratio [23s / 16s]:	1.6
RNA Integrity Number (RIN):	10 (B.02.10, Anomaly Threshold(s) manually adapted)
Result Flagging Color:	
Result Flagging Label:	RIN:10

Fragment table for sample 8 : FKRN210040945-1A

Name	Start Time [s]	End Time [s]	Area	% of total Area
16S	39.68	42.29	100.2	21.7
23S	45.25	47.51	155.9	33.8

PAO1-L-DS_stationary_3



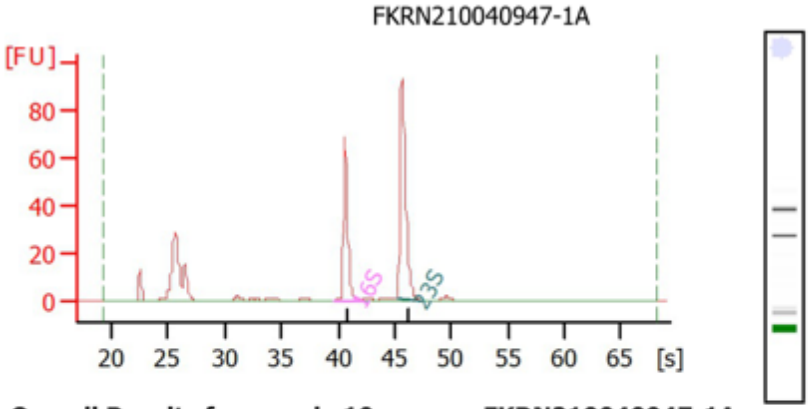
Overall Results for sample 9 : FKRN210040946-1A

RNA Area:	328.5
RNA Concentration:	157 ng/µl
rRNA Ratio [23s / 16s]:	1.6
RNA Integrity Number (RIN):	10 (B.02.10, Anomaly Threshold(s) manually adapted)
Result Flagging Color:	
Result Flagging Label:	RIN:10

Fragment table for sample 9 : FKRN210040946-1A

Name	Start Time [s]	End Time [s]	Area	% of total Area
16S	39.92	42.34	79.3	24.1
23S	45.20	47.27	127.2	38.7

ΔABCDEFXY_stationary_1



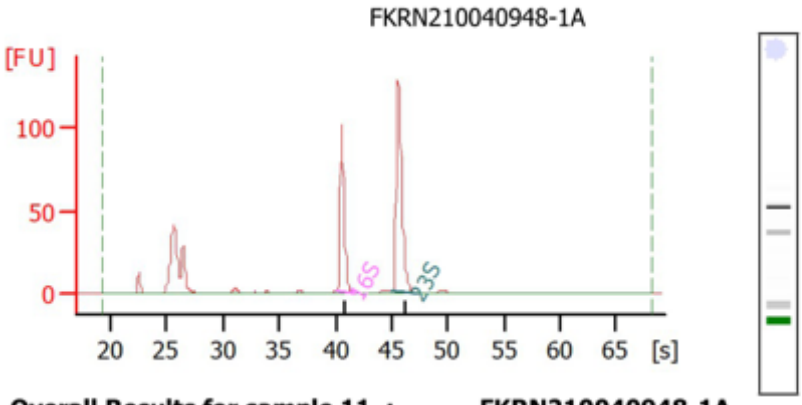
Overall Results for sample 10 : FKRN210040947-1A

RNA Area:	333.3
RNA Concentration:	159 ng/µl
rRNA Ratio [23s / 16s]:	1.6
RNA Integrity Number (RIN):	10 (B.02.10, Anomaly Threshold(s) manually adapted)
Result Flagging Color:	
Result Flagging Label:	RIN:10

Fragment table for sample 10 : FKRN210040947-1A

Name	Start Time [s]	End Time [s]	Area	% of total Area
16S	39.56	42.13	72.5	21.7
23S	45.15	47.27	114.7	34.4

ΔABCDEFXY_stationary_2



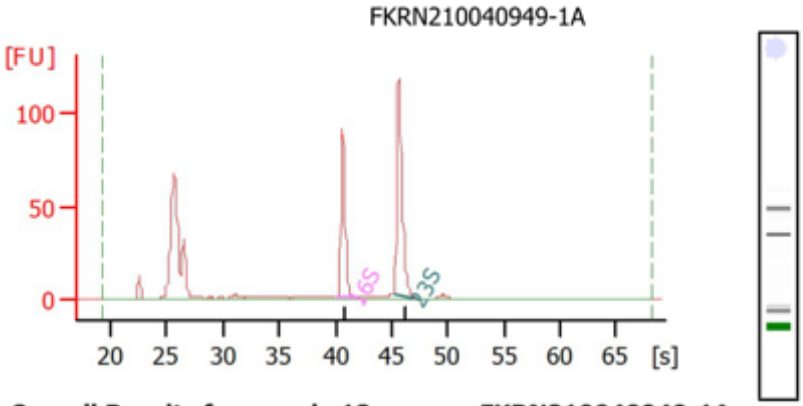
Overall Results for sample 11 : FKRN210040948-1A

RNA Area:	495.3
RNA Concentration:	237 ng/µl
rRNA Ratio [23s / 16s]:	1.5
RNA Integrity Number (RIN):	9.9 (B.02.10, Anomaly Threshold(s) manually adapted)
Result Flagging Color:	
Result Flagging Label:	RIN: 9.90

Fragment table for sample 11 : FKRN210040948-1A

Name	Start Time [s]	End Time [s]	Area	% of total Area
16S	40.15	41.69	106.7	21.5
23S	45.05	47.27	159.7	32.2

ΔABCDEFXY_stationary_3



Overall Results for sample 12 : FKRN210040949-1A

RNA Area:	548.1
RNA Concentration:	262 ng/µl
rRNA Ratio [23s / 16s]:	1.4
RNA Integrity Number (RIN):	9.5 (B.02.10, Anomaly Threshold(s) manually adapted)
Result Flagging Color:	
Result Flagging Label:	RIN: 9.50

Fragment table for sample 12 : FKRN210040949-1A

Name	Start Time [s]	End Time [s]	Area	% of total Area
16S	40.10	41.64	97.6	17.8
23S	45.15	47.37	135.4	24.7

Appendix X: Scripts used for RNA-Seq analysis

```
-------------------------------------------

SCRIPT FOR RNAseq ANALYSIS

Danielle Scales

University of Nottingham

-------------------------------------------

### SCRIPT 1: ASSESS QUALITY OF RAW SEQUENCING DATA USING FASTQC AND
MULTIQC


# Go to directory where paired reads are stored and run:

> fastqc -t 24 *.fq


# Compile FastQC results into a single report using MultiQC. Go to
directory where FastQC output files are stored and run:

> multiqc .


-------------------------------------------

### SCRIPT 2: DATA PRE-PROCESSING USING TRIMMOMATIC


> java -jar trimmomatic-0.35.jar PE -phred33 R1_1.fq.gz R1_2.fq.gz
  R1_1_paired.fq.gz R1_1_unpaired.fq.gz R1_2_paired.fq.gz
  R1_2_unpaired.fq.gz ILLUMINACLIP:TruSeq3-PE.fa:2:30:10 LEADING:3
  TRAILING:3 SLIDINGWINDOW:4:15 MINLEN:36


-------------------------------------------

### SCRIPT 3: RE-ASSESS READ QUALITY USING FASTQC AND MULTIQC


# Go to directory where paired reads are stored and run:

> fastqc -t 24 *.fq
```

```
# Compile FastQC results into a single report using MultiQC. Go to
directory where FastQC output files are stored and run:
> multiqc .

-------------------------------------------
### SCRIPT 4: DE NOVO ASSEMBLIES USING BOWTIE2

# Create Bowtie2 index database for reference genome:
> bowtie2-build GSE94113_NC_002516.inverted.RGP42insertion.fasta
PAO1_inversion

# Check quality of database:
> bowtie2-inspect -n PAO1_inversion

# Map reads against the PAO1_inversion genome database:
> bowtie2 -x PAO1_inversion -1 R1_1.fq -2 R1_2.fq -S
bowtie2_R1_inversion.sam

-------------------------------------------
### SCRIPT 5: ASSESS ALIGNMENT QUALITY USING MULTIQC

# Go to directory where bowtie2 output files are stored and run:
> multiqc .

-------------------------------------------
### SCRIPT 6: CONVERT .SAM FILES TO .BAM FILES USING SAMTOOLS

> samtools view -S -b bowtie2_R1_inversion.sam > bowtie2_R1_inversion.bam

-------------------------------------------
```

```
### SCRIPT 7: COUNT MAPPED READS FOR GENOMIC FEATURES USING SUBREAD
FEATURECOUNTS

> featurecounts -T 4 -t CDS,exon -p –fraction -O -g gene_id -a
GSE94113_NC_002516.inverted.RGP42insertion.gtf -o counts_R1.txt
bowtie2_R1_inversion.bam

# Extract gene_id and sample counts columns:
> cut -f1,7-18 counts_R1.txt > countsmatrix_R1.txt

# Remove header:
> sed 1d countsmatrix_R1.txt > countsmatrix2_R1.txt

-----------------------------------------------
### SCRIPT 8: DIFFERENTIAL GENE EXPRESSION USING DESEQ2

library(tidyverse)
library(DESeq2)

# Load data:
> countdata <- (as.matrix(read.table("~/countsmatrix2_R1.txt", header =
  TRUE, row.name = 1)))

# View count distribution:
> ggplot(data) +
> geom_histogram(aes(x = bowtie2_R1_inversion.bam), stat = "bin", bins =
  200) +
> xlab("Raw expression counts") +
> ylab("Number of genes")
```

```
# Plot mean versus variance to determine whether data should be modelled
using Poisson or negative binominal distribution:
> mean_counts <- apply(countdata[, 10:12], 1, mean)
> variance_counts <- apply(countdata[, 10:12], 1, var)
> df <- data.frame(mean_counts, variance_counts)

> ggplot(df) +
> geom_point(aes(x=mean_counts, y=variance_counts)) +
> geom_line(aes(x=mean_counts, y=mean_counts), color="#EE3377", size=1) +
> scale_x_log10(breaks = 10^c(2,4,6), labels = trans_format("log10",
  math_format(10^.x)), limits = c(1,10000000), expand = c(0, 0)) +
> scale_y_log10(breaks = 10^c(2,5,8,11), labels = trans_format("log10",
  math_format(10^.x)), limits = c(1,1000000000000), expand = c(0, 0)) +
> xlab("Mean") +
> ylab("Variance")

# Create DESeq2Dataset object:
> dds <- DESeqDataSetFromMatrix(countData=round(countdata), colData =
  coldata, design = ~Strain)

# Check size counts:
> dds <- estimateSizeFactors(dds)
> sizeFactors(dds)

> normalized_counts <- counts(dds, normalized = TRUE)
> write.table(normalized_counts, file = "~/normalized_counts.txt", sep =
  "\t", quote=F, col.names = NA)

# Transform counts for data visualization:
> rld <- rlog(dds, blind=TRUE)
```

```
# Extract the rlog matrix from the object:
> rld_mat <- assay(rld)

# Compute pairwise correlation values:
> rld_cor <- cor(rld_mat)
> head(rld_cor)

# Plot PCA:
> pcaData <- plotPCA(rld, intgroup=c("Strain","growth_phase"),
  returnData=TRUE)
> percentVar <- round(100 * attr(pcaData, "percentVar"))

> ggplot(pcaData, aes(PC1, PC2, color=Strain, shape=growth_phase)) +
> geom_point(size=3) +
> xlab(paste0("PC1: ",percentVar[1],"% variance")) +
> ylab(paste0("PC2: ",percentVar[2],"% variance")) +
> labs(shape = "Growth phase") +
> scale_x_continuous(expand = c(0, 0), limits = c(-40,40)) +
> scale_y_continuous(expand = c(0, 0.1), limits = c(-10,10)) +
> scale_colour_manual(values = c("PAO1-L" = "#440154FF", "ABCDEFXY" =
  "#4AC16DFF"), labels = c("PAO1-L" = "PAO1-L", "ABCDEFXY" = "ΔABCDEFXY"))
  +
> guides(color = guide_legend(order = 1), shape = guide_legend(order = 2))
  +
> coord_fixed(ratio=2/1)

# Plot heatmap:
> heat.colors <- brewer.pal(6, "PinkYl")
> heatmap <- pheatmap(rld_cor, color = heat.colors, border_color = NA)
```

```
# Normalise counts:
> normalized_counts <- counts(dds, normalized=TRUE)
> normalized_counts2 <- normalized_counts %>%

> data.frame() %>%
> rownames_to_column(var="gene") %>%
# remove gene- string in front of each gene number
> mutate(gene = str_replace(gene, "gene-", "")) %>%
> as_tibble() %>%
> left_join(gene_names)

> write.table(normalized_counts2$gene, file = "~/gene_names1.txt", sep =
  "\t")

# Total number of raw counts per sample:
colSums(counts(dds))

# Total number of normalized counts per sample:
colSums(counts(dds, normalized=T))

# Plot dispersion estimates:
plotDispEsts(dds)

# Define contrasts, extract results table, and shrink the log2 fold
changes:
#NB. The order of the names determines the direction of fold change that is
reported. The factor level given last is the base level for the comparison
ie. the name provided in the second element is the level that is used as
baseline. So for example, if we observe a log2 fold change of -2 this would
mean the gene expression is lower in PAO1-L_exponential relative to
ABCEEFXY_exponential.
```

```
> contrast_exponential <- c("Strainnames", "ABCDEFXY_exponential", "PAO1-
  L_exponential")
> res_tableexponential_unshrunken <- results(dds, contrast =
  contrast_exponential, alpha = 0.05)
> res_tableexponential <- lfcShrink(dds, contrast = contrast_exponential,
  res = res_tableexponential_unshrunken, type = "ashr")

> contrast_stationary <- c("Strainnames", "ABCDEFXY_stationary", "PAO1-
  L_stationary")
> res_tablestationary_unshrunken <- results(dds, contrast =
  contrast_stationary, alpha = 0.05)
> res_tablestationary <- lfcShrink(dds, contrast = contrast_stationary, res
  = res_tablestationary_unshrunken, type = "ashr")

# Convert to df and keep the significant genes:
> padj.cutoff <- 0.05
> l2fc.cutoff <- 1.0

> res_tableexponential_tb <- res_tableexponential %>%
> data.frame() %>%
> rownames_to_column(var="gene") %>%
> filter(padj < padj.cutoff & abs(log2FoldChange) > l2fc.cutoff) %>%
> arrange(desc(log2FoldChange)) %>%
# remove gene- string in front of each gene number
> mutate(gene = str_replace(gene, "gene-", "")) %>%
> as_tibble() %>%
> left_join(gene_names) %>%
# remove deleted genes from dataset
> filter(!gene_name %in% c("mexA", "mexB", "oprM", "mexC", "mexD", "oprJ",
  "mexE", "mexF", "oprN", "mexX", "mexY"))
```

```
> res_tablestationary_tb <- res_tablestationary %>%
> data.frame() %>%
> rownames_to_column(var="gene") %>%
> filter(padj < padj.cutoff & abs(log2FoldChange) > l2fc.cutoff) %>%
> arrange(desc(log2FoldChange)) %>%
# remove gene- string in front of each gene number
> mutate(gene = str_replace(gene, "gene-", "")) %>%
> as_tibble() %>%
> left_join(gene_names) %>%
> filter(!gene_name %in% c("mexA", "mexB", "oprM", "mexC", "mexD", "oprJ",
  "mexE", "mexF", "oprN", "mexX", "mexY"))

# Volcano plots:
> VP_exponential <- ggplot(res_tableexponential_tb, aes(x = log2FoldChange,
  y = -log10(padj), label = gene)) +
> geom_point(aes(colour = cut(log2FoldChange,c(-Inf, -1, 1, Inf))), size =
  2.5) +
> geom_text_repel(data = subset(res_tableexponential_tb, log2FoldChange < -
  1 | log2FoldChange > 1), aes(label = gene_name), size = 3, max.overlaps =
  11, box.padding = unit(0.35, "lines"), point.padding = unit(0.3,
  "lines")) +
> ggtitle("A. Exponential phase") +
> xlab("log2 fold change") +
> ylab("-log10 adjusted p-value") +
> scale_y_continuous(expand = c(0, 0), limits = c(0,50.5)) +
> scale_x_continuous(expand = c(0, 0), limits = c(-4,4), breaks = c(-4,-3,-
  2,-1,0,1,2,3,4)) +
> scale_color_manual(name = "Expression:", values = c("(-Inf,-1]" =
  "#EE3377", "(-1,1]" = "grey60", "(1, Inf]" = "#f08c33"), labels =
  c("Downregulated", "Not significant", "Upregulated"))
```

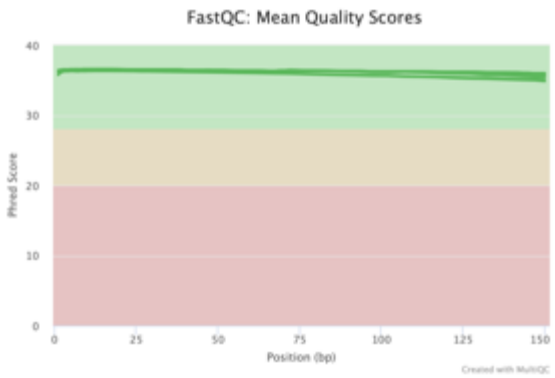
```
> VP_stationary <- ggplot(res_tablestationary_tb, aes(x = log2FoldChange, y
  = -log10(padj), label = gene)) +
> geom_point(aes(colour = cut(log2FoldChange,c(-Inf, -1, 1, Inf))), size =
  2.5) +
> geom_text_repel(data = subset(res_tablestationary_tb, log2FoldChange < -1
  | log2FoldChange > 1), aes(label = gene_name), size = 3, max.overlaps =
  13, box.padding = unit(0.35, "lines"), point.padding = unit(0.3,
  "lines")) +
> ggtitle("B. Stationary phase") +
> xlab("log2 fold change") +
> ylab("-log10 adjusted p-value") +
> scale_y_continuous(expand = c(0, 0), limits = c(0,50.5)) +
> scale_x_continuous(expand = c(0, 0), limits = c(-4,4), breaks = c(-4,-3,-
  2,-1,0,1,2,3,4)) +
> scale_color_manual(name = "Expression:", values = c("(-Inf,-1]" =
  "#EE3377", "(-1,1]" = "grey60", "(1, Inf]" = "#f08c33"), labels =
  c("Downregulated", "Not significant", "Upregulated"))
```

Appendix Y: Quality control of RNA-Seq reads A) Sequence length distribution B) Mean quality score C) Per sequence quality scores D) Per base N content E) Sequence duplication levels F) Adapter content

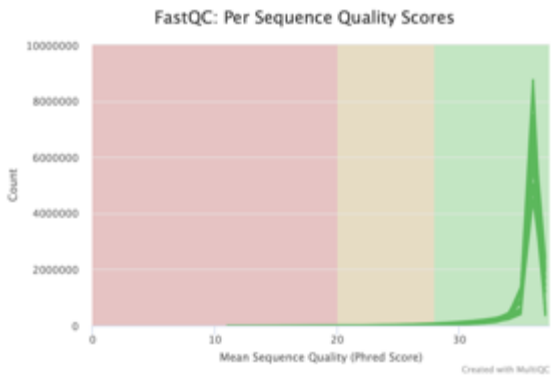
A

All samples have sequences of a single length (150bp).

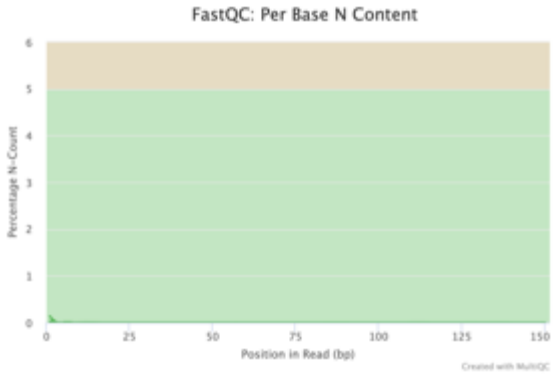
B



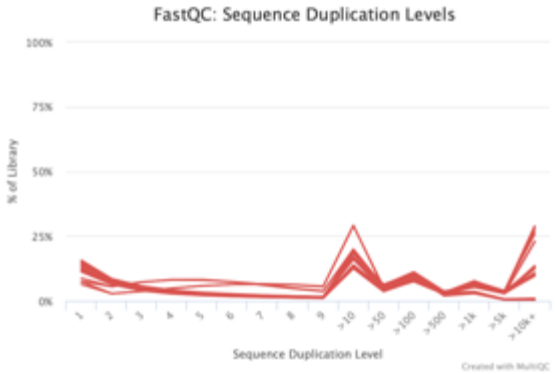
C



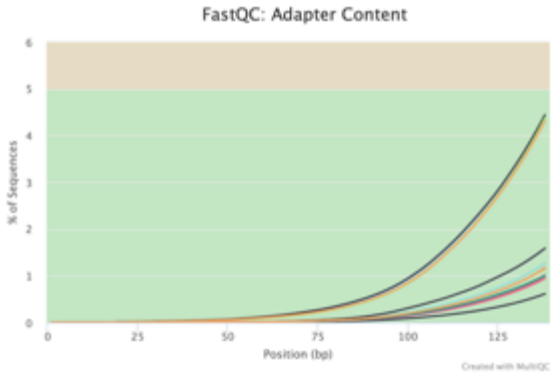
D



E



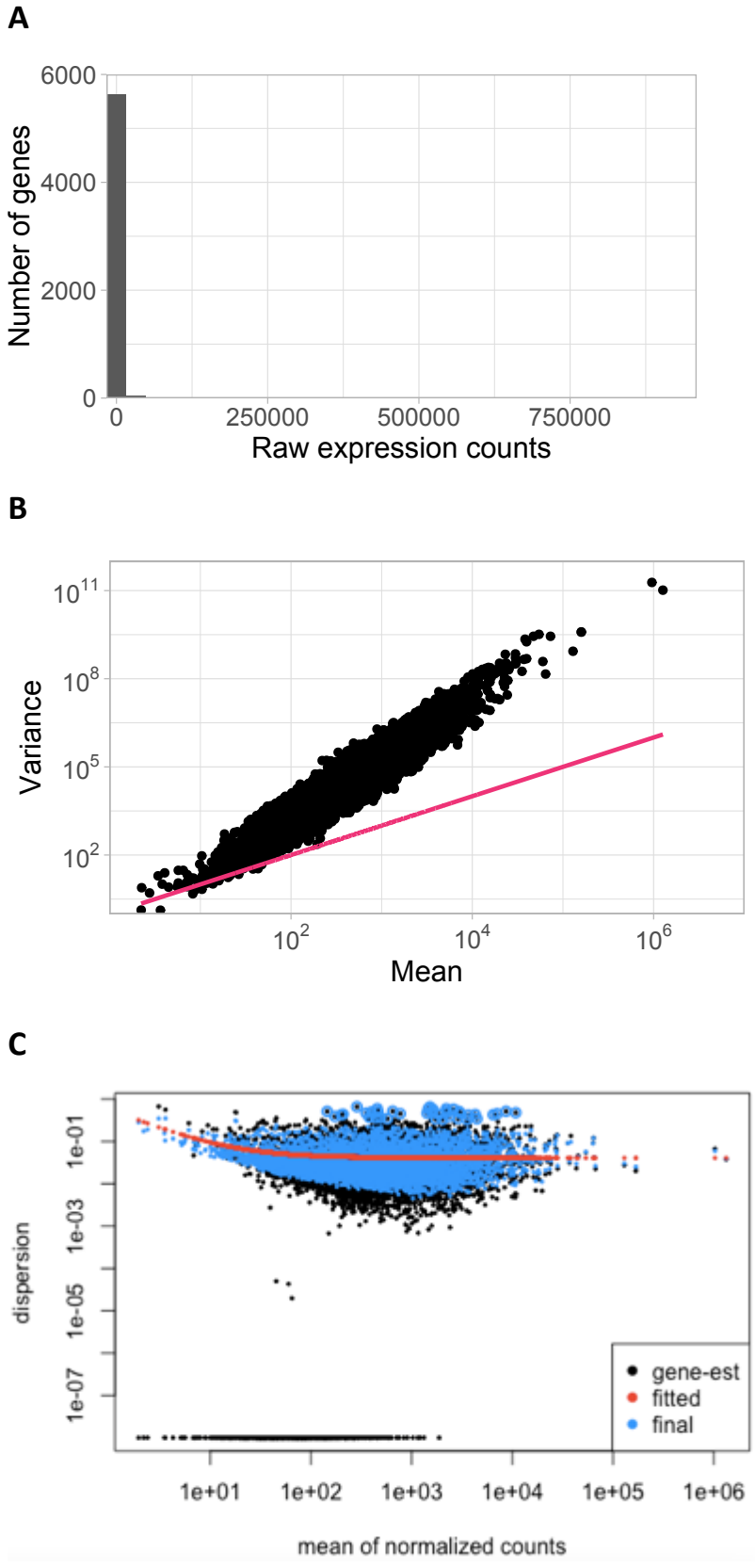
F



Appendix Z: Bowtie2 mapping statistics for each sample against the PAO1-UW_inversion reference sequence.

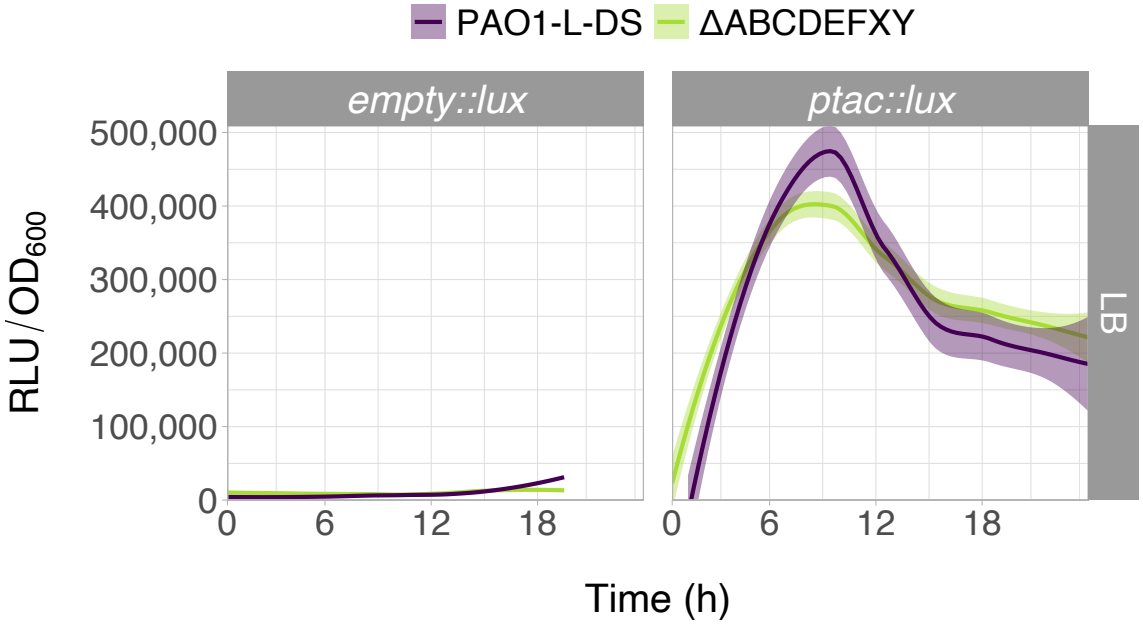
Sample	Total reads	Total mapped reads	Uniquely mapped reads	Multiple mapped reads	Total mapping rate (%)	Uniquely mapping rate (%)	Multiple mapping rate (%)
PAO1-L-DS_exponential_1	9129248	9039855	8912072	127783	99.02	97.62	1.4
PAO1-L-DS_exponential_2	7851511	7777371	7688819	88552	99.06	97.93	1.3
PAO1-L-DS_exponential_3	8828116	8664050	8548501	115549	98.14	96.83	1.31
ΔABCDEFXY_exponential_1	9839095	9747191	9610127	137064	99.07	97.67	1.39
ΔABCDEFXY_exponential_2	10958882	10866127	10710646	155481	99.15	97.73	1.42
ΔABCDEFXY_exponential_3	10023349	9935615	9824052	111563	99.12	98.01	1.11
PAO1-L-DS_stationary_1	9544143	9362016	9283367	78649	98.09	97.27	0.82
PAO1-L-DS_stationary_2	9433457	9246948	9167000	79948	98.02	97.18	0.85
PAO1-L-DS_stationary_3	11614068	11279108	11146944	132164	97.12	95.98	1.14
ΔABCDEFXY_stationary_1	9765388	9635342	9556941	78401	98.67	97.87	0.81
ΔABCDEFXY_stationary_2	11143823	10955228	10843870	111358	98.31	97.31	1
ΔABCDEFXY_stationary_3	9855401	9710529	9626629	83900	98.53	97.68	0.85

Appendix AA: DEseq2 gene-level differential expression analysis. A) Count distribution B) Relationship between mean and variance of counts C) Dispersion plot of gene-wise estimates.

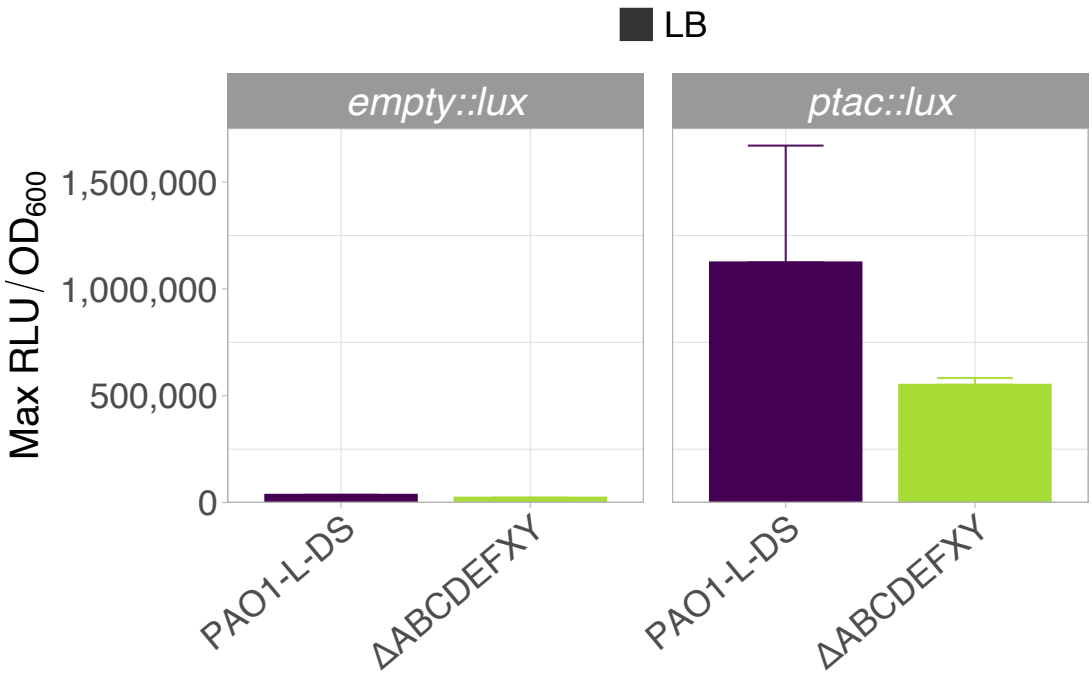


Appendix AB: Controls for transcriptional promoter fusion assays. Strains PAO1-L-DS and ΔABCDEFXY were tagged with the empty pMiniCTX*::lux* (*empty::lux*) vector or P*tac::lux* and grown in LB medium at 37°C. i) Light output (RLU) and OD_{600} readings were taken every 30 minutes and promoter expression is displayed over 18 h (*empty::lux*) or 24 h (P*tac::lux*). The dark line for each strain represents the normalized mean (RLU/OD_{600}) at each time point while lighter shading represents ± 1SD ii) The maximum expression of each gene was calculated and normalized for growth (Max RLU/OD600) ± 1SD

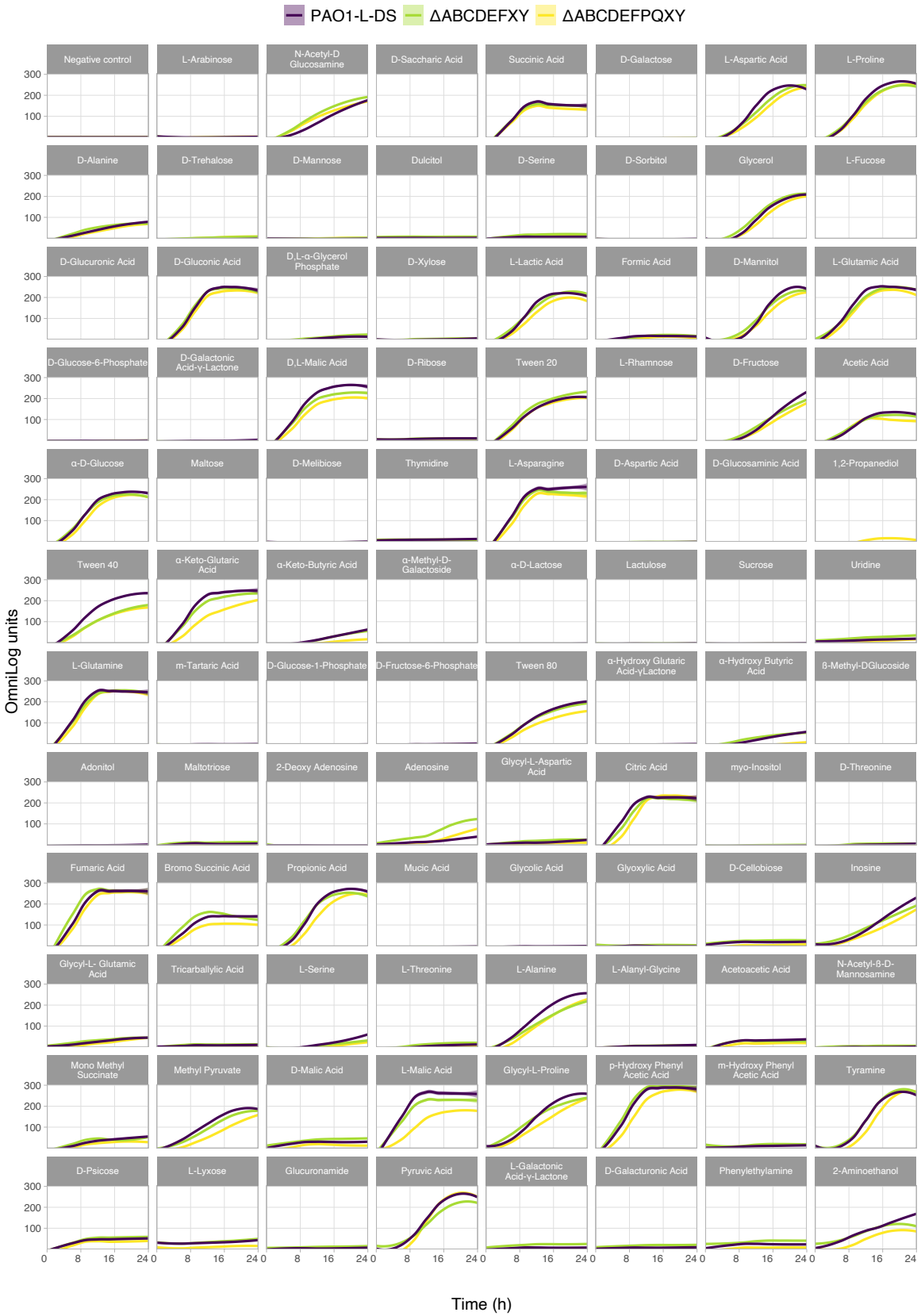
i.



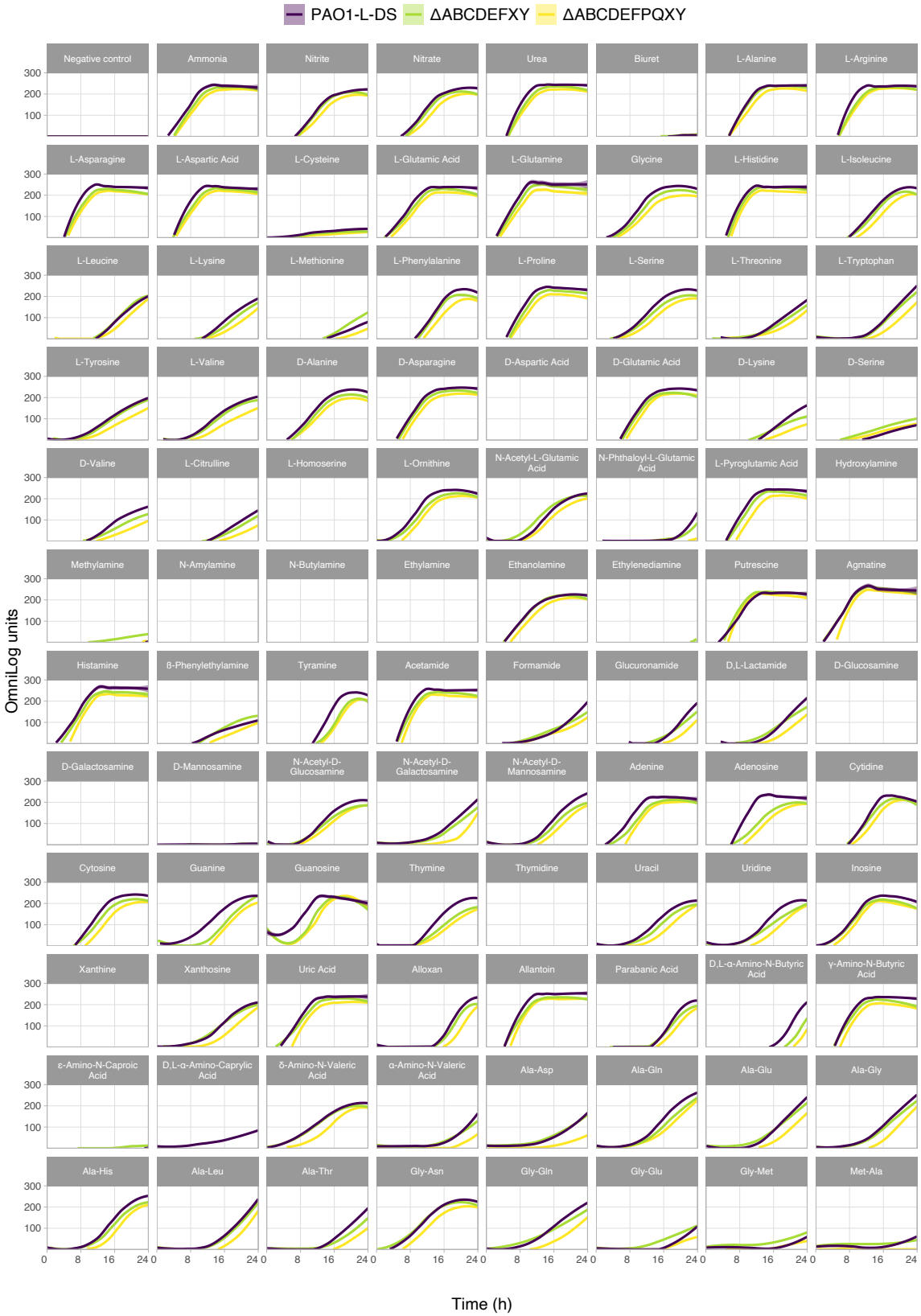
ii.



Appendix AC: Carbon utilisation of PAO1-L-DS, ΔABCDEFXY and ΔABCDEFPQXY on Biolog microplate PM1. Plates were incubated at 37°C for 24 h and readings were taken every 15 mins. Microbial respiration is presented as OmniLog units normalized to the negative control well.



Appendix AD: Nitrogen utilisation of PAO1-L-DS, ΔABCDEFXY and ΔABCDEFPQXY on Biolog microplate PM3B. Plates were incubated at 37°C for 24 h and readings were taken every 15 mins. Microbial respiration is presented as OmniLog units normalized to the negative control well.



Appendix AE: Phosphorus and sulphur utilisation of PAO1-L-DS, ΔABCDEFXY and ΔABCDEFPQXY on Biolog microplate PM4A. Plates were incubated at 37°C for 24 h and readings were taken every 15 mins. Microbial respiration is presented as OmniLog units normalized to the negative control well.



Appendix AF: K2732 and K2733 maximal promoter activity. *P. aeruginosa* K2732 (blue) and K2733 (Δ*mexAB-oprM*, Δ*mexCD-oprJ*, Δ*mexEF-oprN* and Δ*mexXY-oprM*) (green) containing the transcriptional fusions: *lasI::lux*, *lasB::lux*, *rhlI::lux*, *rhlA::lux*, *mexA::lux*, *phzA1::lux*, *pqsA::lux*, *lecA::lux* and the constitutive promoter P*tac::lux* which acted as a positive control of gene transcription. Promoter activity is reported as Relative Light Units (RLU) normalized to cell density (OD_{600}). Strains were cultured in LB at 37 °C for 22 hours and the average of three independent replicates is presented (± 1SD). Taken from J. Grey MRes. Thesis (2017).

